April 30, 1971 LMSC-D007915

PB 200 143

FLYWHEEL FEASIBILITY STUDY AND DEMONSTRATION

FINAL REPORT

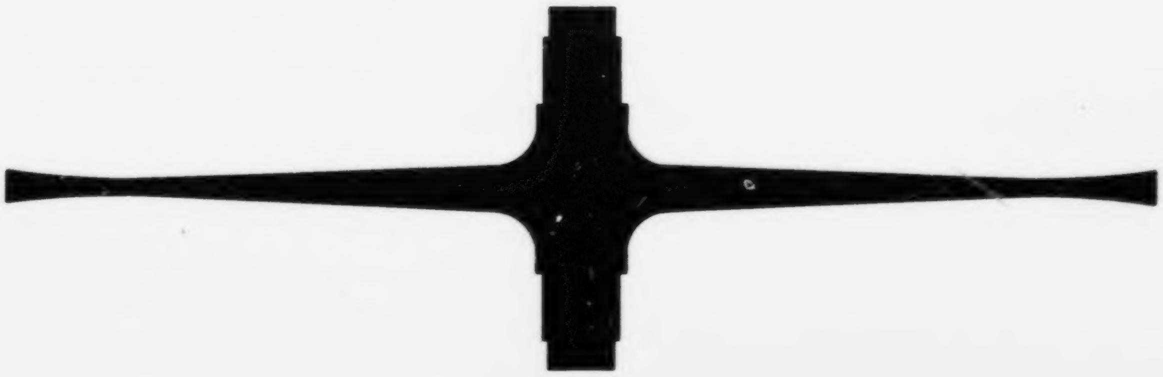

TO

ENVIRONMENTAL PROTECTION AGENCY
Air Pollution Control Office

Reproduced by
NATIONAL TECHNICAL
INFORMATION SERVICE
Springfield, Va. 22151

GROUND VEHICLE SYSTEMS

LOCKHEED MISSILES AND SPACE COMPANY
SUNNYVALE, CALIFORNIA

165

PB 200 143

BIBLIOGRAPHIC DATA SHEET	1. Report No.	2.	3. Recipient's Accession No.

4. Title and Subtitle

Flywheel Feasibility Study and Demonstration

5. Report Date

30 April 1971

6.

7. Author(s)

R.R. Gilbert, J.R. Harvey, G.E. Hever, L.J. Lawson

8. Performing Organization Rept. No. LMSC D0079115

9. Performing Organization Name and Address

Ground Vehicle Systems
Lockheed Missiles and Space Co.
1111 Lockheed Way
Sunnyvile, California 94088

10. Project/Task/Work Unit No.

11. ~~Contract~~/Grant No.

EHS 70-104

12. Sponsoring Organization Name and Address

Environmental Protection Agency
Office of Air Programs
5 Research Drive
Ann Arbor, Mich. 48103
Division of Advanced Automotive Power Systems Development
Hybrids and Electrical Systems Branch

13. Type of Report & Period Covered

14.

15. Supplementary Notes

16. Abstracts

The report presents

A study of the feasibility of application of Flywheel only and flywheel hybrid propulsion systems to four classes of vehicles.

A

17. Key Words and Document Analysis. 17a. Descriptors

Flywheels

Hybrid Propulsion Systems

Vehicle Propulsion

17b. Identifiers/Open-Ended Terms

17c. COSATI Field/Group

18. Availability Statement

19. Security Class (This Report) UNCLASSIFIED

20. Security Class (This Page) UNCLASSIFIED

21. No. of Pages 165

22. Price $3.00

FORM NTIS-35 (10-70)

USCOMM-DC 40329-P71

c

April 30, 1971 LMSC-D007915

FLYWHEEL FEASIBILITY STUDY AND DEMONSTRATION

FINAL REPORT

Contract No. EHS 70-104

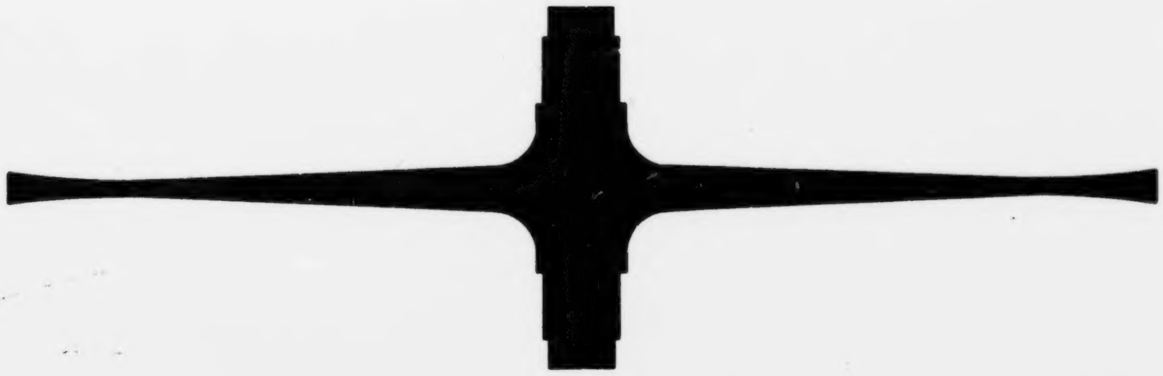

TO

ENVIRONMENTAL PROTECTION AGENCY
Air Pollution Control Office

BY

R. R. GILBERT, J. R. HARVEY, G. E. HEUER AND L. J. LAWSON

GROUND VEHICLE SYSTEMS

LOCKHEED MISSILES AND SPACE COMPANY
SUNNYVALE, CALIFORNIA

CONTENTS

Section		Page
	ILLUSTRATIONS	vii
	TABLES	xi
	UNITS CONVENTION	xiii
	SUMMARY	xv
	Results and Conclusions	xv
	Recommendations	xvi
1	INTRODUCTION	1-1
	Emissions From 1967 and 1970 Model Cars	1-1
	Clean Air Act of 1970	1-3
	Kinetic-Energy Storage As An Acceptable Solution	1-4
	Purpose of the Flywheel Feasibility Study	1-6
	Kinetic-Energy Storage Vehicle Background	1-7
2	APPROACH	2-1
3	APPLICABILITY STUDIES	3-1
	Development of Vehicle Specifications	3-1
	Family Car Specifications	3-1
	Commuter Car Specifications	3-11
	City Bus Specifications	3-14
	Delivery/Postal Van Specifications	3-19
	Vehicle/Configuration Selection	3-23
4	CONFIGURATION TRADEOFFS	4-1
	Transmission Selection	4-1

Section Page

Transmission Requirements 4-1
Ratios 4-1
Ratio Range 4-2
Recuperation 4-2
Efficiency 4-2
Compatibility With Current Practice 4-2
Transmission Controls 4-2
Total Kinetic Energy Control 4-3
Transmission Configurations 4-5
Transmission Types 4-7
Hydrostatic Transmission 4-7
Electric Transmissions 4-8
Power Splitting Transmissions 4-16
Family Car Transmission Comparison 4-22
Bus Transmission Comparison 4-23
Heat Engine Selection 4-24
Heat Engine Survey 4-24
Engine Trend Data 4-26
Spark-Ignition Engines 4-27
Diesel Engines 4-33
Gas Turbine Engines 4-34
Steam (Rankine Cycle) Engines 4-38
Engine Comparison 4-42
5 FLYWHEEL DESIGN STUDIES 5-1
Flywheel Geometries 5-1
Pierced Disc Flywheels 5-2
Rim Flywheels 5-2
Flat Disc Flywheels 5-5
Exponential Disc Flywheels 5-5
Conical Disc Flywheels 5-8
Bar-Type Flywheels 5-8

Section Page

Flywheel Materials 5-10
Computer-Aided Flywheel Screening 5-13
Selection of Hybrid Vehicle Flywheel Designs 5-15
Flywheel Gyrodynamic Considerations 5-17
Flywheel Safety 5-19
  Conservative Design and Inspection 5-20
  Shielding 5-21
Flywheel Accessories 5-21
  Flywheel Housing 5-22
  Flywheel Bearings and Seals 5-23
  Evacuation System 5-25
6 FLYWHEEL DETAIL DESIGN, FABRICATION, AND TESTING 6-1
Detailed Design of Family Car Flywheel 6-1
Fabrication of Family Car Flywheel 6-2
Testing of Family Car Flywheel 6-5
  Nondestructive Tests 6-5
  Tensile Specimen Tests 6-5
  Flywheel No. 1 – Spin Testing 6-5
    Pumping Losses Test 6-5
    Disintegration Test 6-6
  Flywheel No. 2 – Spin Testing 6-8
    Power Density Tests 6-8
    Spindown Tests 6-10
    Acoustic Test 6-10
Detailed Design of City Bus Flywheel 6-15
  Body Taper Design 6-15
  Hub Design 6-17
Fabrication of City Bus Flywheel 6-18
Testing of City Bus Flywheel 6-19
  Fatigue Properties 6-19
  Tensile Specimen Tests 6-19

Section Page

Creep Tests 6-19
No. 1 Glass Flywheel Tests 6-20
  Spindown 6-20
  Disintegration Speed Tests 6-20
No. 2 Glass Flywheel Spin Tests 6-23
7 HYBRID DESIGN CONFIGURATION 7-1
Family Car 7-1
City Bus 7-2
8 CONCLUSIONS AND RECOMMENDATIONS 8-1
9 FUTURE PROGRAM PLANS 9-1
Program 1 – Flywheel/Hybrid Drive System Development 9-2
Program 2 – Integration of a Flywheel/Spark-Ignition Hybrid Drive System into Prototype Passenger Cars 9-3
Program 3 – Integration of a Flywheel/Spark-Ignition Hybrid Drive System into Prototype City Buses 9-3
10 REFERENCES 10-1

Appendixes

A NAPCA VEHICLE DESIGN GOALS – SIX-PASSENGER AUTOMOBILE (REVISION A, NOVEMBER 30, 1970) A-1
B COMPUTER PROGRAM DESCRIPTIONS B-1
C HEAT-ENGINE TREND DATA C-1
D COMPUTER-AIDED STRESS ANALYSIS OF DISC TYPE FLYWHEELS D-1
E ANALYSIS FLYWHEEL/HYBRID FAMILY CAR PERFORMANCE IN DOT HIGH-SPEED PASS MANEUVER E-1

ILLUSTRATIONS

Figure		Page
1-1	Flywheel/Hybrid Drive System	1-5
1-2	Oerlikon Electrogyro Bus	1-7
3-1	DHEW Urban Dynamometer Driving Schedule – Velocity vs. Time and Acceleration vs. Time (Revised November 10, 1970 Federal Register)	3-5
3-2	DHEW Urban Dynamometer Driving Schedule – Acceleration Histogram (Revised November 10, 1970 Federal Register)	3-6
3-3	Family Car Road Power for Various Loaded Weights and Grades	3-7
3-4	Grade Velocity Variance With hp to Road for 4,700-lb Loaded Weight Family Car	3-8
3-5	Grade Velocity Variance With hp to Road for 5,000-lb Loaded Weight Family Car	3-9
3-6	Grade Velocity Variance With hp to Road for 5,300-lb Loaded Weight Family Car	3-10
3-7	Velocity vs. Grade for the Commuter Car	3-13
3-8	Velocity vs. Time for City Bus Driving Schedule	3-16
3-9	Acceleration vs. Time for City Bus Driving Schedule	3-16
3-10	Velocity vs. Grade for City Bus	3-18
3-11	Velocity vs. Time for Delivery/Postal Van Driving Schedule	3-20
3-12	Acceleration vs. Time for Delivery/Postal Van Driving Schedule	3-20
3-13	Velocity vs. Grade for Delivery/Postal Van	3-22
4-1	Control System Block Diagram	4-5
4-2	Basic Transmission Configurations	4-6
4-3	Block Diagrams of Hydrostatic Transmissions	4-8
4-4	Weight vs. Rated Speed for a Hydrostatic Motors and Pumps	4-9
4-5	Efficiency vs. Rated Speed for a Hydrostatic Transmission	4-9
4-6	Electric Transmissions	4-10

Figure		Page
4-7	Torque-Speed Characteristics for Squirrel Cage Induction Motor	4-11
4-8	Weight vs. Rated Torque for Squirrel Cage Induction Motors	4-12
4-9	Volume vs. Rated Torque for Squirrel Cage Induction Motors	4-13
4-10	Cost vs. Rated Torque for Squirrel Cage Induction Motors	4-14
4-11	Efficiency vs. Rated Power for Squirrel Cage Induction Motors	4-15
4-12	Efficiency vs. Speed for Combined Motor Inverter	4-17
4-13	Weight vs. Rated Power for Aircraft Generators	4-18
4-14	Volume vs. Rated Power for Aircraft Generators	4-19
4-15	Efficiency vs. Rated Power for Aircraft Generators	4-20
4-16	Power Splitting Transmission	4-21
4-17	Power Splitting Transmission Configurations	4-21
4-18	Efficiency vs. Speed for a Power Splitting Transmission	4-22
4-19	HC Emissions vs. Continuous Horsepower	4-28
4-20	CO Emissions vs. Continuous Horsepower	4-29
4-21	NO_x Emissions vs. Continuous Horsepower	4-30
4-22	Spark-Ignition Cost vs. Continuous Horsepower	4-32
4-23	Spark-Ignition Specific Fuel Consumption vs. Continuous Horsepower	4-32
4-24	Spark-Ignition Weight vs. Continuous Horsepower	4-32
4-25	Spark-Ignition Volume vs. Continuous Horsepower	4-32
4-26	Diesel Cost vs. Continuous Horsepower	4-35
4-27	Diesel Specific Fuel Consumption vs. Continuous Horsepower	4-35
4-28	Diesel Weight vs. Continuous Horsepower	4-35
4-29	Diesel Volume vs. Continuous Horsepower	4-35
4-30	Gas Turbine Cost vs. Continuous Horsepower	4-37
4-31	Gas Turbine Specific Fuel Consumption vs. Continuous Horsepower	4-37
4-32	Gas Turbine Weight vs. Continuous Horsepower	4-37
4-33	Gas Turbine Volume vs. Continuous Horsepower	4-37
4-34	Steam Engine Cost vs. Continuous Horsepower	4-41
4-35	Steam Engine Specific Fuel Consumption vs. Continuous Horsepower	4-41

Figure		Page
4-36	Steam Engine Weight vs. Continuous Horsepower	4-41
4-37	Steam Engine Volume vs. Continuous Horsepower	4-41
4-38	Comparison of Cost vs. Continuous Horsepower	4-44
4-39	Comparison of Specific Fuel Consumption vs. Continuous Horsepower	4-44
4-40	Comparison of Weight vs. Continuous Horsepower	4-44
4-41	Comparison of Volume vs. Continuous Horsepower	4-44
5-1	Stress Plots for a Pierced Disc Flywheel	5-3
5-2	Stress Plots for a Rim Flywheel	5-4
5-3	Stress Plots for a Flat Disc Flywheel	5-6
5-4	Stress Plots for an Exponential Disc Flywheel	5-7
5-5	Stress Plots for a Conical Disc Flywheel	5-9
5-6	Bar Flywheel Configuration	5-10
5-7	Windage Loss vs. Pressure for 0.5 kw-hr Family Car Flywheel	5-24
6-1	Stress Plots for the Family Car Flywheel	6-3
6-2	Steel Flywheel – 0.5 kw-hr	6-4
6-3	Closeup of Occlusion in Failed Steel Flywheel	6-7
6-4	Failed Steel Flywheel	6-7
6-5	Pit After Disintegration of No. 1 Steel Flywheel	6-8
6-6	Spindown Test, EPA/APCO No. 2 Steel Flywheel	6-11
6-7	No. 2 Steel Flywheel Acoustic Noise Test Calibration	6-12
6-8	No. 2 Steel Flywheel Acoustic Noise Test Background Level	6-12
6-9	No. 2 Steel Flywheel Acoustic Noise Test–22,800 rpm	6-13
6-10	No. 2 Steel Flywheel Acoustic Noise Test–19,500 rpm	6-13
6-11	No. 2 Steel Flywheel Acoustic Noise Test–19,000 rpm	6-14
6-12	No. 2 Steel Flywheel Acoustic Noise Test–18,600 rpm	6-14
6-13	No. 2 Steel Flywheel Acoustic Noise Test–9,800 rpm	6-15
6-14	Bar-Type Flywheel	6-16
6-15	Bar Flywheel Hub Prior to Assembly	6-17
6-16	Grinding the Glass Bar Flywheel	6-18
6-17	Spindown Tests, EPA/APCO No. 1 Glass Flywheel	6-20

Figure		Page
6-18	No. 1 Glass Flywheel After Disintegration	6-22
6-19	No. 1 Glass Flywheel Hub and Bearing Support After Flywheel Disintegration	6-22
6-20	No. 2 Glass Flywheel After Disintegration	6-23
6-21	Major Pieces of No. 2 Glass Flywheel After Disintegration	6-24
7-1	Drivetrain Arrangement for Conventional Engine-Mounted Hydrokinetic Transmission	7-3
7-2	Drivetrain Arrangement for Engine-Mounted Flywheel/Hybrid Transmission	7-3
7-3	Engine-Mounted Flywheel/Hybrid Transmission Layout	7-4
7-4	Drivetrain Arrangement for Transaxle Flywheel/Hybrid Transmission	7-5
7-5	Transaxle Flywheel/Hybrid Transmission Layout	7-6
7-6	Transaxle Flywheel/Hybrid Transmission Configuration	7-7
7-7	Drivetrain Arrangement for Conventional City Bus	7-8
7-8	Drivetrain Arrangement for Flywheel/Hybrid City Bus	7-9
7-9	Layout of Flywheel/Hybrid Transmission for City Bus	7-10

TABLES

Table		Page
1-1	Exhaust Emissions From Eight Pre-1967 Model Cars	1-2
1-2	Exhaust Emissions From Seven Model Year 1970 Cars	1-2
1-3	Comparison of Present Car and Clean Air Act Emissions	1-4
2-1	Vehicle Configuration Selection	2-2
3-1	Vehicle Specifications	3-2
3-2	Accessory Power Requirements for Family Car	3-4
3-3	Accessory Power Requirements for Commuter Car	3-12
3-4	City Bus Cycle	3-15
3-5	American Transit Association Statistics for City Buses	3-15
3-6	Accessory Power Requirements for City Bus	3-17
3-7	Delivery/Postal Van Cycle	3-19
3-8	Accessory Power Requirements for Delivery/Postal Van	3-21
3-9	Required Flywheel Capacities for Flywheel-Only Vehicles	3-24
3-10	Flywheel Sizes and Weights for Flywheel-Only Design	3-25
3-11	Required Flywheel Capacities for Flywheel/Hybrid Vehicles	3-26
4-1	Family Car Transmission Comparison	4-23
4-2	Bus Transmission Comparison	4-23
4-3	Quantity of Engines Investigated	4-26
4-4	Heat-Engine Sizing for Hybrid Vehicles	4-43
4-5	Family Car Engine Selection	4-45
4-6	Family Car Emissions	4-45
4-7	Bus Engine Selection	4-46
4-8	City Bus Emissions	4-46
5-1	Flywheel Shape Factors for Various Geometries	5-2
5-2	Flywheel Materials	5-11
5-3	Hybrid Flywheels	5-16

Tables Page

5-4 Flywheel Gyrodynamic Forces 5-18
6-1 Comparison of Power Loss Calculations 6-6
6-2 Results of Power Density Test, No. 2 Steel Flywheel 6-9
6-3 Ratio, Longitudinal to Transverse Interleaves 6-16
6-4 No. 1 S-Glass Flywheel Test Data 6-21

UNITS CONVENTION

This report employs the foot-pound-second system of units. Where heat-engine or vehicle performance comparisons are involved, power is expressed in horsepower. In order to facilitate comparison with other means of energy storage, however, power density is expressed in watts per pound (w/lb) and energy density in watt-hours per pound (w-hr/lb).

BLANK PAGE

SUMMARY

The purpose of this study is to determine the feasibility of the flywheel as a means of attaining low-emission propulsion systems for urban vehicles. A further objective is the demonstration and performance evaluation of full-scale flywheels for hybrid applications.

RESULTS AND CONCLUSIONS

The flywheel/heat-engine hybrid drive appears to be a technically feasible means of emission reduction for the family car, commuter car, city bus, and delivery/postal van.

A flywheel/hybrid family car using a spark-ignition engine may approach the Clean Air Act emission standards.

A flywheel/hybrid family car using one of several engines of projected 1975 availability might have emissions below the Clean Air Act standards.

A flywheel/hybrid city bus using a presently available spark-ignition engine would have not only substantially less emissions than a conventional city bus, but a lower operating cost as well.

Pure flywheel drives are presently suitable only for limited-range vehicles such as the city bus where recharge could be accomplished at intervals of approximately 10 miles or less.

The spark-ignition engine is the best available heat engine for flywheel/hybrid vehicles at this time, both on the basis of minimum cost and on the basis of minimum emissions.

At the present time, the optimum flywheel is the high-strength steel constant-stress disc. Tests conducted on steel disc flywheels suitable for the family car showed a usable power density in excess of 5,000 w/lb and a usable energy density of 12 w-hr/lb with suitable safety factors. The fiberglass bar-type flywheels sized for a city bus failed prematurely at approximately 75 percent of design speed. Specific energy at burst was about 7 w-hr/lb.

RECOMMENDATIONS

Development and testing of prototype hybrid vehicles is recommended – family cars because of high population; city buses because of concomitant cost advantages.

Recommended prototype development includes the following:

- Further tests on flywheels in the areas of fatigue, failure control, and aerodynamic shrouding
- Transmission studies and design
- Control system design
- Drive system dynamometer testing with emission sampling

Section 1
INTRODUCTION

In our highly competitive automotive industry there apparently have been inadequate incentives for the individual vehicle manufacturer to apply air pollution control technology to automotive vehicles in advance of his competitors. Similarly, there have been insufficient motivations for the individual fuel producer to introduce products with improved pollution characteristics in advance of his competitors.

One factor which may help account for the apparent unconcern of the automotive-related industries to the problems they have helped create is the significant factor of lead time. In order to meet competitive standards of reliability and economy in a mass-produced product such as a car or truck, substantial time is required for the design, testing, and manufacturing of new automotive components. This lead time is a real factor that should be considered in any prediction of the time at which new propulsion systems for automobiles may appear.

State and Federal Government agencies have acted to impose planned programs to reduce vehicle emissions. As a result, during the past decade a series of increasingly tough limitations on vehicle emissions have become public law. Thus far the automotive industry has met these limitations for new vehicles by the incorporation of relatively minor modifications such as positive crankcase ventilation (PCV), spark timing, leaner mixtures, air injection kits, and evaporation control. In general, improvements made to automobiles have followed the "burn fuel better" concept as a means to reduce emissions.

EMISSIONS FROM 1967 AND 1970 MODEL CARS

The results of modifications made to passenger automobiles have been reviewed using emissions data provided by EPA/APCO. A tabulation of exhaust emissions based upon actual test data for eight pre-1967 passenger cars is presented in Table 1-1. A similar tabulation for seven model year 1970 cars is presented in Table 1-2.

Table 1-1

EXHAUST EMISSIONS FROM EIGHT PRE-1967 MODEL CARS

Car No.	Engine Type	Exhaust Emissions (gm/mile)		
		Unburned Hydrocarbons (HC)	Carbon Monoxide (CO)	Nitrogen Oxides (NO_X)
1	V-8	7.64	87.88	1.40
2	V-8	4.40	42.76	2.04
3	V-8	7.08	69.37	3.03
4	6	7.75	63.19	1.91
5	V-8	5.75	62.01	2.32
6	6	5.09	43.07	1.63
7	V-8	17.76	97.38	2.50
8	V-8	10.35	123.03	2.10

Table 1-2

EXHAUST EMISSIONS FROM SEVEN MODEL YEAR 1970 CARS

Car No.	Engine Type	Exhaust Emissions (gm/mile)		
		Unburned Hydrocarbons (HC)	Carbon Monoxide (CO)	Nitrogen Oxides (NO_X)
1	V-8	3.89	27.88	3.17
2	V-8	3.64	25.35	2.71
3	V-8	3.20	35.21	3.04
4	V-8	3.15	32.42	3.10
5	V-8	3.36	57.95	2.85
6	V-8	2.74	42.24	3.61
7	V-8	2.74	37.49	4.09

Both tables present data from recent 1972 Federal Procedure Tests conducted by EPA/APCO. This procedure specifies a cold start, a nonrepetitive driving schedule, and mass emissions determined by the constant-volume sampling technique. True mass emissions are expressed as grams per vehicle mile. Hydrocarbon (HC) masses assume an average carbon-to-hydrogen ratio of 1:1.85. Oxides of nitrogen (NO_X) are expressed as nitrogen dioxide (NO_2).

The data of Tables 1-1 and 1-2 show that HC and CO values were reduced by changes implemented by the automobile manufacturers. However, one of these changes, the use of leaner mixtures, results in substantially higher levels of nitrogen oxides.

The emission levels shown in Table 1-2 are representative of new cars with carburetors adjusted for a lean mixture. Since the use of lean mixtures may incur some driveability penalty, the temptation may exist for owners to adjust carburetors for better performance, thus negating some of the emission control.

CLEAN AIR ACT OF 1970

The recent passage of the Clean Air Act of 1970 has greatly changed the complexion of the automotive air pollution control problem. The emission standards established by this Act are substantially below those being met by present vehicles. This has prompted many comments by automotive manufacturers to the effect that the new standards will be difficult to meet in the prescribed timeframe.

Table 1-3 contrasts the Clean Air Act emission requirements for passenger cars with the average of the previously presented 1970 passenger car levels.

A quick comparison of the 1970 cars with the Clean Air Act emission standards shows that a nearly 8:1 improvement in all three emission types is required. Achievement

Table 1-3

COMPARISON OF PRESENT CAR AND CLEAN AIR ACT EMISSIONS

Item	Exhaust Emission (gm/mile)		
	HC	CO	NO_X
Average of Seven 1970 Cars	3.25	36.9	3.22
Clean-Air Act Requirements	0.46(a)	4.7(a)	(b)

(a) Effective Date Model Year 1975 (may be extended to Model Year 1976)
(b) Undetermined at present

of these goals by just "burning fuel better" even in conjunction with "burning better fuel" (which may be developed by oil companies) appears to be doubtful at this time. Additional approaches being contemplated, such as the use of solid-state electronic carburetion/ignition timing, thermal reactors, and catalytic mufflers, also may be incapable of achieving the goals, particularly over the useful life of the car. In addition, these approaches must be such that the tests of customer acceptance (initial cost, performance, energy cost, and maintenance cost) and allowable depletion of resources (nickel, platinum, and oil) are met.

The conclusion is thus reached that additional improvements well beyond those presently being implemented by automotive manufacturers will be required to meet the Clean Air Act standards.

KINETIC-ENERGY STORAGE AS AN ACCEPTABLE SOLUTION

A third means of reducing automotive emissions (after "burning fuel better" and "burning better fuel") is "burning less fuel." This can be accomplished by lighter-weight/lower-performance vehicles or by recuperation of vehicle kinetic energy during braking operations. The former (now available) offers only a partial solution to the air pollution problem because the fuel consumption is reduced only by about 2:1, while the Clean Air Act of 1970 requires an 8:1 improvement. Further, the small, "sub-compact" car is not acceptable as the sole transportation means for most automobile owners.

The passenger car with a recuperative transmission and an onboard means of storing vehicle kinetic energy in a flywheel offers many improvements in emission characteristics. A basic configuration considered for such a hybrid vehicle drive is shown in the block diagram of Fig. 1-1.

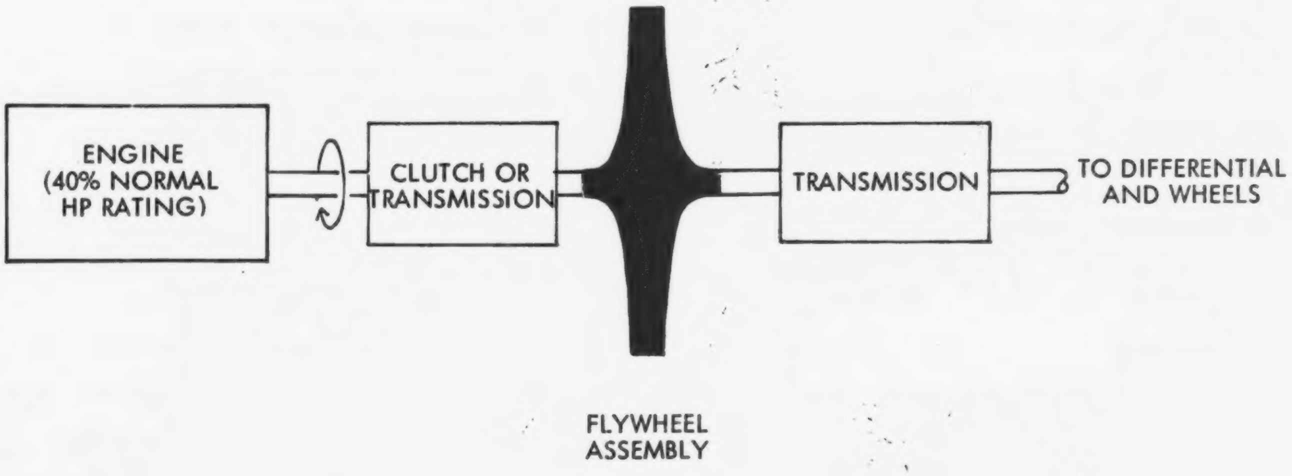

Fig. 1-1 Flywheel/Hybrid Drive System

The first obvious improvement is the conservation of energy resulting in less fuel burned. The availability of a bilateral kinetic-energy storage system in the vehicle with the high power recuperative characteristics (or power density) needed to recover vehicle kinetic energy during braking provides several additional means of reducing emissions. The more important of these improvement potentials brought about by the presence of the flywheel are as follows:

- The flywheel can provide the power required for vehicle acceleration, thereby reducing the required installed engine horsepower to 40 percent of that now used for the desired performance. This leads to the possibilities of either using a smaller engine or modifying the present-size engine for much lower emissions.
- The energy-storage flywheel permits the engine to be operated primarily at a single point on the torque/speed curve (or over a single line of limited range on the torque/speed curve) such that emissions may be reduced.

- No rapid engine accelerations (which presently contribute substantially to vehicle emissions) are necessary with the flywheel available to provide for vehicle acceleration requirements.

In the flywheel/hybrid configuration described, no reduction in vehicle size is required and, similarly, no compromise in vehicle performance from present levels is envisioned. In addition, improvements being made to present types of automotive engines are all applicable to the hybrid vehicle and further improve emission control potentials. Finally, when developments in low-emission Rankine and Brayton cycle engines or modified Diesel engines become available, these may possibly be applied to the flywheel/hybrid for additional air pollution reduction.

PURPOSE OF THE FLYWHEEL FEASIBILITY STUDY

The purpose of the present study is to determine the feasibility of the flywheel as a means of attaining low-emission propulsion systems for urban vehicles. A further objective is the demonstration and performance evaluation of full-sized kinetic-energy flywheels.

This program is a part of the overall plan of the Advanced Automotive Power Systems (AAPS) Program. The goal of AAPS is the demonstration within 5 years of a very low pollution automobile in accordance with the February 10, 1970, Message on Environment by the President. The planning philosophy of the AAPS Program is to investigate various technical approaches to very low pollution automobiles (including gas turbines, steam engines, Diesels, stratified-charge engines, electric hybrids, flywheel hybrids and flywheel-only systems) and to later select from these the most promising candidates, which will then be developed into prototype systems.

The work done on this Flywheel Feasibility Study and Demonstration Program as described in this report along with other flywheel activities being conducted by EPA/APCO will assist EPA/APCO in a preliminary screening to determine the best hybrid approach – electric battery or flywheel.

KINETIC-ENERGY STORAGE VEHICLE BACKGROUND

The use of the flywheel for the operation of urban vehicles is not new. The most recent and commercially significant application to date of flywheel energy storage to land transportation is the Oerlikon Electrogyro (Ref. 1-1).

Twenty years ago, the Oerlikon Engineering Company of Zurich, Switzerland, began operating the Electrogyro, a passenger bus powered solely by a 5.25-ft diam flywheel. Initial success led to the production of these buses and their application in Switzerland, Germany, Belgium, and the Congo. The last Electrogyro went out of revenue service in 1969.

A pictorial representation of the Oerlikon Electrogyro is shown in Fig. 1-2. In operation, three-phase ac power was collected, as shown, from an overhead pole by three collector arms. This power was used to energize a two-pole squirrel cage induction

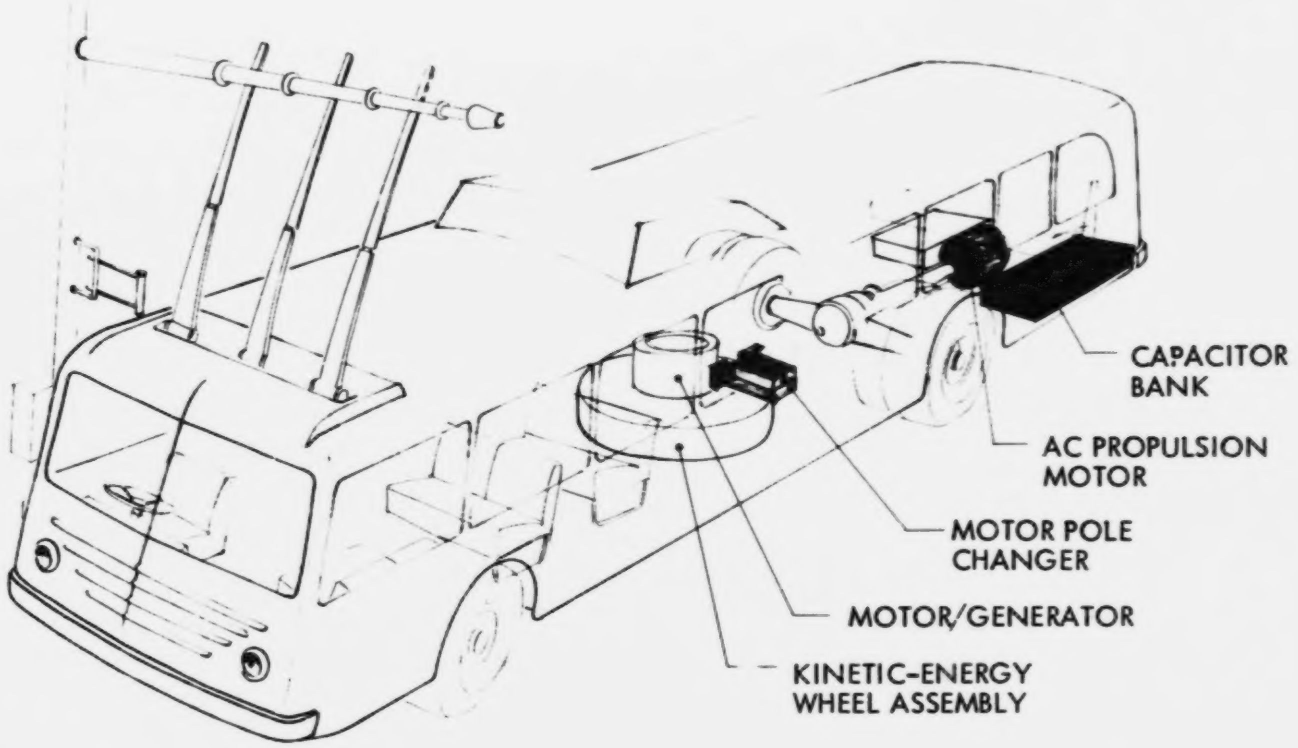
CAPACITOR BANK
AC PROPULSION MOTOR
MOTOR POLE CHANGER
MOTOR/GENERATOR
KINETIC-ENERGY WHEEL ASSEMBLY

Fig. 1-2 Oerlikon Electrogyro Bus

motor which spun the flywheel (operated in 0.7 atmosphere of hydrogen) up to a speed of about 3,000 rpm (synchronous speed for 50-Hz operation). The bus then operated using a pole-changing induction drive motor up to an average distance of three quarters of a mile on power obtained from the kinetic energy stored in the spinning flywheel. The flywheel was then recharged during a 40-sec dwell at the next charging pole. In operating the bus, a considerable degree of skill was required by the operator in that he had to switch drive motor poles at just the right moment, perhaps as many as 12 times for each stop/start sequence.

The background of the Electrogyro and other applications form the basis for the updating of flywheel technology in which advantage can be taken of new materials, electronic controls, improved testing techniques, quality control concepts, and recent developments in seal and bearing technology.

Section 2
APPROACH

The Flywheel Feasibility Study and Demonstration conducted for the Air Pollution Control Office of the Environmental Protection Agency was intended to be an objective assessment of the suitability of flywheel energy storage, either alone or in a heat-engine hybrid configuration, to propulsion systems for low-pollution urban vehicles. The program was structured to evaluate the flywheel as a drive system component for vehicles capable of meeting "real world" operating specifications. These requirements were based on typical existing vehicles with full accessory loads – including air conditioning – and presently available performance in acceleration, maximum speed, and vehicle range. The final results of the program were to show whether the flywheel, using presently available materials and technology, is worthy of continued consideration as an alternative means of propulsion for low-pollution urban vehicles. Demonstrations were based on the design, manufacture, and evaluation of full-scale flywheels.

The approach used in conducting the initial study portions of the program was first to perform applicability studies to find the optimal vehicle/flywheel combinations. These studies established performance requirements for various vehicles and resulted in comparative evaluation of various flywheel system configurations. Next, tradeoff studies were made to evaluate complete drive systems – consisting of flywheels, transmissions, and engines – for the two selected vehicles from the standpoint of comparative emissions, cost, size, weight, and availability. Finally, a series of design studies and tests were performed to evaluate flywheel geometries, materials, failure control, and gyrodynamics.

The applicability study was directed toward four common vehicle types – the city bus, the delivery/postal van, the family car, and the commuter car – in various configurations as shown in Table 2-1. For each of the four vehicle types, the flywheel was

Table 2-1

VEHICLE CONFIGURATION SELECTION

System Configurations	Vehicles			
	City Bus	Delivery/ Postal Van	Family Car	Commuter Car
Flywheel Only	A	F	K	P
Flywheel/Diesel	B	G	L	Q
Flywheel/Rankine Cycle	C	H	M	R
Flywheel/Gas Turbine	D	I	N	S
Flywheel/Spark Ignition	E	J	O	T
	Select One	Select One		

considered both as the sole means of propulsion and as a hybrid system component, e.g., the flywheel in conjunction with the Diesel engine, the Rankine cycle engine, the Brayton cycle (gas-turbine) engine, and the Otto cycle (spark-ignition) engine. In selecting the two optimum configurations for the study, special consideration was given to the city bus. Therefore, one of the five configurations shown in Table 2-1 was selected as an optimum flywheel system applicable to a city bus. In addition, one of the 15 flywheel-only or flywheel/heat-engine hybrid configurations was selected for one of the three smaller urban vehicles.

After selecting the two best applications of the flywheel, a detailed study using a computer-aided methodology was carried on to review the tradeoffs relating to various drive configurations – flywheels, engines, and transmissions – with respect to vehicle performance requirements and emissions resulting from operation over typical operating profiles. In the drive configuration tradeoff studies, the vehicle operating profiles used for both the family car and the commuter car were the DHEW Urban Dynamometer Driving Schedule, as published in the Federal Register of November 10, 1970. This 7.5-mile driving cycle – consisting of 18 stops and starts –

represents a portion of Los Angeles streets and freeways. It represents a realistic city driving profile and was used to quantitatively compare the suitability of various drives used for passenger cars. The city bus drive configurations were evaluated using a cycle based on city bus operations data collected for LMSC by the American Transit Association. The postal van was evaluated for operations over a predicted cycle representative of typical postal pick-up cycles within the city. These drive configuration tradeoff studies resulted in the recommendation of optimum flywheel drives for the two previously selected vehicles on the basis of emission reduction potentials in combination with cost and availability considerations.

In the same timeframe, a series of flywheel design studies were conducted. In these studies, attention was directed toward the various available flywheel geometries, materials, and fabrication techniques. Tests were conducted to evaluate prospective flywheel materials, and consideration was given to system components such as bearings, seals, vacuum systems, housings, and flywheel assembly suspension systems. In addition, the gyrodynamic or precession effects experienced with flywheels were investigated and quantified. The design studies also considered the problems and potential methods of flywheel failure control.

The results of the flywheel design studies were used in the computer-aided design of two flywheel types, one for the city bus and one for the selected smaller vehicle. A large number of plausible flywheel designs provided the opportunity for an objective choice of the two best candidates. The two designs selected then were detailed and used to fabricate two flywheels of each type in full-size configurations representative of typical flywheels which might be applied to future urban vehicles.

A test program was conducted on the four flywheels to verify their energy storage capabilities and power density characteristics during charge and discharge. Spindown losses of the flywheels at various vacuum levels also were measured and acoustical noise levels over operating speed ranges were assessed. Final tests on the two flywheel types included overspeed testing until flywheel failure occurred. The results of these tests then were evaluated and used to determine the suitability of the flywheel as a component for urban vehicle propulsion systems.

On the basis of the results of the applicability studies, drive configuration studies, design studies, and flywheel tests, a series of recommended future program plans have been prepared and are presented. These program plans present a logical sequence of activities for applying the flywheel energy storage principle to future low-emission urban vehicles having the maximum potentials for near-term air pollution control.

Section 3
APPLICABILITY STUDIES

Applicability studies were conducted to determine the most promising configuration (flywheel only or flywheel/hybrid) for the city bus, and to determine the most promising combination of vehicle and configuration for the other three smaller vehicles. First, specifications were developed for each of the vehicles; then, based on concurrent flywheel studies, the flywheel size and volume were determined for each flywheel only and flywheel/hybrid vehicle configuration. Finally, a comparison of flywheel size and weight requirements with allowances, in conjunction with other considerations, led to the selection of vehicles and configurations.

DEVELOPMENT OF VEHICLE SPECIFICATIONS

Specifications for each of the four vehicles under consideration were developed in conjunction with the Air Pollution Control Office. These specifications are summarized in Table 3-1.

FAMILY CAR SPECIFICATIONS

The family car is a difficult candidate in which to effect emission improvements because of the severe cost constraints. Despite this, the family car is the prime candidate for emission reduction because its large population causes the bulk of automotive air pollution. For this reason, the particular type of family car chosen is that which has had the highest market percentage – the full-sized six-passenger family sedan. It is assumed that emission reduction techniques suitable for the family car could readily be applied to the rest of the automotive population.

The performance specifications in this section for the family car are as outlined in the Advanced Automotive Power System Program, "Vehicle Design Goals – Six-Passenger

Table 3-1

VEHICLE SPECIFICATIONS

Item	Family Car	Commuter Car	City Bus	Delivery/Postal Van	Remarks
Stops/Mile	(a)	0.02 to $5^{(b)}$	10	5	Number of stops that vehicle makes per mile necessitated by traffic or commercial constraints
$\overline{V}$ operation (mph)	(a)	4 to $62^{(b)}$	12	20	Length of trip/route divided by time vehicle is on trip/route $\cong \ell_{range}/\Delta t_{range}$
V max (mph)	(a)	70	40	40	Maximum sustained cruise velocity
V grade @ grade (mph @ %)	65 @ 5	33 @ 12	6 @ 20	8 @ 20	Maximum sustained velocity on the specified grade
Grade length (miles)	Continuous	4	0.5	0.5	
$\bar{a}$ max (mph/sec)	4.44 to 60 mph	5	3.2	4	Maximum acceleration achievable [proportional to V (0 to cruise)/Δt (to reach cruise)]
Δt stop (sec)	(a)	60 to $300^{(b)}$	15 to $300^{(b)}$	60 to $300^{(b)}$	Length of time vehicle is stopped (V = 0) while all accessories are operating. Stop necessitated by traffic or commercial considerations (such as loading/unloading passenger from bus) only.
ℓ_{range} (miles)	200	1 to $50^{(b)}$	$18^{(c)}$	60	Length of a trip or duty cycle. Maximum value of one trip if it is given as a variable is the maximum length of a trip/duty cycle possible without supplementing vehicle energy system. Note: For the flywheel-only city bus, ℓ range may be achieved by one duty cycle with "recharge" between duty cycles. The ratio of recharge time to duty cycle time shall not exceed 7 percent.
W_p (lb)	–	–	10,000	2,500	Payload weight for commercial vehicles
Number of Seats	6	2	44	–	Occupant capacity (passengers and driver) for noncommercial vehicles
W_c (lb)	4,300 max	1,400	20,000	4,500	Curb weight
W_ℓ (lb)	5,300 max	1,700	30,000	7,000	Fully loaded total vehicle weight
W_s (lb)	1,600 max	600	6,000	1,700	Weight assignable to all propulsion system components including energy storage, controls, etc.
Vol_s (cu ft)	35	16	175	42	Maximum volume assignable to propulsion system components including energy storage controls, etc.
Δt power (sec)	45	60	180	180	Time from start-up to usable power output
A (sq ft)	$A \cdot C_d = 13$	18	80	42	Frontal cross-sectional area suitable for the calculation of aerodynamic drag
C_d		0.35	0.85	0.85	Drag coefficient
Jerk (mph/sec^2)	(a)	5 max	2 max	4 max	–

(a) Not specified.
(b) The range (a to b) means a continuous variable bounded by a and b. Any calculations made should be dense enough over the range (a to b) to show the effect of the variable.
(c) Limit for flywheel-only vehicles.

NOTES:

1. Any calculations of rolling resistance due to tires should be made on the basis of currently available tires and include the effect of tire width. Decreasing rolling resistance due to tires by assuming a type of tire that has unsafe traction characteristics by virtue of low rolling resistance is not allowed.

2. With respect to the city bus, the average acceleration ($\bar{a}$ max) must not be achieved by any instantaneous accelerations or rate of acceleration that would cause passenger discomfort.

3. Any resulting weight distribution that results in possible handling characteristics significantly different from the normal expected by drivers of the vehicles should be noted specifically.

4. Any decrease in gross vehicle weight achieved, for example in the lighter family car and the commuter car, must not compromise safety considerations.

5. Operation of the vehicle should not be compromised by ambient weather considerations. Ambient weather is defined as -25° to 110° F.

6. Noise aspects of the various components should be considered.

Automobile," (Revision A, November 30, 1970), contained in Appendix A.* These specifications are in general agreement with the performance capability of present-day automobiles with the exception that the maximum cruise velocity for the specification vehicle is in the neighborhood of 80 mph. (Although not specified explicitly, this maximum cruise velocity results from the specified velocity requirement of 65 mph on a 5-percent grade.) Present-day family cars have velocity capabilities considerably in excess of 80 mph; however, this is felt to be not so much a requirement per se, but rather a result of concurrent requirements for good acceleration performance and economy up to about 80 mph.

Accessory power requirements for each of the four vehicles were estimated by LMSC. Accessory power requirements for the family car are given in Table 3-2. Air conditioning and power steering loads are somewhat less than for present-day family cars because the flywheel drive provides a more narrow speed range power takeoff.

In accordance with the requirements stated in "Vehicle Design Goals," emissions for the family car are calculated on the basis of the revised "DHEW Urban Dynamometer Driving Schedule" published in the Federal Register of November 10, 1970. This driving cycle, based on an actual driving experience on Los Angeles roadways, is 7.5 miles long and includes 18 starts and stops. Velocity and acceleration plots of this DHEW cycle are shown in Fig. 3-1. In order to accommodate limitations of the chassis dynamometers used for emission measurement, the measured accelerations were limited to ± 3.3 mph/sec. This clipping is evident in the acceleration plot. An acceleration histogram of the DHEW cycle is shown in Fig. 3-2. Except for the acceleration clipping (and an apparent preference for certain least significant digits in data taking), the histogram follows the expected distribution.

The sensitivity of road power required for the family car to velocity, grade, and vehicle weight is shown in the plots of Fig. 3-3. These same data are also replotted for convenience in Figs. 3-4, 3-5, and 3-6.

---

*Since the completion of this work there has been a further revision (Revision B, February 11, 1971) in which vehicle rolling resistance and air drag are slightly reduced and vehicle speed and weight are increased. The net result is that the applicability of the flywheel is increased somewhat by this latest revision, because of the lower ratio of nonrecoverable losses (rolling resistance and air drag) to recoverable loss (acceleration).

Table 3-2

ACCESSORY POWER REQUIREMENTS FOR FAMILY CAR

Accessories	Power Requirements	
	Watts	hp
Service Lights – High Beam	46.8	
Service Lights – Rear	24.0	
License Plate Lights	18.0	
Windshield Wiper Motor	12.0	
Defroster Fan Motor	24.0	
Heater/Air Conditioning Fan Motor	24.0	
Clock	0.6	
Radio	60.0	
Dash Lights	18.0	
Alternator Status	1.2	
Energy Storage Status	1.2	
Engine Temperature Status	1.2	
Total Electrical Load	231.0	
Alternator Losses (Eff. = 0.85)	40.8	
Alternator Input	271.8	0.4
Power Steering Pump		0.6
Air Conditioning Compressor		4.0
Total Accessory Load		5.0

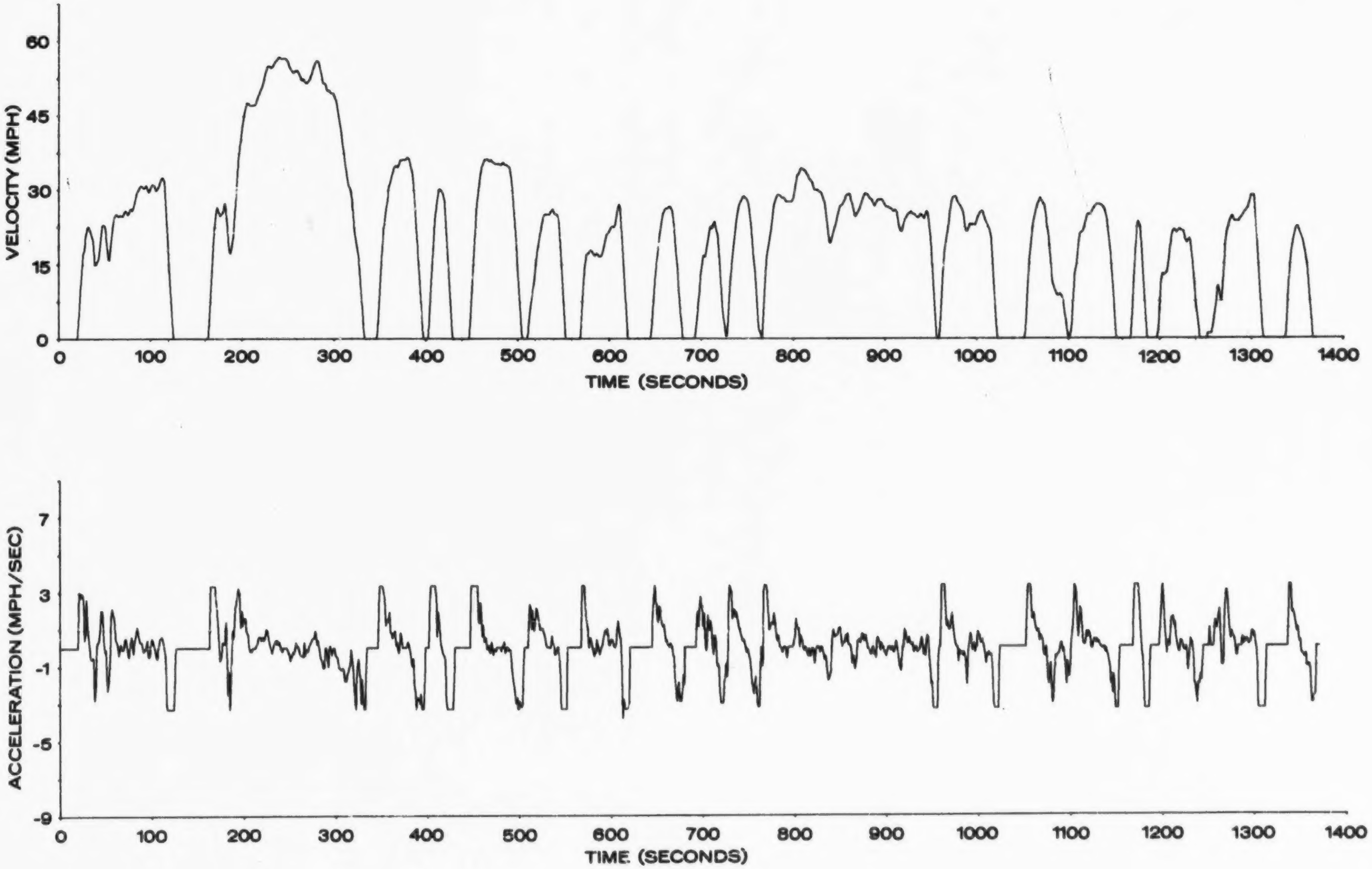

Fig. 3-1 DHEW Urban Dynamometer Driving Schedule – Velocity vs. Time and Acceleration vs. Time (Revised November 10, 1970 Federal Register)

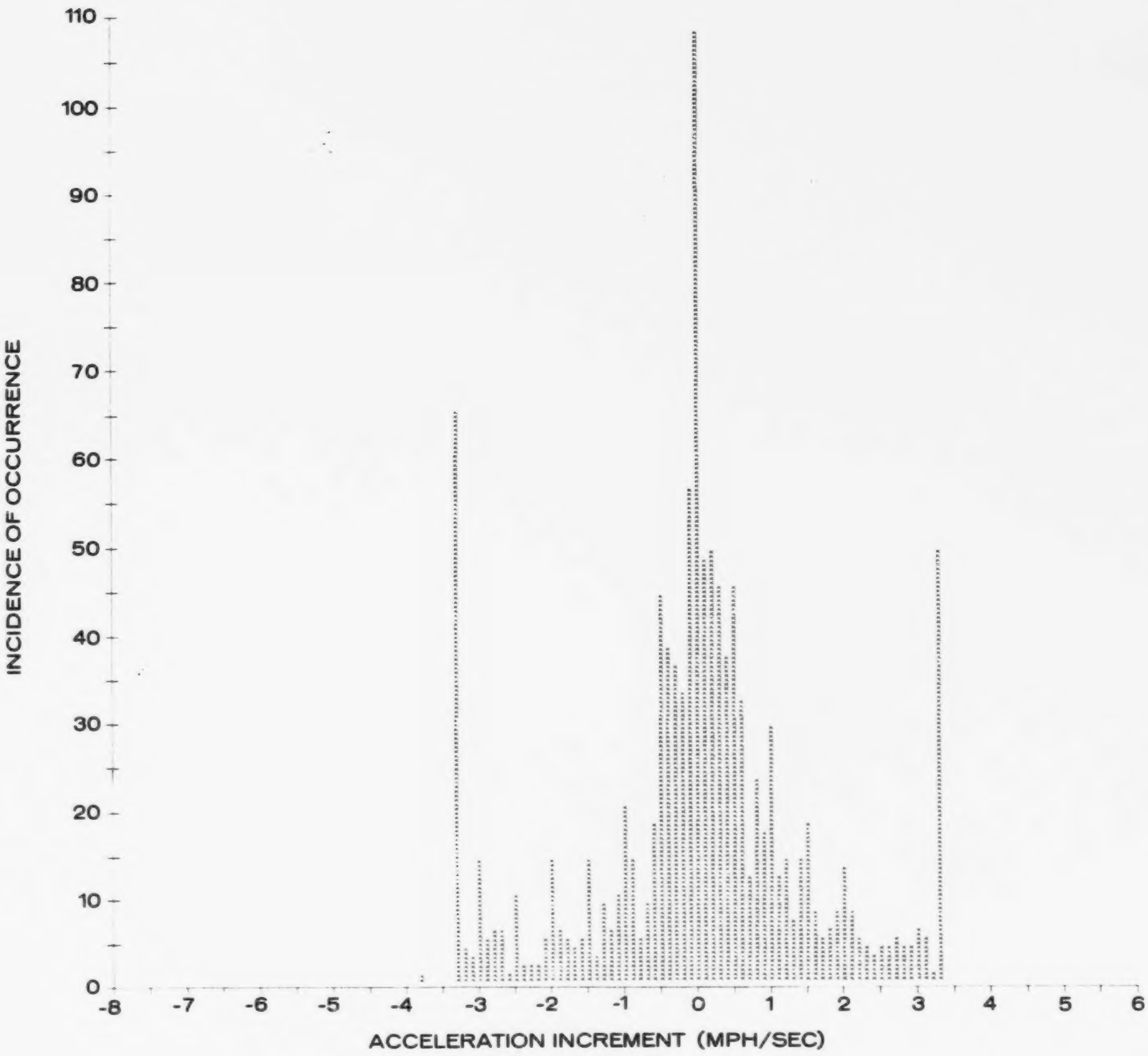

Fig. 3-2 DHEW Urban Dynamometer Driving Schedule – Acceleration Histogram (Revised November 10, 1970 Federal Register)

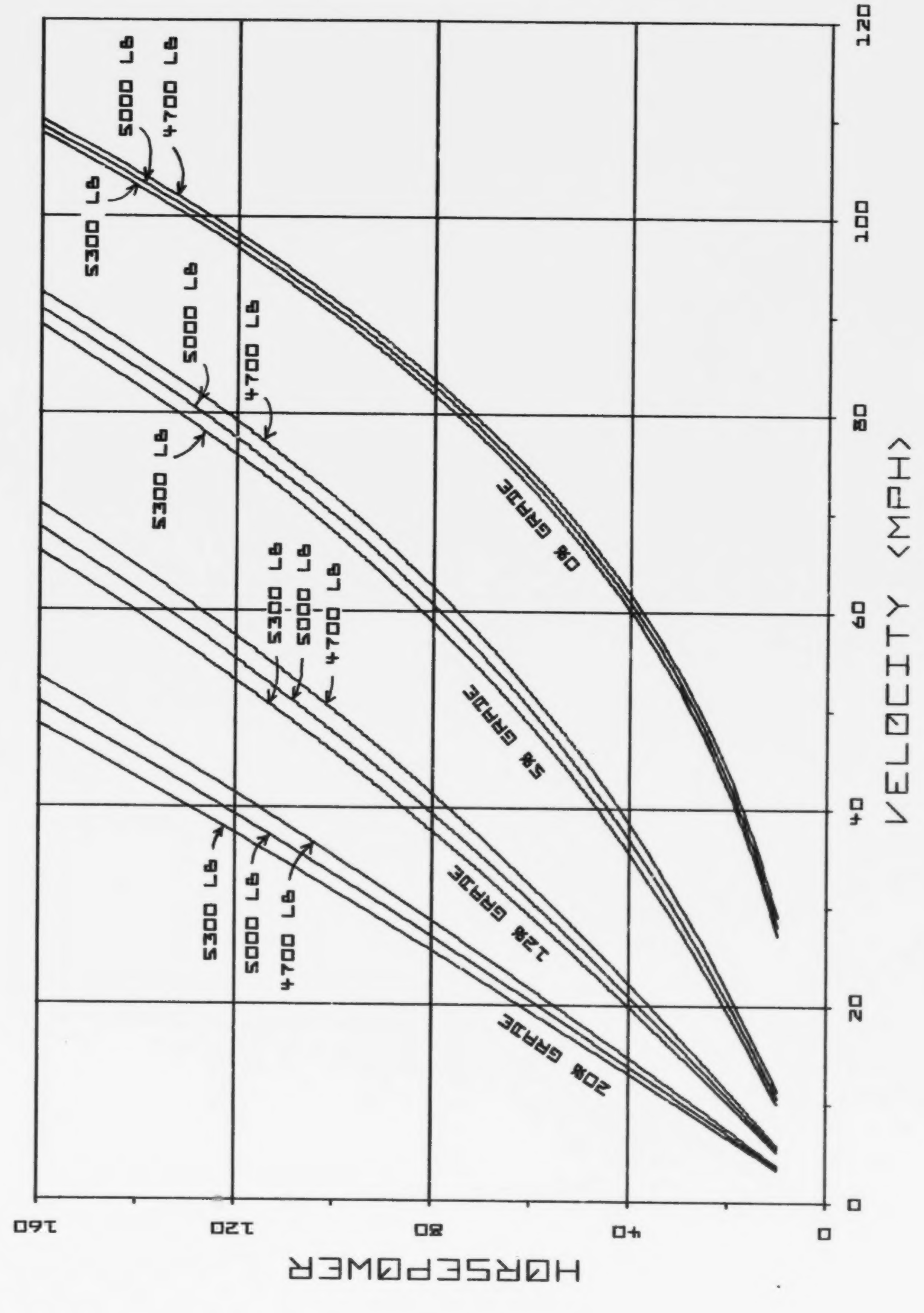

Fig. 3-3 Family Car Road Power for Various Loaded Weights and Grades

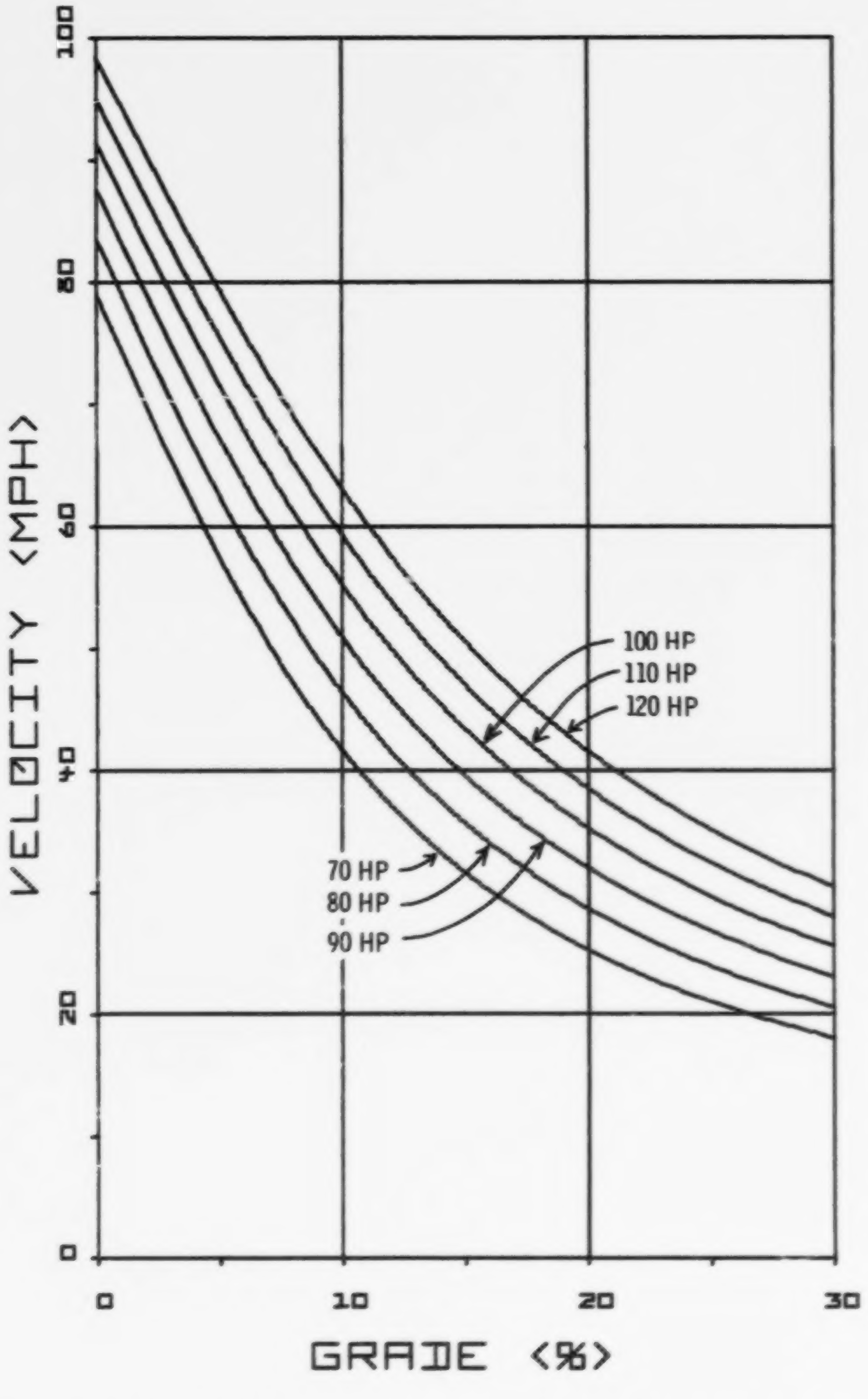

Fig. 3-4 Grade Velocity Variance With hp to Road for 4,700-lb Loaded Weight Family Car

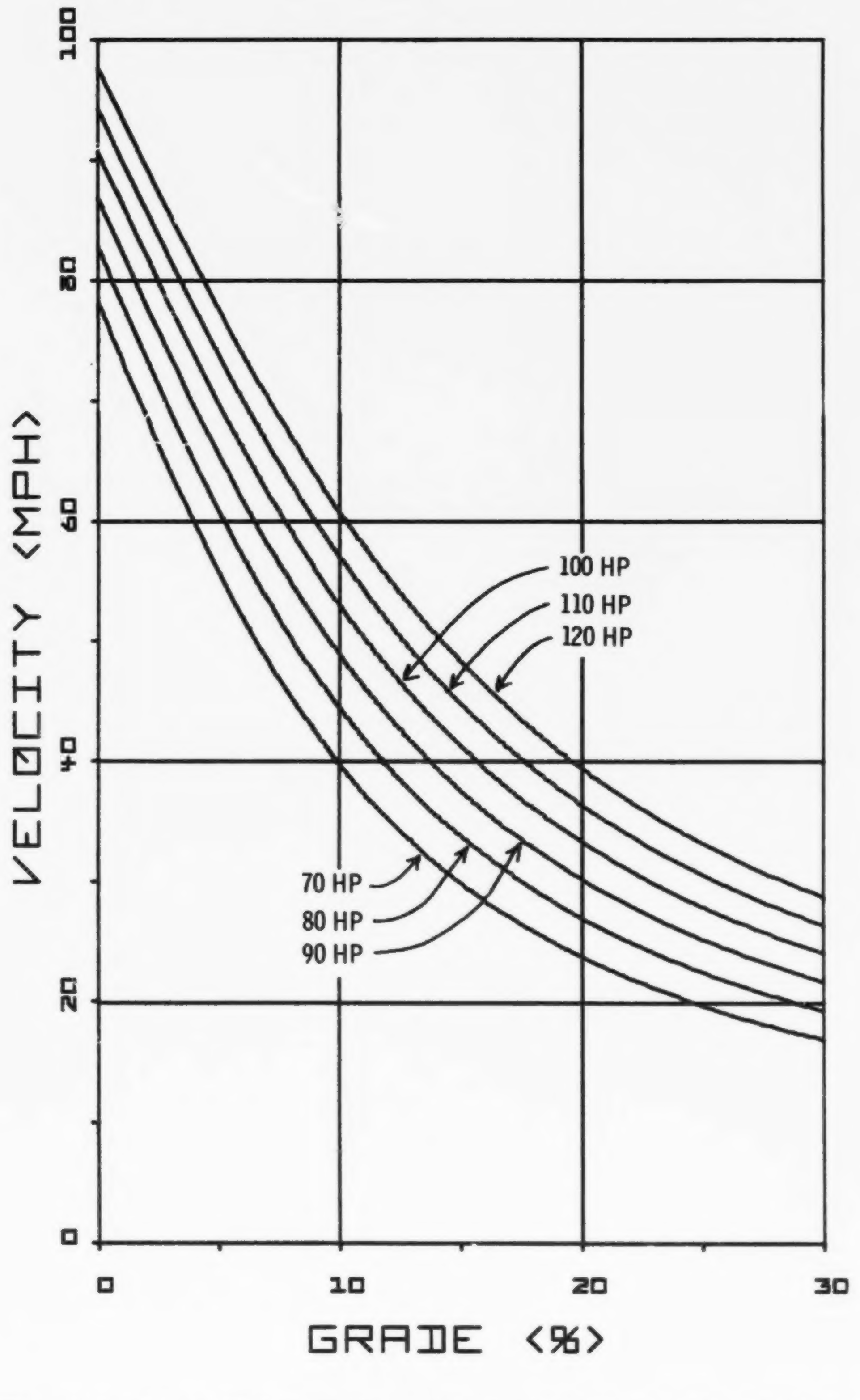

Fig. 3-5 Grade Velocity Variation With hp to Road for 5, 000-lb Loaded Weight Family Car

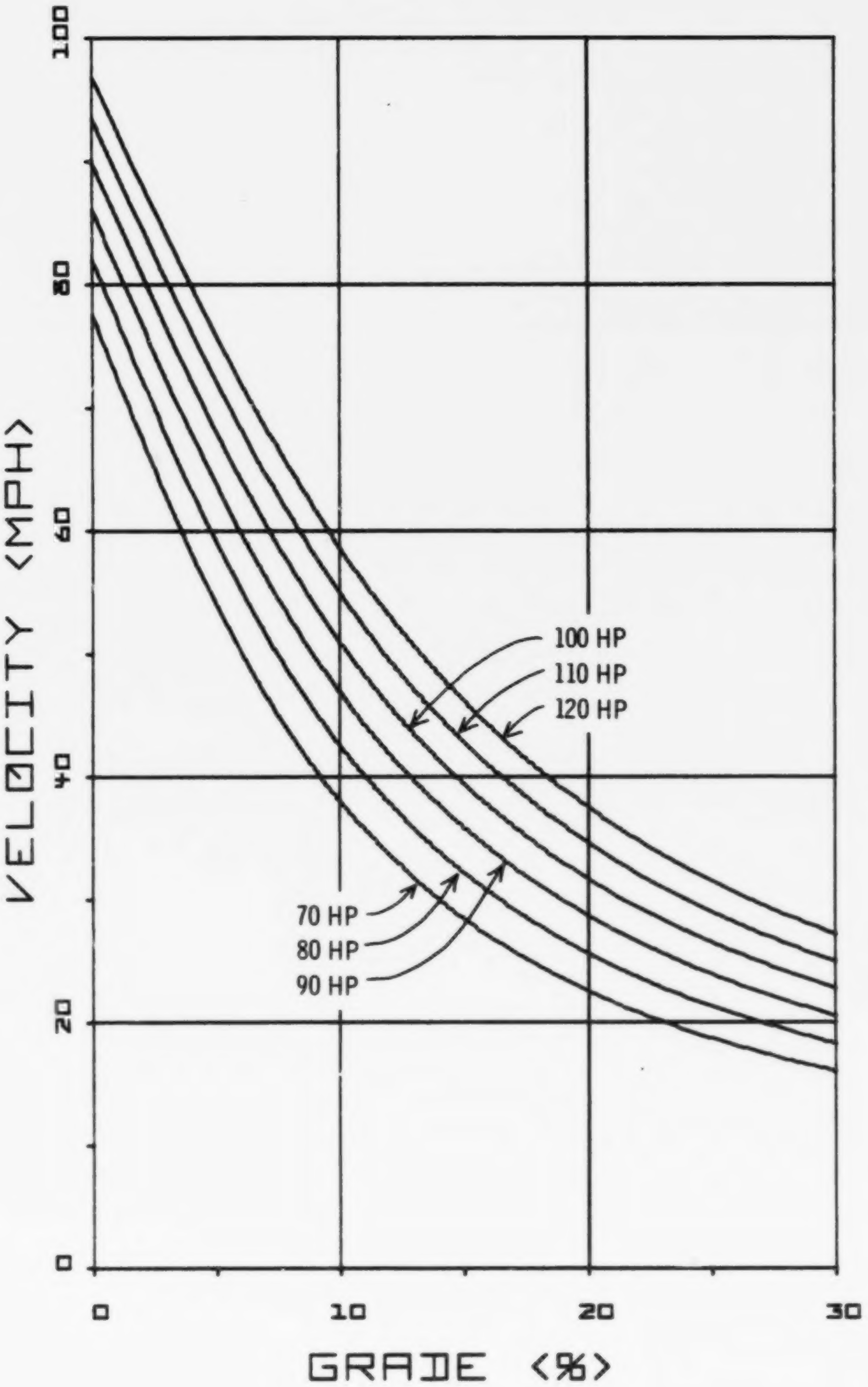

Fig. 3-6 Grade Velocity Variation With hp to Road for 5, 300-lb Loaded Weight Family Car

COMMUTER CAR SPECIFICATIONS

The commuter car, as defined in Table 3-1, is of the same general class as the Austin Mini and Fiat 850. The commuter car, however, seats only two, has a top speed of 70 mph, and a range of only 50 miles. The specification obviously bends to accommodate a low-emission energy storage means, but is intended to represent the minimum that the general public would accept as a commuting automobile.

The availability of nonpolluting commuter cars would probably have little effect on total automotive air pollution during the next decade. Nevertheless, the commuter car could be a suitable first application for a nonpolluting energy storage device which, with further development, might gradually be applied to larger automobiles.

The driving cycle used for emission determination is the same DHEW cycle used for the family car.

Accessory loads for the commuter car are given in Table 3-3, and a plot of velocity vs. grade is shown in Fig. 3-7.

Table 3-3

ACCESSORY POWER REQUIREMENTS FOR COMMUTER CAR

Accessories	Power Requirements	
	Watts	hp
Service Lights – High Beam	46.8	
Service Lights – Rear	24.0	
License Plate Lights	18.0	
Windshield Wiper Motor	12.0	
Defroster Fan Motor	18.0	
Heater/Air Conditioning Fan Motor	18.0	
Clock	0.6	
Radio	60.0	
Dash Lights	18.0	
Alternator Status	1.2	
Energy Storage Status	1.2	
Engine Temperature Status	1.2	
Total Electrical Load	219.0	
Alternator Losses (Eff. = 0.85)	38.6	
Alternator Input	257.6	0.3
Air Conditioning Compressor		3.0
Total Accessory Load		3.3

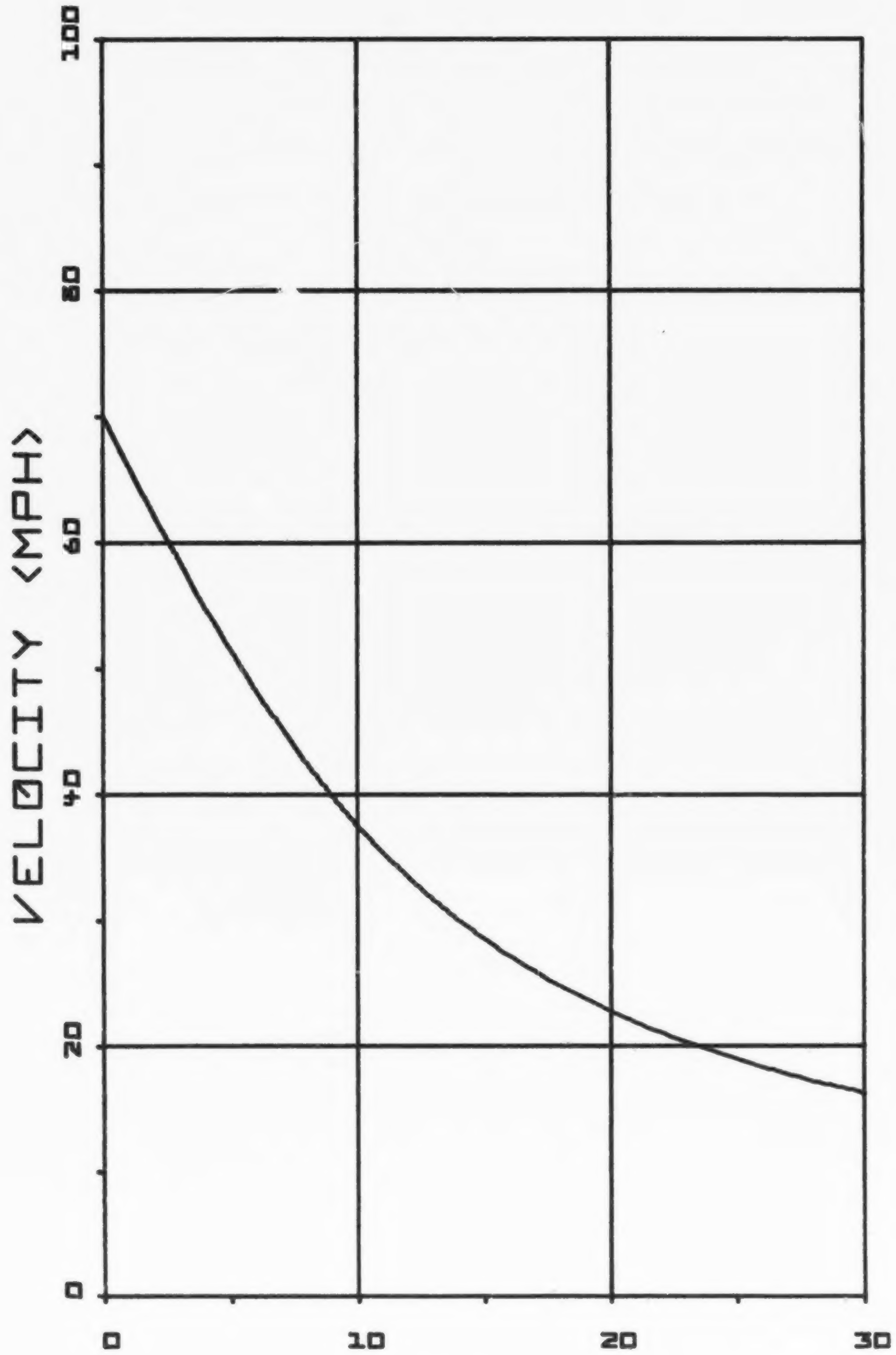

Fig. 3-7 Velocity vs. Grade for the Commuter Car

CITY BUS SPECIFICATIONS

The city bus is an attractive candidate for low-pollution propulsion systems because of the relatively soft constraints in the size, weight, and cost. In addition, the Federal Government has existing means to subsidize low-pollution city buses through capital-improvement grants. However, the need for low operating cost is still critical because this cost is borne by the operator of the bus system. Since the highest single operating cost is for drivers' wages, the performance capability of the bus is very important. (Improved vehicle performance can result in reduced route times which in turn permit a reduction in the number of buses and drivers required to handle peak load conditions.) In addition, the cycle life of any energy storage means must be great enough so that operating cost is not seriously affected.

The city bus performance requirements shown in Table 3-1 are representative of current production vehicles. The driving cycle used as the basis for emission calculations is given in Table 3-4. Velocity and acceleration plots for this schedule are given in Figs. 3-8 and 3-9, respectively. These performance requirements and driving cycle are based in part on data compiled for LMSC by the American Transit Association (Table 3-5).

Accessory loads are shown in Table 3-6. Again a limited speed range power takeoff was assumed for the air conditioner compressor and power steering pump.

A plot of velocity vs. grade for the city bus is shown in Fig. 3-10.

Table 3-4

CITY BUS CYCLE

Velocity Mode (mph)	Time (sec)	Distance (ft)	Acceleration Rate(a) (mph/sec)
0 to 19.2	6.0	99	3.2
19.2	3.0	112	0
19.2 to 25.2	3.0	71	2
25.2	2.0	112	0
25.2 to 0	9.0	132	-2.8
0	13.0	0	
	36	529	
Average Velocity = 10 mph			
Stops = 10/mile			

(a) Accelerations at constant road hp except maximum jerk = 2 mph/sec^2

Table 3-5

AMERICAN TRANSIT ASSOCIATION STATISTICS FOR CITY BUSES

City	Maximum Speed (mph)	Average Speed (mph)	Maximum Route Length (miles)	Median Route Length (miles)	Maximum Grade (percent)	Stops per Mile
Los Angeles	24	12.8	17.3	7	7 to 10	11
New York	–	9.3	12.07	5	13.0	10
San Francisco	–	15.99	12.18	5.79	21.0	9–15

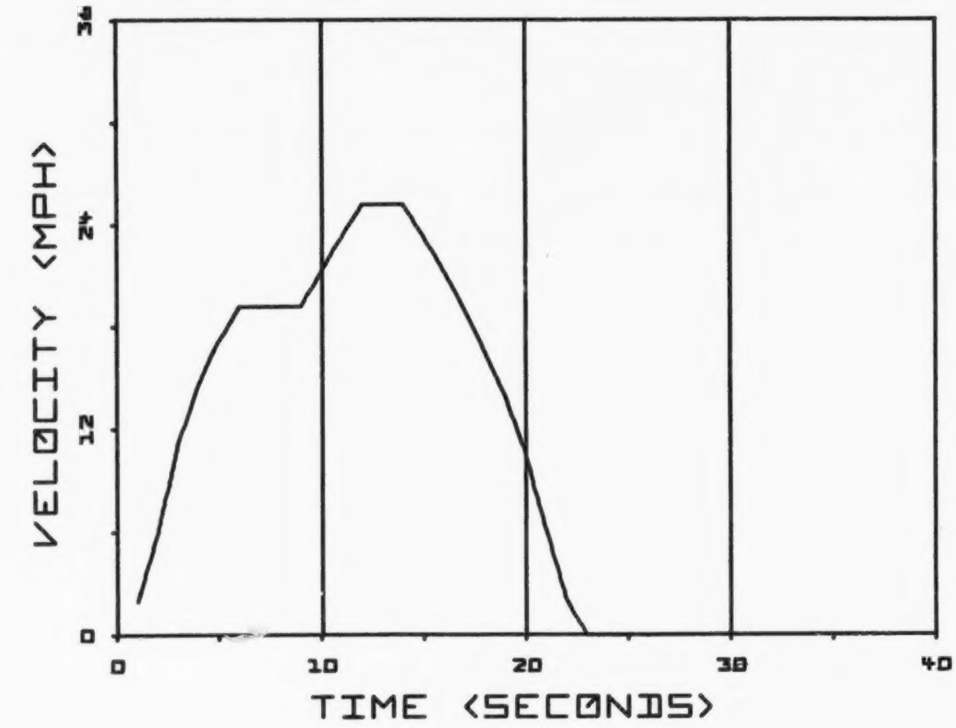

Fig. 3-8 Velocity vs. Time for City Bus Driving Schedule

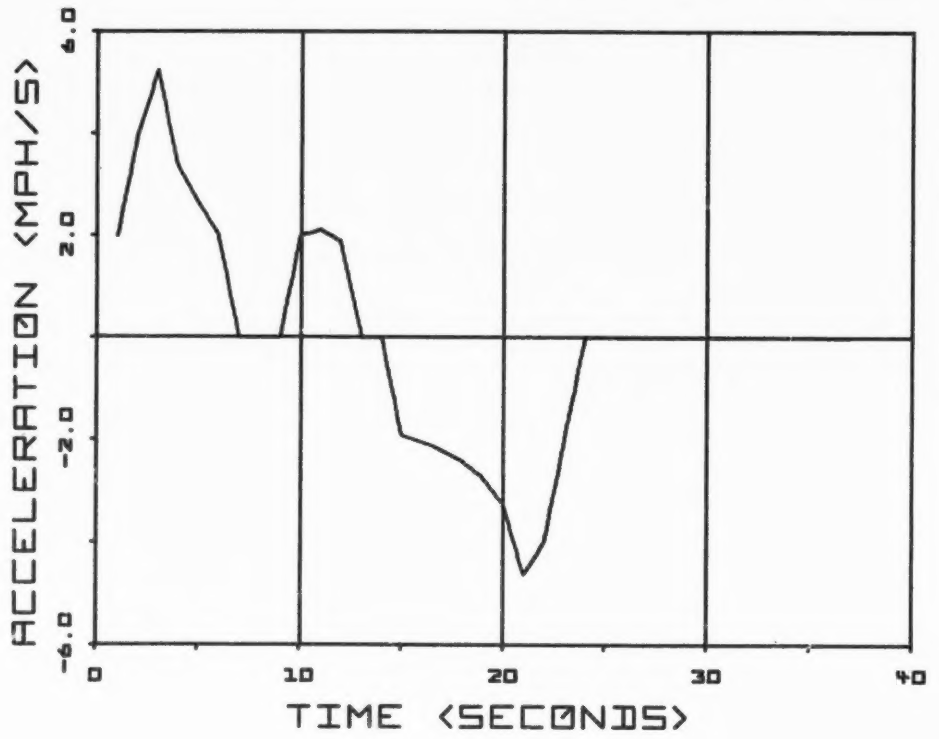

Fig. 3-9 Acceleration vs. Time for City Bus Driving Schedule

Table 3-6

ACCESSORY POWER REQUIREMENTS FOR CITY BUS

Accessories	Power Requirements	
	Watts	hp
Service Lights – Regular Beam	50	
Service Lights – Rear	40	
License Plate Lights	36	
Destination Sign Light	36	
Interior Lights (5 at 40 w)	200	
Identification Lights (2)	20	
Entrance/Exit Lights (2)	Intermittent	
Clearance Lights (4)	40	
Windshield Wiper Motor	24	
Defroster Fan Motor	48	
Clock	0.6	
Dash Lights	36.0	
Alternator Status	1.2	
Energy Storage Status	1.2	
Other Gages	18.0	
Total Electrical Load	551.0	
Alternator Losses (Eff. = 0.9)	61.2	
Alternator Inputs	612.2	0.8
Power Steering Pump		1.5
Air Conditioning Compressor and Fan		18.0
Total Accessory Load		20.3

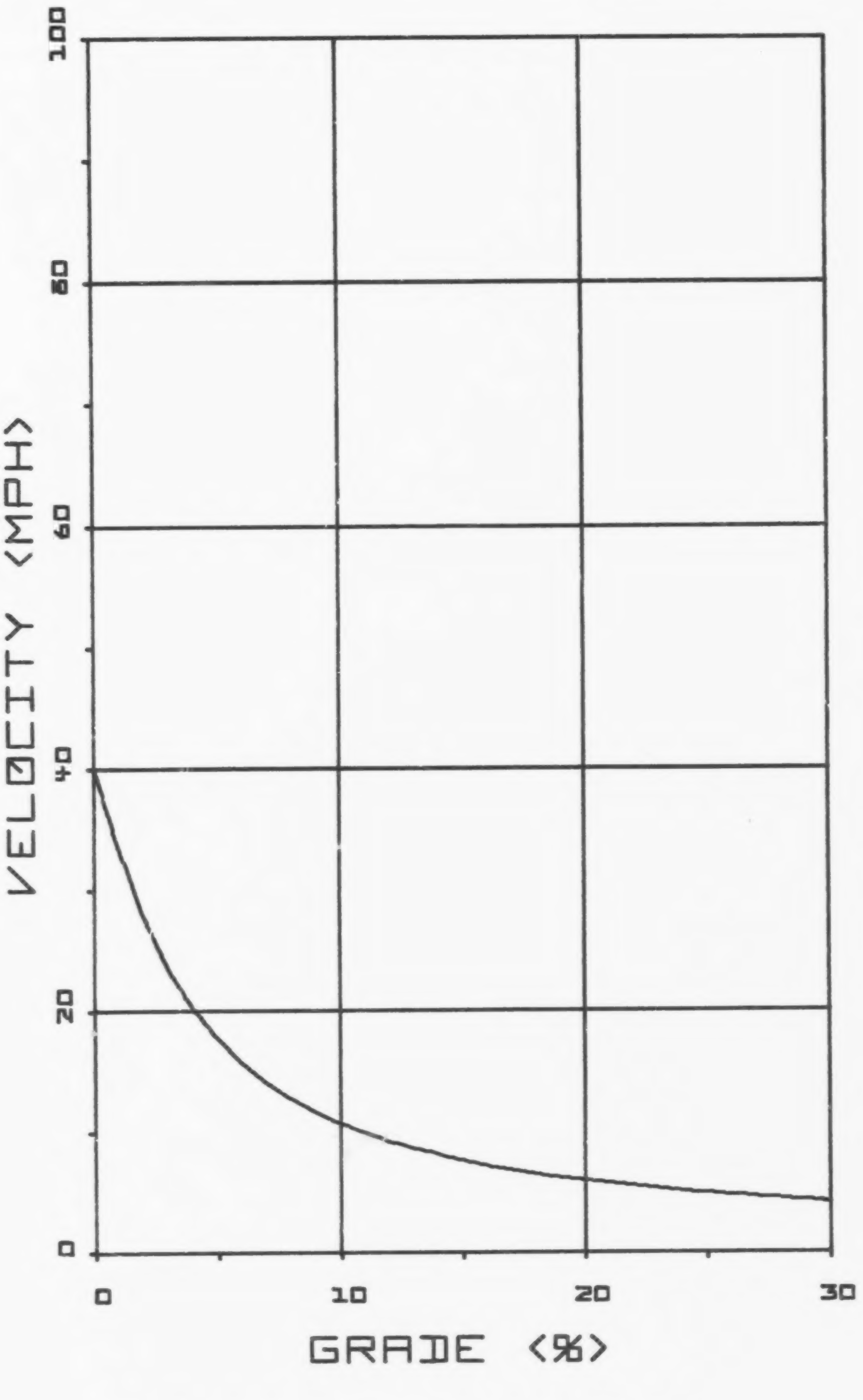

Fig. 3-10 Velocity vs. Grade for City Bus

DELIVERY/POSTAL VAN SPECIFICATIONS

The delivery/postal van, although of small population, could be an attractive first application of a low-pollution propulsion system. As in the case of the city bus, size, weight, and cost constraints for the delivery/postal van are soft, and the purchase of postal vans by the Federal Government could be directed toward low-pollution vehicles. The delivery/postal van specifications are given in Table 3-1; and the driving schedule in Table 3-7. These are representative of current vehicles involved in urban delivery and mail collection. Velocity and acceleration plots for this schedule are given in Figs. 3-11 and 3-12, respectively.

As shown in Table 3-8, the accessory loads are almost negligible.

Figure 3-13 shows a plot of velocity vs. grade for the delivery/postal van.

Table 3-7

DELIVERY/POSTAL VAN CYCLE

Velocity Mode (mph)	Time (sec)	Distance (ft)	Acceleration Rate (mph/sec)
0 to 16	4	73	4.0
16	11	396	–
16 to 32	4	92	4.0
32	9	330	–
32 to 0	8	165	-4.0
0	60	0	–
	96	1,056	
Average Velocity = 7.5 mph			
Stops = 5/mile			

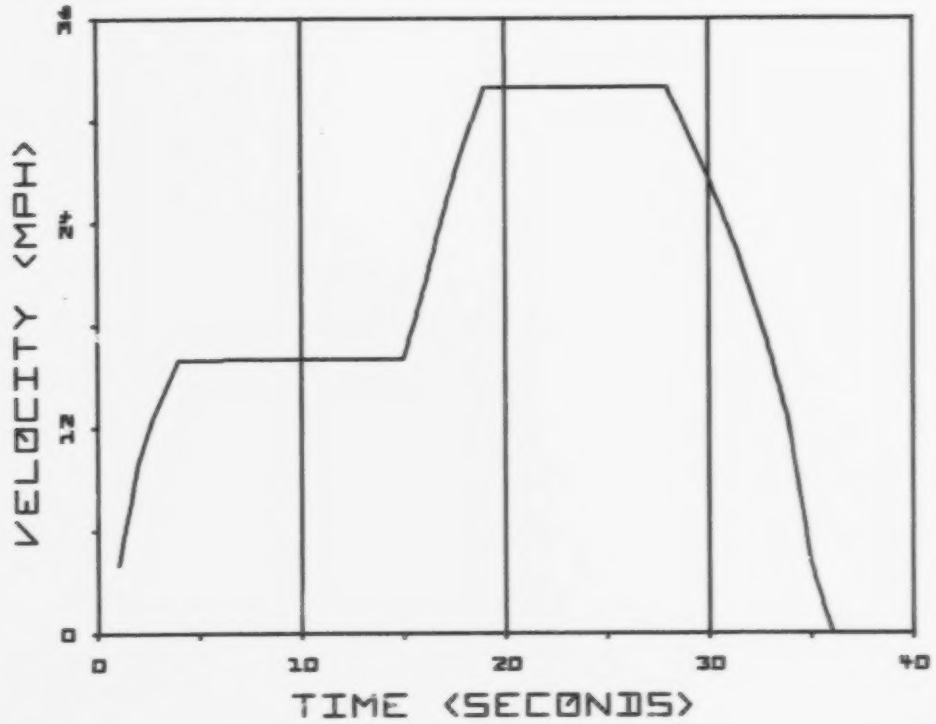

Fig. 3-11 Velocity vs. Time for Deliver/Postal Van Driving Schedule

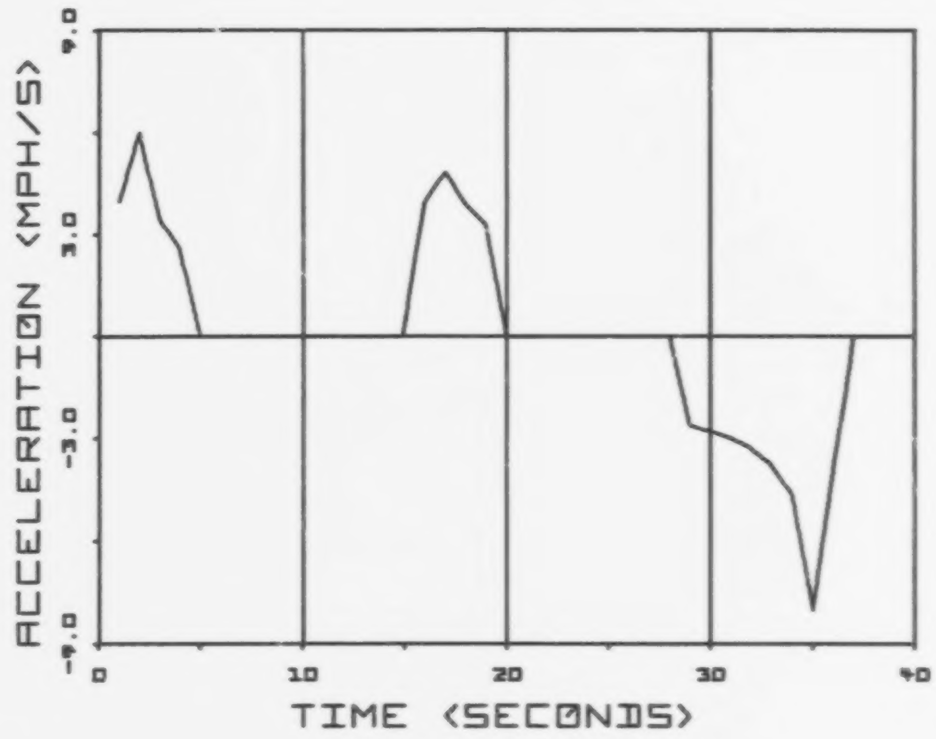

Fig. 3-12 Acceleration vs. Time for Delivery/Postal Van Driving Schedule

Table 3-8

ACCESSORY POWER REQUIREMENTS FOR DELIVERY/POSTAL VAN

Accessories	Power Requirements	
	Watts	hp
Service Lights – High Beam	46.8	
Service Lights – Rear	24.0	
License Plate Lights	18.0	
Windshield Wiper Motor	12.0	
Defroster Heater Fan Motor	24.0	
Clock	0.6	
Dash Lights	18.0	
Alternator Status	1.2	
Energy Storage Status	1.2	
Engine Temperature Status	1.2	
Total Electrical Load	147.0	
Alternator Losses (Eff. = 0.85)	25.9	
Alternator Input	172.9	0.2
Total Accessory Load		0.2

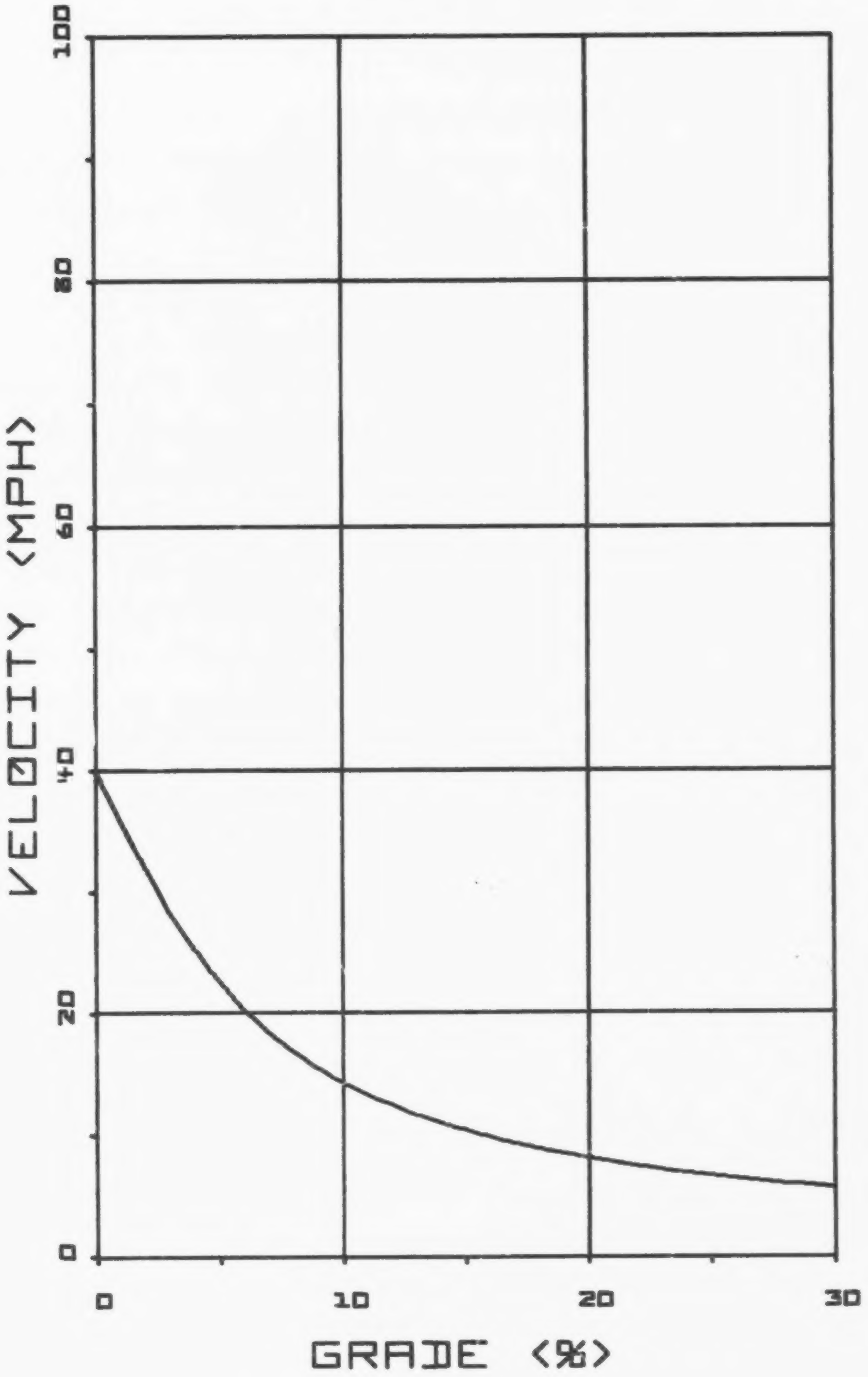

Fig. 3-13 Velocity vs. Grade for Delivery/Postal Van

VEHICLE/CONFIGURATION SELECTION

Preliminary flywheel size and weight estimates were made for both flywheel only and flywheel/hybrid configurations of each of the four vehicles. This was done to eliminate from further consideration those combinations of vehicle and configuration that are not feasible because of excessive flywheel size or weight.

Flywheel design studies (described in Section 5) showed two types of flywheels that appeared attractive – one, a uniform biaxial-stress steel disc; the other, a uniaxial-stress bar (or log) type flywheel of glass filaments. The bar-type flywheel has the higher theoretical energy density (w-hr/lb) but lower energy per unit volume (w-hr/cu ft), so size and weight estimates were made for both types of flywheels.

For flywheel-only vehicles, the required flywheel capacities to meet various parts of the performance specifications are given in Table 3-9. The resulting flywheel sizes and weights are as shown in Table 3-10. For the family car, commuter car, and delivery/postal van, the required flywheel weight exceeds the maximum allowable weight of the entire propulsion system. The bar flywheel for the city bus has a volume greater than that allowed for the total propulsion system. The only remaining possibility, then, is the city bus with a steel disc flywheel. The flywheel weight, however, is over 2/3 the total propulsion system weight. This flywheel weight is excessive, but if the range (between recharging) of the bus were reduced to approximately 10 miles, then the flywheel-only bus would appear to be feasible. Because of the excessive size and weight of flywheels for the flywheel-only vehicles, further consideration was limited to flywheel/hybrid vehicles.

The flywheels for the hybrid vehicles are sized on the basis of vehicle kinetic energy at maximum speed. The rationale for sizing the flywheel in this manner is the "Total Kinetic Energy Control" technique. By means of a linear control loop, heat-engine output is controlled so as to maintain the sum of the vehicle kinetic energy and the flywheel kinetic energy at a fixed value approximately equal to the vehicle kinetic energy at maximum speed. Thus, the flywheel supplies the power required for

Table 3-9

REQUIRED FLYWHEEL CAPACITIES FOR FLYWHEEL-ONLY VEHICLES

Vehicle	Energy Required for Maximum Grade Operation (kw-hr)	Energy Required for Vmax Over Range (kw-hr)	Energy Required for Trip Profile Over Range (kw-hr)
Family Car	–	136[(a)]	114[(a)]
Commuter Car	2.91	17.2	14.1
City Bus	10.0	52.0	97.2
Delivery/Postal Van	1.88	42.5	51.5

(a) 200 miles per NAPCA "Vehicle Design Goals – Six-Passenger Automobile," (see Appendix A).

acceleration, and the heat engine supplies the power necessary to overcome aerodynamic drag, rolling resistance, grade, and associated drivetrain losses. This "Total Kinetic Energy Control" method is discussed more fully in Section 4.

The flywheel energy capacities required for each of the four hybrid vehicles are shown in Table 3-11. These capacities are such that the resulting weights and volumes are only a small fraction of the allowable values for the total propulsion system. Therefore all four hybrid vehicles – using either flywheel type – are feasible with respect to flywheel weight and volume.

Although each of the smaller hybrid vehicles were shown to be potentially feasible, the family car was chosen for further study because it causes the bulk of today's automotive air pollution.

The applicability studies thus resulted in the following choice of vehicles for further study:

- Flywheel/hybrid family car
- Flywheel/hybrid city bus

Table 3-10

FLYWHEEL SIZES AND WEIGHTS FOR FLYWHEEL-ONLY DESIGN

Vehicle Type	Required Flywheel Capacity (kw-hr)	Maximum Allowable Propulsion System Weight(a) (lb)	Maximum Allowable Propulsion System Volume(a) (cu ft)	Constant Stress Maraging Steel Flywheel (23. 6 w-hr/lb, 6. 8 w-hr/cu in.)		Bar Flywheel (S-1014) (25. 1 w-hr/lb, 0. 226 w-hr/cu in.)	
				Weight (lb)	Volume (cu ft)	Weight (lb)	Volume (cu ft)
Family Car	136	1,500	28	5,763	11.57	5,418	348
Commuter Car	17.2	600	16	729	1.46	685	44.0
City Bus	97.2	6,000	175	4,119	8.27	3,873	249
Delivery/ Postal Van	51.5	1,700	42	2,182	4.38	2,052	132

(a) Propulsion system includes flywheel, transmission, clutches, driveshaft, differential, axle, and controls.

Table 3-11

REQUIRED FLYWHEEL CAPACITIES FOR FLYWHEEL/HYBRID VEHICLES

Vehicle	Required Flywheel Capacity (w-hr)
Family Car	372
Commuter Car	115
City Bus	665
Delivery/Postal Van	155

Section 4
CONFIGURATION TRADEOFFS

As a result of the applicability studies (Section 3), the flywheel/hybrid family car and the flywheel/hybrid city bus were selected for further study. Configuration tradeoffs therefore were directed toward selecting the best transmission type and the best heat-engine type for each of these two vehicles.

TRANSMISSION SELECTION

The function of a transmission for a flywheel/hybrid vehicle is to couple together the heat engine, the flywheel, and the vehicle such that emissions from the heat engine are reduced with minimum sacrifice in overall vehicle performance. To achieve this, acceleration loads are handled by a reversible exchange of kinetic energy between the vehicle and the flywheel, while cruise power is supplied by the heat engine.

TRANSMISSION REQUIREMENTS

Ratios. Torque provided by the flywheel is proportional to the rate of change of flywheel speed; thus, infinitely variable (stepless) ratios are required in the flywheel-vehicle path in order to produce reasonably smooth torque and preclude excessive shifting losses. Similarly, the transmission speed ratio must not wander or oscillate because this would cause objectional variations in vehicle acceleration and possible operational instability.

Ratio Range. To provide reasonably good efficiency, the vehicle must operate over a fairly wide speed range without intentional dissipation (clutch slipping). Thus, a vehicle speed range (without dissipation) of 10:1 was assumed. Since the flywheel slows as the vehicle accelerates, the overall ratio range required is approximately 10 times the flywheel speed range.

The selection of flywheel speed range is a tradeoff between required flywheel size and required transmission size. The portion of the flywheel energy that is available is given by

$$W_A/W_T = 1 - R^{-2}$$

where

W_A/W_T = ratio of available flywheel energy to total flywheel energy*
R = flywheel speed range

Increasing the flywheel speed range increases the transmission speed range that is required, and therefore may increase transmission size; but it also reduces the flywheel size that is required.

Recuperation. The exchange of kinetic energy between the flywheel and the vehicle must be reversible. When the vehicle is moving forward, the flywheel must deliver power to the vehicle during acceleration and recuperate power from the vehicle during braking. When the vehicle is reversing, flywheel power may be desirable but is not essential, and recuperation during braking in reverse is of little value.

Efficiency. In order to effect maximum heat-engine emission reduction, the transmission must be efficient over a wide range of vehicle speeds. Efficiency is especially critical in the flywheel-vehicle path because in urban driving high rates of acceleration and repetitive recuperation can cause the average power to and from the road to be several times the average engine power. Thus, a given percentage loss in flywheel-vehicle path could be reflected as a much larger percentage increase in engine brake specific fuel consumption and resulting emissions.

Compatibility With Current Practice. The flywheel transmission must be compatible with current automotive practice if it is to go into production in the next 5 or 10 years. The usual design constraints of size, weight, and component availability are largely inflexible in this time span. Transmission noise should not be worse than with current vehicles and driver feel should not be adversely affected. Maintenance and repair must be capable of being accomplished using presently available facilities with a minimum of personnel training.

---

*Flywheel weight does not vary inversely with this expression since allowable working stress is affected by stress range for the same cycle life.

TRANSMISSION CONTROLS

One of the first items for consideration in the transmission studies was the determination of flywheel speed as a function of vehicle speed. The simplest approach might be to control the heat engine in an on-off (full throttle on – declutched off) mode so as to drive the flywheel up to approximately its half-energy speed, reserving the remainder of the flywheel capacity for recuperative braking. This control mode, however, has two drawbacks: first, the flywheel size is double that required for vehicle acceleration from 0 to maximum speed; second, the flywheel energy and therefore the performance capability of the vehicle is history dependent. For example, a vehicle cruising for some time just below maximum sustained cruise speed would have a flywheel charged to one half total capacity. This would permit a rapid pass maneuver at speeds well above the maximum sustained cruise speed. Immediately following such a maneuver, however, the flywheel energy might be completely exhausted. Then if an identical maneuver is attempted, the vehicle will "bog down" with its speed limited to maximum sustained cruise speed. In fact, the loss of available power could occur in mid-maneuver. The dangers inherent in such vehicle behavior are readily apparent.*

After considering several other control techniques, a control method was devised which can be used to minimize history dependence of vehicle performance and which obviates flywheel oversizing for recuperation capacity. This approach is the Total Kinetic Energy (TKE) control concept.

TOTAL KINETIC ENERGY CONTROL

The basic idea of the TKE approach is to control the heat-engine output so as to hold at a constant value the sum of the kinetic energies of the flywheel and the vehicle. The speed of the vehicle is squared and scaled to give the vehicle kinetic energy. Likewise, the flywheel speed is squared and scaled to yield the flywheel kinetic energy. These two kinetic energy values are added to give the total kinetic energy of the flywheel-vehicle combination. From this TKE value is subtracted a predetermined quantity, essentially equal to the kinetic energy of the fully loaded vehicle at maximum cruise velocity. The resulting error signal is then used as a feedback signal to control the heat-engine output so as to minimize the error signal and thereby hold the TKE fixed.

---

*An analysis of flywheel/hybrid family car performance in the DOT High-Speed Pass Maneuver is given in Appendix E.

The net result of this TKE control approach is that the flywheel provides power for vehicle acceleration (and stores power during vehicle deceleration) while the heat engine supplies only cruise power and accessory power. The cruise power includes losses due to rolling resistance, aerodynamic drag, grade, and associated transmission and flywheel losses. It should be noted that neglecting transmission losses, a sudden and sustained acceleration of the vehicle does not affect the TKE if the heat engine continuously supplies cruise power.

In order to minimize emissions as fully as possible, this basic TKE approach may be modified somewhat. For instance, it may be desirable to allow an excess of TKE during regenerative braking on downhill runs in order to convert the potential energy of the vehicle into flywheel kinetic energy. In no case, of course, would it be permissible to allow the flywheel to overspeed.

Because of the necessary lag in heat-engine response to a control error signal, the driver hears a slow build-up in engine noise sometime after making a sudden acceleration. This inherently disconcerting affect can be eliminated by means of the compensated feedback control system as shown in Fig. 4-1. The Power Control separates the accelerator pedal power command signal into an acceleration power signal and a cruise power signal. The cruise power is estimated as a direct function of vehicle speed, and this cruise power signal is subtracted from the commanded power to give the acceleration power signal. The cruise power signal adjusts the speed of the heat engine. The heat engine throttle is preprogrammed on the basis of engine speed for minimum emissions. The Gear Ratio Control divides the acceleration power by vehicle speed to give a torque command which in turn is integrated to give a gear ratio command to the vehicle transmission. The TKE (vehicle plus flywheel) tends to drift due to cruise power estimation error and grade power, so a separate loop is used to calculate the TKE and compare it to a preset reference. The resultant error signal is used to linearly override the power signal to the heat engine so that the TKE is maintained constant. This control scheme results in a vehicle feel for the driver which is very close to that of a conventional family car except that engine noise is only slightly affected by acceleration.

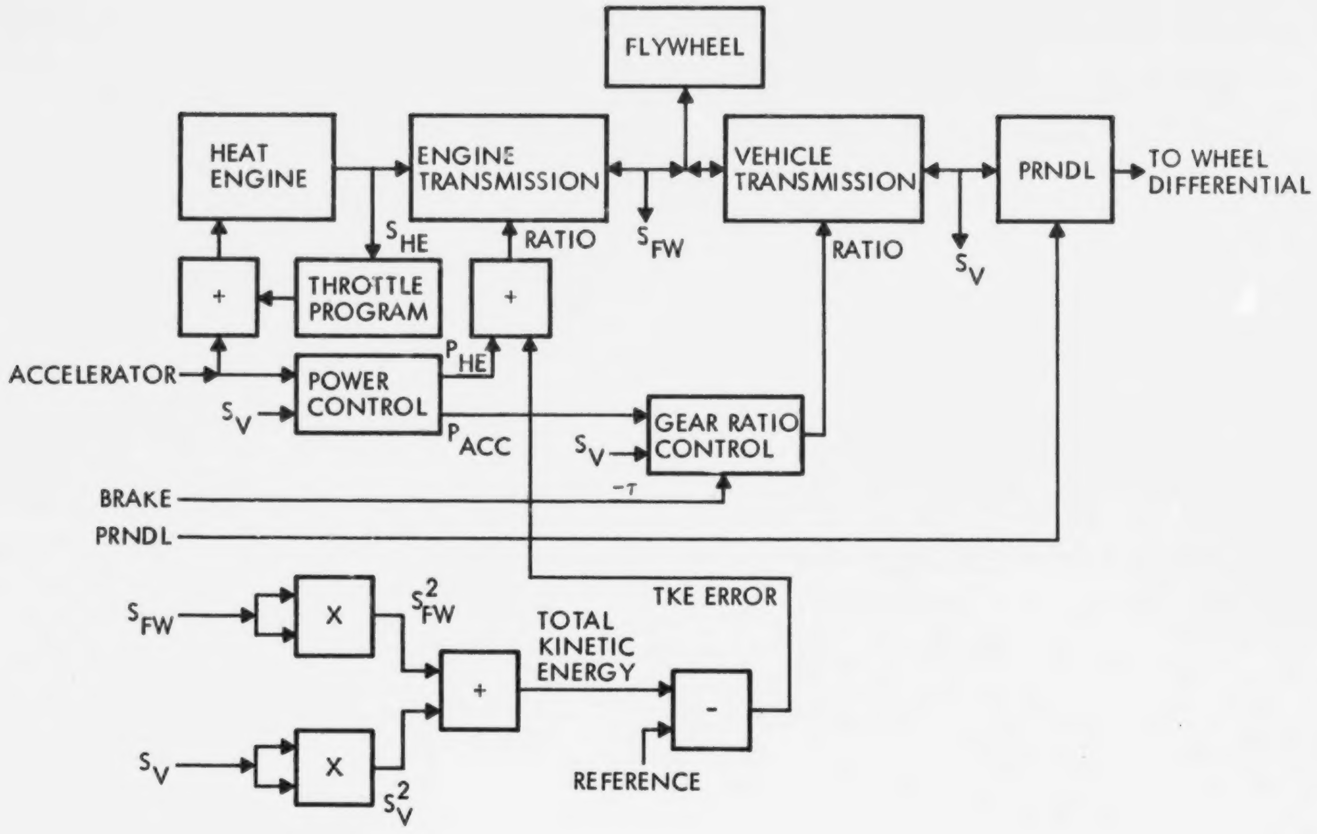
FLYWHEEL
HEAT ENGINE
ENGINE TRANSMISSION
VEHICLE TRANSMISSION
PRNDL
TO WHEEL DIFFERENTIAL
S_{HE}
RATIO
S_{FW}
RATIO
S_V
+
THROTTLE PROGRAM
+
ACCELERATOR
P_{HE}
POWER CONTROL
S_V
P_{ACC}
S_V
GEAR RATIO CONTROL
BRAKE
-T
PRNDL
S_{FW}
X
S_{FW}^2
TKE ERROR
TOTAL KINETIC ENERGY
+
-
S_V
X
S_V^2
REFERENCE

Fig. 4-1 Control System Block Diagram

The final form of the transmission controls is dependent upon required future testing both of emissions and vehicle "feel" in various control modes. Since testing of prototype vehicles in various control modes is necessary, the use of all-electronic controls for prototype vehicle propulsion systems is strongly recommended. Production control systems may or may not be all-electronic because of cost.

TRANSMISSION CONFIGURATIONS

The two basic transmission configurations that were considered are shown in Fig. 4-2. The double transmission, as the name implies, is really two transmissions: a wide-range transmission between the flywheel and the vehicle, and a narrow-range transmission between the flywheel and the engine. The single transmission is a wide-range transmission linking the vehicle with the flywheel and/or engine, where the flywheel and heat engine may be clutched in and out independently.

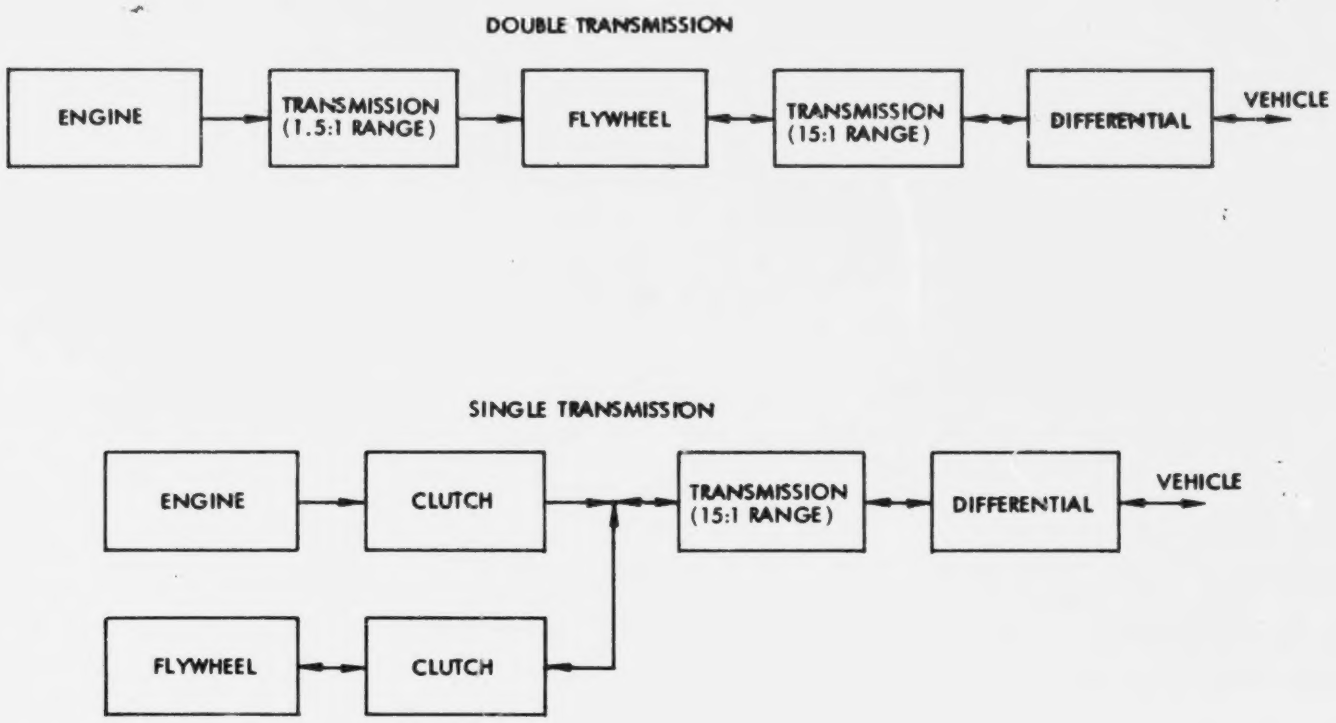
DOUBLE TRANSMISSION
ENGINE
TRANSMISSION (1.5:1 RANGE)
FLYWHEEL
TRANSMISSION (15:1 RANGE)
DIFFERENTIAL
VEHICLE
SINGLE TRANSMISSION
ENGINE
CLUTCH
TRANSMISSION (15:1 RANGE)
DIFFERENTIAL
VEHICLE
FLYWHEEL
CLUTCH

Fig. 4-2 Basic Transmission Configurations

The double transmission offers complete control flexibility since the heat-engine speed may be controlled independent of either flywheel speed or vehicle speed. Cruise efficiency, however, tends to be degraded by having two transmissions in the engine-vehicle path.

The single transmission has better cruise efficiency by virtue of having only one transmission in the engine-vehicle path, but heat-engine speed is tied directly to flywheel speed. Since the flywheel must slow down as the vehicle speeds up, so must the heat engine slow down as the vehicle speeds up. This means that maximum engine speed occurs at vehicle standstill, while at maximum vehicle speed the heat engine is at two thirds of its maximum speed (still assuming a 1.5:1 flywheel speed range). These speed relationships mean that the heat engine is being used in an awkward fashion.

In addition, driver "feel" is upset because of engine sound. The single transmission, however, is lighter, smaller, and less expensive than the double transmission.

For prototype vehicles it is recommended that a double transmission be employed so that all control modes of interest may be investigated. The single transmission would be simulated by "locking-up" the engine/flywheel transmission.

Both single and double configurations were given continued consideration in the configuration tradeoffs.

TRANSMISSION TYPES

Initially, four types of transmissions were to be given consideration – mechanical, hydrostatic, hydrokinetic, and electric. Each type was evaluated in terms of its applicability to the flywheel/vehicle transmission. This transmission constitutes the major technical challenge since it involves providing a bilateral power flow between two large inertias. The engine/flywheel transmission represents no significant technical challenge. Purely mechanical gear transmissions are not suitable because they cannot provide the stepless changes in gear ratio required for reasonably smooth and efficient operation. Hydrokinetic transmissions are not applicable for the overall transmission because their output torque is controlled by the input/output speed ratio.

Hydrostatic Transmissions. The hydrostatic transmission consists of a hydraulic pump connected hydraulically to a hydraulic motor. Variable control can be obtained either by means of bypass valving or by a variable stroke in one or both units. Because of the need for high efficiency, only the variable stroke types were considered.

Block diagrams of double and single configurations of hydrostatic transmissions are shown in Fig. 4-3. For both configurations, the hydrostatic units would be integrated into a single transmission assembly. The single transmission would be rather conventional, but the double transmission would be special because of the integration of an additional pump.

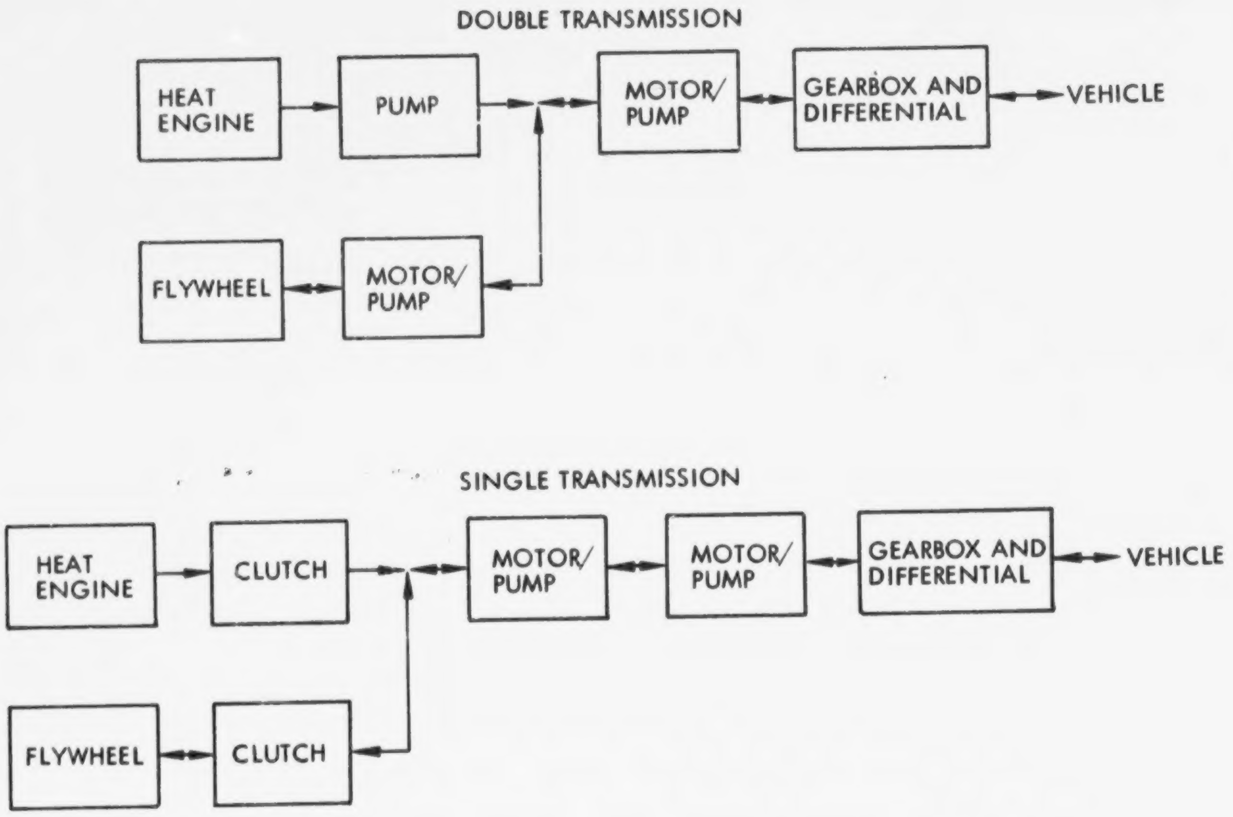
DOUBLE TRANSMISSION
HEAT ENGINE
PUMP
MOTOR/ PUMP
GEARBOX AND DIFFERENTIAL
VEHICLE
FLYWHEEL
MOTOR/ PUMP
SINGLE TRANSMISSION
HEAT ENGINE
CLUTCH
MOTOR/ PUMP
MOTOR/ PUMP
GEARBOX AND DIFFERENTIAL
VEHICLE
FLYWHEEL
CLUTCH

Fig. 4-3 Block Diagrams of Hydrostatic Transmissions

Conventional industrial-type hydrostatic transmissions are excessively heavy (and therefore also too costly) for mass-produced vehicles. Sizing therefore was based on aircraft-type components. A curve of weight versus rated power for aircraft-type hydrostatic pumps and motors is shown in Fig. 4-4. Volume was estimated by LMSC at 24 cu in./lb, and cost at \$1.00/lb for passenger cars and \$2.00/lb for commercial vehicles.

Efficiency versus speed for a hydrostatic transmission is given in Fig. 4-5.

Electric Transmissions. Electric transmissions can take many forms, employing ac machines with thyristor cycloconverters or dc link inverters or dc machines with thyristor choppers. The dc machine plus chopper was ruled out because in high-volume production it is larger, heavier, and more expensive than the ac machine with its power conditioning. Cycloconverters were ruled out because of the 2:1 oversizing of the

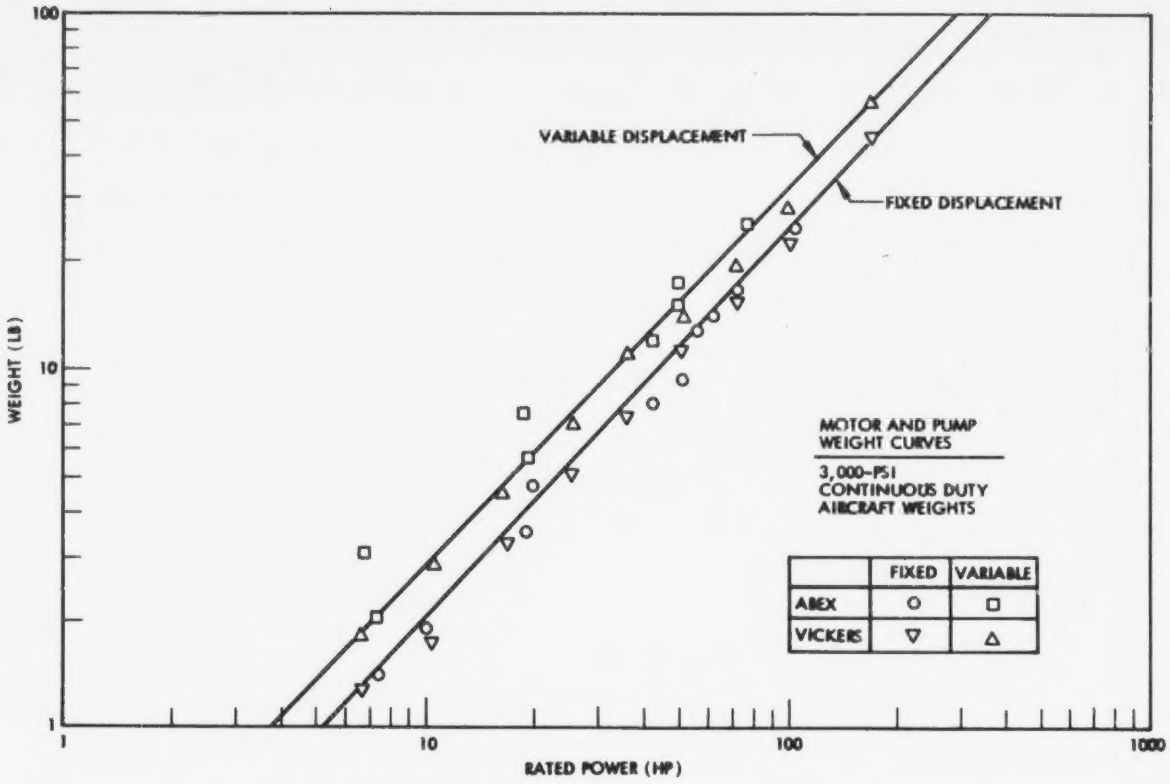

Fig. 4-4 Weight vs. Rated Speed for Hydrostatic Motors and Pumps

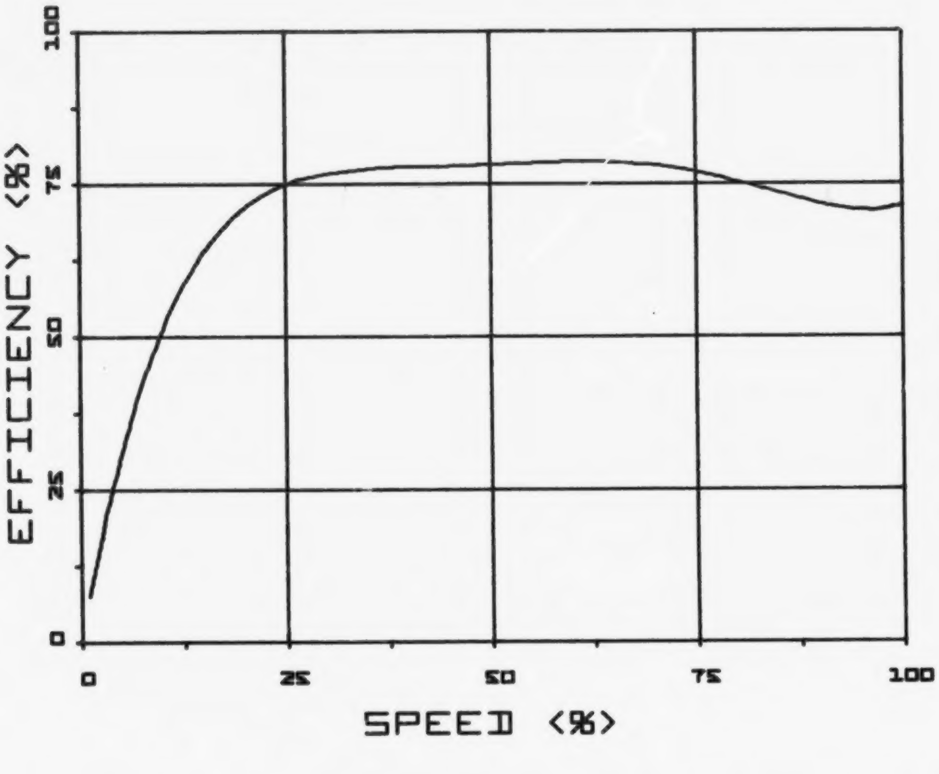

Fig. 4-5 Efficiency vs. Rated Speed for a Hydrostatic Transmission

generator (Ref. 4-1) and the speed relationships which they require. Consideration, then, was limited to ac machines with inverters operating in dc link systems. The single and double configurations of these systems are shown in Fig. 4-6. In both configurations, during regenerative braking, the motors and inverters function in the negative slip region as generators and rectifiers.

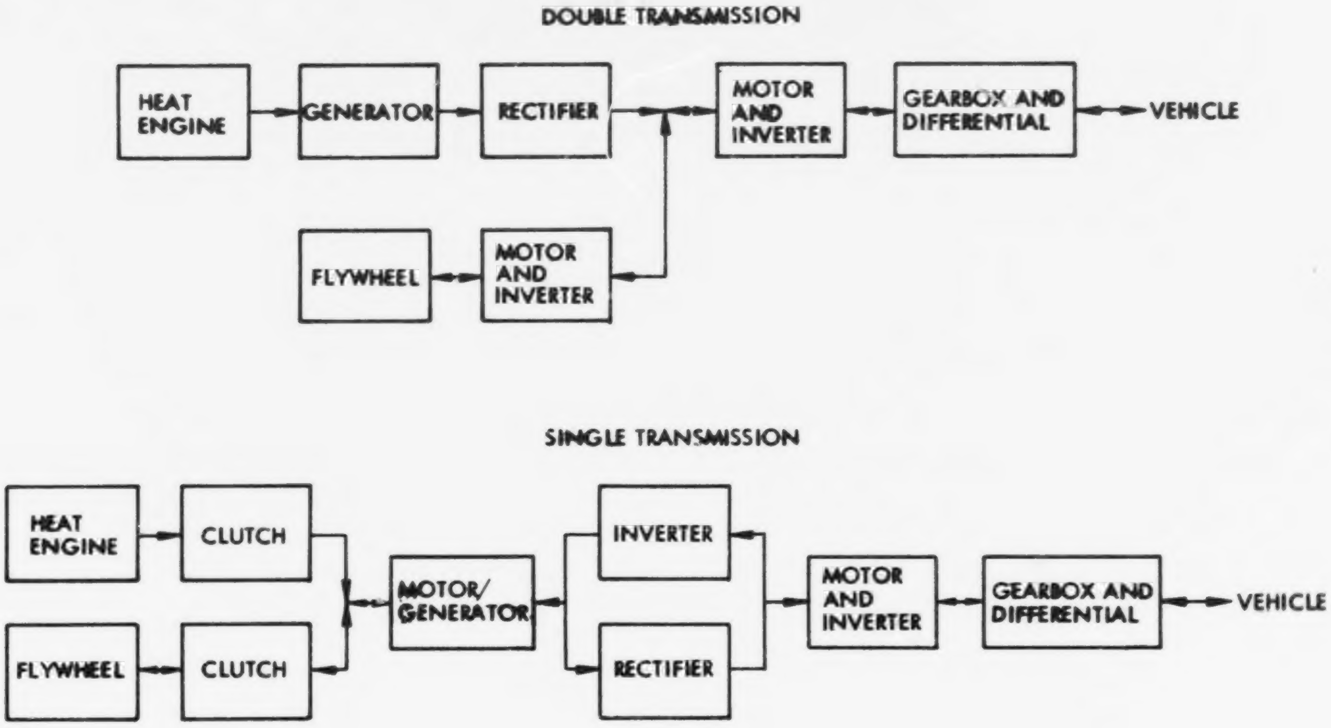
DOUBLE TRANSMISSION
HEAT ENGINE
GENERATOR
RECTIFIER
MOTOR AND INVERTER
GEARBOX AND DIFFERENTIAL
VEHICLE
FLYWHEEL
MOTOR AND INVERTER
SINGLE TRANSMISSION
HEAT ENGINE
CLUTCH
FLYWHEEL
CLUTCH
MOTOR/ GENERATOR
INVERTER
RECTIFIER
MOTOR AND INVERTER
GEARBOX AND DIFFERENTIAL
VEHICLE

Fig. 4-6 Electric Transmissions

Variable speed experimental ac motor drive systems using inverters and cycloconverters to energize the motor have been described extensively in literature. Motor speeds of about 12,000 rpm have been generally reported, and in some cases motor speeds as high as 20,000 rpm are used. By proper control of the frequency, the ac motor can be made to have a speed torque characteristic (as shown in Fig. 4-7) similar to the dc series motor used for traction application. The ac motor thus can provide high starting and acceleration torque several times the rated torque of the motors.

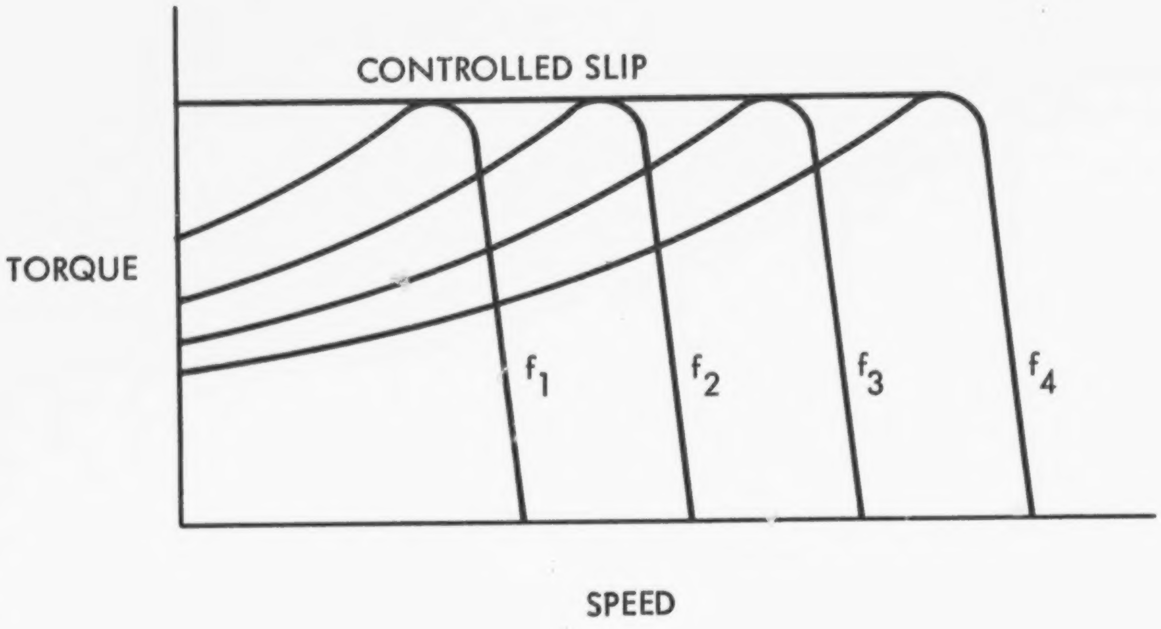

Fig. 4-7 Torque-Speed Characteristics for Squirrel Cage Induction Motor

Weight, volume, and cost versus rated torque for catalog squirrel cage induction motors are given in Figs. 4-8, 4-9, and 4-10, respectively.

Cost of the modified high-speed motors in high-volume production was estimated by LMSC to be the same as the single quantity cost of a simpler standard catalog machine. The cost is very close to $1.00/lb.

Efficiency versus power rating for a line of squirrel cage induction motors is shown in Fig. 4-11. The general trend is one reason why electric transmissions are used in Diesel locomotives and large mine trucks, but not in smaller vehicles. Below about 1,000 hp the machine losses become too large. Although experimental electric drives can show substantially higher efficiencies, the cost of such systems is presently prohibitive for application to family cars.

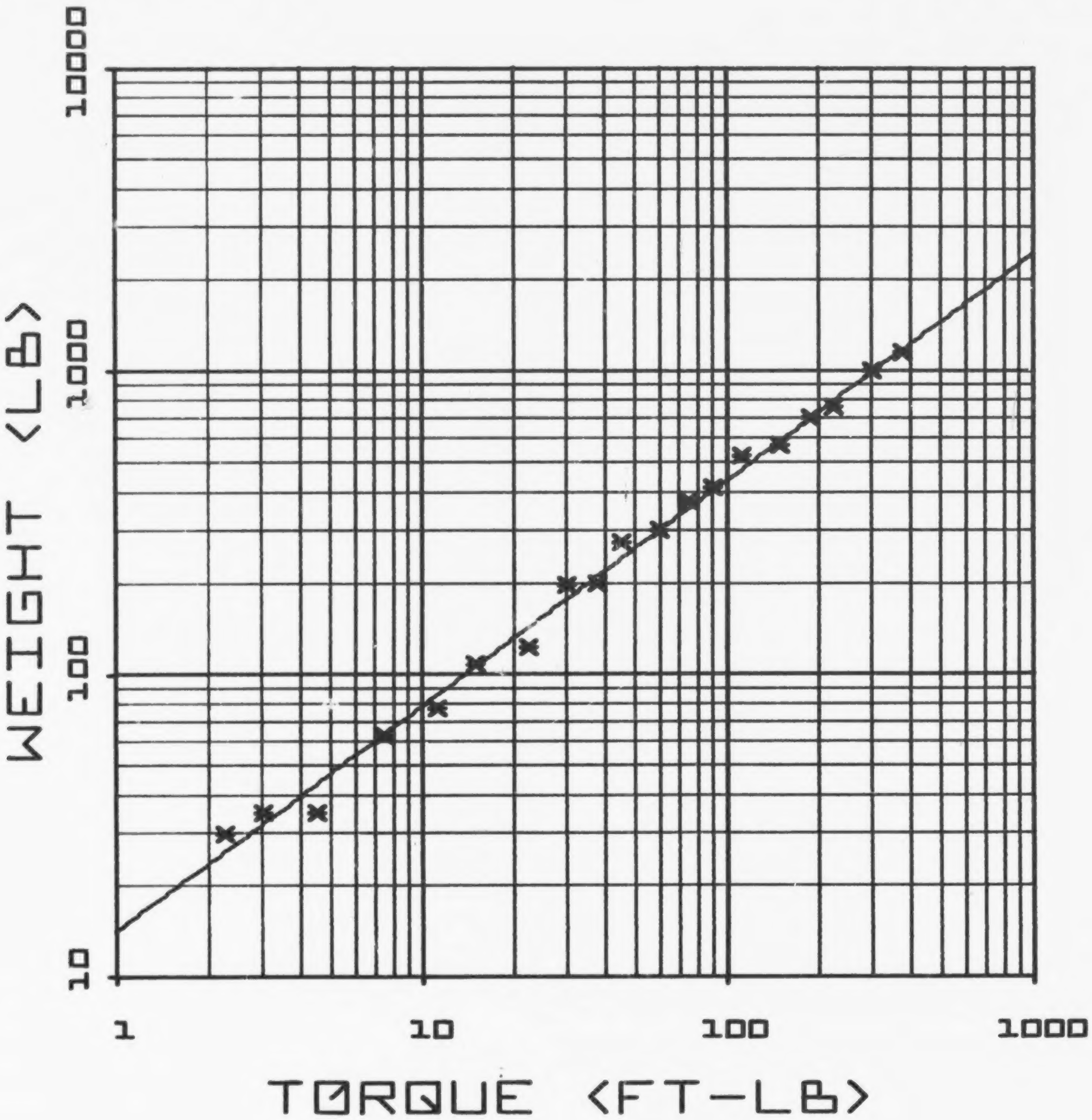

Fig. 4-8 Weight vs. Rated Torque for Squirrel Cage Induction Motors

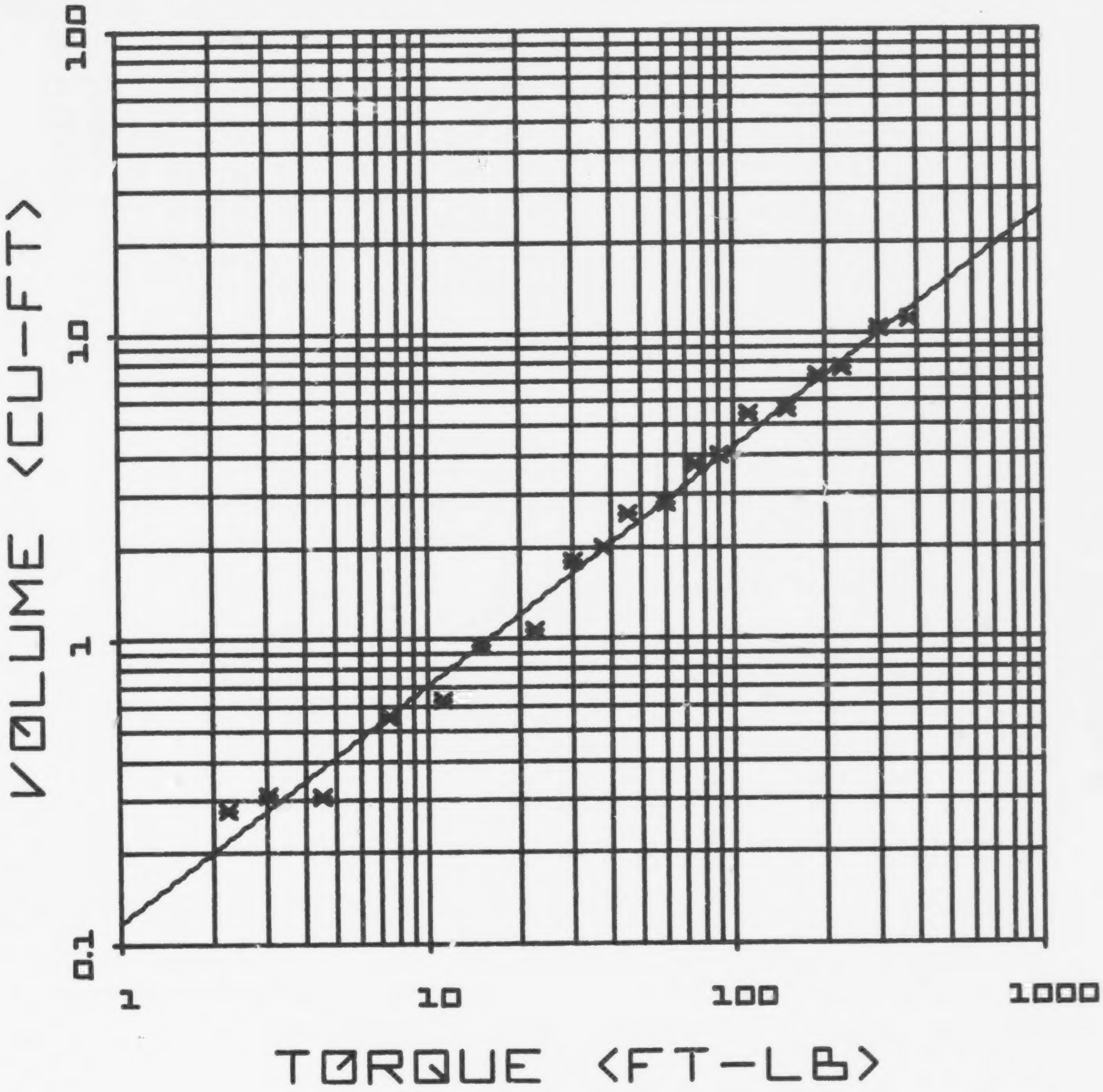

Fig. 4-9 Volume vs. Rated Torque for Squirrel Cage Induction Motors

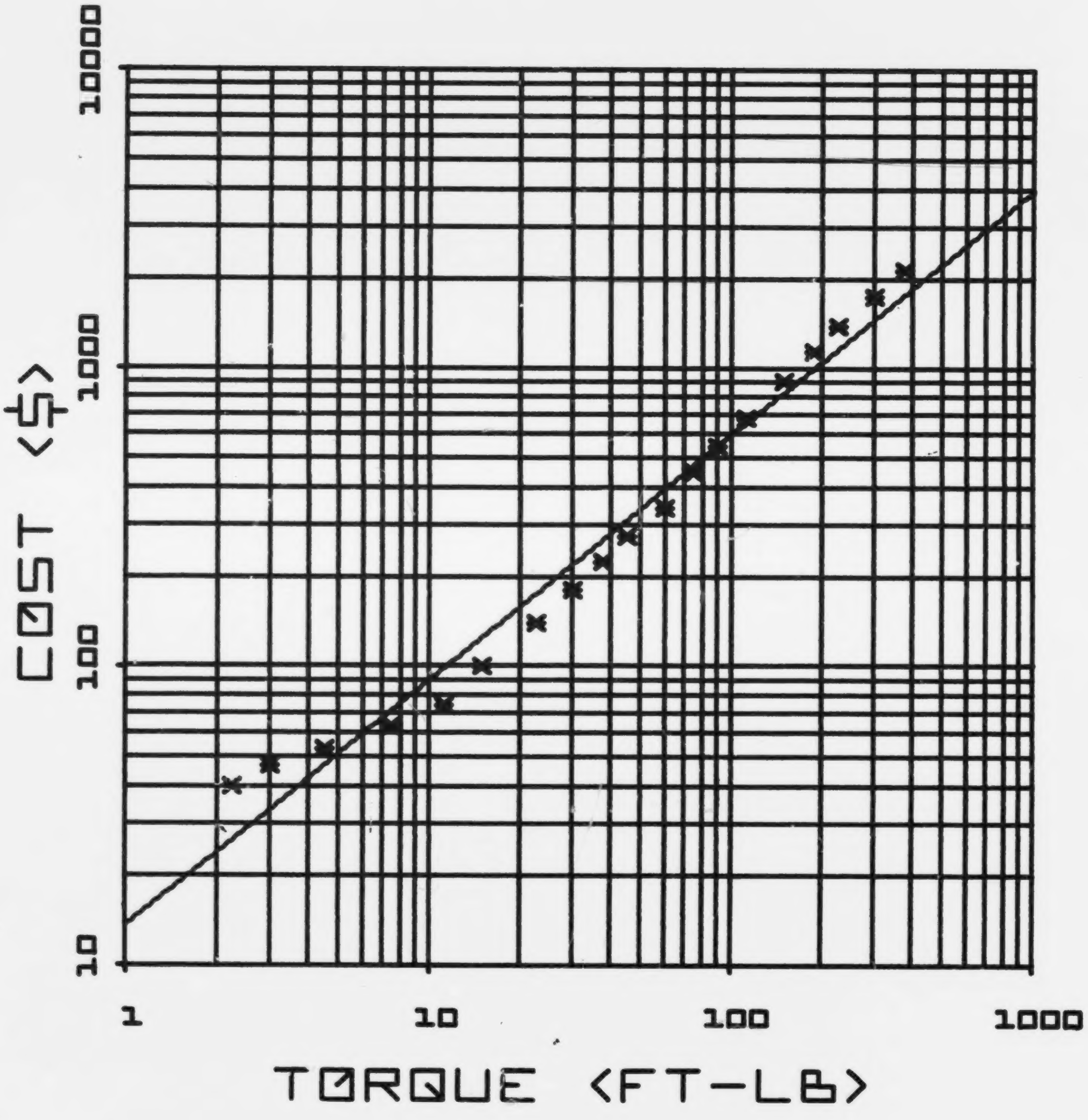

Fig. 4-10 Cost vs. Rated Torque for Squirrel Cage Induction Motors

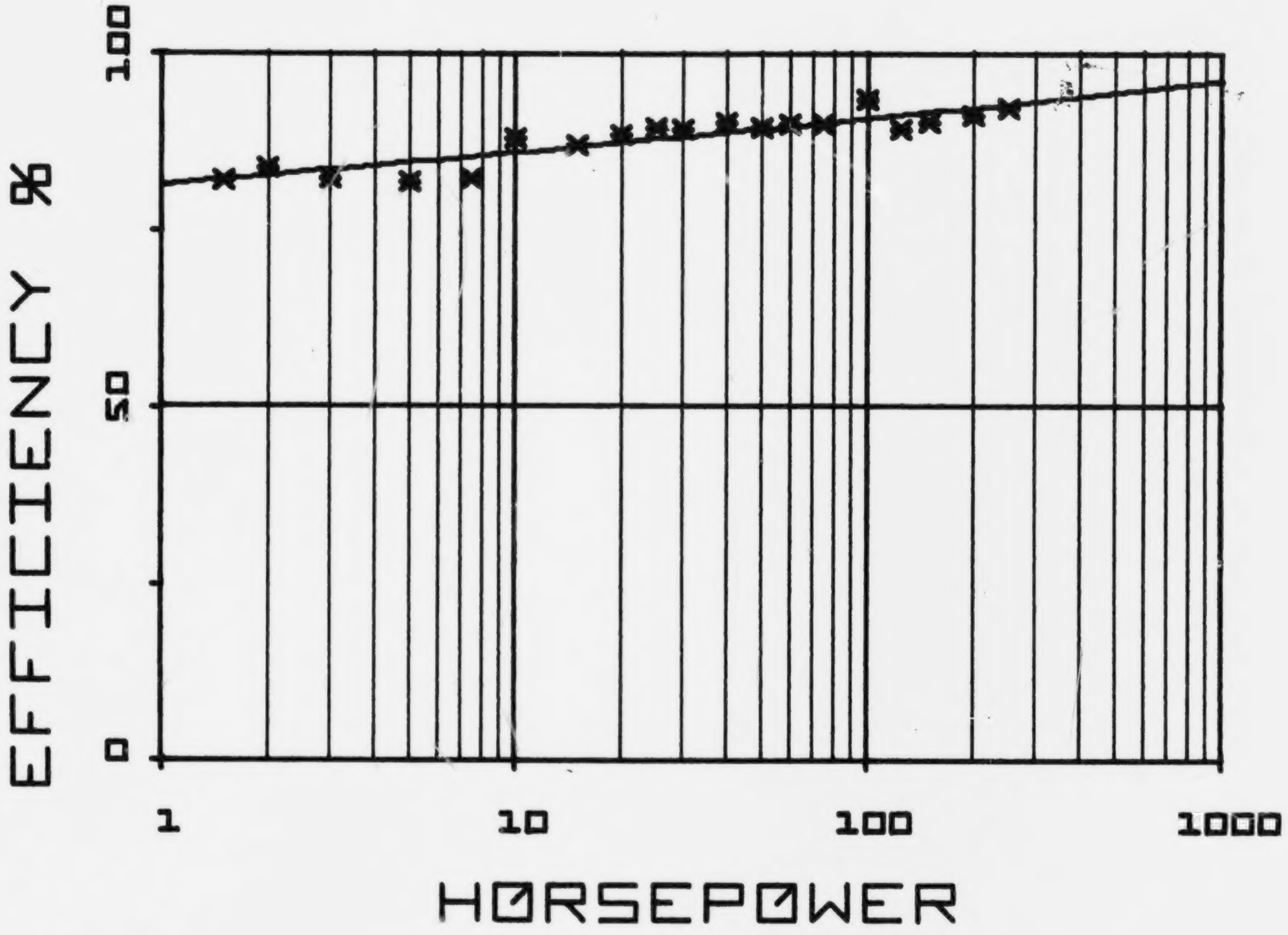

Fig. 4-11 Efficiency vs. Rated Power for Squirrel Cage Induction Motors

Efficiency as a function of speed for combined motor and inverter is shown in Fig. 4-12. This curve is based on LMSC motor testing. Again, better efficiencies have been attained with high-cost experimental drives.

Weight and volume curves for a line of aircraft generators is shown in Figs. 4-13 and 4-14, respectively. These curves were used without modification. Cost was estimated by LMSC at $1.00/lb for passenger cars and $2.00/lb for commercial vehicles.

Full load efficiency versus rated power for this line of aircraft generators is shown in Fig. 4-15. As mentioned before in discussing motors, the low efficiency at the lower power ratings has limited the application of electric transmissions to high-power (greater than 1,000 hp) vehicles.

Power Splitting Transmissions. In addition to the four types of transmissions (mechanical, hydrostatic, hydrokinetic, and electric) initially given consideration, a fifth type – the power splitting transmission – was also studied. The power splitting transmission, as shown in Fig. 4-16, is a combination of a mechanical-differential and a hydrostatic transmission. The mechanical-differential gearing is normally planetary and the hydrostatic transmission can tie between the second input of the differential and either the output or the other input. Input coupling was assumed because the relatively narrow speed range of the flywheel provides a better tie point than the infinite speed range of the vehicle.

The power splitting transmission configurations are shown in Fig. 4-17. Operation is similar to that of the hydrostatic transmission, but the power splitting transmission has better efficiency since much of the power is handled mechanically. The power splitting transmission, despite its greater size and weight, has lower cost than the hydrostatic.

A curve of efficiency versus speed for a power splitting transmission is shown in Fig. 4-18. This particular transmission is the Sundstrand DMT-250 which is slated for high-volume production for on-the-road truck application by the end of 1972. Size, weight, and cost estimates, by LMSC, also were based on extrapolations of data for this transmission.

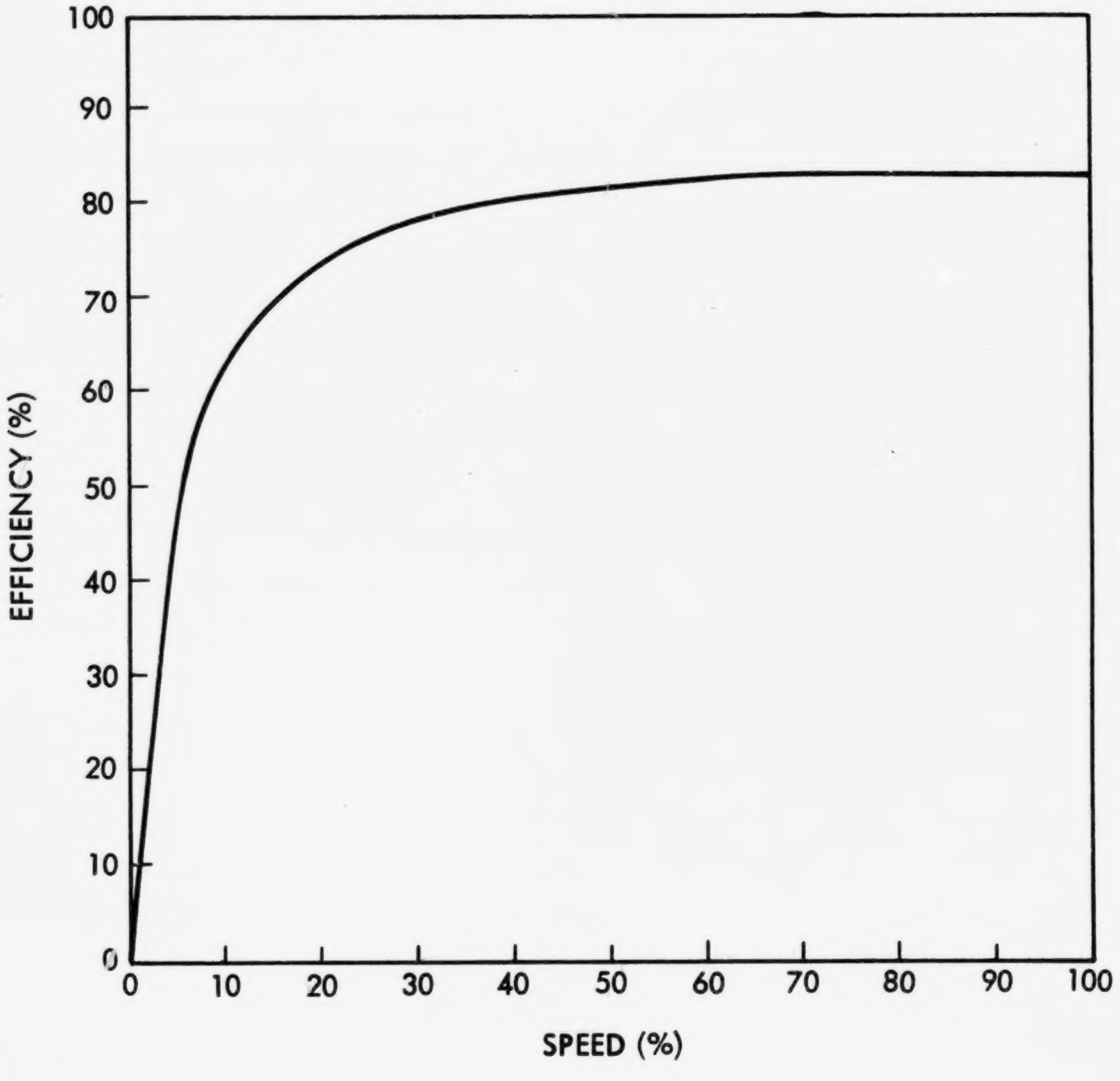

Fig. 4-12 Efficiency vs. Speed for Combined Motor and Inverter

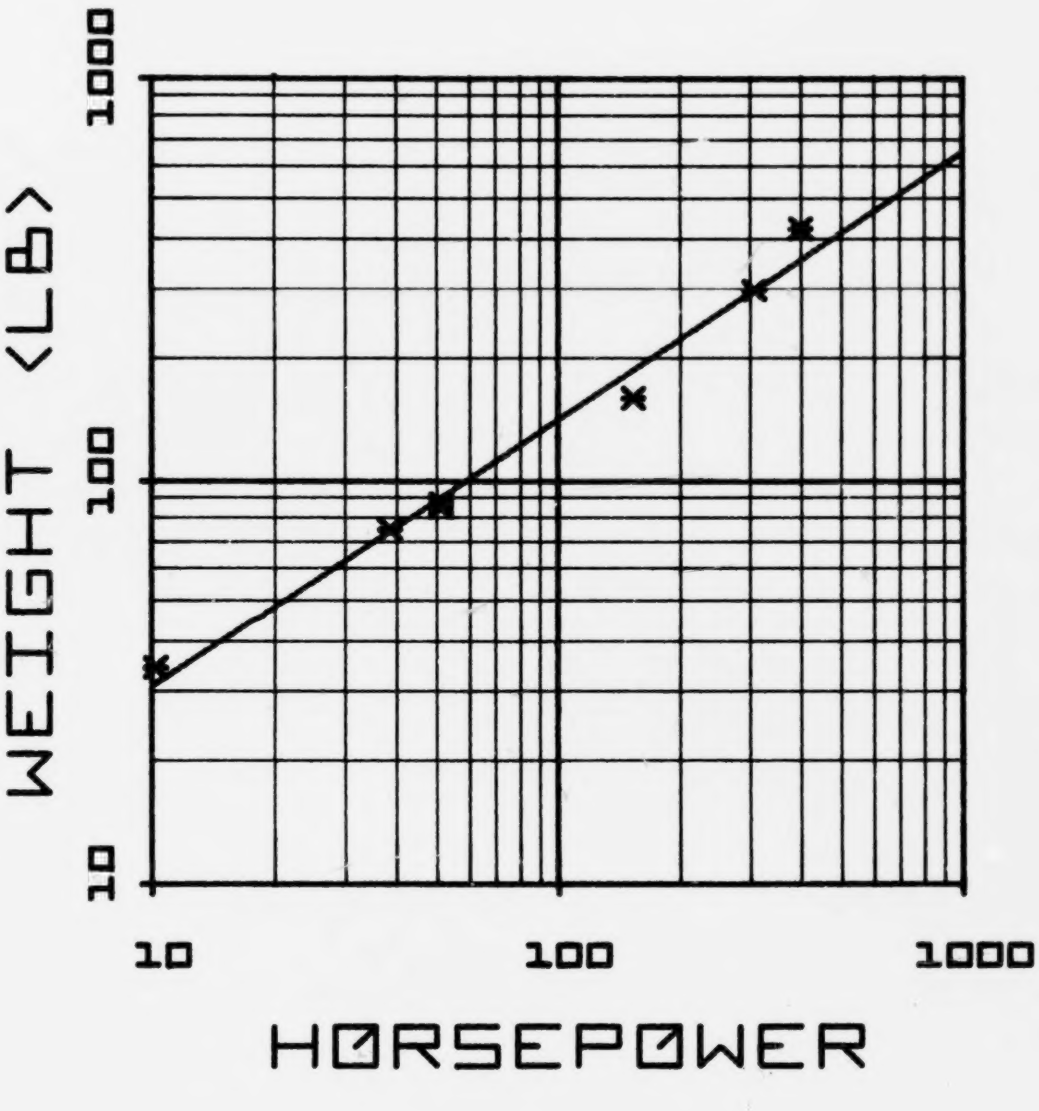

Fig. 4-13 Weight vs. Rated Power for Aircraft Generators

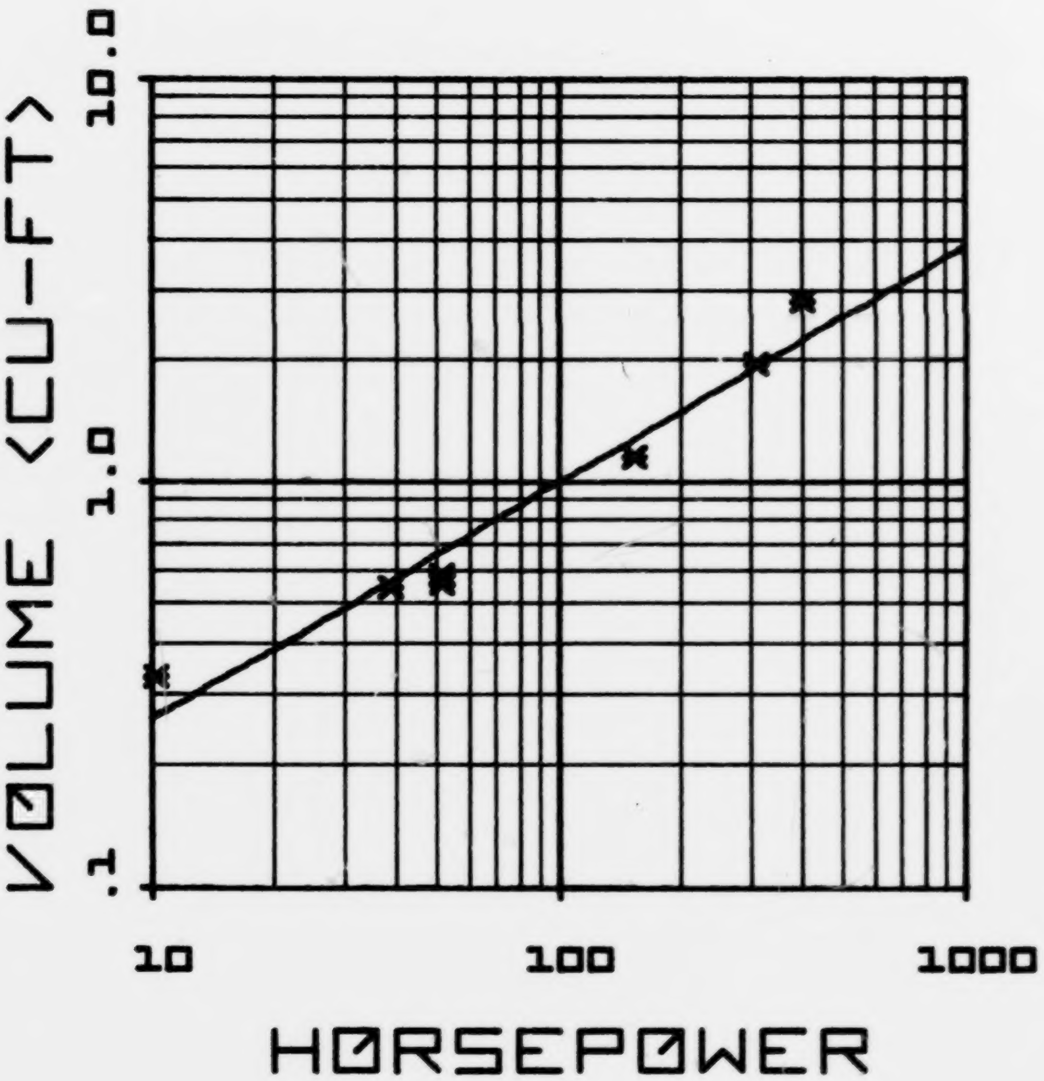

Fig. 4-14 Volume vs. Rated Power for Aircraft Generators

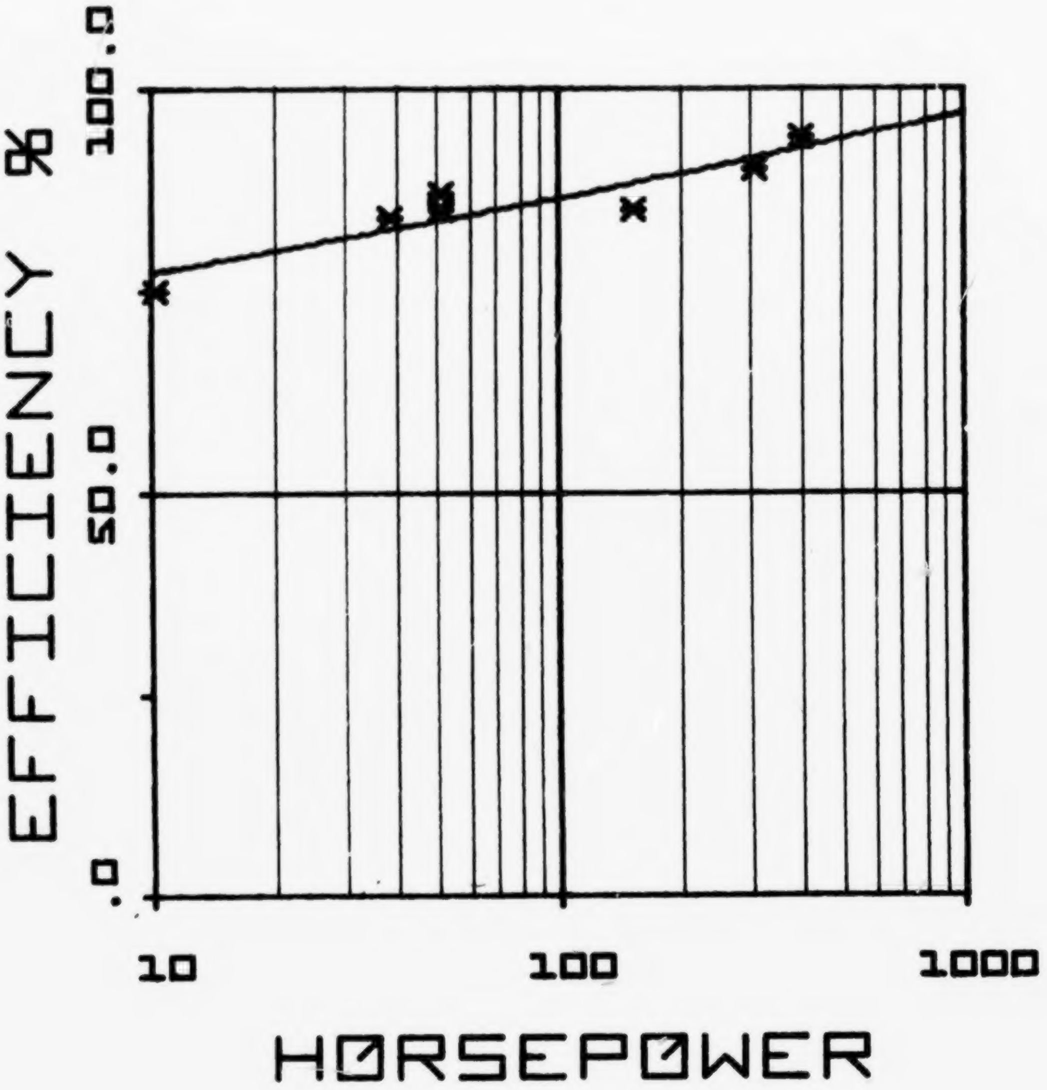

Fig. 4-15 Efficiency vs. Rated Power for Aircraft Generators

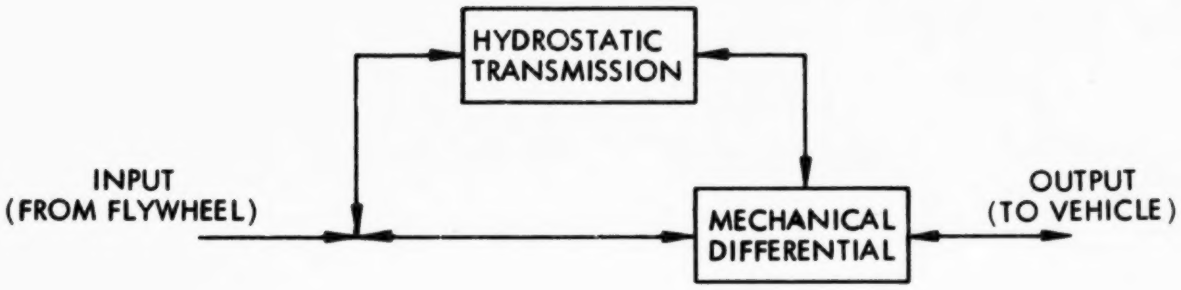
HYDROSTATIC TRANSMISSION
INPUT (FROM FLYWHEEL)
MECHANICAL DIFFERENTIAL
OUTPUT (TO VEHICLE)

Fig. 4-16 Power Splitting Transmission

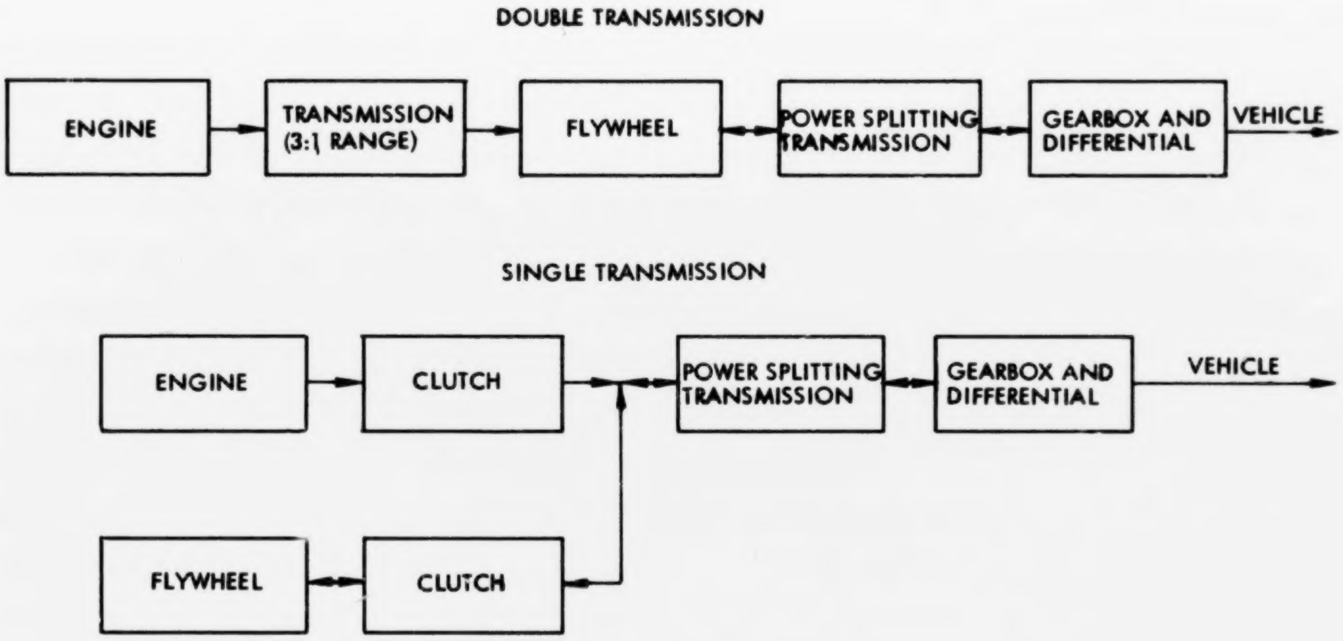
DOUBLE TRANSMISSION
ENGINE
TRANSMISSION (3:1 RANGE)
FLYWHEEL
POWER SPLITTING TRANSMISSION
GEARBOX AND DIFFERENTIAL
VEHICLE
SINGLE TRANSMISSION
ENGINE
CLUTCH
POWER SPLITTING TRANSMISSION
GEARBOX AND DIFFERENTIAL
VEHICLE
FLYWHEEL
CLUTCH

Fig. 4-17 Power Splitting Transmission Configurations

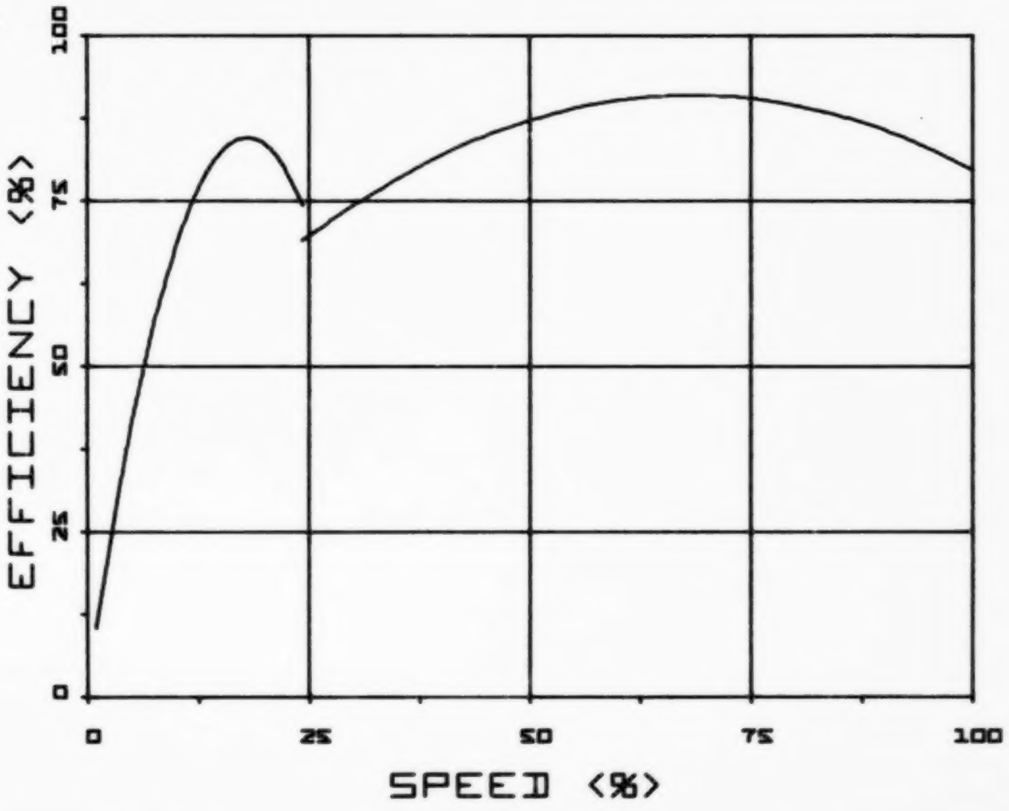

Fig. 4-18 Efficiency vs. Speed for a Power Splitting Transmission

Family Car Transmission Comparison. A comparison of electric, hydrostatic, and power splitting transmissions for both single and double transmissions suitable for application to the family car is shown in Table 4-1. The efficiency is based on operation of the specified family car over the DHEW Urban Dynamometer Driving Schedule with the assumption that all braking is recuperative. The efficiencies of each transmission type are normalized on the basis of 1.00 efficiency for the best configuration (power splitting single).

The size, weight, and cost figures for the various transmissions represent estimates by LMSC based on equivalent production quantities. The electric transmissions are worst on all accounts; the costs are probably prohibitive. The best transmission on the basis of highest efficiency (which minimizes emissions) and lowest cost is the power splitting transmission. The weight and volume of the power splitting transmission, although greater than those of the hydrostatic, are not excessive.

Table 4-1
FAMILY CAR TRANSMISSION COMPARISON

Item	Electric		Hydrostatic		Power Splitting	
	Single	Double	Single	Double	Single	Double
DHEW Schedule Efficiency (Normalized)	0.588	0.369	0.745	0.626	1.000	0.835
Volume (cu ft)	3.4	4.0	3.3	3.7	3.7	5.1
Weight (lb)	488	536	280	289	311	391
Cost ($)	641	689	403	469	261	341

On these bases, therefore, the power splitting transmission was chosen as the best one for the flywheel/hybrid family car.

Bus Transmission Comparison. A comparison of electric, hydrostatic, and power splitting transmissions for both single and double transmissions suitable for application to the city bus is shown in Table 4-2. The efficiency is based on operation of the specified fully loaded bus over the city bus cycle with the assumption that all braking is recuperative. The efficiencies of each transmission type are normalized on the basis of 1.00 efficiency for the best configuration (power splitting single).

Table 4-2
BUS TRANSMISSION COMPARISON

Item	Electric		Hydrostatic		Power Splitting	
	Single	Double	Single	Double	Single	Double
Profile Efficiency (Normalized)	0.6254	0.4267	0.7681	0.6615	1.000	0.8495
Volume (cu ft)	16	17	20.6	23.8	25.5	35.5
Weight (lb)	2,023	2,077	1,937	2,085	2,255	2,922
Cost ($)	6,088	6,291	3,335	3,900	2,205	2,872

The size, weight, and cost figures for the various transmissions represent estimates by LMSC based on equivalent production quantities. As with the case of the family car, the electric transmission types are seen to be prohibitively expensive. Again, on the bases of best efficiency and lowest cost, the power splitting transmission was chosen as being the best for the city bus.

HEAT ENGINE SELECTION

The heat engines to be considered are the spark-ignition, Diesel, gas turbine, and Rankine cycle engines. Primary attention was given to cost, size, weight, efficiency, and emission rates of carbon monoxide (CO), unburned hydrocarbons (HC), and oxides of nitrogen (NO_x), but the engine study also considered engine sound level and smoke emission.

HEAT ENGINE SURVEY

To support the configuration tradeoffs, realistic heat-engine data in the range of 20 to 200 hp were required, representing the most desirable engine characteristics that could reasonably be expected to be commercially available in the near future. Data for this purpose were acquired by means of an exploratory survey of applicable heat engines available, and letters of inquiry to the manufacturers of the engines of interest.

The specific objectives of the engine data survey were to derive the relationships between engine continuous power rating and cost, specific fuel consumption, weight, envelope volume, and exhaust emissions. For each engine type studied, these relationships were established in a form suitable for input to the computerized parametric study. It was recognized that the usefulness and validity of the study depends on the availability, in the 1971–1975 timeframe, of commercial versions of the engines considered, in appropriate sizes, substantially in accordance with the performance attributed to them and without the necessity for implemental development funding. Thus, the stratified-charge engine, which may offer improvements over the common spark-ignition engine if it becomes available over a range of sizes in the near future, was not included. Similarly, rotating combustion engine data were not used because this engine's 1975 commercial availability in a range of sizes is not assured at this time even though such engines are now used in automobiles (the NSU RO-80 for example). The Stirling engine concept was considered to be in an inadequate state of vehicular development for 1975 availability.

Engine preliminary data sources are listed in Refs. 4-2 through 4-7. Final data for the engines of interest were obtained directly from the manufacturers. Exhaust emission data were obtained primarily from Ref. 4-8 and were in part confirmed by a small amount of data obtained from engine manufacturers. Information on engine developmental status was derived in part from Ref. 4-9.

In order to simplify the task of sorting the most promising Diesel and spark-ignition engines for use in the study, a selective elimination of engines from Refs. 4-2, 4-3, and 4-4 was performed. As a weight, volume, and cost consideration, all low- and medium-speed engines were eliminated from consideration on the basis that these engines would be heavy and costly. In general, only engines of 1,800 rpm or more were considered. As a "noise pollution" consideration, turbosupercharged engines were eliminated. (Ref. 4-10. Also see the NAPCA Vehicle Design Goals, Appendix A.) This process of elimination resulted in a quantity of 160 eligible Diesel engines within the range of 15 to 150 continuous horsepower, and 100 eligible spark-ignition engines.

All turbine engines determined to be within the range of 15 to 150 hp were considered, and all "small" Rankine engines were considered.

Engine weights and piston displacements versus continuous horsepower were plotted for the eligible Diesel and spark-ignition engines, and then straight lines were drawn through the weight and displacement data in such a way that an adequate range of engines lay below the lines. These Diesel and spark-ignition engines were regarded as the preferred engines for purposes of the study, and was the subject of letters of inquiry to the manufacturers to obtain confirming and additional data. Letters of inquiry were also sent to all known or possible manufacturers of small turbine and Rankine engines for whom addresses could be determined. A quantitative summary of engines investigated, inquiries made, and responses obtained is given in Table 4-3.

Table 4-3

QUANTITY OF ENGINES INVESTIGATED

Type	Domestic Engines	Foreign Engines	Total
SPARK-IGNITION			
Eligible Engines	97	3	100
Manufacturer's Data Requested	37	3	40
Useful Response Received	23	3	26
DIESEL			
Eligible Engines	34	126	160
Manufacturer's Data Requested	22	37	59
Useful Response Received	21	12	33
GAS TURBINE			
Eligible Engines	4	2	6
Manufacturer's Data Requested	7	2	9
Useful Response Received	5	0	5
RANKINE			
Eligible Engines		Indeterminate	
Manufacturer's Data Requested	14	1	15
Useful Response Received	3	1	4

ENGINE TREND DATA

The parameters of cost, specific fuel consumption, weight, and volume all vs. continuous horsepower were evaluated by a computerized "least squares curve fit" to determine the most appropriate equation relating each parameter to the continuous power rating. For each parameter, curves of the following type were compared with the actual data:

$$Y = A + (BX)$$

$$Y = A(\epsilon)^{BX}$$

$$Y = A(X)^B$$

$$Y = A + \left(\frac{B}{X}\right)$$

$$Y = \frac{1}{A + (BX)}$$

$$Y = \frac{X}{A + (BX)}$$

where

Y = value of the parameter (cost, specific fuel consumption, weight, and volume)

X = corresponding continuous power rating

ϵ = base of natural logarithms

A = Y intercept

B = factor

The equations of these curves were then used to determine the parameters at particular values of continuous rated power. A compilation of the data used to establish these trend curves is given in Appendix C.

Emission curves for the various engines were supplied by EPA/APCO. These curves are based on rather rudimentary data and do not include any cold start factors. Much more data is needed and many more calculations must be made to properly calculate the emissions. The emission figures quoted in this report should be considered only approximate and preliminary results. These curves of HC, CO, and NO_x as a function of continuous horsepower are shown in Figs. 4-19, 4-20, and 4-21, respectively. These curves were used as the basis for all emission calculations.

Spark-Ignition Engines. The conventional automobile spark-ignition engine is constrained by its cycle to a range of air/fuel ratios (between extremes of approximately 8 and 17), and in order to avoid detonation is limited to relatively low compression ratios (less than approximately 12) compared with the Diesel. Its exhaust emissions therefore

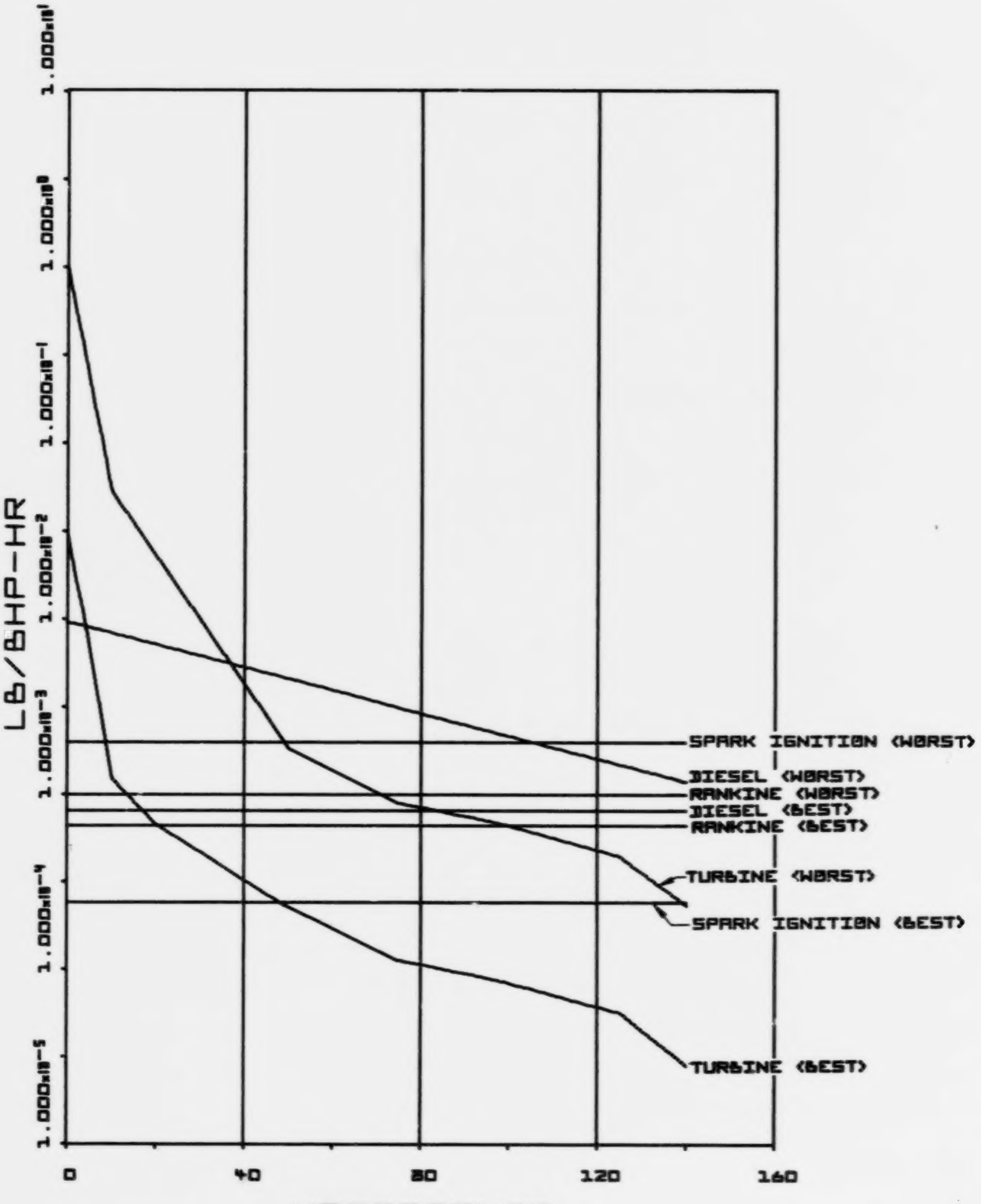

Fig. 4-19 HC Emissions vs. Continuous Horsepower

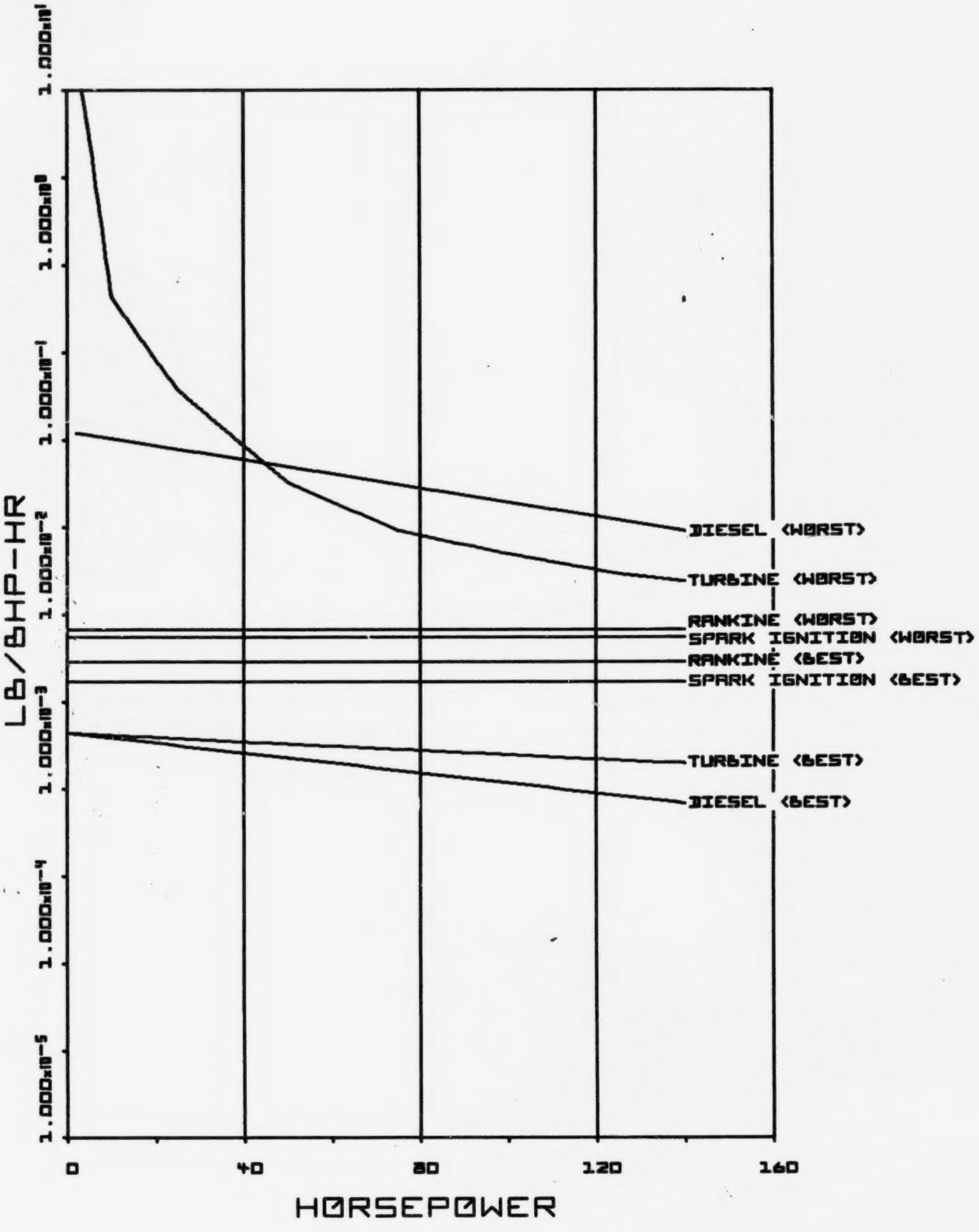

Fig. 4-20 CO Emissions vs. Continuous Horsepower

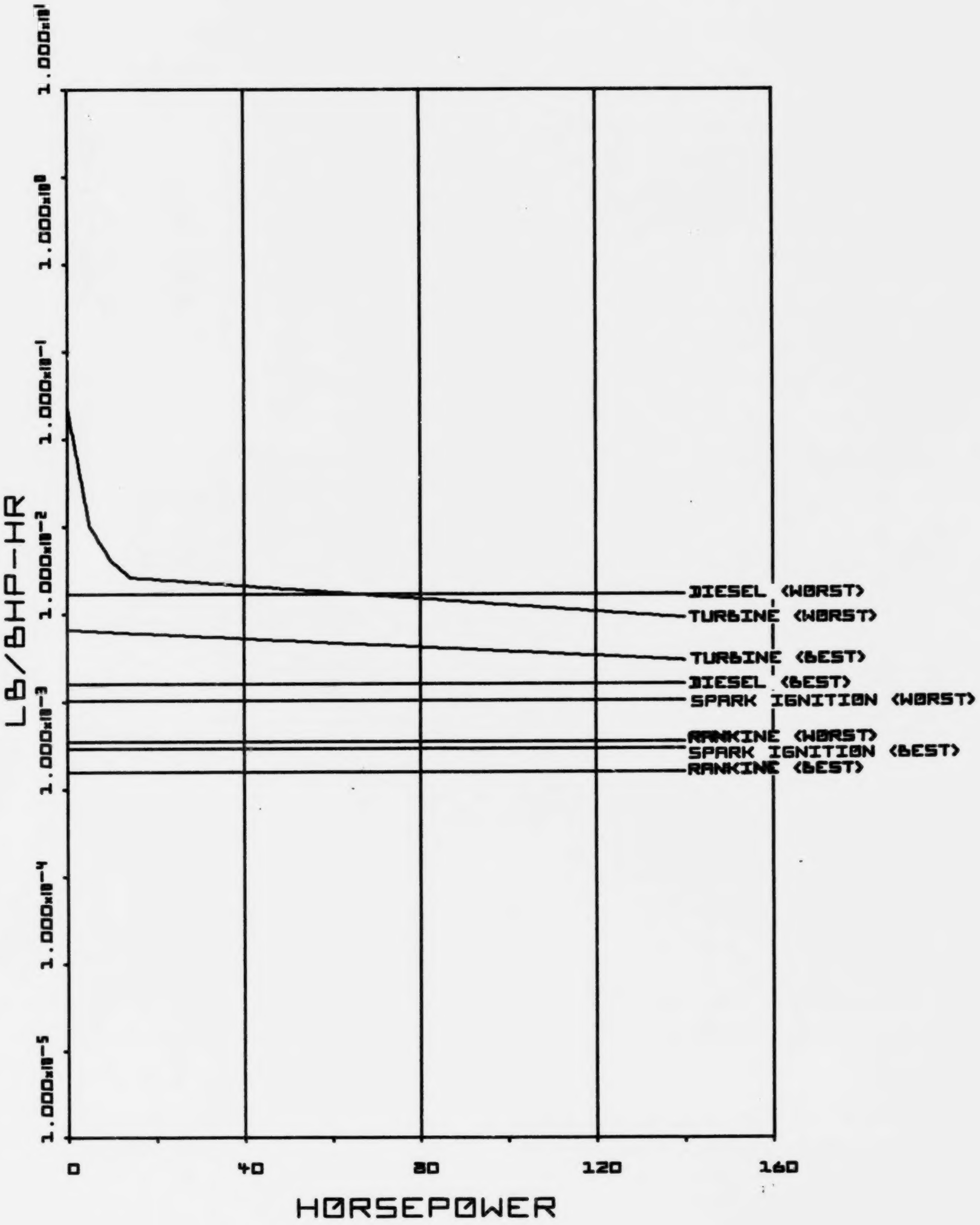

Fig. 4-21 NO_x Emissions vs. Continuous Horsepower tend to follow a characteristic pattern, and largely must be controlled external to the cylinder or by avoiding power transients and idling conditions. The high state of development of the basic engine and its high rate of production over a range of power values results in a relatively compact, light, low-cost, readily available engine.

From Table 4-3 it is seen that letters of inquiry were sent to manufacturers representing 40 percent of the total quantity of eligible engine models. These represented the most promising models for the application, derived by selective and preferential elimination processes. Useful responses were received covering 65 percent of the engines so investigated. However, emissions data were so meager as to be useless for establishment of trends; hence, Ref. 4-8 was concluded to be unmodified by manufacturer's information, and was regarded as the effective emissions data source for this study.

For the spark-ignition engine, the following relations were used to express the values of the parameters:

Function	Ordinates	Equation
Cost vs. hp	Y vs. X	$Y = A(X)^B$
Specific Fuel Consumption vs. hp	Y vs. X	$Y = A + \left(\frac{B}{X}\right)$
Weight vs. hp	Y vs. X	$Y = A(X)^B$
Volume vs. hp	Y vs. X	$Y = A(X)^B$

The computer plots of the four parameters showing all data points used for the curve fit are shown in Figs. 4-22 through 4-25.

Specific fuel consumption, volume, cost and weight charts do not include the effect of advanced emission control techniques and therefore are only approximate.

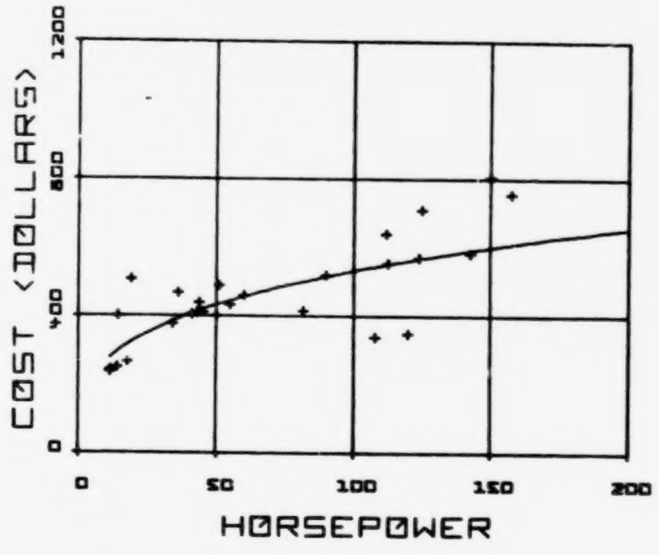

Fig. 4-22 Spark-Ignition Cost vs. Continuous Horsepower

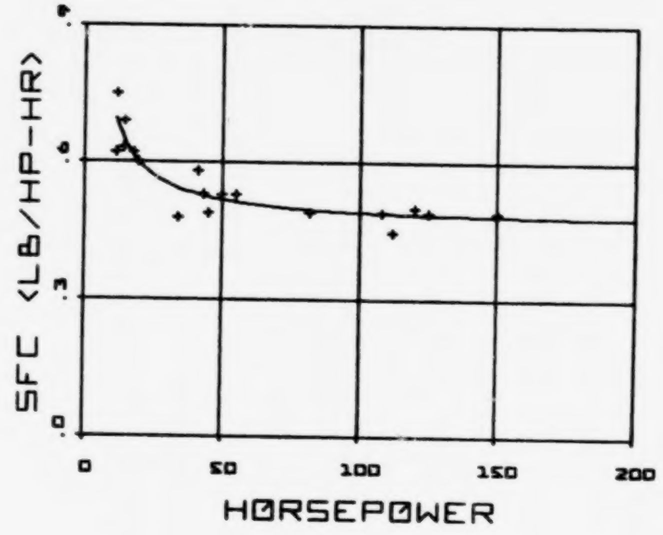

Fig. 4-23 Spark-Ignition Specific Fuel Consumption vs. Continuous Horsepower

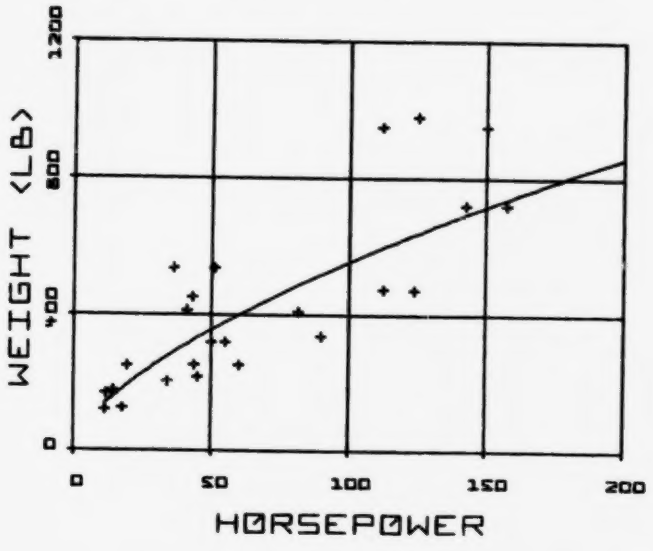

Fig. 4-24 Spark-Ignition Weight vs. Continuous Horsepower

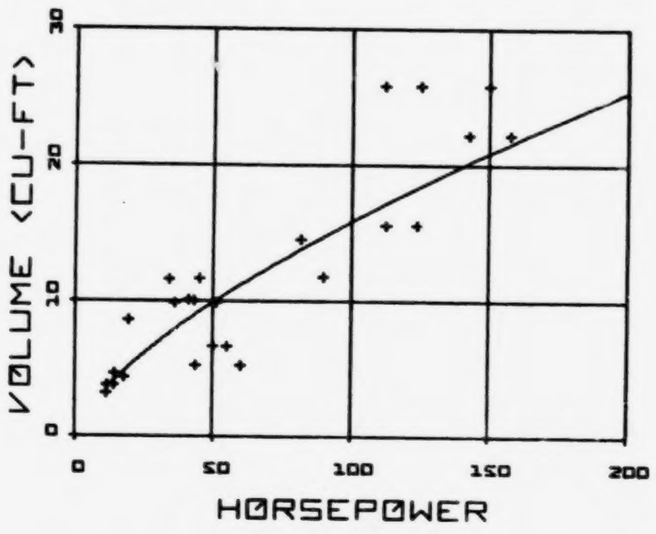

Fig. 4-25 Spark-Ignition Volume vs. Continuous Horsepower

Diesel Engines. The Diesel cycle inherently permits operation over a wide range of air/fuel ratios, and permits higher compression ratios than the spark-ignition engine, thereby providing lower specific fuel consumption. Due to its greater size and weight, costly fuel-metering and injection system, and lower production rate, the Diesel is more expensive than the spark-ignition. It also is noisier because of the rapid rate of pressure rise in the cylinder and injection system noise. Its higher air/fuel ratio tends to result in much lower CO content in the exhaust, and HC content can be lower with appropriate attention given to design of injection equipment. Despite the fact that its higher air/fuel ratios tend to result in lower NO_x, its high combustion temperature and pressure cause NO_x to be high.

Letters of inquiry were sent regarding 37 percent of the total quantity of eligible Diesel models. Useful responses covered 56 percent of the models so investigated. As with the spark-ignition engines, these represented the most promising Diesels for the application, derived by two processes of elimination.

Extensive emissions data were received from one manufacturer, which provided a general confirmation of the data of Ref. 4-8 for Diesels. Only meager emissions data were received from the remainder of the manufacturers.

The parameters were again evaluated by computer curve fit to determine the best equations relating the parameters to the continuous power rating. The following relations were used:

Function	Ordinates	Equation
Cost vs. hp	Y vs. X	$Y = A(X)^B$
Specific Fuel Consumption vs. hp	Y vs. X	$Y = \frac{1}{A + (BX)}$
Weight vs. hp	Y vs. X	$Y = A(X)^B$
Volume vs. hp	Y vs. X	$Y = A(X)^B$

The computer plots of the four parameters showing all data points are shown in Figs. 4-26 through 4-29.

Any reductions in cost, weight, or NO_x emissions would make the Diesel more attractive.

Gas Turbine Engines. In comparison with the reciprocating internal combustion engine, the nonregenerative gas turbine is much lighter, smaller, and simpler mechanically. However, continuously sustaining the high gas temperatures necessary to obtain acceptable thermal efficiency and maintaining the production tolerances necessary require expensive metallurgical, design, and production processes. For this reason, turbine costs are generally appreciably higher. The turbine operates with overall air/fuel ratios much higher than the spark-ignition engine, and higher than the Diesel, in order to limit turbine inlet temperatures. Because its combustion process is continuous – not intermittent as with the reciprocating engines – and occurs in a continuously hot combustor, it tends to be a very low producer of CO and HC. Its high air flow rates require special attention to intake and exhaust design to avoid bothersome noise levels.

Turbines may be attractive for flywheel applications because of the good speed compatibility.

The references used to collect engine data indicate that very few turboshaft gas turbines exist in the range of 20 to 200 continuous shaft horsepower. For this engine category, Refs. 4-2 and 4-4 indicate half a dozen such engines available. Letters of inquiry were sent regarding these engines, and to several additional manufacturers from Ref. 4-6. A total of five useful responses were obtained, an insufficient quantity to support the drawing of trend curves. No emissions data were received. Data related to fuel consumption, weight, and envelope volume were so diverse as to prohibit any conclusion regarding a curve shape. The probable reason for this is the strong growth of turbine power with time. Three of the turbines are growth versions

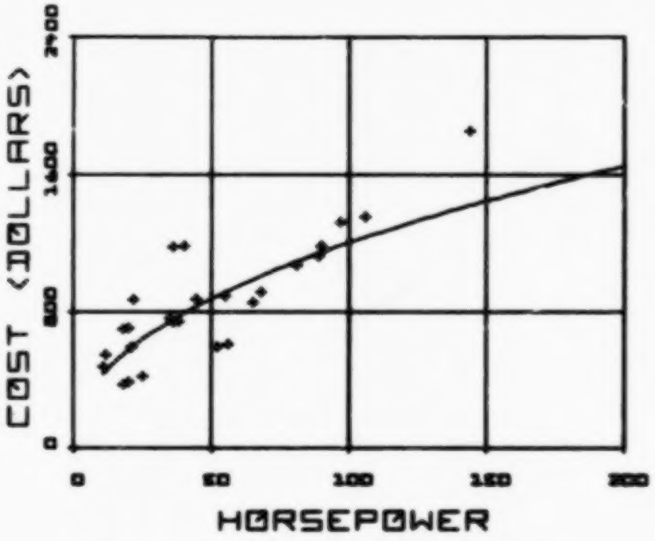

Fig. 4-26 Diesel Cost vs. Continuous Horsepower

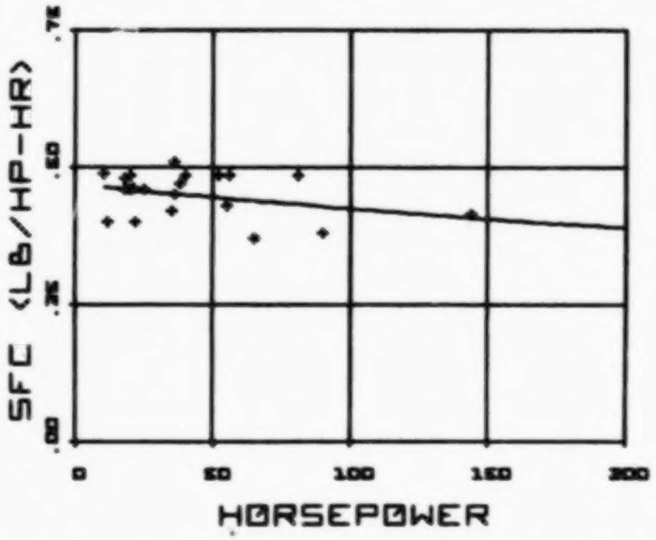

Fig. 4-27 Diesel Specific Fuel Consumption vs. Continuous Horsepower

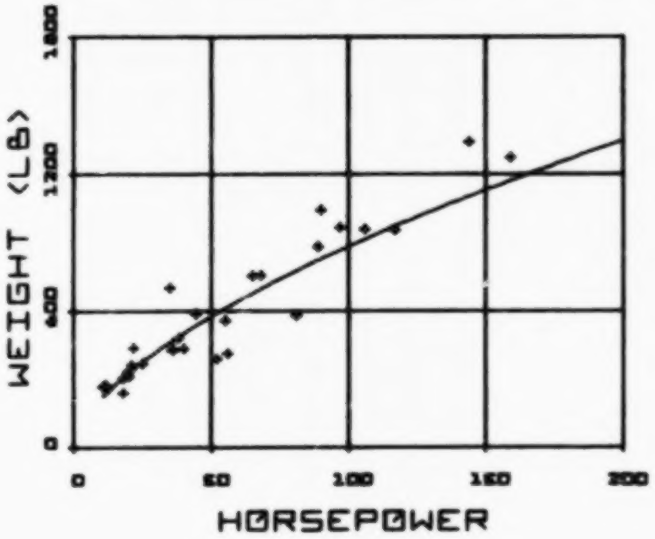

Fig. 4-28 Diesel Weight vs. Continuous Horsepower

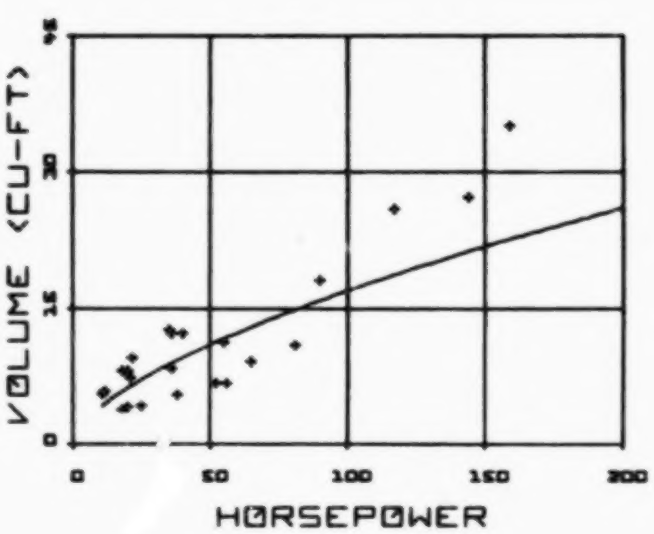

Fig. 4-29 Diesel Volume vs. Continuous Horsepower

of approximately 1960 technology, which would tend to show lower values of specific fuel consumption, weight, and volume. Another of the turbines is a new development and has the capability of doubling its present power in a few years, but it would require funding to accomplish this. The fifth turbine appears to be just in the planning stage. Only three of the responses included cost figures.

In view of the small amount of useful small-turbine data, supplemental data were used to derive curve shapes.

a. The three cost values, when plotted versus power, lay very nearly on a straight line. As a check, four other points were added for known engine costs within the power range of 300 to 800 hp. These supplemental points verified the applicability of the small-engine cost data, and permitted the establishment of a cost curve of the form $Y = A + (BX)$. This plot with the points used is shown in Fig. 4-30.

b. The five specific fuel consumption data points would not support the establishment of a curve in which confidence could be placed. Therefore, data from an additional 30 turbine engines were taken from Ref. 4-4, covering continuous power values up to 1, 150 hp. These data, representing a more or less average degree of engine growth, were combined on a plot with the five small engines, and the computer curve fit program employed to determine the relationship of specific fuel consumption to continuous power. Investigating the same curve forms as for the spark-ignition and Diesel engines, the relation used was

$$Y = A(X)^B$$

This computer plot with the points is shown in Fig. 4-31.

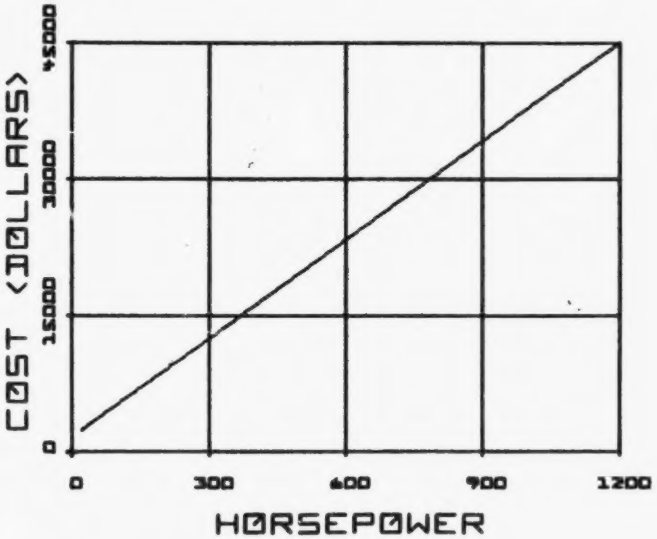

Fig. 4-30 Gas Turbine Cost vs. Continuous Horsepower

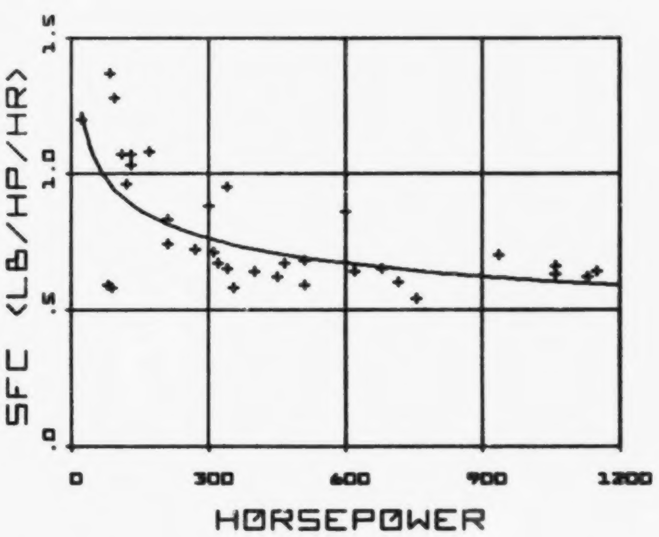

Fig. 4-31 Gas Turbine Specific Fuel Consumption vs. Continuous Horsepower

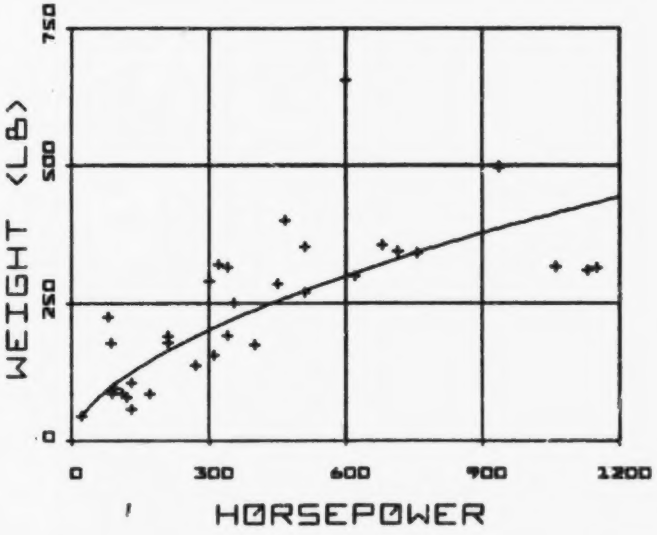

Fig. 4-32 Gas Turbine Weight vs. Continuous Horsepower

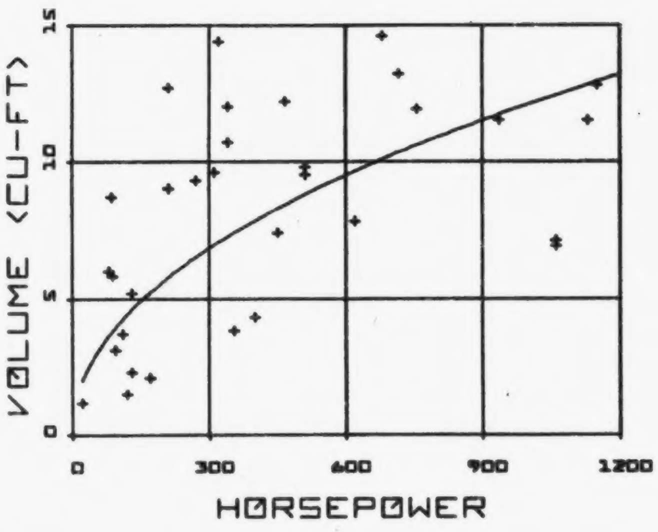

Fig. 4-33 Gas Turbine Volume vs. Continuous Horsepower

c. Weight data for the five small turbines were not considered reliable for 1975 engine weight prediction. Two engine weights were only prediction estimates, and the other two engine weights were abnormally low because the engines are at an advanced state of power growth. Again, Ref. 4-4 data for 30 additional engines were used to supplement the small-engine data. The resultant relationship between weight and continuous rated power used was

$$Y = A(X)^B$$

This plot with points is shown in Fig. 4-32.

d. Precisely the same comments noted for weight also apply to the small-engine volume data. Reference 4-4 data again were used as a supplement, and the resultant relationship used was

$$Y = A(X)^B$$

This computer plot with points is shown in Fig. 4-33.

To regard these equations as being applicable to a specific range of 1975 production engines is somewhat unrealistic. Any turbine engine that is expected to reach production status by 1975 must now be in the planning stage, and will need to go into design promptly. Therefore, the only small turbines whose availability can really be depended upon are those few for which the data were obtained; moreover, the parametric relations derived do not necessarily "fit" these specific engines. However, the relations are considered to be fair representations of small-turbine-engine capability, and as such are appropriate for use in the study.

Rankine Cycle Engines. The Rankine cycle engine and its associated equipment constitute a larger and heavier system than the other engine types considered, and its efficiency is considerably below that of reciprocating engines. For purposes of combustion efficiency and smoke elimination it is operated over a narrow range of air/fuel ratios with approximately 10 to 20 percent excess air over that required for optimum combustion with the fuel used. It has the potential of being a very low producer of CO, HC, and NO_x because combustion is continuous and complete, occurring at moderately high temperatures in a hot chamber, and because the air/fuel ratio is higher than the stoichiometric mixture. System cooling size and weight requirements are high because the working fluid must be condensed and recirculated. In contrast to the production status of reciprocating engines, and the emerging production status of automotive turbines, there is no evidence of the availability of large-scale production plans or facilities for the Rankine cycle engine.

The status of steam or vapor engines applicable to this study was indeterminate; therefore, letters of inquiry were sent to all of the potential data sources indicated by Refs. 4-5, 4-6, and 4-7. The relatively small number of useful responses – 4 out of 15 – might be due to the small size of most companies dealing with small vapor engines, or to a reluctance, in the face of a potential future vapor engine market, to share useful technical information which has been acquired by individually sponsored research and efforts. The small response made necessary a considerable degree of extrapolation to derive parametric relations for vapor engines.

Since both water and organic working fluid Rankine engine systems are presently under investigation, with several proponents for each type fluid, a decision was required regarding the fluid on which to base the study input data. It was decided to base the inputs on a water (steam) cycle, primarily on the basis that a higher efficiency appears attainable with steam than with the organic fluids reviewed. Other considerations were the strong historical familiarity with steam and the better availability of steam engine data. Data are based on the use of a reciprocating expander, rather than a steam turbine, because of its better efficiency at partial loads.

a. The relationship of cost to continuous power rating of the steam power system involved some degree of approximation, with very little data available. One item of data was an auto manufacturer's estimate that a 100-hp steam power system would cost approximately 40 to 86 percent more than the 220-hp spark-ignition engine system which it would hypothetically replace. (The comparison included an automatic transmission, drive shaft, and rear axle for each system.) Correcting the spark-ignition engine maximum output to continuous power by an assumed factor of 75 percent, the comparison then applies between a 100-hp steam system and a 165-hp spark-ignition system.

A steam engine manufacturer estimated that a steam engine would cost about as much as a spark-ignition engine including semi-automatic transmission. Using these values, the following estimates were made:

Spark-Ignition Power (hp)	Equivalent Steam Power (hp)	Engine Cost ($)	Automatic Transmission Cost ($)	1.6× Spark-Ignition Cost ($)	Spark-Ignition Engine + Transmission Cost ($)
90	54.5	510	70	816	580
165	100	700	165	1120	865

Based on the above, it was decided to estimate the steam engine cost at approximately twice the spark-ignition engine cost at the same horsepower. This computer plot is shown in Fig. 4-34.

b. The specific fuel consumption relation was based on assumed brake thermal efficiency of 15 percent at the 10-hp engine size, 20 percent at the 160-hp engine size, and a fuel heating value of 18,400 Btu/lb, with linear interpolation between these points. This plot with the points used is shown in Fig. 4-35.

c. The engine weight curve was based upon the response from one source, which indicated a weight of 500 lb for a 36-hp system and 950 lb for a 95-hp system. A straight line interpolation was assumed between these points, and was extrapolated from them. This plot with point used is shown in Fig. 4-36. It is noteworthy that the weight at 95 hp is approximately verified by the value of 957 lb cited for a 100-hp system in Ref. 4-11.

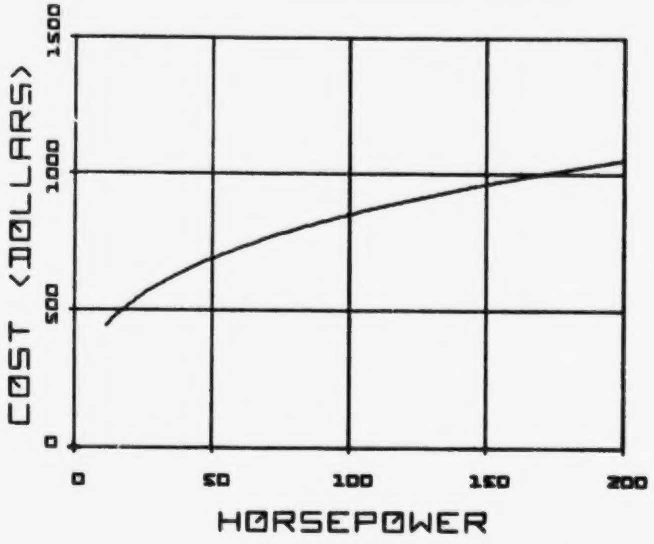

Fig. 4-34 Steam Engine Cost vs. Continuous Horsepower

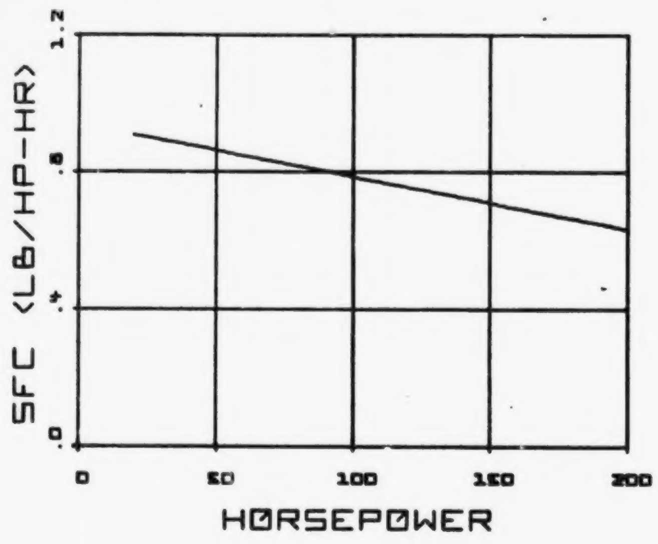

Fig. 4-35 Steam Engine Specific Fuel Consumption vs. Continuous Horsepower

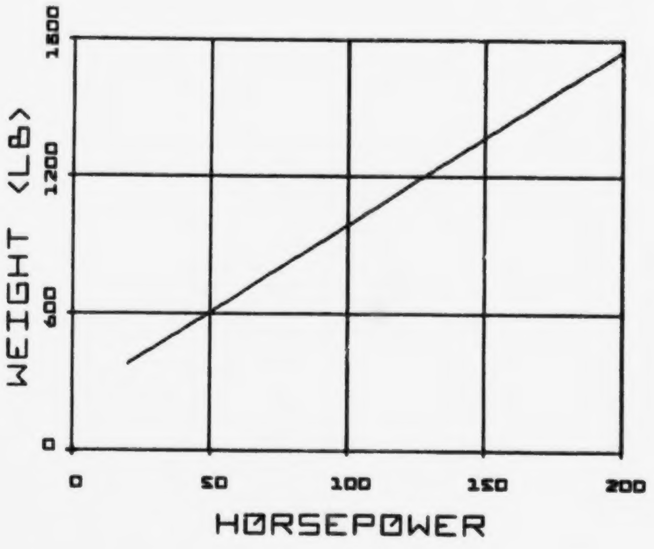

Fig. 4-36 Steam Engine Weight vs. Continuous Horsepower

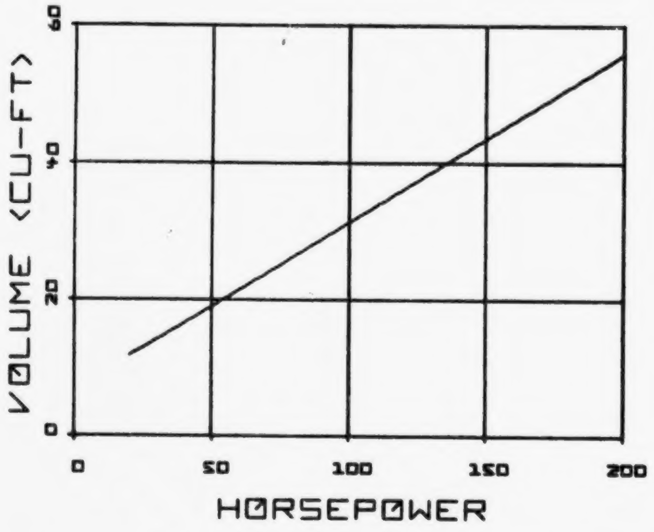

Fig. 4-37 Steam Engine Volume vs. Continuous Horsepower

d. The displacement volume curve was based on a value of 15.6 cu ft at 36 hp, from the data of one of the responses, and a value of 8.0 cu ft at 5 hp from another data input. A straight line was drawn through these points, and then was generally verified by an estimated value of 34.5 cu ft at 100 hp, derived from another data input by proportioning. This plot with points used is shown in Fig. 4-37.

In summary, the following relations are determined to be most applicable to Rankine engines:

Function	Ordinates	Equation
Cost vs. hp	Y vs. X	$Y = A(X)^B$
Specific Fuel Consumption vs. hp	Y vs. X	$Y = A + (BX)$
Weight vs. hp	Y vs. X	$Y = A + (BX)$
Volume vs. hp	Y vs. X	$Y = A + (BX)$

ENGINE COMPARISON

Plots of cost, specific fuel consumption, weight, and volume as a function of continuous horsepower for all four engine types are replotted in Figs. 4-38, 4-39, 4-40, and 4-41, respectively. The gas turbine is seen to be excessively expensive, and the Rankine engine to have excessive volume. The Diesel and spark-ignition engines are acceptable on the basis of all four parameters. The spark-ignition engine has the lowest cost, and the Diesel the lowest specific fuel consumption.

The heat-engine power rating required for the hybrid configuration of each of the four vehicles is shown in Table 4-4. These road power requirements are based on vehicle performance requirements: for the family car, a sustained 65 mph on a 5-percent grade, and for the other vehicles, sustained maximum speed on the level. As shown in Table 4-4, the heat-engine power required is the sum of the road power, drivetrain losses, and accessory loads. The drivetrain losses are based on the efficiency characteristics of the power-splitting transmission.

Table 4-4
HEAT-ENGINE SIZING FOR HYBRID VEHICLES

Item	Road Power (hp)	Drivetrain Losses (hp)	Accessory Load (hp)	Engine Power (hp)
Family Car	87.9	9.8	5.0	102.7
Commuter Car	22.8	5.7	3.3	31.8
City Bus	101.6	25.4	32.3	159.3
Delivery/Postal Van	32.4	8.1	0.2	40.7

The resultant heat-engine power ratings for the family car and city bus were used in conjunction with the engine trend curves to determine heat-engine weight, volume, cost, and specific fuel consumption for these two vehicles.

Emissions for these engines were calculated by computer-running each of the engines in both the city bus and the family car. Emission characteristics were those supplied by EPA/APCO. For the family car, the operating profile was the DHEW Urban Dynamometer Driving Schedule; for the city bus the profile used was the City Bus Cycle. For both vehicles, a model of the previously selected power splitting transmission was used.

At each discrete second of cycle time, the engine power was calculated as the sum of rolling resistance, aerodynamic drag, accelerator power, transmission loss, and accessory loads. This power level was used in conjunction with the emission curves to determine HC, CO, and NO_x emissions for the 1-sec interval. The emissions for each second were then summed to yield the total emissions which in turn was divided by the total cycle distance to give the emissions per mile.

The results of these computer runs for the family car are shown in Table 4-5. Emission and parameter values for an average 1970 family car are included for comparison. On the basis of minimum cost and emissions, the spark-ignition engine was chosen as

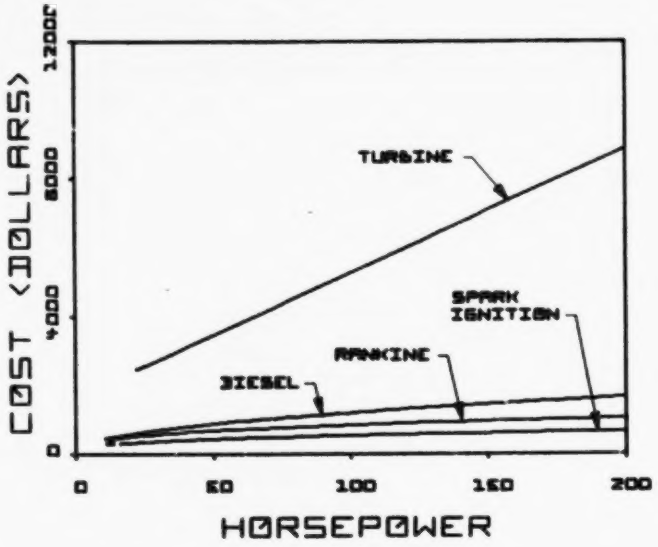

Fig. 4-38 Comparison of Cost vs. Continuous Horsepower

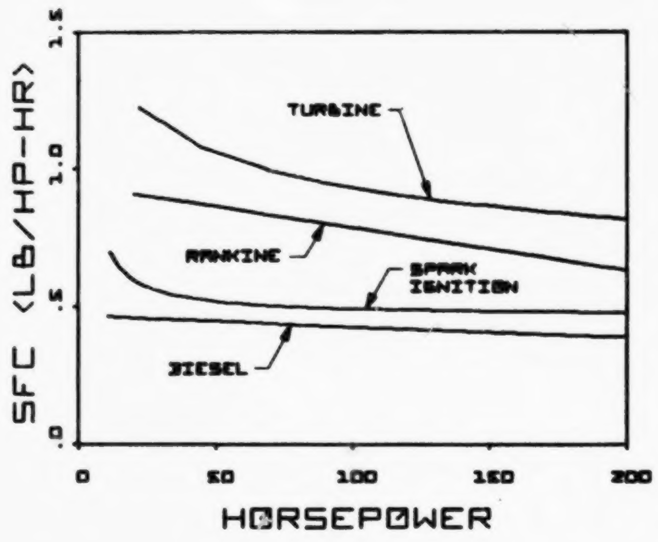

Fig. 4-39 Comparison of Specific Fuel Consumption vs. Continuous Horsepower

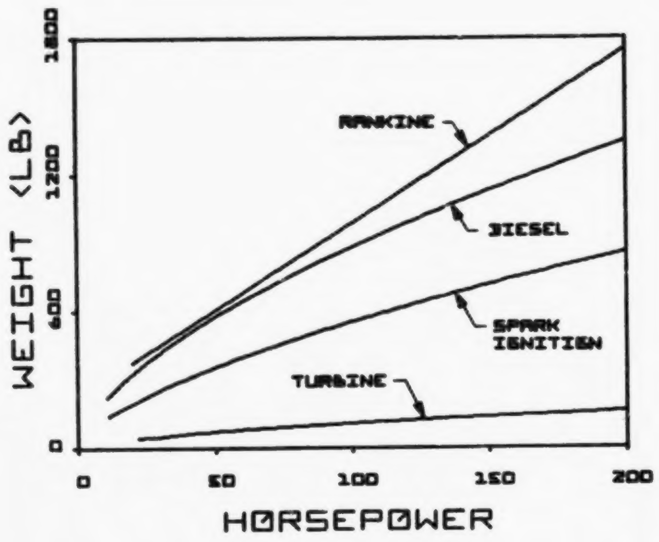

Fig. 4-40 Comparison of Weight vs. Continuous Horsepower

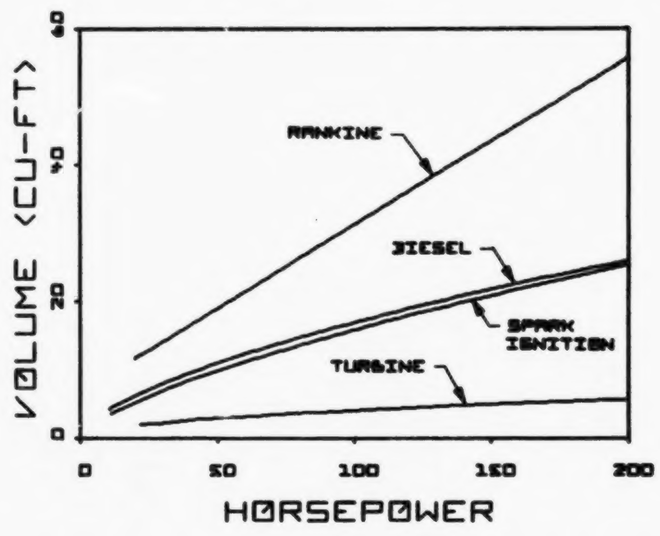

Fig. 4-41 Comparison of Volume vs. Continuous Horsepower

best for the family car. A comparison of these emissions with various standards is presented in Table 4-6. Again, the results are estimates and more refined analysis with better data including cold start effects is needed.

Table 4-5

FAMILY CAR ENGINE SELECTION

Item	1970 Family Car	Power Splitting Transmission							
		Spark-Ignition		Diesel		Turbine		Rankine	
Volume (cu ft)	16	21.0		24.2		8.5		37.2	
Weight (lb)	817	1,034		1,390		672		1,492	
Cost ($)	958	1,050		1,771		5,749		1,476	
Cruise Specific Fuel Consumption (lb/hp-hr)	0.47	0.486		0.424		0.919		0.774	
Emissions (gm/mile)[a]		Best	Worst	Best	Worst	Best	Worst	Best	Worst
HC	3.25	0.083	0.695	0.278	0.487	0.016	0.127	0.229	0.347
CO	36.9	1.42	2.57	0.308	11.6	0.503	5.84	1.88	2.85
NO_x	3.22	0.591	1.11	1.39	4.52	1.94	3.43	0.434	0.650

(a) Includes air conditioning and other accessories.

Table 4-6

FAMILY CAR EMISSIONS

Item	Emissions (gm/mile)			
	1975 Standard	Average New 1970 Car	Flywheel/Hybrid Car	
			With Worst Gasoline Engine	With Best Gasoline Engine
HC	0.45	3.25	0.69	0.08
CO	4.7	36.9	2.57	1.42
NO_x[a]	0.5	3.22	1.11	0.59

(a) Effective Date: Model Year 1976.

The results of computer runs to determine city bus emissions are presented in Table 4-7. Parameter values for a typical 1970 city bus are included for comparison. Table 4-8 shows a comparison of these emissions for the spark-ignition engine and Diesel engine with the 1973 California standard. On the basis of minimum cost and emissions, the engine chosen as best for the city bus is the spark-ignition engine.

Table 4-7

BUS ENGINE SELECTION

Item	1970 Bus	Power Splitting Transmission							
		Diesel		Turbine		Rankine		Spark-Ignition	
Volume (cu ft)	76.5	55.8		31.8		70.9		47.6	
Weight (lb)	4,688	3,743		2,594		3,834		3,181	
Cost ($)	8,138	4,318		9,648		3,748		3,238	
Cruise Specific Fuel Consumption (lb/hp-hr)	0.38	0.404		0.859		0.703		0.480	
Emissions (gm/mile)(a)		Best	Worst	Best	Worst	Best	Worst	Best	Worst
HC		1.81	2.65	0.063	0.520	1.49	2.26	0.540	4.52
CO		1.85	67.8	3.17	34.8	12.2	18.5	9.27	16.7
NO_x		9.04	29.4	12.2	21.3	2.83	4.23	3.84	7.23

(a) Includes all accessories.

Table 4-8

CITY BUS EMISSIONS

Item	Emission (gm/mile)				
	1973 California Standard	Flywheel/Hybrid Bus			
		Worst Gasoline Engine	Best Gasoline Engine	Worst Diesel Engine	Best Diesel Engine
HC	11	4.52	0.54	2.65	1.81
CO	17	16.7	9.27	67.8	1.85
NO_x	25	7.23	3.84	29.4	9.04

Section 5
FLYWHEEL DESIGN STUDIES

In the same time frame as the applicability study and configuration tradeoff study portions of the program, design studies relating to flywheel technology were conducted. These design studies were later specifically directed toward the flywheel sizes and capacities which were established on the basis of the completed configuration tradeoffs.

FLYWHEEL GEOMETRIES

The large variety of flywheel geometries may be categorized into a few basic types. For the purpose of the design studies, consideration was given to six basic types – a pierced uniform disc (i.e., having constant thickness normal to the plane of rotation and a center hole), an unpierced uniform disc, a constant-stress disc, a truncated conical disc (having the manufacturing advantages of the uniform disc while approaching the energy storage efficiency of the ideal constant-stress disc), a rim-type flywheel, and a "bar" type of configuration. In the last, the material is arranged in a prismatic or cylindrical bar rotated about an axis perpendicular to the diameter at its midpoint.

If constraints other than those due to stress considerations are removed from peripheral velocity, flywheel specific energy (in in.-lb/lb) is equal to the ratio of working stress (in lb/in.^{2}) to density (in lb/in.^{3}) times a dimensionless shape factor for the particular flywheel geometry. Flywheel shape factors for various geometries are given in Table 5-1.

Characteristics of the six flywheel geometries are presented in the succeeding paragraphs.

Table 5-1

FLYWHEEL SHAPE FACTORS FOR VARIOUS GEOMETRIES

Geometry	Shape Factor
Pierced Disc (ID/OD = 0.1)	0.305
Bar (Single Filament)	0.333
Thick Rim (ID/OD = 0.8)	0.438
Thin Rim (ID/OD = 1)	0.500
Disc (No Hole)	0.606
Truncated Conical Disc	0.806
Exponential Disc (t_{hub}/t_{tip} = 5.48)	0.807

PIERCED DISC FLYWHEELS

Figure 5-1 shows a computer-generated plot of the shape (half-thickness) of the pierced disc along with the tangential and radial stresses as a function of radius. Since the stresses at the hole edge approach twice that at the center of a solid disc, the pierced disc makes poor use of material unless the material is built up at the proximity of the center hole to overcome the effect of the tangential stress buildup.

RIM FLYWHEELS

The rim-type flywheel is probably the most familiar flywheel geometry. In the rim-type flywheel, material is concentrated near the periphery. The rim material is stressed primarily as a hoop in the tangential direction with a minimal web attaching the hoop material to the center hub or shaft of the flywheel. The shape of the rim-type flywheel is shown in the computer plot of Fig. 5-2 along with tangential and radial stress plots. The rim flywheel appears to be an excellent candidate geometry for filamentary composite materials such as fiberglass bonded with epoxy. These

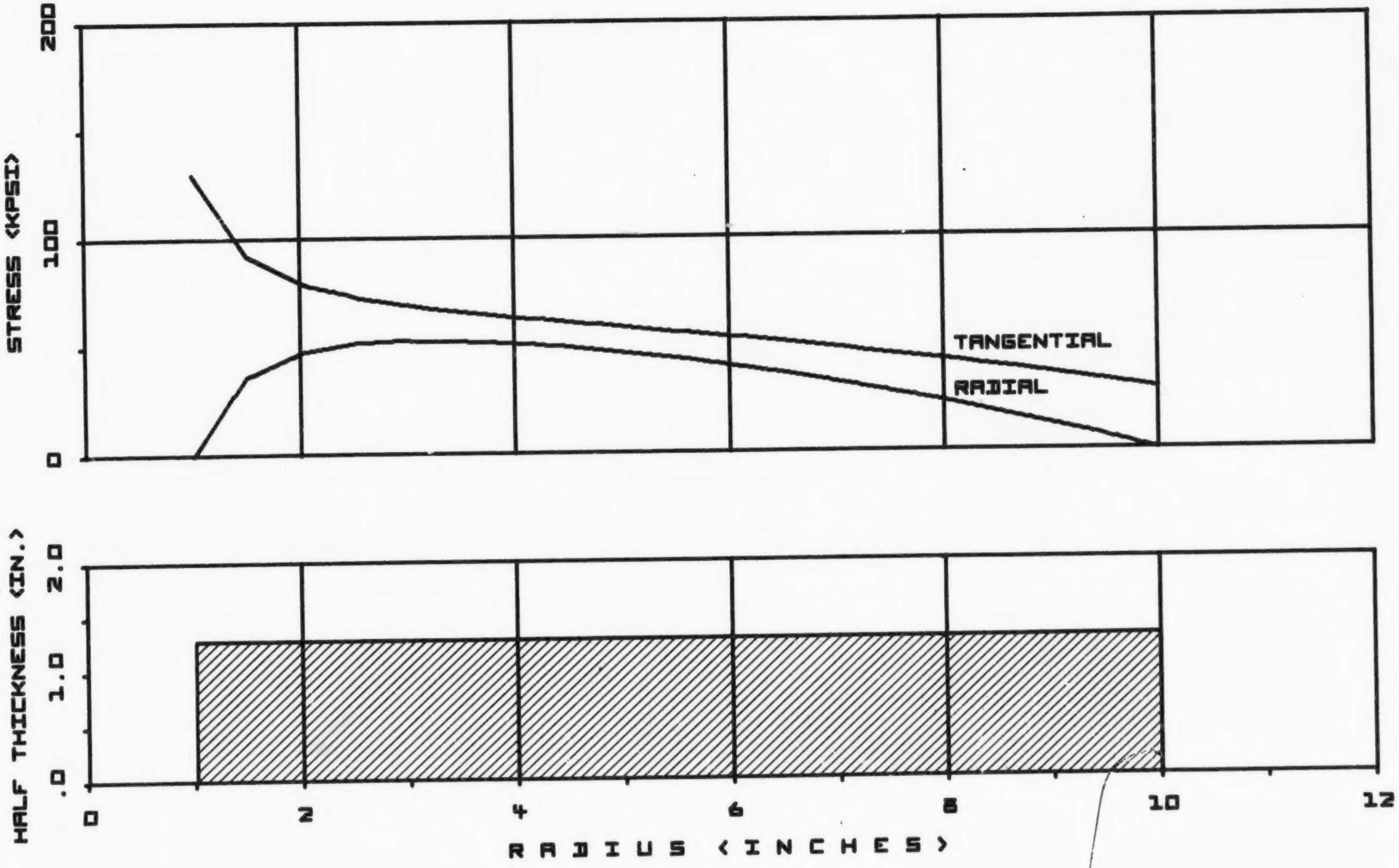

Fig. 5-1 Stress Plots for a Pierced Disc Flywheel

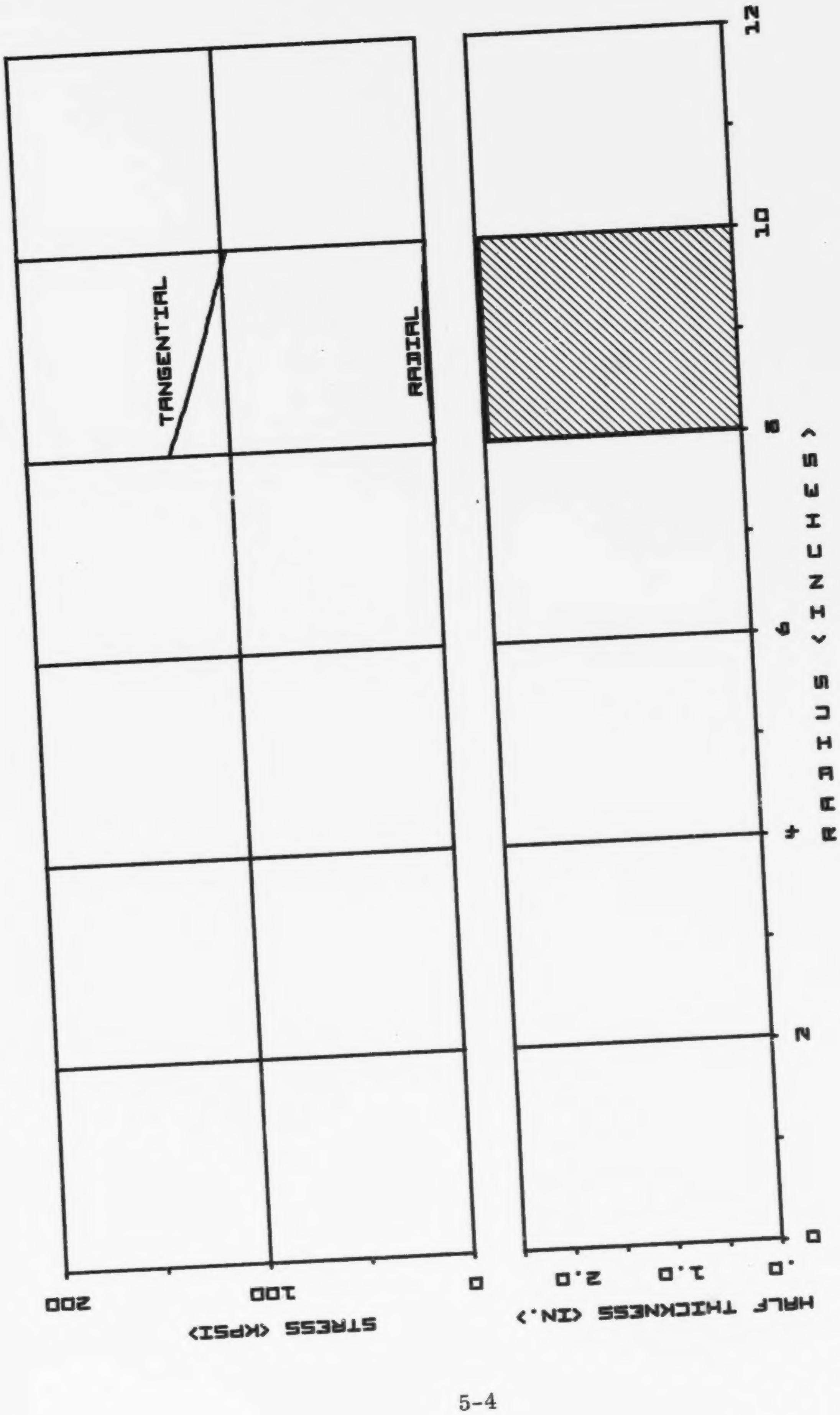

Fig. 5-2 Stress Plots for a Rim Flywheel

materials characteristically have high strength in the direction of the filaments and offer the possibility of being wound onto the web to support the high levels of tangential (or hoop) stress. Investigations have shown, however, that strain incompatibilities between a filament-wound rim and a homogeneous web present serious problems of rim separation. In addition, difficulties are envisioned in accomplishing the necessary balance without cutting filaments and thereby degrading the primary strength of the rim.

FLAT DISC FLYWHEELS

Theoretically, the flat disc flywheel with an unpierced center offers twice the energy storage capability as the same weight of material in a pierced disc without a reinforced hub. The geometry of a flat disc flywheel is shown in the computer plot of Fig. 5-3 along with the radial and tangential stress plots. The flat disc geometry is also used in many applications, often by virtue of the fact that it makes good use of isotropic materials, such as metals, which can be stressed biaxially.

EXPONENTIAL DISC FLYWHEELS

Analyses dating back to the turn of the century show that for maximum energy density a flywheel of isotropic material takes the form of a disc with exponentially varying thickness, as shown in the computer plot of Fig. 5-4. For any given material, this geometry is nearly twice as efficient as the common rim-type flywheel design previously discussed. The plots of the tangential and radial stresses for the exponential disc flywheel, as shown in Fig. 5-4, reflect that the material is stressed at a relatively constant level over almost its entire mass of material except near the tip. The shape factor of the exponential disc flywheel increases as the ratio of disc thickness at the center to disc thickness at the rim is increased. The ultimate exponential disc flywheel would thus have an infinite edge radius with a zero rim thickness, but of course practical considerations dictate a finite radius.

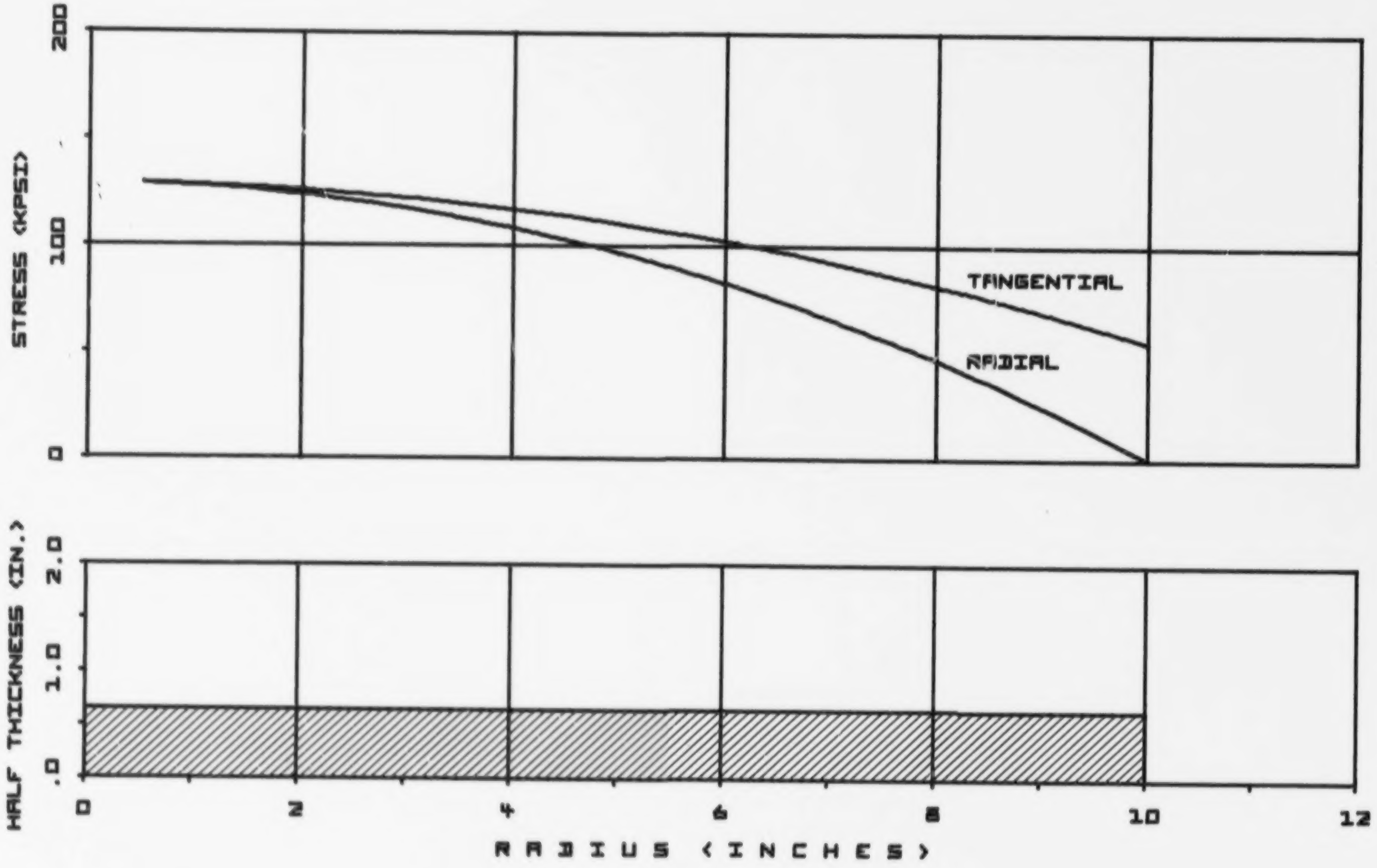

Fig. 5-3 Stress Plots for a Flat Disc Flywheel

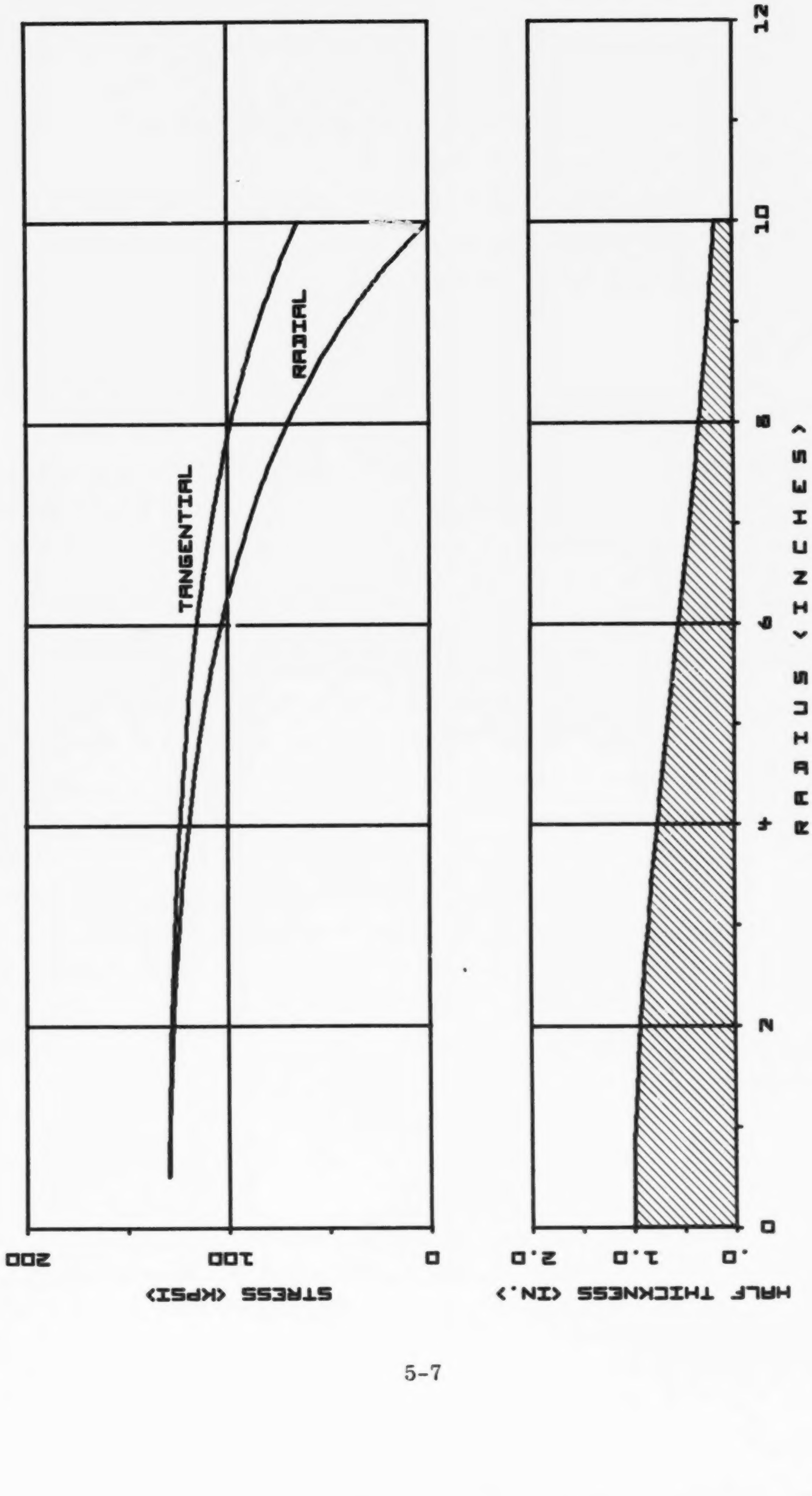

Fig. 5-4 Stress Plots for an Exponential Disc Flywheel

CONICAL DISC FLYWHEELS

A conical disc represents an intermediate case between the flat unpierced disc and the constant-stress disc flywheels. A computer plot of a typical conical flywheel is shown in Fig. 5-5 along with tangential and radial stress plots. The conical disc has almost the same energy density as the constant stress geometry, and the essential simplicity from the standpoint of manufacture of the conical disc often makes it a more desirable shape than the constant stress geometry.

BAR-TYPE FLYWHEELS

The bar flywheel geometry makes use of a log or bar rotated about a transverse axis and was included in the flywheel design studies because of the suitability of this shape for the utilization of filamentary composite materials having high-strength uniaxial characteristics. The bar flywheel configuration is shown in Fig. 5-6.

A simple means of considering the energy density capabilities of the bar flywheel may be obtained by comparing a single filament rotated about its midpoint with a single filament in a theoretical rim. In the rim, the filament would be stressed uniformly throughout its entire length. However, in the single filament bar the stress decreases with the distance from the center of rotation of the filament, and, as seen in Table 5-1 the single filament bar has an energy density only two-thirds that of a single filament thin-rim flywheel. Improvement in the energy density characteristics of the bar flywheel can be brought about by shaping the cross-section of the bar exponentially, again making use of the filamentary material only in its uniaxial direction. In the ultimate case, the shaped bar-type flywheel can approach the energy density of the theoretical rim. This shaping, however, imposes shear property requirements on the bonding matrix which may be difficult or impossible to meet.

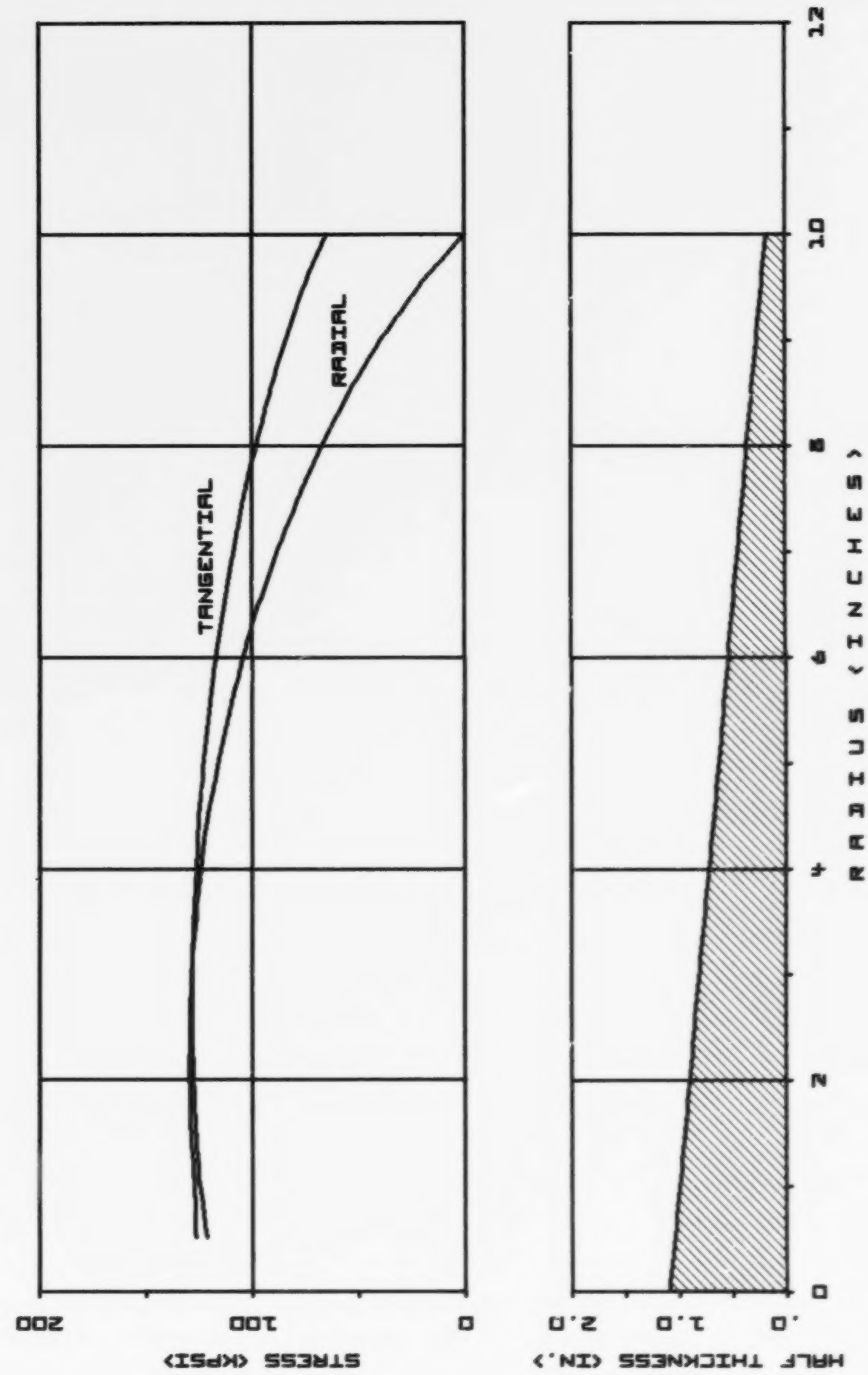

Fig. 5-5 Stress Plots for a Conical Disc Flywheel

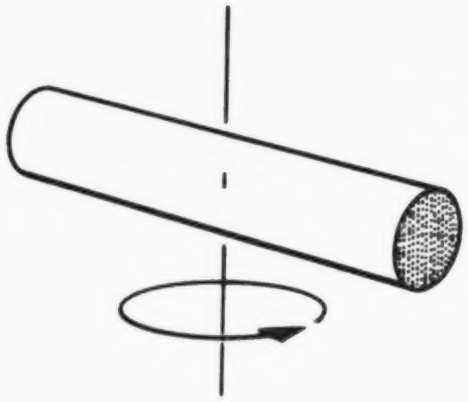

Fig. 5-6 Bar Flywheel Configuration

FLYWHEEL MATERIALS

A survey of materials that could be obtained in mill-run quantities was conducted as a part of the flywheel design studies. Only materials with known characteristics that could be applied to the design, fabrication, and testing of flywheels within the time-frame of the present contract were considered. A total of 11 materials were chosen on the basis of high strength and/or low cost, and are shown in Table 5-2. Recommended working stress was derived from design studies in which the design cycle life of the flywheel was assumed to be 10 million cycles. Material cost was based on mill-run quantities.

In order to facilitate a quantitative comparison, a normalized cost was calculated as follows: material cost was divided by the working-stress-to-density ratio and then divided by the resulting value for the least expensive material. Thus, the normalized cost represents the cost for each material to provide an equivalent energy storage capability for a given flywheel configuration.

The first material shown is 18NI-400 maraging steel, which is the highest strength steel currently available in mill-run quantities with an ultimate tensile stress level of 409 ksi and a yield stress of 400 ksi. The material is specified by the supplier as having a cycle life of 10 million when used at a working stress level of 260 ksi. The $2.25/lb cost of the maraging steel in mill-run quantities is expected to remain at approximately this level since maraging steel is composed of relatively large portions

Table 5-2

FLYWHEEL MATERIALS

Material	Density (ρ) (lb/in.^{3})	Poisson's Ratio (ν)	Ultimate Tensile (F_{tu}) ksi	Yield Tensile (F_{ty}) ksi	Working Stress (σ) ksi	$\frac{\sigma}{\rho}$ ($\times 10^6$)	Material Cost ($/lb)	Normalized Cost ($/lb)
18NI-400 (Maraging Steel)	0.289	0.26	409	400	260	0.900	2.25	5.30
18NI-300 (Maraging Steel)	0.289	0.30	307	300	200	0.692	2.25	6.89
4340 Steel	0.283	0.32	260	217	130	0.459	0.60	2.78
1040 Steel	0.283	0.30	87	58	36	0.127	0.30	5.00
1020 Steel	0.283	0.30	68	43	25	0.088	0.30	7.23
Cast Iron	0.280	0.30	55	37	20	0.071	0.30	8.94
2021-T81 (Aluminum)	0.103	0.33	62	52	26	0.252	0.53	4.45
2024-T851 (Aluminum)	0.100	0.33	66	58	35	0.350	0.50	3.03
6Al-4V (Titanium)	0.160	0.32	150	140	82	0.512	4.00	16.55
E-Glass	0.075	0.29	200	–	67	0.890	0.42	1.00
S-Glass	0.072	0.293	260	–	87	1.210	0.75	1.31

of cobalt and nickel. The 18NI-300 maraging steel is quite similar to the 400 grade except that the ultimate and yield tensile stress levels are somewhat lower. This material is expected to have a greater fracture toughness than the 400-grade material and thus ultimately may be more desirable because of its greater resistance to the development and propagation of cracks. It is conceivable that a test program would reveal that the working stress level capability of the 300 grade would approach that of the 400 grade for equivalent cycle life and fracture toughness.

AISI 4340-grade steel is a relatively common high-strength hot-rolled steel that has an attractive combination of characteristics – in particular, low cost and a high recommended working stress level. The \$0.60/lb cost shown in Table 5-2 is for vacuum arc remelted 4340-grade steel, which has excellent stress uniformity and a very high level of homogeneity. AISI 1040 and 1020 steels are common steels used in a wide variety of industrial applications. These materials have much lower working stress levels, but at the same time much lower material cost. Cast iron also was considered as a candidate although its stress level is the lowest of any of the ferrous metals considered.

Two grades of relatively high-strength aluminum are shown in Table 5-2. These materials have merit factors better than those of the low-grade steels and cast irons. Aluminum, however, by virtue of its lower density, has poorer volumetric efficiency when applied to kinetic-energy wheels than the heavier ferrous materials. The remaining isotropic or metallic material considered was titanium, which has a relatively high working stress level along with a low density, but is prohibitively high in cost.

Two nonmetallic materials were considered – E-glass and S-glass filamentary composites. These materials are similar in chemical composition but have substantial differences by virtue of the finishing operations used. S-glass is a premium quality glass fiber that is well suited to filament-winding applications. Its high tensile strength makes it ideal in applications where major considerations are high strength and low weight. It also is used in many parallel lay-down lamination constructions. The characteristics of E-glass are very similar to S-glass, although, as shown in Table 5-2, the recommended working stress level and the material cost of the E-glass are somewhat lower.

The normalized costs shown in the right-hand column of Table 5-2 indicate that the most cost-effective material is E-glass, followed by S-glass and then 4340-grade steel. The filamentary composites, however, seem to be readily applicable to only the bar-type flywheel geometry. These filamentary composites might be used in a rim-type flywheel, but at the present time the web attachment and balancing requirements appear to be significant problems. The 4340-grade steel appears to be an excellent candidate material for application to low-cost flywheels in a disc configuration. The 400-grade maraging steel also appears to be an attractive candidate for many applications by virtue of its high working-stress-to-density ratio; and if flywheel weight is a major consideration, and cost is not critical, maraging steel might be the best material. All 11 materials were considered in the flywheel selection that followed.

COMPUTER-AIDED FLYWHEEL SCREENING

When the results of applicability studies were completed, a computer-aided screening of various flywheels for the two selected vehicles was performed. The study results showed that the flywheel size requirements were relatively small since in hybrid configurations the flywheel is required to provide energy only for vehicle acceleration. In the case of the family car, the required kinetic energy from the flywheel was found to be 395 w-hr. In order to provide a reasonable engineering contingency, it was decided to size the family car flywheel at a level of 500 w-hr. In a similar manner, the configuration tradeoffs showed that the city bus flywheel capacity requirement was 604 w-hr. Again, an engineering contingency was added, raising the total city bus flywheel capacity to 1 kw-hr.

The screening of the two hybrid vehicle flywheel types was accomplished with the use of a digital computer, combining all the input information previously derived for flywheel shapes and materials. The six previously described flywheel geometries, in conjunction with the 11 flywheel materials, gave a possible combination of 66 flywheel configurations. However, this number of configurations was reduced by eliminating certain combinations that would appear to be unreasonable. For example the use of filamentary composites in disc-type flywheels was eliminated because the filamentary materials are not well suited for winding into discs. Similarly, the use of the more expensive isotropic materials such as the maraging steels and titanium in pierced discs and rim-type wheels also was eliminated because of the low energy density associated with these flywheel geometries. On this basis, a total of 33 plausible combinations of the six flywheel geometries and 11 materials were considered. In order to have the flywheel design as accomplished by the computer cover a broad range of dimensional ratios, five variations ranging from maximum reasonable radius to minimum reasonable radius (highest speed) and associated thickness dimensions were utilized. Finally, the two flywheel capacities, 0.5 and 1.0 kw-hr, were considered for the computer-aided flywheel screening. Thus, the combination of 33 plausible geometry/materials, along with five dimensional ratios and two capacities, gave 330 possible flywheel configurations to be screened by the computer.

The computer calculated flywheel weight and dimensions along with maximum flywheel speed. In addition, the computer calculated the flywheel assembly weight, volume, and cost. Here, the assembly was assumed to incorporate a housing suitable for maintaining a vacuum, bearings, and seals. Flywheel assembly cost was estimated as three times flywheel material cost plus $3.00/lb for the housing.

To reduce the amount of data to be reviewed, several constraints were applied to the computer to eliminate flywheel types which for one reason or another would be unreasonable for final consideration. The first of these constraints was flywheel assembly weight. It was assumed that the flywheel assembly weight should not exceed half the weight specified for the entire vehicle propulsion system, whether family car or bus. The second constraint was on flywheel assembly volume, where again it was assumed that the assembly volume should not exceed 50 percent of the total volume specified for the propulsion system for either the car or the bus. The third set of constraints was applied to the dimensions of the flywheel assemblies. In the case of the family car, it was assumed that the flywheel assembly radius should not exceed 2 ft and that the assembly height should not exceed 1 ft. These constraints were assumed to represent maximum realistic values for fitting the flywheel assembly into a family car.

Similar dimensional constraints were applied for the city bus; flywheel assembly radius would not exceed 3 ft, nor the assembly height 2 ft. A speed constraint of 24,000 rpm also was applied. The selection of this speed was based on the availability of relatively inexpensive high-quality seals and bearings as a function of speed. The high availability of seals and bearings up to about 24,000 rpm is probably due to the common use of 400 Hz electrical power for the operation of two-pole electric motors as is common practice in commercial and military aircraft systems. Bearings and seals for large rotating masses at speeds higher than 24,000 rpm generally must be specifically designed, are relatively high in cost, and are not readily available.

A final constraint placed upon the flywheel assembly was that of cost. The assumption used was that for family cars or city buses a cost greater than \$0.50/w-hr of energy stored would be unreasonably high. The constraints were then applied by the digital computer which selected 24 acceptable candidate flywheels suitable for application to the flywheel/heat-engine hybrid vehicles. The computer-calculated values of size, weight, and cost for these flywheel assemblies are shown in Table 5-3.

SELECTION OF HYBRID VEHICLE FLYWHEEL DESIGNS

Of the 24 acceptable hybrid flywheels, 11 are suitable for application to the family car with the energy storage capacity of 500 w-hr. These flywheels include pierced disc, flat disc, conical disc, and exponential geometries, but exclude all bar and rim geometries by virtue of the imposed constraints. The optimum flywheel for the family car from the standpoint of minimum assembly cost, size, and weight is shown in Table 5-3 to be the constant-stress disc of 4340-grade steel. The cost shown represents the projected assembly cost in automotive quantities after amortization of necessary tooling. Thus, the decision was made to fabricate two identical 46-lb, 24,000-rpm flywheels from 4340-grade steel in the exponential geometry, as described in Section 6.

The acceptable hybrid flywheel configurations suitable for the city bus are seen in Table 5-3 to cover essentially the same range as those for the family car with the exception that two of the filamentary composite flywheels in the bar configuration are shown

Table 5-3

HYBRID FLYWHEELS

Capacity (kw-hr)	Material	Geometry	Flywheel Speed (rpm)	Flywheel Weight (lb)	Assembly Weight (lb)	Assembly Volume	Assembly Cost ($)[a]
0.5	4340	Pierced Disc	21,749	111.7	124.8	0.75	240.44
0.5	4340	Solid Disc	22,821	57.6	74.9	0.39	155.65
0.5	1040	Solid Disc	13,453	206.6	222.0	1.39	232.40
0.5	2021-T81	Solid Disc	13,394	105.0	127.9	1.95	235.65
0.5	2024-T851	Solid Disc	21.940	75.8	91.5	1.45	160.70
0.5	4340	Conical	23,410	52.0	69.1	0.20	145.18
0.5	2021-T81	Conical	18,698	92.1	112.3	1.0	201.08
0.5	2024-T851	Conical	22,970	66.2	82.5	0.75	148.17
0.5	4340	Constant-Stress	24,000	42.4	59.5	0.12	127.51
0.5	2021-T81	Constant-Stress	24,000	75.2	90.9	0.56	166.50
0.5	2024-T851	Constant-Stress	24,000	56.62	73.52	0.43	135.63
1.0	4340	Pierced Disc	17,308	225.9	242.0	1.52	454.85
1.0	4340	Solid Disc	21,746	115.1	133.7	0.78	262.86
1.0	1040	Solid Disc	10,678	413.1	433.1	2.78	431.52
1.0	2021-T81	Solid Disc	13,394	210.1	233.0	3.89	402.60
1.0	2024-T851	Solid Disc	17,714	151.5	171.7	2.89	287.88
1.0	4340	Conical	22,873	99.5	119.3	0.4	238.26
1.0	2021-T81	Conical	18,097	180.2	199.5	2.0	344.30
1.0	2024-T851	Conical	20,857	130.8	149.8	1.49	293.22
1.0	4340	Constant-Stress	24,000	83.8	104.8	0.22	213.66
1.0	2021-T81	Constant-Stress	24,000	150.3	166.0	1.10	286.00
1.0	2024-T851	Constant-Stress	24,000	110.0	127.9	0.83	218.56
1.0	E-Glass	Bar	15,132	87.6	136.5	9.90	260.59
1.0	S-Glass	Bar	19,199	63.3	108.9	7.63	274.54

(a) Assembly cost elements are described on p. 5-14.

to fall within the constraints. The much greater volume that is available for the flywheel assembly in the city bus permits the glass bar flywheels to be acceptable candidates although the volumetric efficiencies of these flywheel configurations are relatively low as previously noted. Review of the 1.0 kw-hr flywheel designs of Table 5-3 again reveals that the 4340-grade steel flywheel in an exponential configuration has the highest cost effectiveness of any of the designs. This design then appears to be the logical choice for fabrication and testing of flywheels suitable for hybrid city busses. However, it was decided that little additional information would result from fabrication and test of the 1.0 kw-hr flywheel in essentially the same configuration and of the same material as chosen for the 0.5 kw-hr flywheel. Thus, the decision was made to fabricate a flywheel in a very different configuration – the bar flywheel of S-glass filamentary composite bonded with epoxy. Although the cost effectiveness of the S-glass flywheel is shown in Table 5-3 to be somewhat less than that for the E-glass design, the potential of continued cost reduction in the basic S-glass material is highly probable. Thus, in the time period of ultimate production of flywheels in this configuration, the S-glass bar would likely be the type having the greatest cost effectiveness.

FLYWHEEL GYRODYNAMIC CONSIDERATIONS

The gyrodynamic torques which result from the rotation of a flywheel perpendicular to its axis of rotation ~~are simply~~ the product of flywheel momentum and the applied angular rate. Since the flywheel kinetic energy is proportional to the product of flywheel moment of inertia and the square of flywheel rotational speed, while momentum is related to the moment of inertial times the rotational speed, the gyrodynamic forces may be minimized by decreasing the flywheel moment and increasing design speed.

An analysis of gyrodynamic forces was made based on the chosen family car flywheel design. The 0.5-kw-hr family car flywheel with a maximum operating speed of 24,000 rpm has a moment of inertia of 0.42 lb-ft/sec^2. In normal vehicle driving operations, the maximum vertical acceleration that is assumed to be applied to the sprung mass of the car is 0.3 g. The flywheel system is assumed to be in the sprung mass. This level is based on vehicle ride studies indicating that 0.3g is the vertical acceleration tolerance limit for most drivers (Ref. 5-1). Similarly, the assumption can be made that the maximum turning velocity at which the car would be operated is one radian per second or a 0.9g turn at 20 mph. Table 5-4 shows the equivalent pitch, roll, or yaw forces that would be applied to the front, side, or rear of the family car resulting from flywheel effects during maximum assumed maneuvers. These maximum force values are shown in Table 5-4 for three orthogonal flywheel spin axis orientations. With the flywheel spin axis vertical, the maximum pitch force that would be experienced due to vertical acceleration would be equivalent to a 25-lb upward or downward force on the hood of the car directly above the front axle. Similarly, the maximum roll force (applied as an upward or downward force at the car door handle) resulting from vertical acceleration is ±43 lb. These force levels are seen to be relatively small in contrast to force variations on the suspension which can occur due to vehicle loading. Although these forces are small, they may cause a different driver "feel" than conventional systems, but these effects can only be assessed properly in a prototype vehicle.

In the case of the longitudinal flywheel spin axis orientation (such as the engine flywheel in most existing cars), Table 5-4 shows that the maximum pitch force resulting from vehicle turning is ±100 lb. The equivalent yaw force (applied to the side of the front or rear fender above the wheel) which results from the vertical acceleration is ±25 lb.

The final case shown in Table 5-4 – the transverse flywheel orientation – results in a maximum roll force due to vehicle turning of ±167 lb, which is roughly equivalent to the effect on the suspension of the addition of a 250-lb passenger near the car door.

Table 5-4

FLYWHEEL GYRODYNAMIC FORCES

Flywheel Spin Axis	Maximum Pitch Force (lb)	Maximum Roll Force (lb)	Maximum Yaw Force (lb)
Vertical	± 25	± 43	–
Longitudinal	± 100	–	± 25
Transverse	–	± 167	± 25

As an additional comparison, it can be shown that the summation of family car wheel and tire momentum values can be approximately half that of the 0.5 kw-hr flywheel. Similarly, the present engine flywheel momentum is nearly one-third that of the proposed hybrid flywheel. Since these momentum values have little effect on the handling characteristics of the present car, it is concluded that the flywheel gyrodynamic forces in the family car are only a minor consideration. Further, it may be concluded that the choice of flywheel spin axis orientation can be based primarily on vehicle packaging considerations. Thus, gyrodynamic considerations do not appear to constrain the vehicle designer. The effect of these forces on a vehicle operating in an environment with a low coefficient of friction (e.g., ice) needs to be studied further.

Precession forces also tend to reduce flywheel bearing life; in fact, the largest bearing loads are those due to precession. Assuming a bearing spacing of 6 in., the peak precession forces on the bearings are approximately 2,000 lb for maneuvers previously described.

Similar conclusions regarding gyrodynamic forces can be drawn for the hybrid city bus flywheel. The larger vehicle dimensions and heavier suspension of the bus serve to minimize the effect of the increased forces.

FLYWHEEL SAFETY

The hazard of an uncontained flywheel failure is so great that it must be positively prevented. Among the possible causes of flywheel failure are the following:

- Material defect
- Accidental overspeed
- Bearing failure
- Vacuum failure
- Vehicle accidents

Generally, there are three modes of flywheel failure: (1) elastic/plastic deformation, which is the usual result of overspeed or excessive heating of a sound flywheel; (2) disintegration, which can result from fatigue stress or material defects; and (3) dislocation, which can result from the failure of both bearings as might occur with a vehicle accident. There are two basic approaches to flywheel failure control: (1) avoid failure by conservative design and inspection, and (2) shield so that a flywheel failure can do no damage.

CONSERVATIVE DESIGN AND INSPECTION

The most common current practice for minimizing the hazards of flywheel and rotor failures is to provide adequate design safety factors in combination with quality control of materials, processes, and finished parts. This approach is commonly used in automotive, aircraft, and industrial systems. In the case of the automotive engine flywheel failure, the bell housing is incapable of containing flywheel disintegration; however, material design margins assure a reasonable degree of safety against failure. The considerable technical effort that has been directed toward turbine rotor safety is applicable to flywheels because of the similarity in design considerations and geometries.

In addition to being designed so as to avoid failure, flywheels may also be designed so as to fail in a nonhazardous manner. For instance, turbine rotors commonly employ a necked section just inside the buckets so that bucket failure will not cause failure of the rest of the rotor. Circumferential grooves may be cut in homogeneous disc flywheels so that crack propagation is inhibited and overspeed will result in bands of material being thrown off in succession from the outside inward. Filamentary composite thick-rim flywheels may be expected to exhibit this type failure. Computer programs are available for designing flywheel shapes so that stresses can be arranged for graceful failure, which can be contained by a relatively light housing.

Inspection requirements for flywheels may be classified into production inspection, periodic inspection, and continuous in-situ inspection. Applicable nondestructive production test techniques include x-ray, ultrasonic, magnaflux techniques, and overspeed testing. Unshielded flywheels should receive overspeed testing and ultrasonic (or x-ray) testing on a 100-percent sample basis. Periodic testing is best accomplished by overspeed testing, and could be conducted during periodic vehicle inspections. In-situ inspection can be accomplished with noncontact probes that sense elastic or plastic deformation, and possibly by detection of the acoustic signature that has been found to accompany incipient crack propagation (Ref. 5-2).

SHIELDING

The second basic approach to flywheel failure control is shielding. This approach is necessary if accidental overspeed cannot be positively prevented. Annular shields can be used to completely contain the flywheel in case of a failure. For the type of flywheels involved in vehicle propulsion, however, the weight of the annular shield may be several times the weight of the flywheel itself. This technique may also incorporate inertia bands – annular rings that absorb much of the flywheel energy in coming up to rotational speed as the impacting flywheel or flywheel pieces slow down. Another possibility is the use of lightly stressed peripheral bands integral with the flywheel.

Other techniques that are currently used for rotor burst protection, but which do not appear attractive for this application, are: target shields, where only personnel and critical equipment are shielded; deflectors, which deflect flywheel pieces away from personnel and critical equipment; and plane orientation, where personnel and critical equipment are kept out of the plane of flywheel rotation.

The decision was made to design the flywheels for this program on the basis that no containment would be provided. This approach is in keeping with current automotive practice. Because of the greater energy stored, flywheel containment by lightweight, low cost methods is certainly an area that deserves future study.

FLYWHEEL ACCESSORIES

The environmental requirements of a flywheel applied to an urban vehicle propulsion system were reviewed as a part of the design studies. The two flywheels considered for the hybrid car and city bus have supersonic peripheral operating speeds. This leads to the requirement for flywheel operation in a low-pressure environment with the concommittant need for a housing, an evacuation system, and rotating seals. In addition, the flywheel must be supported on a bearing system suitable for the speed range and capable of sustaining the shock, vibration, and gyrodynamic loads resulting from vehicle operation.

FLYWHEEL HOUSING

High-energy-density flywheels must be operated in vacuum so that the pumping losses will not be excessive. An empirical relationship, which shows the magnitude of windage power losses, was used to make gross determinations. This equation (supplied by EPA/APCO) is based on the analyses of Daily and Nece (Ref. 5-3) as well as Mann and Marston (Ref. 5-4). The steady-state windage loss calculation is for an unshrouded disc rotating in a noncompressible gas in the subsonic region. Limited test data acquired in the present program have shown the equation to be reasonably accurate (perhaps ±10 percent) for nonshrouded flywheel operation in the supersonic region. The losses with an optimized shroud may be reduced substantially.

The equation is as follows:

$$hp = 0.006 \left(1 + \frac{2.3t}{R_o}\right) \left(\frac{P}{T}\right)^{0.8} \left(\frac{N}{10^4}\right)^{2.8} \left(R_o\right)^{4.6} \left(\mu\right)^{0.2}$$

where

hp = steady-state windage hp
t = tip thickness in in.
R_o = outer radius in in.
P = air pressure in psia
T = temperature in °R
N = rotational speed in rpm
μ = air viscosity in lb/hr-ft

A plot of windage loss as a function of pressure for the 0.5-kw-hr family car flywheel was made based on the following flywheel parameters:

N = 24,000 rpm
R_o = 10.22 in.

t = 0.576 in.
μ = 0.0431 lb/hr-ft (at 60° F)
T = 519.4°R

This plot, shown in Fig. 5-7, indicates that a vacuum level of 0.01 atmosphere (7.6 mm hg) or better is desirable if pumping losses are to be held to 2.5 hp. Even with the use of an optimized shroud, this vacuum level is required if windage losses above 1 hp are unacceptable.

The housing to hold the flywheel bearings and seals must then be capable of withstanding atmospheric pressure. Such a housing is most simply made from a steel or aluminum casting in two halves that can be line-bored for the location of bearings and seals. The ultimate housing design should give full consideration to the tradeoffs involved with material cost, fabrication cost, size, weight, internal (shrouding) contour, bearing and seal replacement, and mounting arrangement with respect to the vehicle.

FLYWHEEL BEARINGS AND SEALS

The constraint placed on flywheel maximum operating speed (24,000 rpm) in the computer-aided flywheel design was imposed so that the selection of bearings and seals could be made from a relatively wide range of commercially available items.

A review of bearing requirements has shown that angular-contact ball bearings are well suited to the hybrid flywheel application for either the bus or car flywheels. The flywheel as mounted on the bearing system is expected to be always rotating in the subcritical mode. Thus, the effective center of mass of the flywheel will rotate in a small circle as permitted by the radial clearance in the bearings. The diameter of this circle of rotation must be held to a minimum in order to prevent excessive radial forces on the bearings. The recommended bearing systems for the flywheels should make provision for preloading the bearings to maintain the proper radial clearance. The angular-contact bearings may be used in either single or tandem configurations

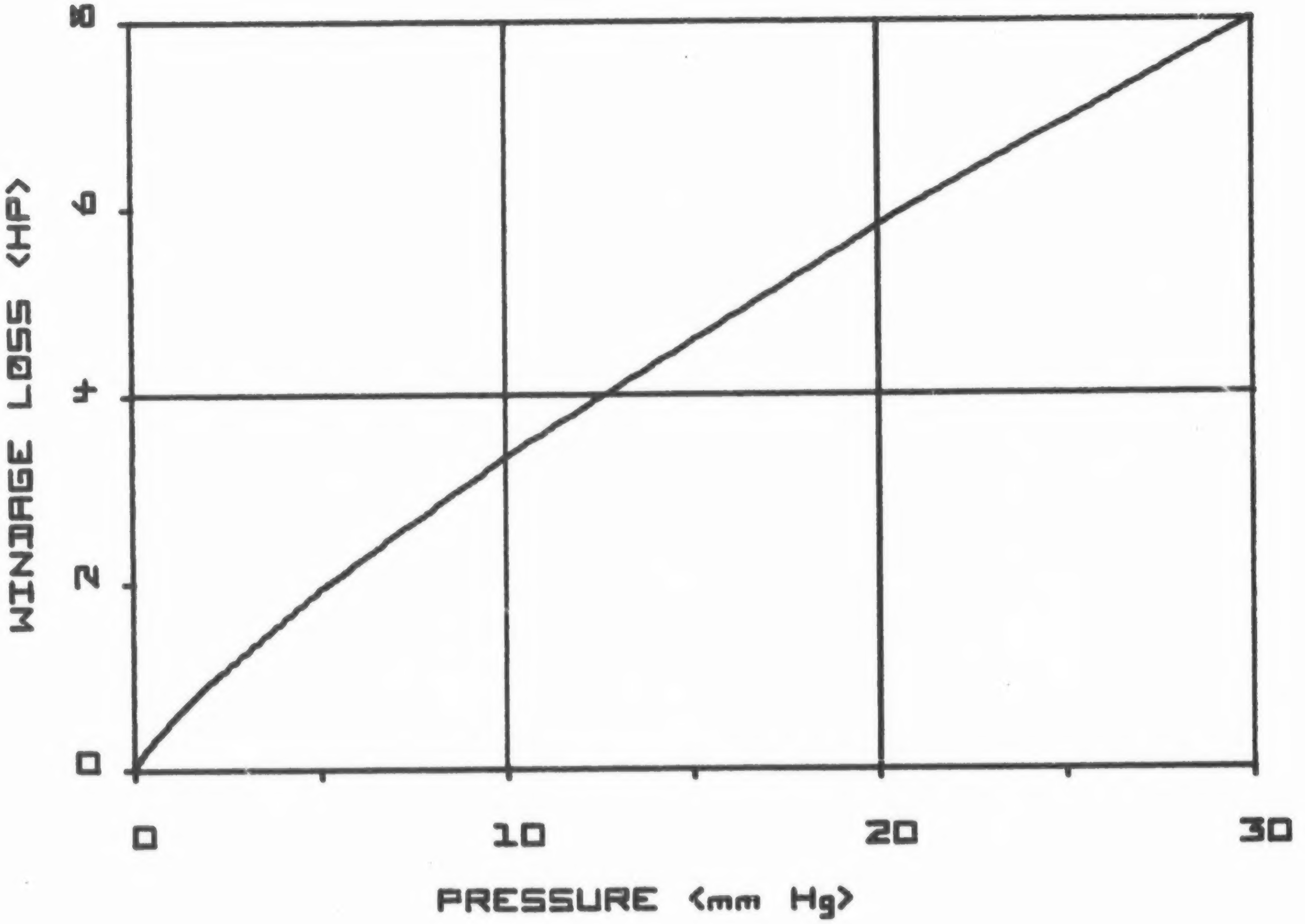

Fig. 5-7 Windage Loss vs. Pressure for 0.5 kw-hr Family Car Flywheel

depending on permissible flywheel unbalance, bearing quality, and life considerations. A lubrication system supplying clean oil or oil/air mist in preference to grease should be provided for the bearings, because of high rotating speeds.

Several rotating seal types suitable for the hybrid flywheel application are commercially available. Since there is no need for a "hard" vacuum, the more exotic aerospace types were not considered. An inexpensive rubbing seal type which appears to be well-suited to the application is the spring-loaded lip seal using low friction carbon-impregnated Teflon. Similarly, the spring-loaded carbon face seal types commonly used in automotive air conditioning compressors appear to be acceptable.

EVACUATION SYSTEM

A relatively simple vacuum system can provide the 0.01 atmosphere evacuation of the flywheel housing. The volume of air to be removed during evacuation is quite small since the hybrid vehicle flywheel housing will be closely contoured to the flywheel. One obvious means of doing most of the evacuation of the housing is by the use of the intake manifold of a reciprocating engine connected through a check valve to the housing. Tests have shown vacuum levels of about 6 in. of Hg or 0.2 atmosphere to be available by this means. The additional evacuation required to reach the 0.01-atmosphere level can be accomplished by several types of simple, inexpensive vacuum pumps. A small flywheel-driven or engine-driven pump could be used. Methods of providing the low-pressure environment is an area that requires further study.

Section 6
FLYWHEEL DETAIL DESIGN, FABRICATION, AND TESTING

The Flywheel Design Studies (Section 5) resulted in selecting an AISI 4340 steel flywheel in the exponential geometry for the family car and an S-glass bar-type flywheel for the city bus. Detailed designs were made for the two types of flywheels; two flywheels of each type were fabricated and tested.

DETAILED DESIGN OF FAMILY CAR FLYWHEEL

The design study recommended a flywheel fabricated of AISI 4340 steel and indicated that a 46-lb weight could be obtained. This weight was based on the configuration shown in Fig. 5-4.

Fatigue data show that AISI 4340 heat treated to 260 ksi can tolerate a static load of 150 ksi, with an imposed sinusoidal load of 27-ksi amplitude for 10-million cycles, with a stress concentration factor of 2.0 applied. This stress concentration factor is more than adequate to account for the flywheel-to-hub transition.

Using such data, it was decided to use a heat treat of 270 ksi and a working stress of 130 ksi.

The following constraints were put upon the design:

(a) Rotational speed (ω) – 24,000 rpm (max.)
(b) Working stress – 130 ksi (max.)
(c) Diameter – 24 in. (max.)
(d) Thickness of the disk $>$ 0.25 in. at any point

The configuration in Fig. 5-4 was used as the initial design. The early dropoff of both the radial and tangential stress made it apparent that more mass could be added to the periphery of the wheel, increasing the stresses throughout most of the flywheel. By increasing the stresses toward the rim, the overall efficiency could be improved. A small rim was added, approximately 0.5 in. deep at the rim and tapering back into the flywheel. Coordinates of the wheel geometry then were put into the data log of the computer, and the stresses were calculated along with a shape factor, which was a measure of the overall efficiency of the configuration. Coordinates then were changed slightly, and a second stress analysis and shape factor were computed. An optimum design was obtained by iterating the design until the shape factor reached a maximum. When the optimum design was plotted and examined, it was noted that the configuration was nearly conical from the start of the hub and out to a radius of 7.25 in. For ease in manufacturing, it was decided to let this part of the configuration become conical. The new configuration is thus a hub section, a conical section extending out to 7.25-in. radius, and a constant radius flare. The major diameter of the flywheel is 20.446 in. with a maximum disk thickness of 0.957 in. at the center and a rim thickness of 0.576 in. Figure 6-1 shows this configuration and a plot of its tangential and radial stresses. The falloff in stress near the hub was deemed desirable in order to offset the stress concentration caused by the shaft. The shape factor was increased to 0.832. Appendix B presents the computer program used for the stress analysis.

FABRICATION OF FAMILY CAR FLYWHEEL

The steel flywheels were fabricated from forged billets of 300M VAR steel – a modified AISI E4340 chromium nickel molybdenum alloy. It is modified by adding vanadium and a higher silicon content to produce high strength levels without the necessity of increasing the carbon content. A vacuum remelt steel was used; this eliminates the major occlusions in the material. Mill run cost of 300M VAR is about $0.60/lb.

After rough forging to produce a radial flow of the disk material, the billets were rough machined and heat treated. This steel will fully harden to a depth in excess of 4 in.; thus, no problems were encountered in achieving full hardening. Samples of the material were heat treated at the same time for material testing. Heat treatment specified was

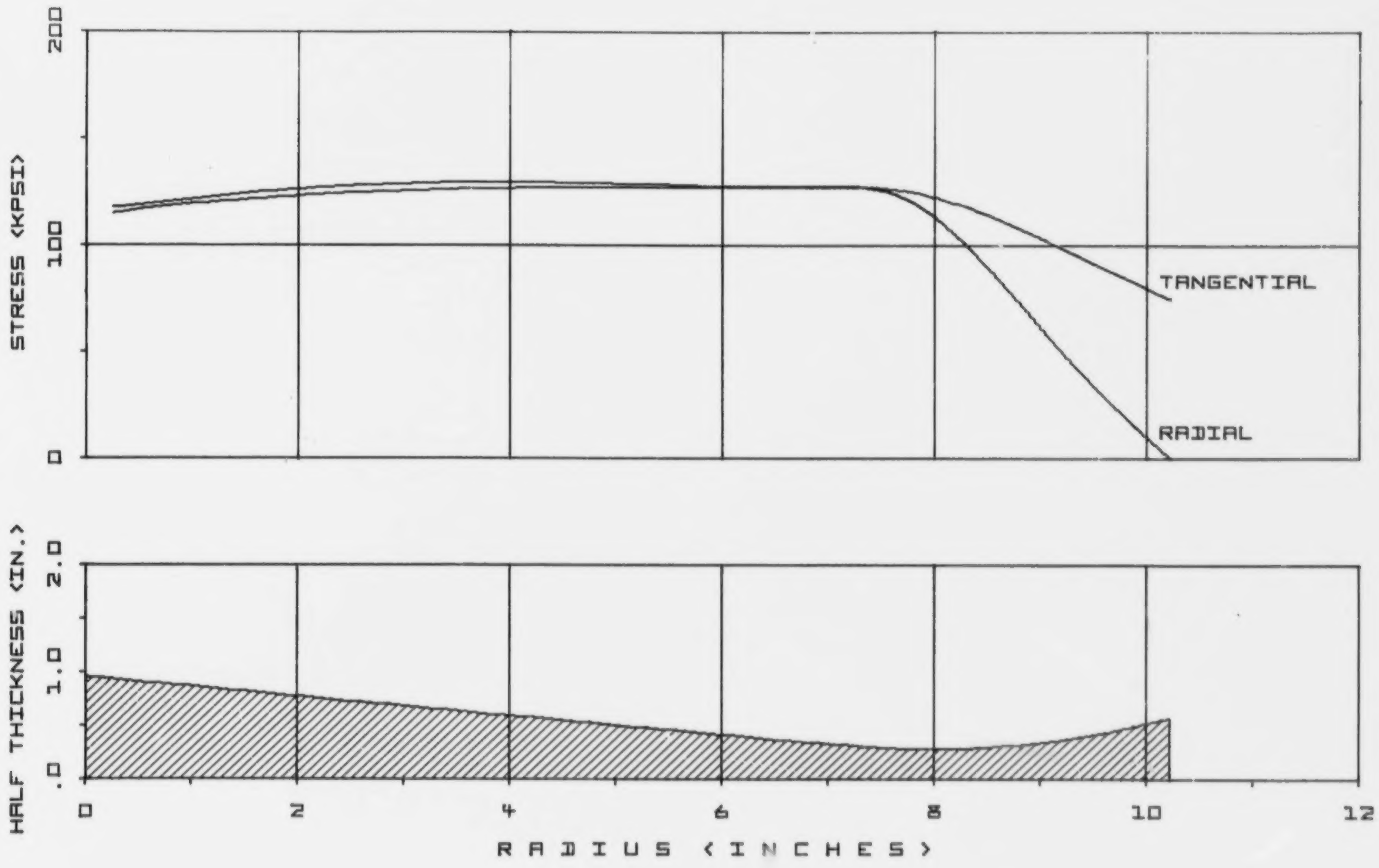

Fig. 6-1 Stress Plots for the Family Car Flywheel

TESTING OF FAMILY CAR FLYWHEEL

NONDESTRUCTIVE TESTS

Nondestructive tests were conducted on the steel flywheels prior to spin testing. These tests are discussed in the section on fabrication.

TENSILE SPECIMEN TESTS

Tensile tests were conducted on specimens fabricated from the same billets that were used to make the steel flywheels. These material tests showed that the steel had an ultimate tensile strength of 290 ksi minimum.

FLYWHEEL NO. 1 – SPIN TESTING

All spin testing was conducted in the LMSC high-speed spin chamber; this is a containment structure of heavy steel plates. The chamber is in a pit below ground level and is sealed to support a vacuum. An air turbine provides spin power, and a disk brake provides high torque levels for extracting power. Torque is measured with a hollow-ring-type torque transducer, and speed is measured with a magnetic pickup and a 60-tooth gear. An automatic digital data reading system was used.

The first steel flywheel was tested to verify pumping losses and energy density (disintegration speed).

Pumping Losses Test. Tests were conducted at various levels of pit vacuum to determine the pumping losses of the flywheel. No actual torque measurements were made; driving torque was estimated from the power output curves of the air turbine at various speeds and inlet line air pressure. Table 6-1 compares the power losses calculated from driving torque and speed with the losses calculated by using the EPA/APCO-supplied equation (see page 5-22).

Table 6-1

COMPARISON OF POWER LOSS CALCULATIONS

Flywheel Speed (rpm)	Vacuum (psia)	Loss (From Turbine Characteristics)	Loss (Calculated From EPA/APCO Equation) (hp)
14,110	8.35	14	15.3
12,530	14.7	13	17.3

Disintegration Test. This test was to determine the speed which would result in flywheel disintegration and thereby would verify the flywheel stress safety factor.

For this test, the flywheel was suspended below the turbine. Two USS T1 steel inertia rings with inside diameters of 24 in. and outside diameters of 35.5 in. were placed between the flywheel and the inside wall of the pit. The rings were 6 and 4 in. in depth, respectively. The inertia rings were to absorb rotational energy of the flywheel at disintegration and protect the inside wall of the pit.

The flywheel was slowly accelerated until disintegration occurred at 35,590 rpm. This represents a peripheral velocity of 3,169.72 ft/sec, an energy density of 26.091 w-hr/lb, and a total energy stored of 1.096 kw-hr.

Failure occurred at a calculated stress of 285,875 psi. This stress compares favorably with an average ultimate tensile stress of 293 ksi measured on four test specimens made from the flywheel material. This verifies that the design analysis is within the accuracy of the measured tensile values of the material.

The flywheel failure may have been initiated at an occlusion on the surface shown in Figs. 6-3 and 6-4.

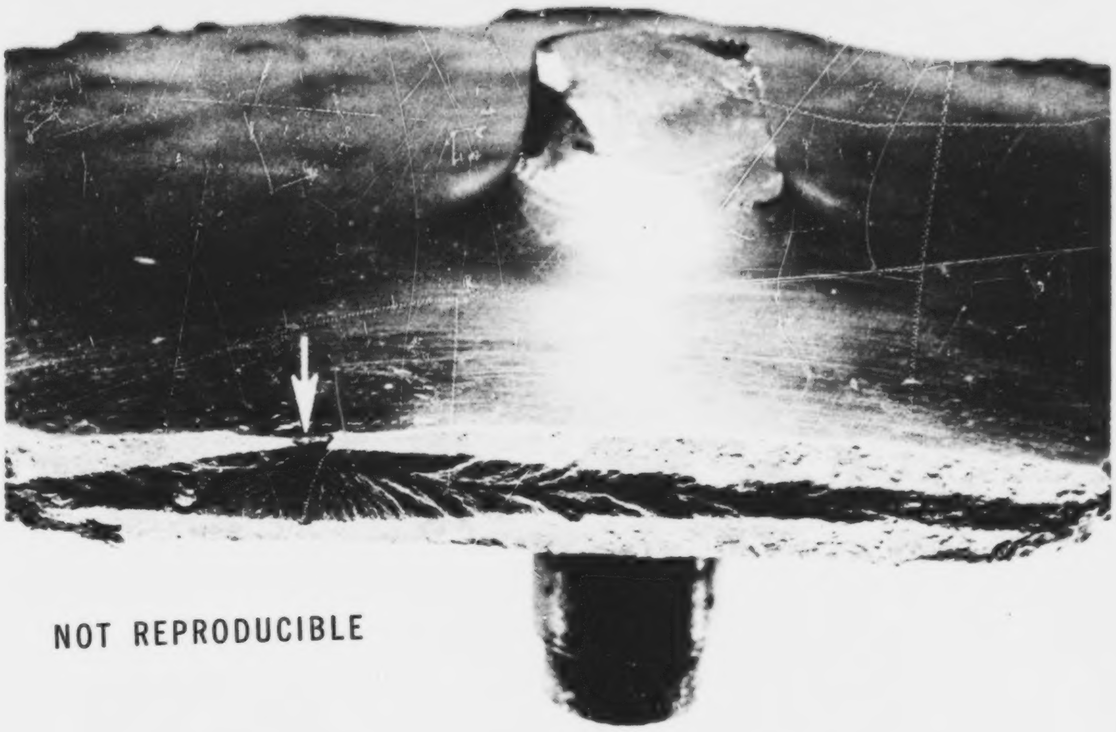

NOT REPRODUCIBLE

Fig. 6-3 Close-up of Occlusion in Failed Steel Flywheel

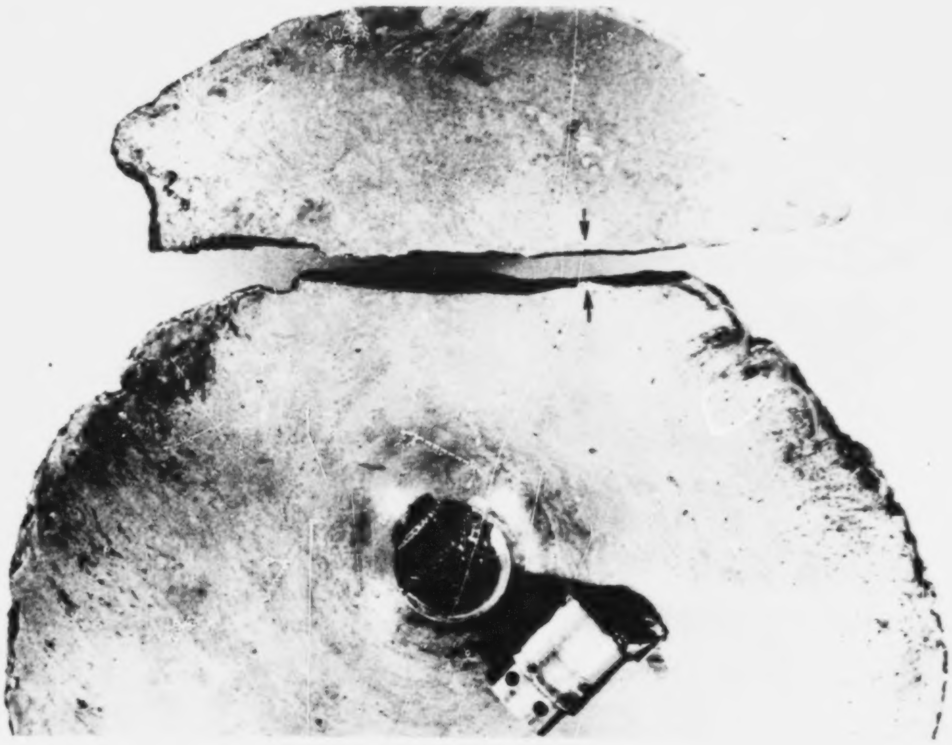

Fig. 6-4 Failed Steel Flywheel

As shown in Figs. 6-4 and 6-5, a large section of the flywheel remained in one piece. The rim and the thin outside section of the flywheel were fragmented by secondary failure.

The effect on the pit was that the inertia rings did not rotate and had been gouged to a depth of approximately 3/4 in. in the worst section.

NOT REPRODUCIBLE

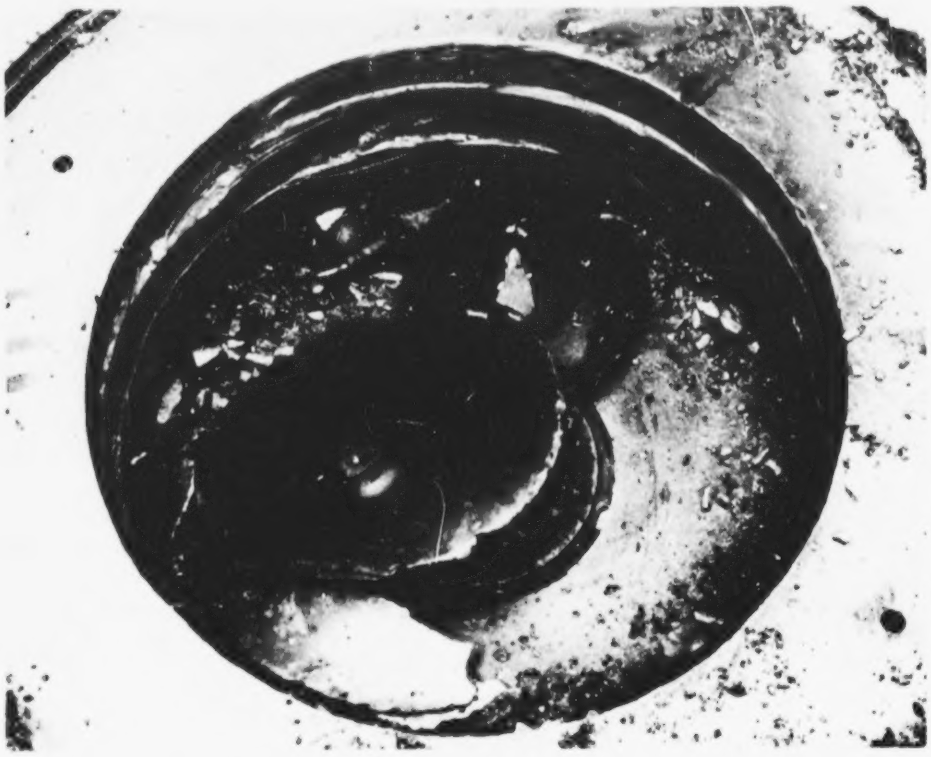

Fig. 6-5 Pit After Disintegration of No. 1 Steel Flywheel

FLYWHEEL NO. 2 – SPIN TESTING

Power density, spindown, and accoustic noise tests were conducted on the No. 2 steel flywheel. During the course of testing the flywheel was cycled over its full speed range 36 times.

Power Density Tests. Power density measurements were made to verify that at least 5,000 w/lb of usable power could be extracted from the flywheel, at various speeds (Table 6-2).

Table 6-2

RESULTS OF POWER DENSITY TEST, NO. 2 STEEL FLYWHEEL

For: 46-lb flywheel $I = 0.4203$ lb-ft-sec^2
Average kw $= 0.142(10)^{-3}\ \tau_{avg.}\ N_{avg.}$
Average kw $= \dfrac{\Delta KE\ (3600)}{\text{interval}}$

Date	Run No.	Speed Increment (rpm)	Average Speed (rpm)	Average Torque (lb-ft)	Average kw Based on Speed and Torque	w/lb Based on Speed and Torque	Initial KE (w-hr)	Final KE (w-hr)	Average kw Based on KE Change	w/lb Based on KE Change
3/4	1	4,570 to 1,850	3,210	69.1	31.5	685	18.13	2.98	54.54	1,186
3/4	2	3,470 to 400	1,935	89.2	24.5	533	10.45	0.14	37.12	807
3/5	1	10,130 to 9,980	10,055	6.9	9.85	215	89.1	86.45	15.17	330
		9,980 to 9,370	9,675	34.9	47.96	1,043	86.45	76.21	62.48	1,359
		9,370 to 8,590	8,980	52.9	67.47	1,466	76.21	64.05	74.20	1,613
		8,590 to 7,750	8,170	61.2	71.02	1,544	64.05	52.13	72.73	1,581
		7,750 to 7,420	7,585	50.3	54.19	1,178	52.13	47.79	26.48	576
3/5	2	11,780 to 11,090	11,435	32.0	51.97	1,130	120.45	106.75	72.56	1,577
		11,090 to 9,620	10,355	88.8	130.61	2,839	106.75	80.33	139.93	3,042
		9,620 to 7,890	8,755	119.1	148.11	3,219	80.33	54.03	139.29	3,028
		7,890 to 7,700	7,795	67.0	74.18	1,612	54.03	51.46	13.61	296
3/5	3	16,530 to 15,520	16,025	28.4	64.64	1,405	237.17	209.08	171.40	3,726
		15,520 to 13,460	14,740	106.9	223.82	4,866	209.08	167.71	252.43	5,487
		13,960 to 13,350	13,655	108.8	211.02	4,587	167.71	154.70	79.38	1,726
		13,350 to 13,260	13,305	16.4	30.99	674	154.70	152.62	12.69	276
3/5	4	23,730 to 22,850	23,290	23.3	73.77	1,603	488.78	453.20	217.10	4,717
		22,850 to 21,860	22,355	70.7	224.50	4,880	453.20	414.78	234.43	5,099
		21,860 to 21,520	21,685	20.9	64.38	1,400	414.78	401.98	78.10	1,698
		21,520 to 21,400	21,460	8.7	26.52	576	401.98	397.51	27.27	593
3/5	5	12,010 to 11,200	11,605	42.5	70.56	1,523	127.08	108.88	111.05	2,414
		11,200 to 9,680	10,440	114.5	169.79	3,691	108.88	81.33	168.10	3,654
		9,680 to 8,070	8,875	121.8	153.54	3,338	81.33	56.53	151.32	3,290
		8,070 to 6,720	7,375	122.2	128.36	2,790	56.53	39.20	105.74	2,299
		6,720 to 6,560	6,640	23.4	22.07	479	39.20	37.35	11.29	246
3/5	6	12,840 to 11,400	12,120	88.3	152.01	3,304	143.10	112.81	184.82	4,017
		11,400 to 10,440	10,920	76.0	117.88	2,563	112.81	94.61	111.09	2,414

The test objective of 5,000 w/lb was exceeded at average speeds of 14,740 rpm and 23,355 rpm on runs 3 and 4, respectively.

Spindown Tests. Spindown tests were conducted by taking the flywheel to 24,000 rpm and uncoupling it from the turbine. The pit was evacuated to 0.2-mm Hg for this test. Rotational speed was measured periodically. After 20 min. of spindown, the pit was vented to the atmosphere. The bearing and the brake disk were the major sources of drag – approximately 3 hp between 24,000 and 20,000 rpm. Bearing drag was high because of oil-flooding of the bearings. The 6-in.-diam. brake disk was running at atmospheric pressure. Figure 6-6 provides a time history of the No. 2 steel flywheel spindown.

Acoustic Test. Prior to the start of the spindown test, a background noise recording was made. All equipment that would not be operating during spindown was turned off. The background noise level was recorded on a General Radio 1525A Data Recorder. The type 1560 P40K preamplifier and microphone was placed 10 ft from the spin pit. System calibration was accomplished with a General Radio Sound Level Calibrator, type 1562A. The noise level was recorded during the entire spindown test. At the conclusion of the test, a post-test calibration was made. Reference sound pressure level (SPL) is 20 micronewtons per square meter.

The data were reduced by playing the tapes back through a Spectral Dynamics Model SD 301 Real Time Analyzer and recording the data on a Mosley X-Y plotter. Figures 6-7 through 6-13 show samples of the reduced data, including sound level and frequency calibration; the only significant noise, above background level, is at the rotational frequency. It should be noted that the maximum sound pressure level (SPL) measured throughout the test was 84.2 dB at 19,500 rpm, at 19,000 rpm the maximum level was 70.2 dB, and at 18,600 rpm the SPL had again increased to 82 dB. From 18,600 rpm, the SPL continually decreased until at 9,800 rpm it was down to 71 dB.

Througnout the test, there was a high SPL recorded at approximately 700 cycles. Because there was no frequency shift of this noise, it was attributed to background machinery, such as a pump, and should not be considered in the noise level of the flywheel.

Obviously, the noise to be expected from a flywheel/hybrid vehicle cannot be extrapolated from these results since the flywheel housing plays an important role in the flywheel assembly acoustical signature.

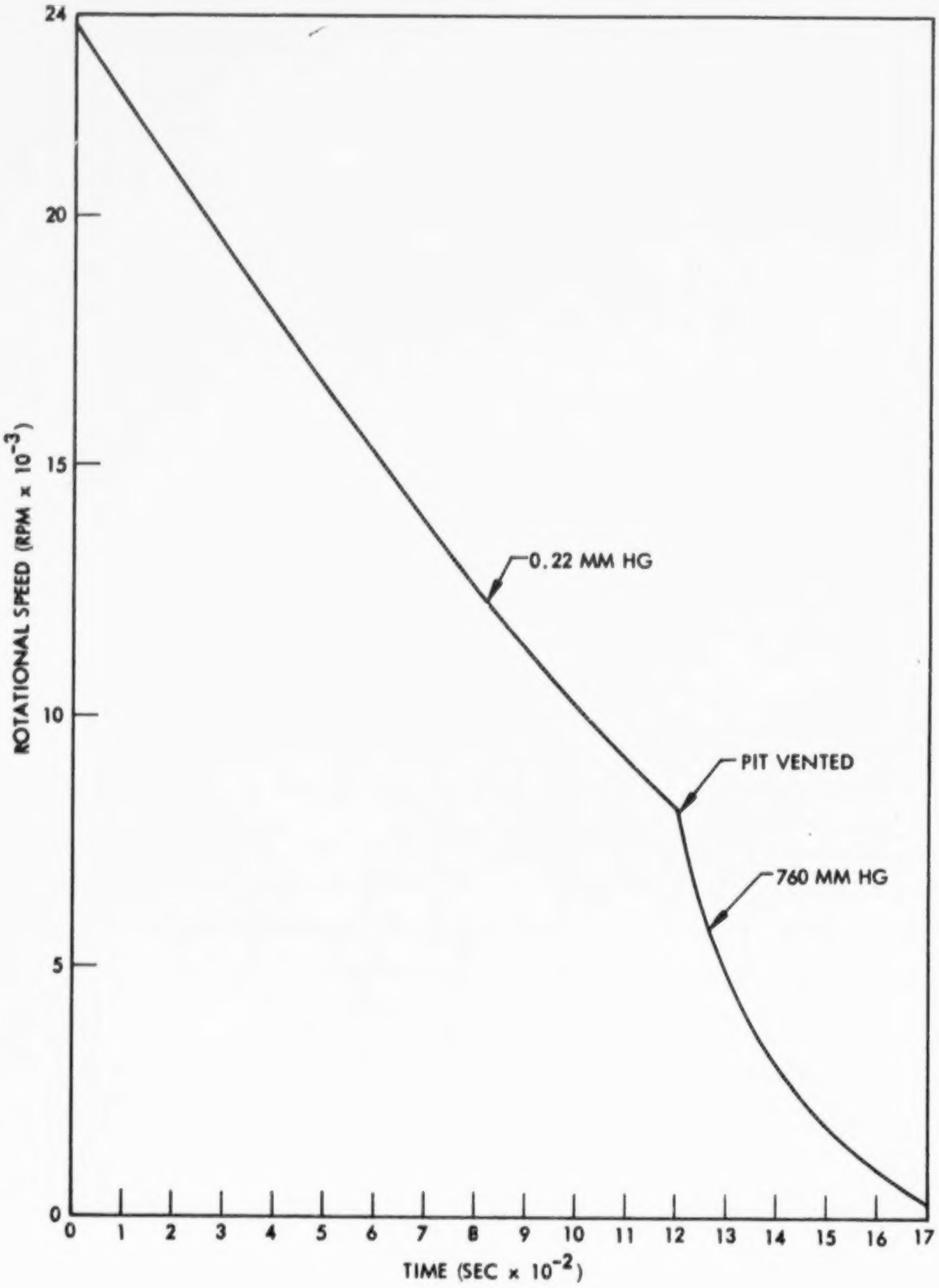

Fig. 6-6 Spindown Test, EPA/APCO No. 2 Steel Flywheel

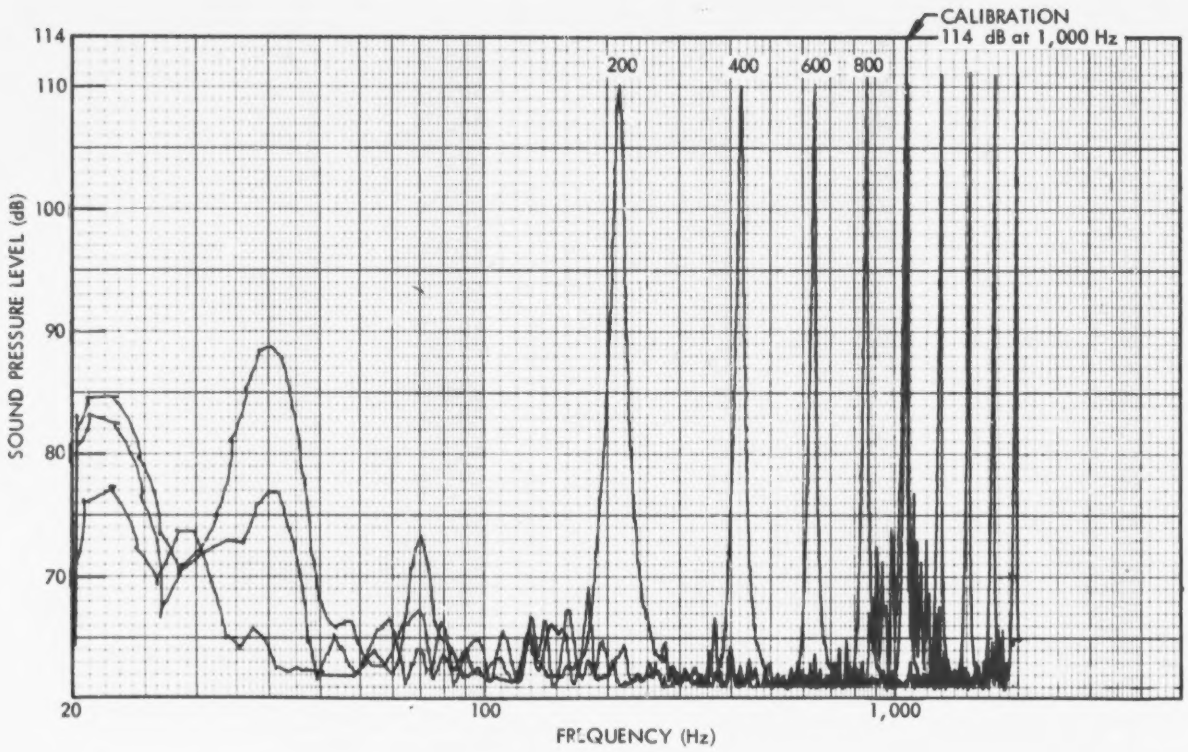

Fig. 6-7 No. 2 Steel Flywheel Acoustic Noise Test Calibration

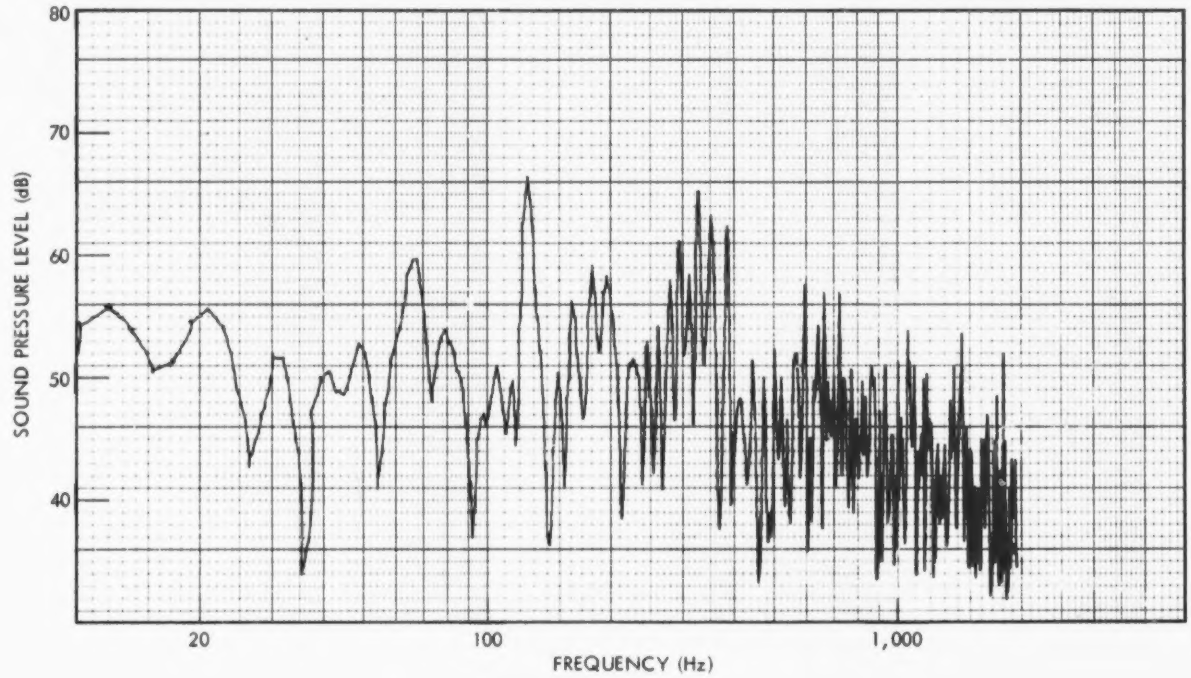

Fig. 6-8 No. 2 Steel Flywheel Acoustic Noise Test Background Level

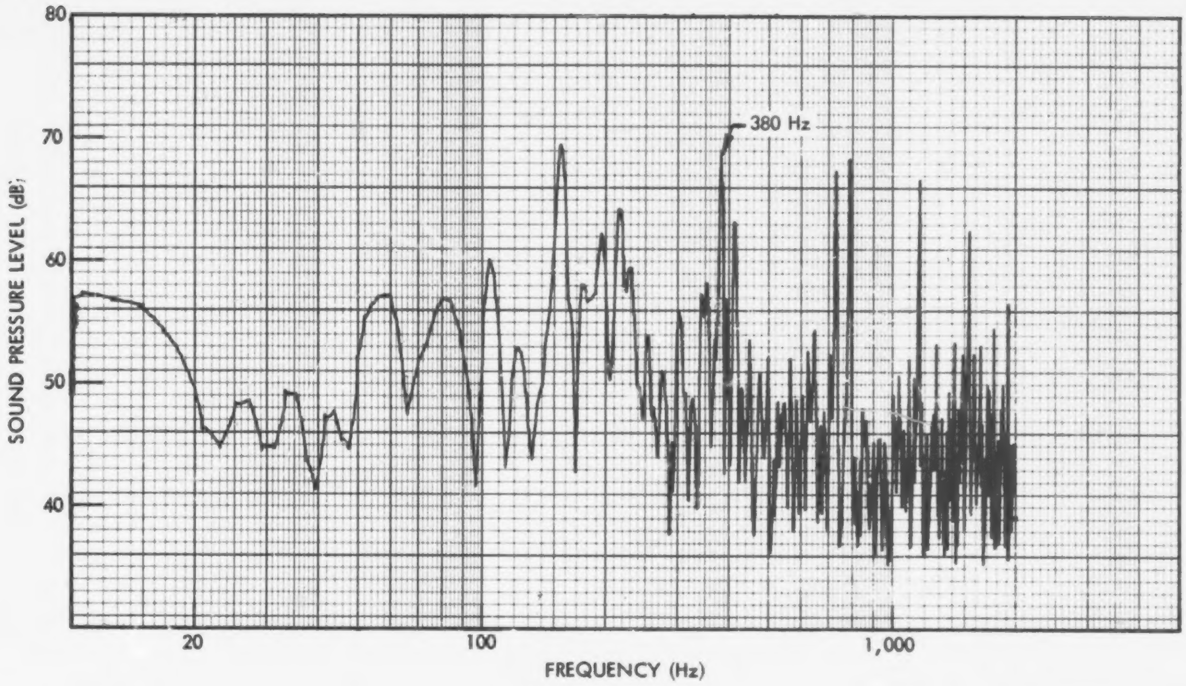

Fig. 6-9 No. 2 Steel Flywheel Acoustic Noise Test – 22,800 rpm

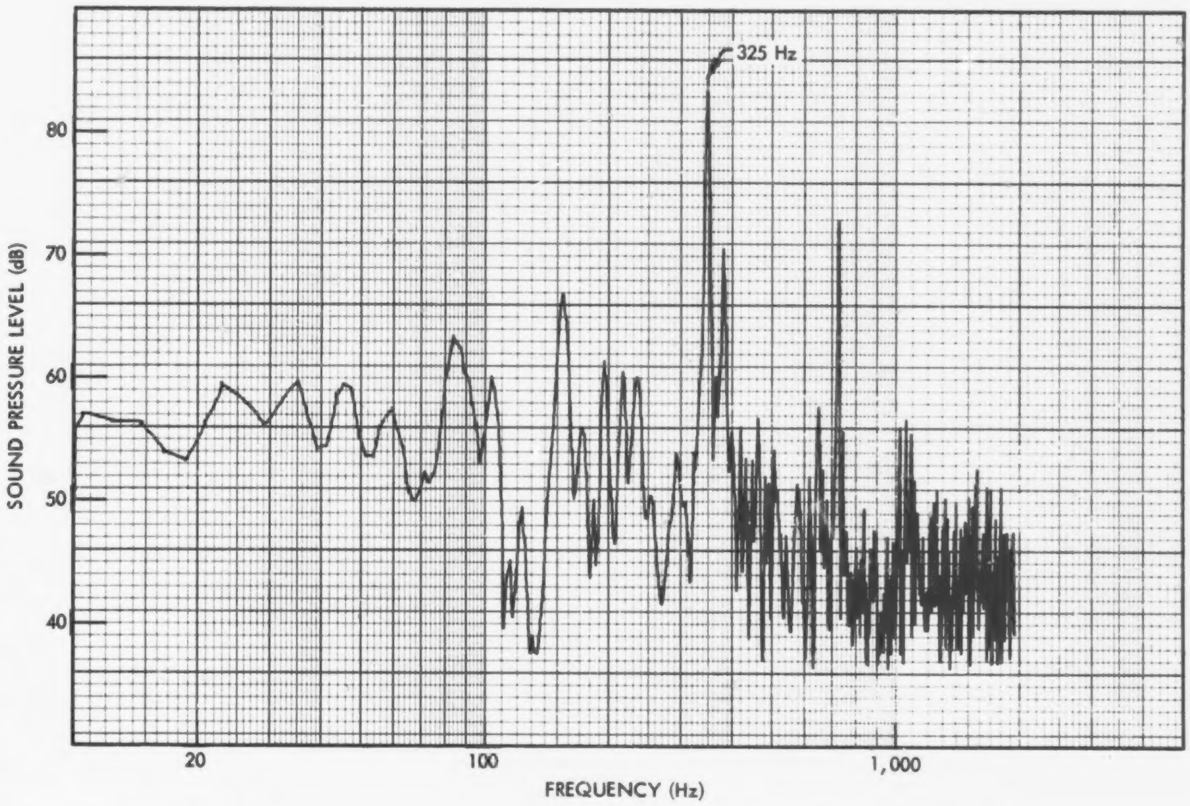

Fig. 6-10 No. 2 Steel Flywheel Acoustic Noise Test– 19,500 rpm

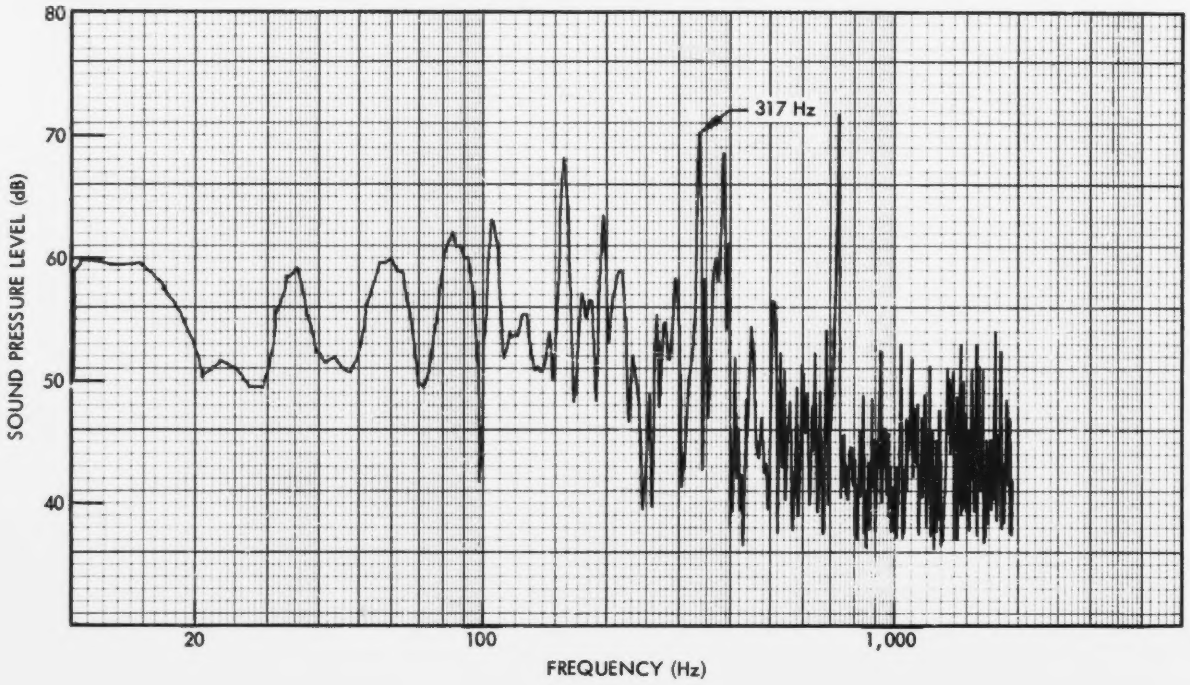

Fig. 6-11 No. 2 Steel Flywheel Acoustic Noise Test – 19,000 rpm

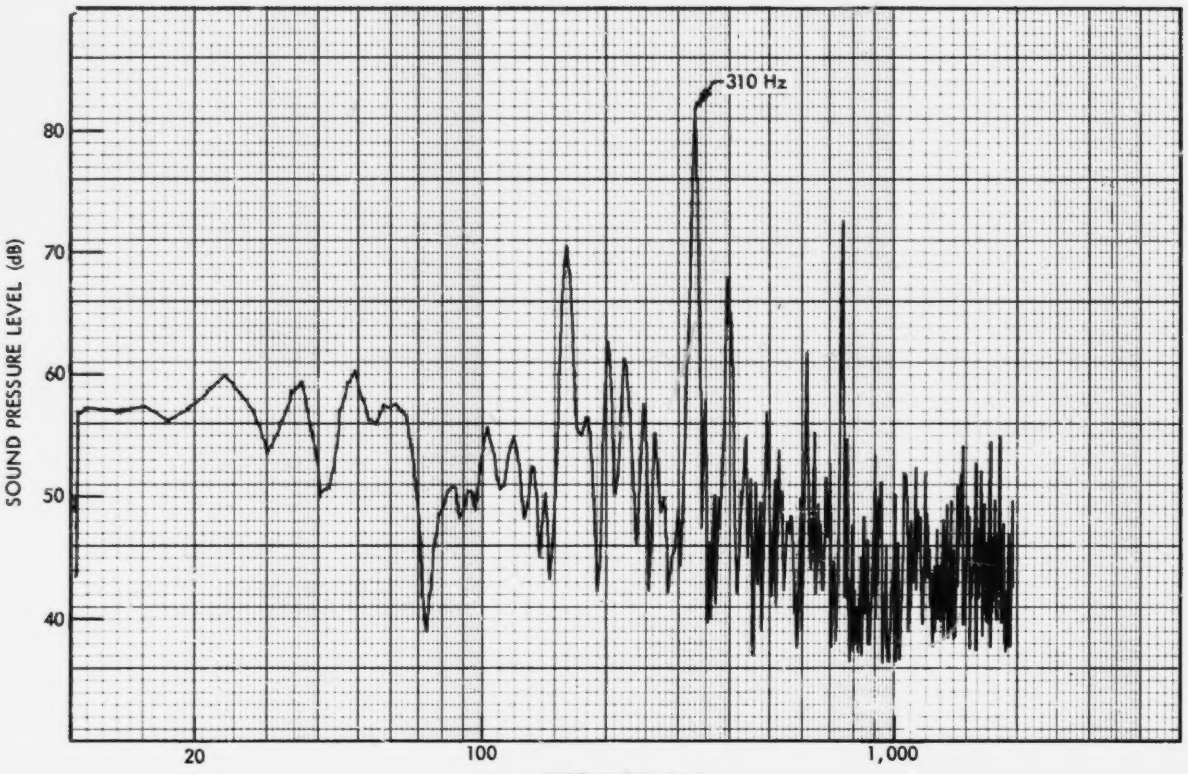

Fig. 6-12 No. 2 Steel Flywheel Acoustic Noise Test – 18,600 rpm

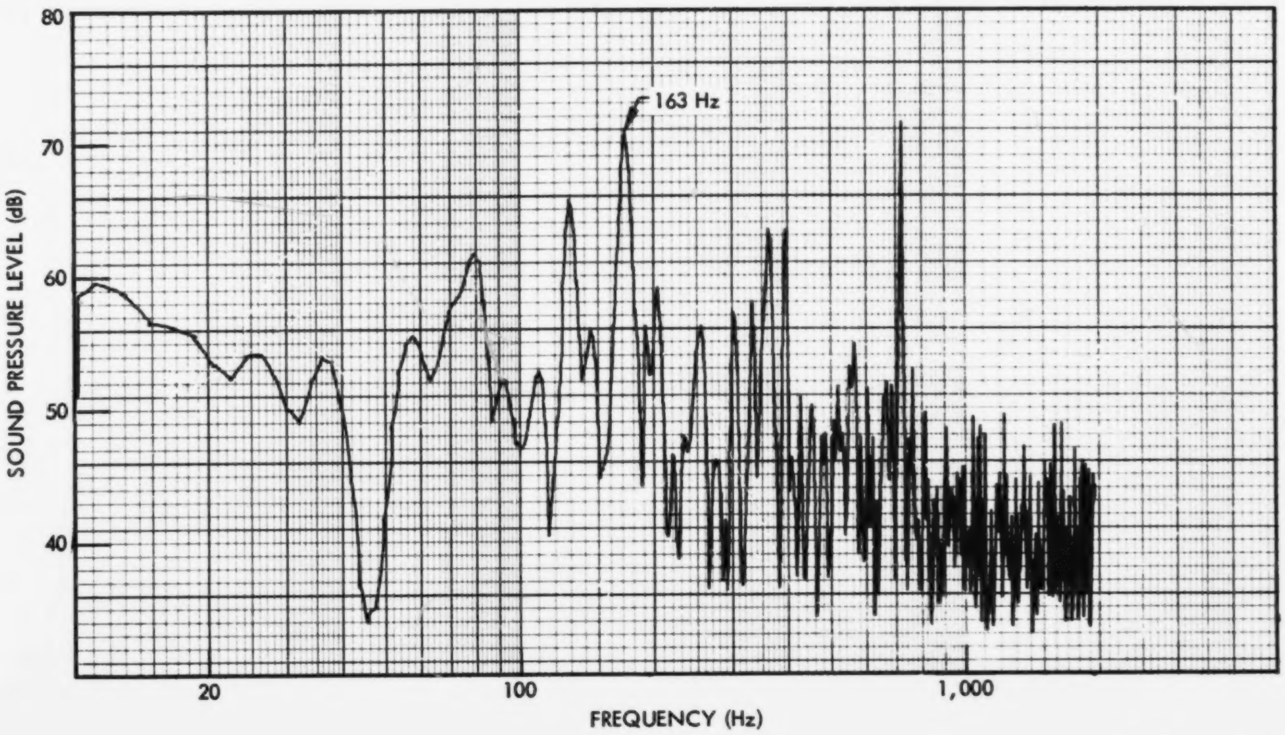

Fig. 6-13 No. 2 Steel Flywheel Acoustic Noise Test – 9,800 rpm

DETAILED DESIGN OF CITY BUS FLYWHEEL

BODY TAPER DESIGN

In a bar-type flywheel, the major stress is longitudinal, i.e., in a direction along the filaments. This longitudinal stress must be carried by the filaments themselves. However, there also is a transverse stress normal to the direction of the filaments. This transverse stress is much lower than the longitudinal stress if the length of the bar is much greater than the width. This transverse stress, as low as it is, can be very important because it must be handled by the epoxy matrix which has a much lower tensile strength than the glass fibers. At the center of the bar the transverse contraction strain caused by longitudinal stress is greater than the lateral elongation caused by lateral stress. On the basis of a strain failure theory, there should be no problem here. However, as the end of the bar is approached, the longitudinal stress goes to zero; thus, so does the lateral contraction resulting from longitudinal stress. The lateral expansion, however, remains undiminished; consequently, there is a danger of splitting or fraying the ends. This splitting would be progressive and would result in a longitudinal delamination of the flywheel. For this reason, the ends of the flywheel were provided with special tapers designed to maintain the lateral strain compressive throughout the length of the flywheel. Although the taper (Fig. 6-14) is required only in the lateral direction, the compound lateral-axial taper was used for ease of fabrication.

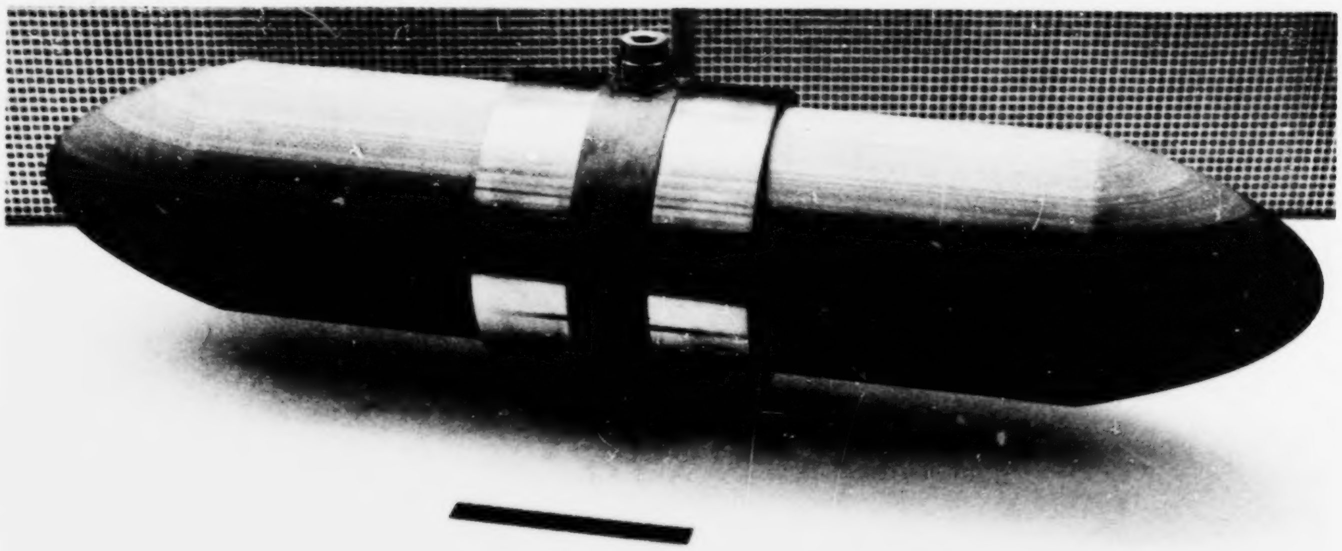

Fig. 6-14 Bar-Type Flywheel

The second bar-type flywheel was identical to the first except that a cross-ply construction was employed to provide additional protection against delamination resulting from lateral stresses. Table 6-3 shows the ratio of longitudinal to transverse interleaves.

Table 6-3

RATIO, LONGITUDINAL TO TRANSVERSE INTERLEAVES

Axial Distance From Centerline (in.)	Longitudinal/Transverse Interleave Ratio
0 to 1.6	3:1
1.6 to 2.2	5:1
2.2 to 2.6	10:1
2.6 to 3.385	1:0

HUB DESIGN

The attachment of the flywheel body to the hub is a major design problem of the bar-type flywheel. At speed, there is a strain incompatibility between the body and the hub; the longitudinal strain in the bar is much greater than that in the hub. Therefore, the attachment must permit relative longitudinal displacement between the body and the hub. However, to maintain balance, there must be very little displacement between the center of gravity of the body and the intended rotating axis of the hub.

Figure 6-16 shows the two pieces of the hub prior to assembly. The slotted sleeve was welded into the hub. This hub assembly then was slipped over the body of the flywheel. The interior surfaces of the hub were coated with mold release, and the flywheel body was prepared for bonding. A potting compound was drawn up the slots and cured. The resulting potted fingers on the body lock with the hub slots to prevent relative rotation or translation, but because the hub surfaces were coated with mold release, relative radial growth caused by centrifugal stress is uninhibited. Translation normal to the longitudinal axis also is prevented because the walls of the hub slots are parallel.

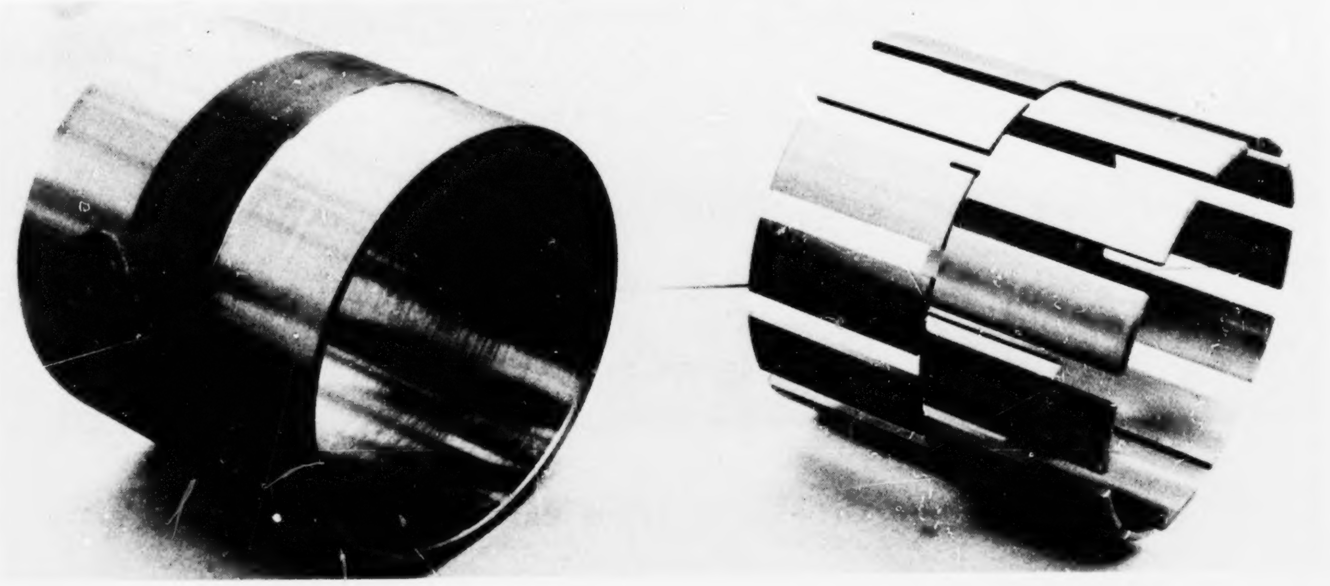

Fig. 6-15 Bar Flywheel Hub Prior to Assembly

FABRICATION OF CITY BUS FLYWHEEL

Two glass bar flywheels were fabricated by using the same configuration but different layup procedures. Both bar flywheels were constructed of Ferro Corporation S-1014 glass fiber with 828/1031/NMA resin. Resin content was 22 percent, by volume.

Prepreg material was laminated to form ten sections approximately 1-in. thick, 36-in. long, and 8-in. wide. These sections were placed in an autoclave for curing, laminated together to form billets 8 in. × 8 in. and 36-in. long, and the entire billet was cured. The final configuration was ground from the billet (Fig. 6-16).

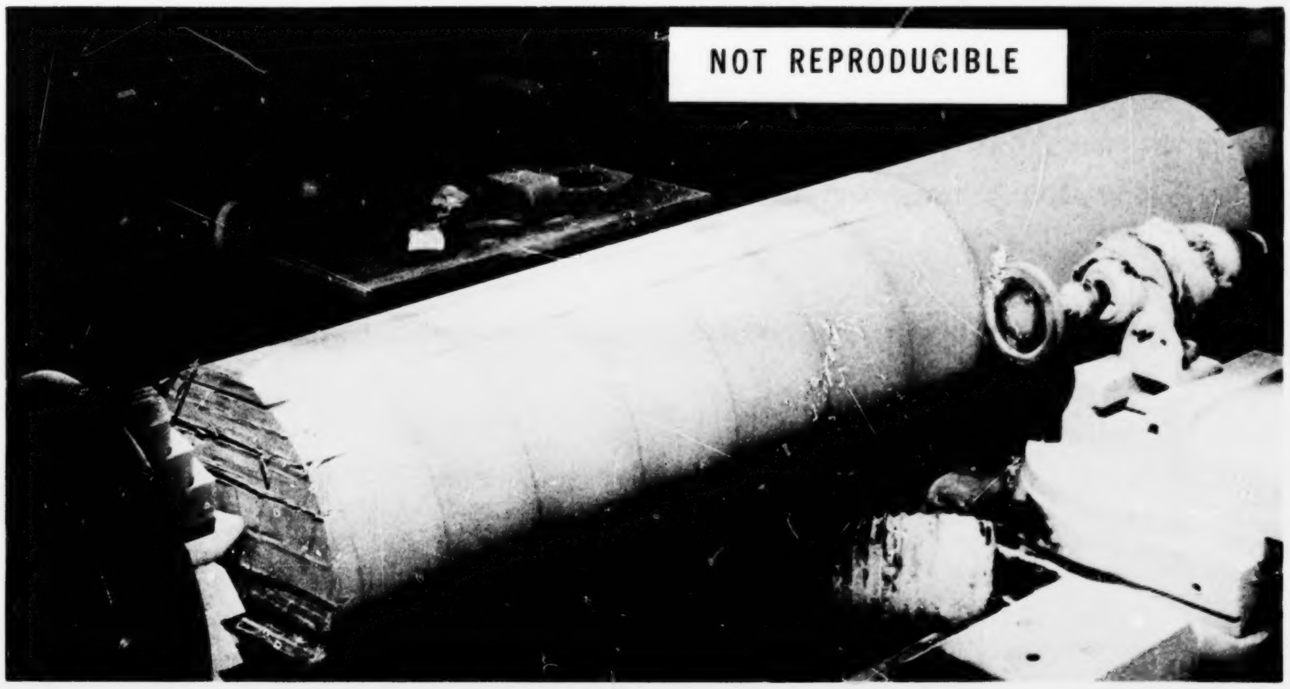

Fig. 6-16 Grinding the Glass Bar Flywheel

When the flywheel grinding was completed, the hub was bonded to the bar. The flywheels then were balanced dynamically to 0.3 in-oz, by grinding material off the tapered ends.

TESTING OF CITY BUS FLYWHEEL

FATIGUE PROPERTIES

Fatigue of uniaxially oriented glass fibers in an epoxy matrix is difficult to test; therefore, little data are available. Because of the very high strength of the material (approximately 280 ksi) and the need to distribute the load evenly into the test specimen, it is difficult to fabricate specimens that can tolerate the dynamic loads required for fatigue testing.

Samples were fabricated and tested in a Sontag Fatigue test machine, but in each case the sample failed because of inadequate bonding of the holding tabs. This test series was discontinued after failure of several specimens.

HITCO, a Division of Armco Steel Corporation, provided information which showed that the ratio of fatigue strength (F_f) to the tensile ultimate (F_{tu}) for fiberglass materials is approximately 0.33 at 10-million cycles. With an $F_{tu} = 260$ ksi, a working stress of 87 ksi can be used.

TENSILE SPECIMEN TESTS

Tensile tests were conducted on specimens fabricated from the same material batching used for the fiberglass wheels. The fiberglass showed an average tensile ultimate of 265 ksi, which was above the allowable required to meet the fatigue requirements.

CREEP TESTS

Creep tests were conducted on fiberglass coupons. Loadings for the creep tests were 125 and 200 ksi. The tests were conducted in an ambient environment. The approximate temperature during the test was 82°F with a relative humidity of 37 percent. Tests were conducted for 30 days. An average creep of 0.003 in. was recorded on all coupons. No creep was experienced after 15 days under load. Some of the measured creep could have been in the attachment of the fiberglass coupons to the metal loading tabs. The fact that no creep was measured during the last 15 days of loading indicates that creep should not cause problems.

NO. 1 GLASS FLYWHEEL TESTS

No. 1 glass flywheel, which was of unidirectional construction, was tested to demonstrate energy density, power density, spindown, and disintegration speed.

The flywheel design speed was 20,000 rpm, but that speed was not reached prior to disintegration.

Table 6-4 provides data from the energy and power density tests.

Spindown. A spindown test was conducted on the flywheel. The spin pit could not be evacuated below 5-mm Hg, so significant drag was experienced (Fig. 6-17).

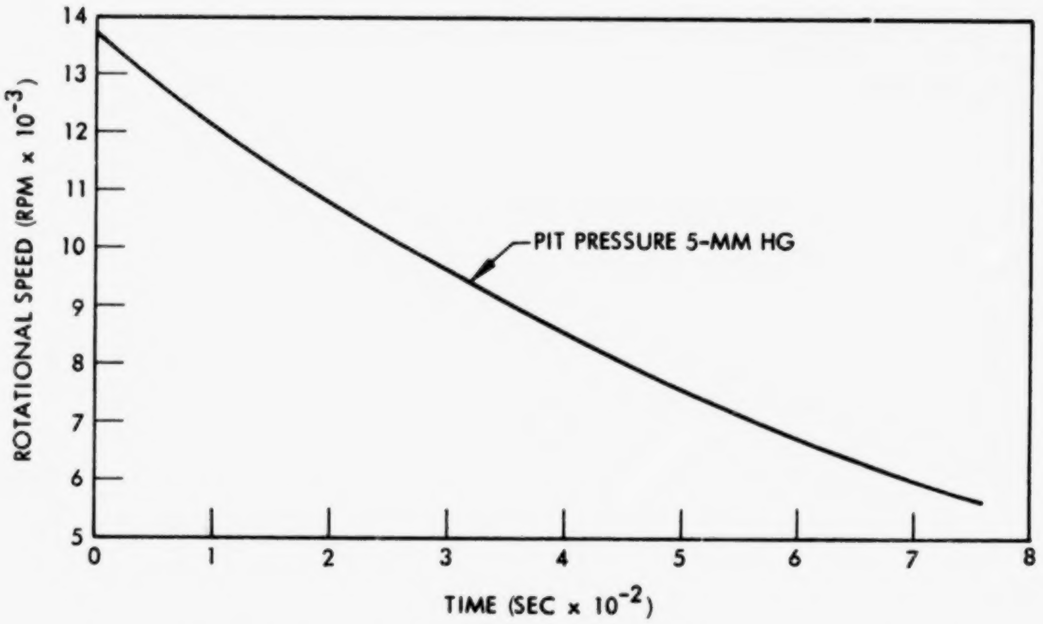

Fig. 6-17 Spindown Tests, EPA/APCO No. 1 Glass Flywheel

Disintegration Speed Test. The No. 1 glass flywheel disintegrated at 15,070 rpm, while an attempt was being made to bring the flywheel to the design speed of 20,000 rpm.

As shown in Figs. 6-18 and 6-19, the flywheel and hub were completely destroyed.

Table 6-4

NO. 1 S-GLASS FLYWHEEL TEST DATA

Energy Density

Test	rpm	w-hr	w-hr/lb
Run 1	13,710	469.91	6.10
Run 2 Prior to Burst	15,070	567.76	7.37

Power Density

Speed Increment (rpm)	Average Speed (rpm)	Average Torque (lb-ft)	Average kw Based on τN	w/lb Based on τN	Initial KE	Final KE	Average kw Based on KE Change	w/lb Based on KE Change
5,030 to 4,990	5,010	4.6	5.88	76.4	63.25	62.25	6.1	79.24
4,990 to 4,930	4,960	12.5	15.82	205.5	62.25	60.76	9.1	118.0
4,930 to 4,850	4,890	15.3	19.096	248.0	60.76	58.80	11.9	155.0
4,850 to 4,750	4,800	19.1	23.4	304.0	58.81	56.41	14.64	190.0
4,750 to 4,630	4,690	24.0	28.7	373.0	56.41	53.59	17.2	223.0
4,630 to 4,540	4,595	22.7	26.6	346.0	53.59	51.53	12.6	163.0
4,440 to 4,310	4,375	3.6	4.02	52.2	49.28	46.44	17.3	225.0
4,310 to 4,120	4,215	31.1	33.5	435.0	46.44	42.43	24.4	317.0
4,120 to 3,880	4,000	43.7	44.6	579.0	42.43	37.63	29.3	380.0
3,880 to 3,750	3,815	48.7	47.4	616.0	37.63	35.16	15.1	196.0
3,660 to 3,530	3,595	12.4	11.4	148.0	33.50	31.15	14.25	185.0
3,530 to 3,280	3,405	39.7	34.5	448.0	31.15	26.90	25.9	337.0
3,280 to 2,910	3,095	66.7	52.7	684.0	26.90	21.17	34.9	454.0
2,910 to 2,520	2,715	78.1	54.1	703.0	21.17	15.88	32.3	419.0
2,520 to 2,120	2,320	89.6	53.1	689.0	15.88	11.24	28.3	368.0
2,120 to 2,000	2,060	78.5	41.3	536.0	11.24	10.00	7.94	98.0

NOT REPRODUCIBLE

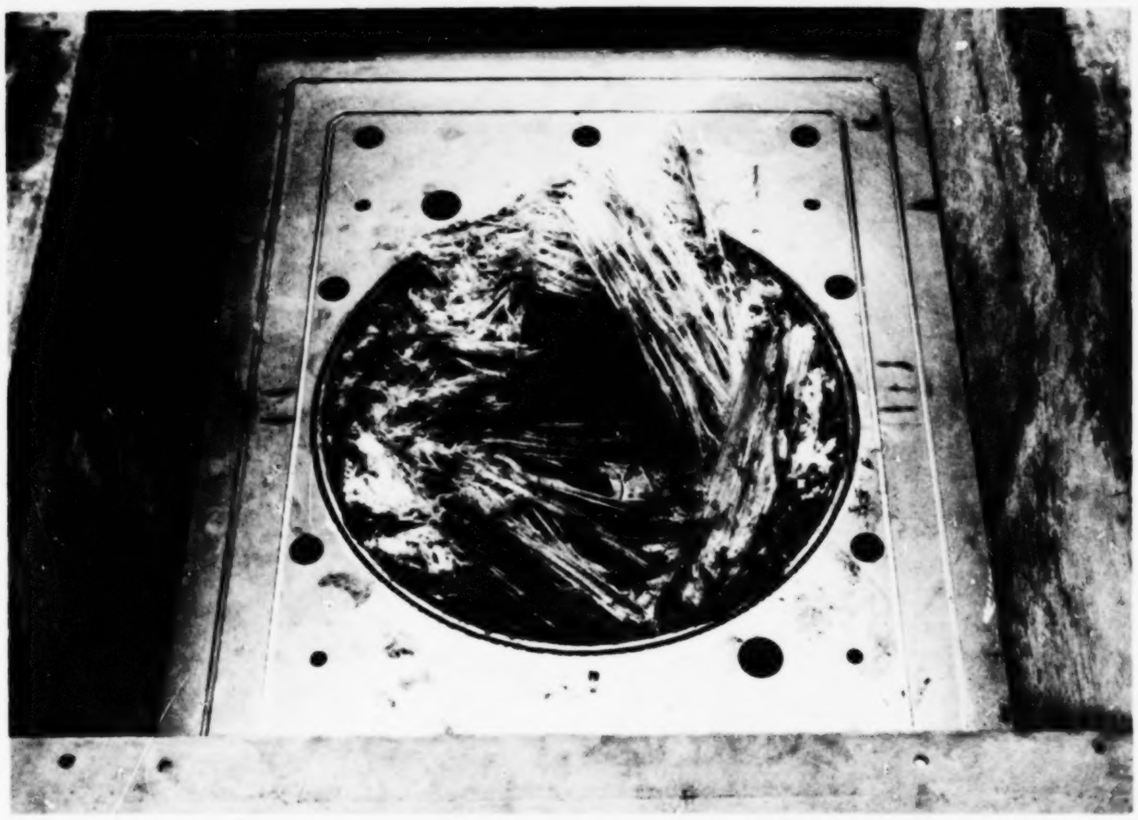

Fig. 6-18 No. 1 Glass Flywheel After Disintegration

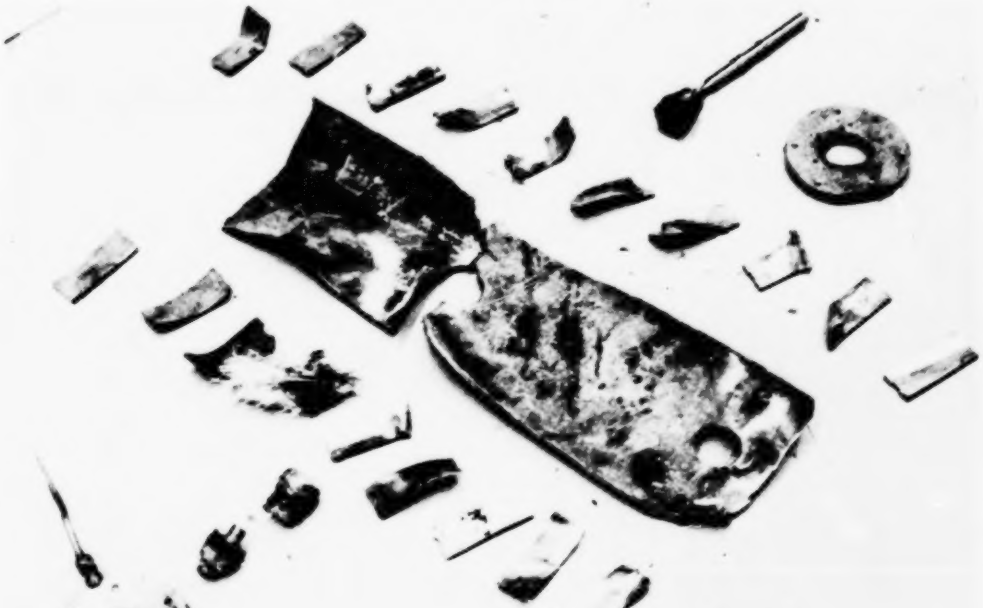

Fig. 6-19 No. 1 Glass Flywheel Hub and Bearing Support After Flywheel Disintegration

The massive disintegration that occurred after failure makes it difficult to determine the failure mode. The break in the hub has the appearance of a tensile failure, thus indicating that a high transverse force was involved. Such a force might be attributed to transverse delamination or a secondary failure of some sort. At burst, the energy density was 7.37 w-hr/lb, and the total energy was 567.8 w-hr.

NO. 2 GLASS FLYWHEEL SPIN TEST

During the energy density test of this flywheel, disintegration occured at 14,690 rpm. As shown in Figs. 6-20 and 6-21, the flywheel and hub were again completely destroyed although the added transverse fibers did serve to hold most of the longitudinal layers together. Again, the hub has the appearance of having been torn apart in tension.

NOT REPRODUCIBLE

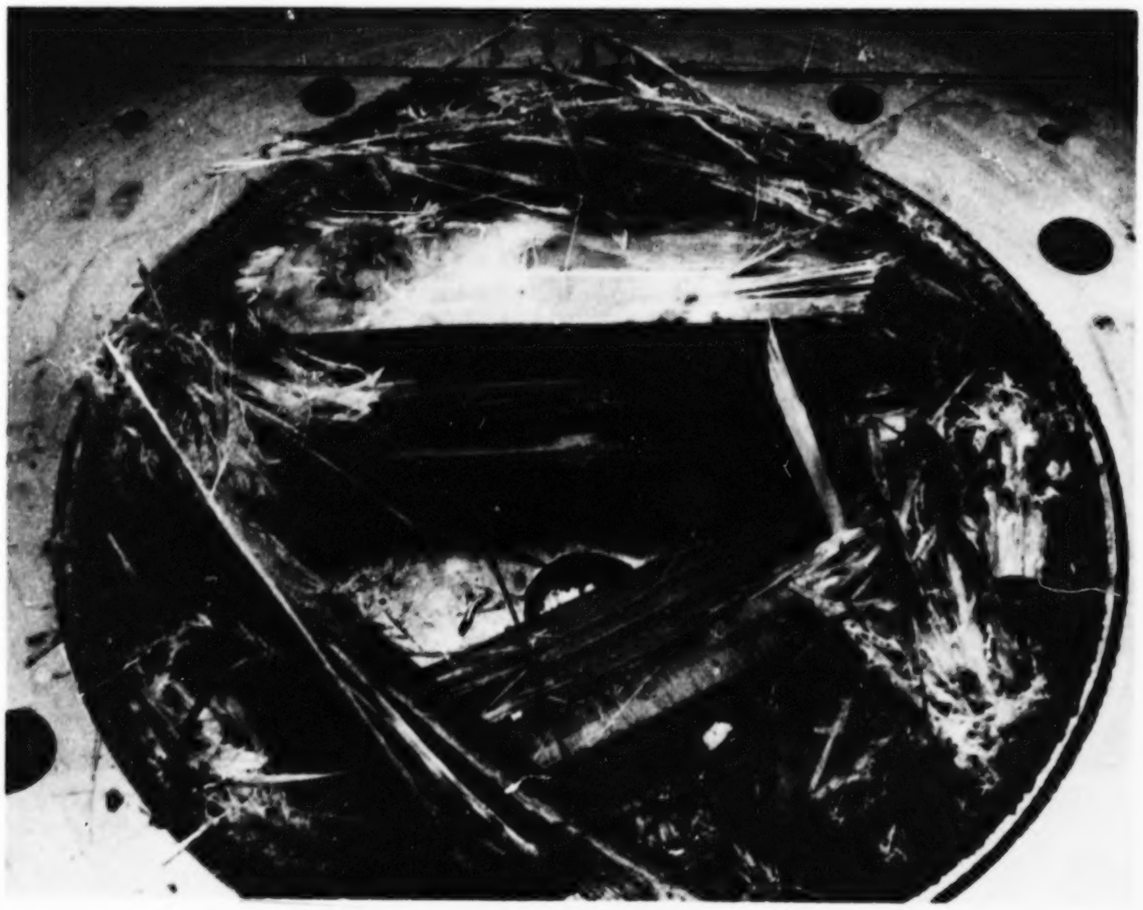

Fig. 6-20 No. 2 Glass Flywheel After Disintegration

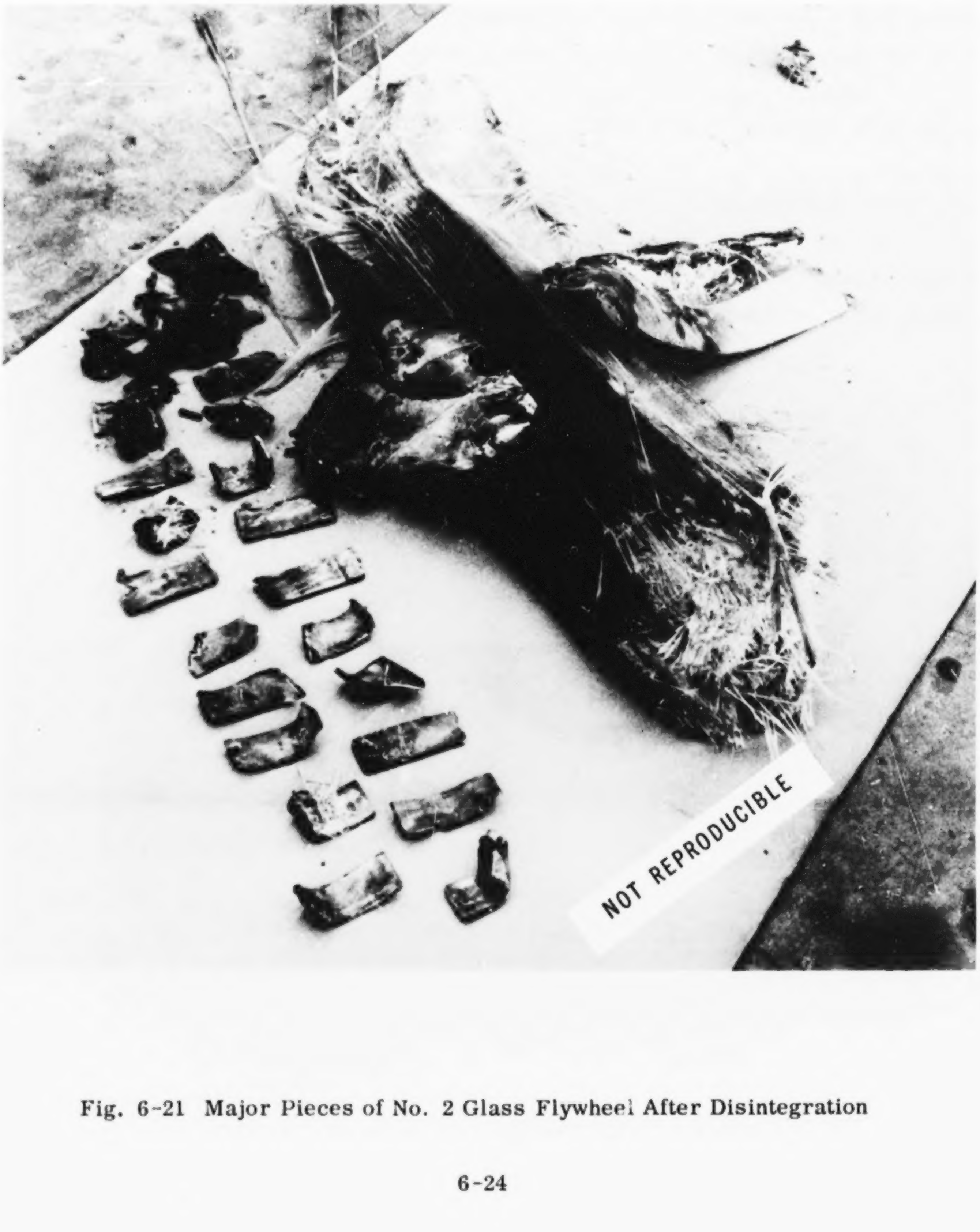
NOT REPRODUCIBLE

Fig. 6-21 Major Pieces of No. 2 Glass Flywheel After Disintegration

The longitudinal layers showed heavy damage, such as might have resulted from a transverse blow, on one end and very little damage on the other end.

On the basis of the above evidence, there is an indication that failure may have occurred by the fiberglass moving longitudinally out of the hub. The severe damage to one end of the fiberglass might be attributed to that end hitting the pit wall. (The running clearance between the fiberglass and the pit wall was approximately 1 in.) The tensile failure of the hub may be attributed to the large transverse force applied to the hub when the fiberglass impacted the pit wall.

The possibility of the fiberglass moving longitudinally out of the hub may be attributed to insufficient lubrication provided in the assembly procedure. As explained on p. 6-17, radial displacement between hub and fiberglass was to have been made possible by the lubricating properties of the mold release. There is, however, a large initial breakaway shear stress involved in mold release lubrication. Thus, the lubrication between the potted fingers on the fiberglass and the hub may have been inhibited by a very large value of initial (one-time-only) stiction. At the moderately high stresses at failure speed, one side of the hub may have overcome this stiction and the resulting sudden longitudinal unbalance may have pulled the fiberglass out of the hub.

If further work with flywheels of this type is desired, any hub/fiberglass interface problems could probably be solved with better lubrication, possibly by teflon-coating the hub prior to assembly.

BLANK PAGE

Section 7
HYBRID DESIGN CONFIGURATION

Results of the applicability studies and configuration tradeoffs have shown that the best flywheel applications are flywheel/heat-engine configurations for city busses and family cars. The configuration tradeoffs also have shown that for both vehicles the optimum transmission is the power-splitting hydrostatic transmission, and the optimum heat engine is the spark-ignition engine. In addition, these studies have shown that no major changes would be required in either the city bus or the family car to accommodate these flywheel/hybrid drives. Several drivetrain layouts were made in order to show a number of ways in which a flywheel/hybrid drive system could be incorporated into current production vehicles.

FAMILY CAR

Figure 7-1 shows a phantom view of a conventional drivetrain arrangement in a full-sized family car. Replacing the conventional hydrokinetic transmission by a flywheel drive transmission, the resulting arrangement would be as shown in Fig. 7-2. The engine has been moved forward to accommodate the greater length of the flywheel drive transmission. Although the same engine size is shown in both cases, a smaller engine could be used with the flywheel/hybrid drive.

Figure 7-3 shows a conceptual layout for an engine-mounted flywheel/hybrid drive transmission. No attempt was made to minimize the length of the transmission, although this could certainly be done.

Another possible arrangement for the flywheel drive is shown in Fig. 7-4. Here the conventional hydrokinetic transmission has been replaced by a simple torque damper. The flywheel drive transmission has been incorporated into an independent rear suspension transaxle package. Conceptual layout of this flywheel transaxle is shown in Fig. 7-5, and a configuration block diagram is shown in Fig. 7-6. Drivetrain packaging advantages are immediately apparent. The smaller engine and removal of the front transmission allow more crumple space to meet head-on collision safety requirements. The transmission hump is no longer required, and the driveshaft tunnel can be substantially reduced or possibly eliminated due largely to the body mounting of the transaxle package. Weight distribution is improved slightly, and more flexibility in choosing weight distribution is provided. The independent rear suspension (IRS) is more expensive than the conventional Detroit solid axle, but offers advantages in handling and ride quality which in themselves have justified IRS for many foreign manufacturers.

CITY BUS

A conventional drivetrain arrangement for a 53-passenger city bus is shown in Fig. 7-7. Figure 7-8 shows a flywheel/hybrid drivetrain arrangement for the city bus, and a conceptual layout of the flywheel/hybrid transmission is shown in Fig. 7-9. Although the flywheel drive transmission is somewhat larger than a conventional bus transmission, its use makes possible a smaller engine – approximately one half the size of the conventional engine – such that the overall package of engine plus transmission is approximately the same or slightly less.

Although these studies did not involve consideration of various types of fuels, the use of fuels such as compressed natural gas (CNG) for the city bus is attractive on the basis of both cost and emissions. When existing engines are converted to CNG, a serious loss in power capability results. The replacement of the existing transmissions with flywheel drives would more than restore the resulting loss in acceleration capability and provide additional reductions in emissions and operating cost.

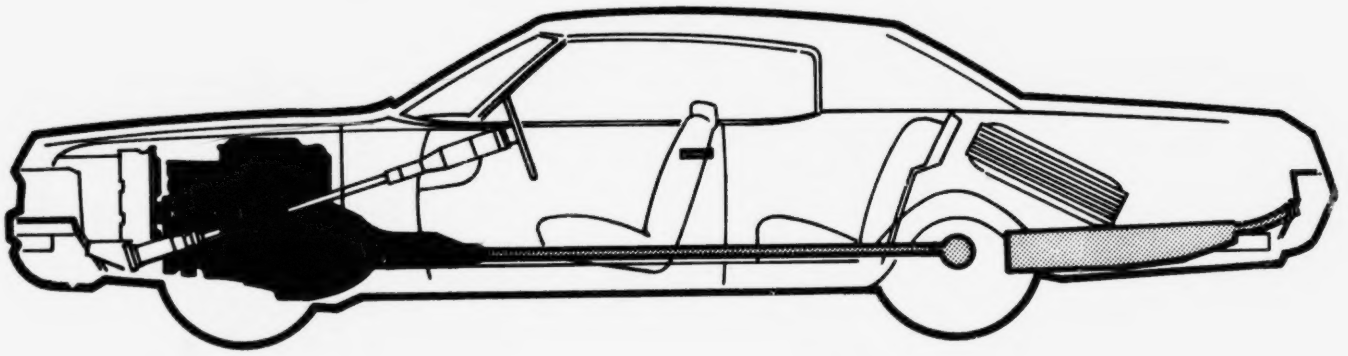

Fig. 7-1 Drivetrain Arrangement for Conventional Engine-Mounted Hydrokinetic Transmission

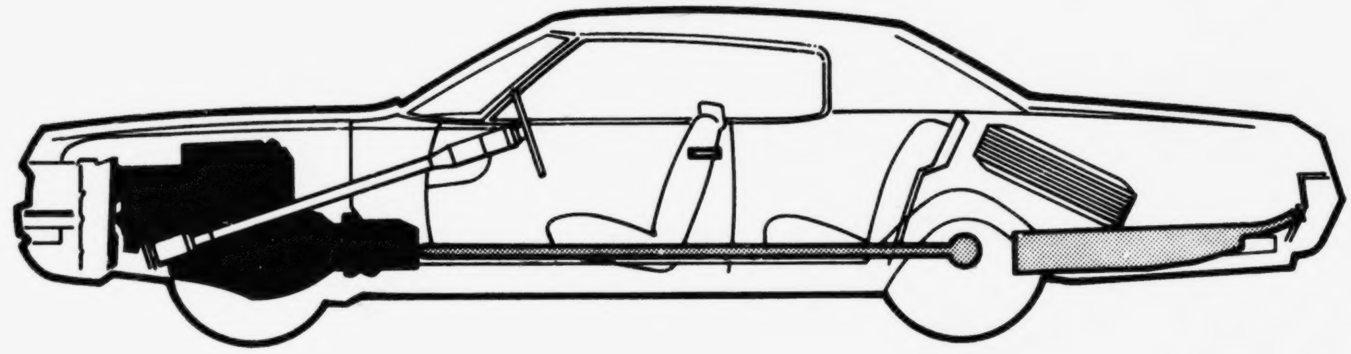

Fig. 7-2 Drivetrain Arrangement for Engine-Mounted Flywheel/Hybrid Transmission

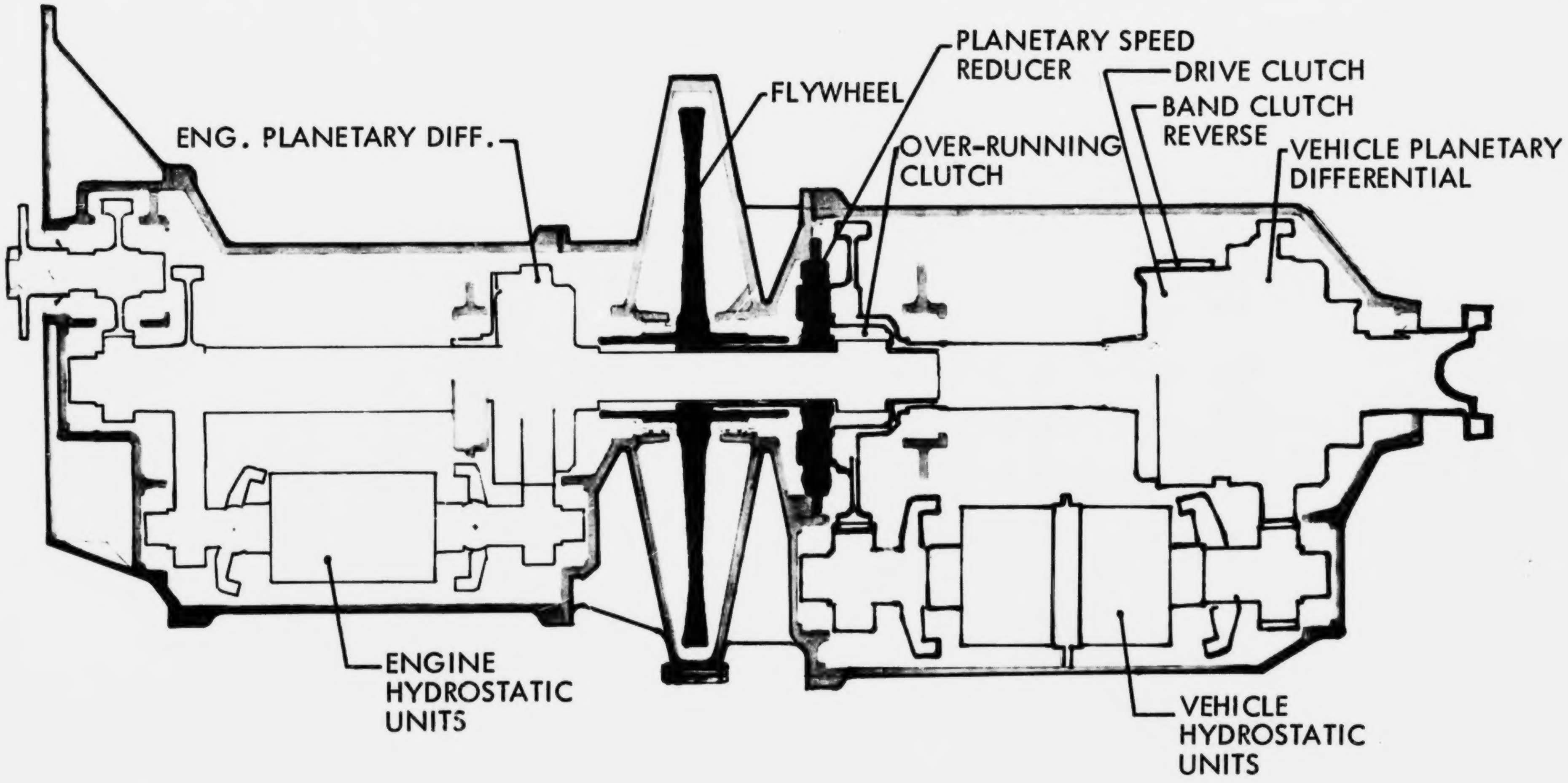
ENG. PLANETARY DIFF.
FLYWHEEL
PLANETARY SPEED REDUCER
OVER-RUNNING CLUTCH
DRIVE CLUTCH
BAND CLUTCH REVERSE
VEHICLE PLANETARY DIFFERENTIAL
ENGINE HYDROSTATIC UNITS
VEHICLE HYDROSTATIC UNITS

Fig. 7-3 Engine-Mounted Flywheel/Hybrid Transmission Layout

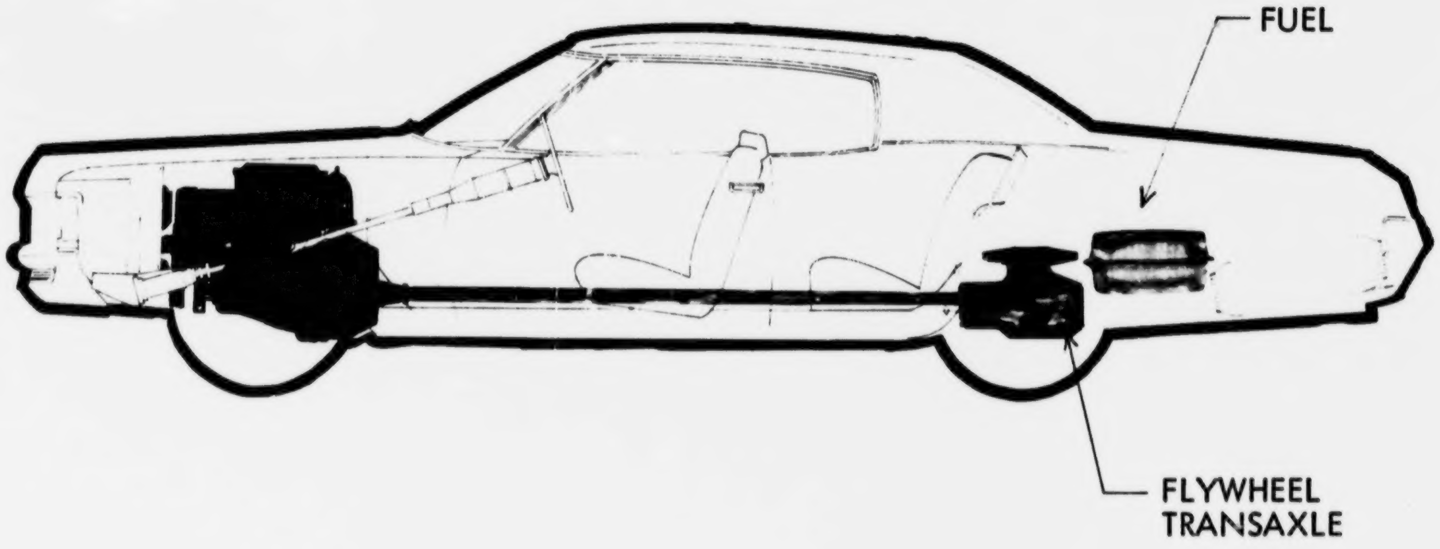
FUEL
FLYWHEEL
TRANSAXLE

Fig. 7-4 Drivetrain Arrangement for Transaxle Flywheel/Hybrid Transmission

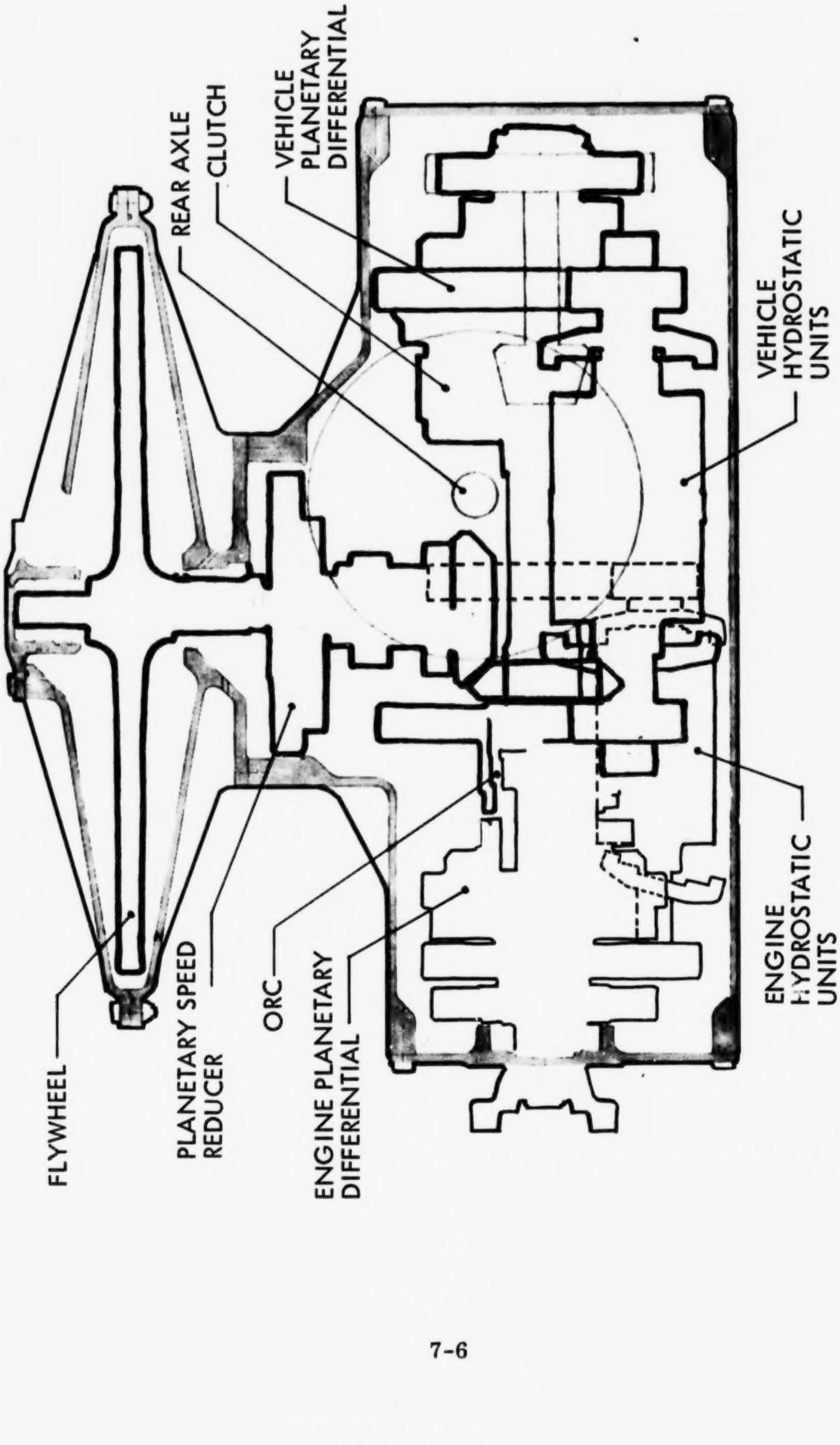
FLYWHEEL
PLANETARY SPEED REDUCER
ORC
ENGINE PLANETARY DIFFERENTIAL
REAR AXLE
CLUTCH
VEHICLE PLANETARY DIFFERENTIAL
VEHICLE HYDROSTATIC UNITS
ENGINE HYDROSTATIC UNITS

Fig. 7-5 Transaxle Flywheel/Hybrid Transmission Layout

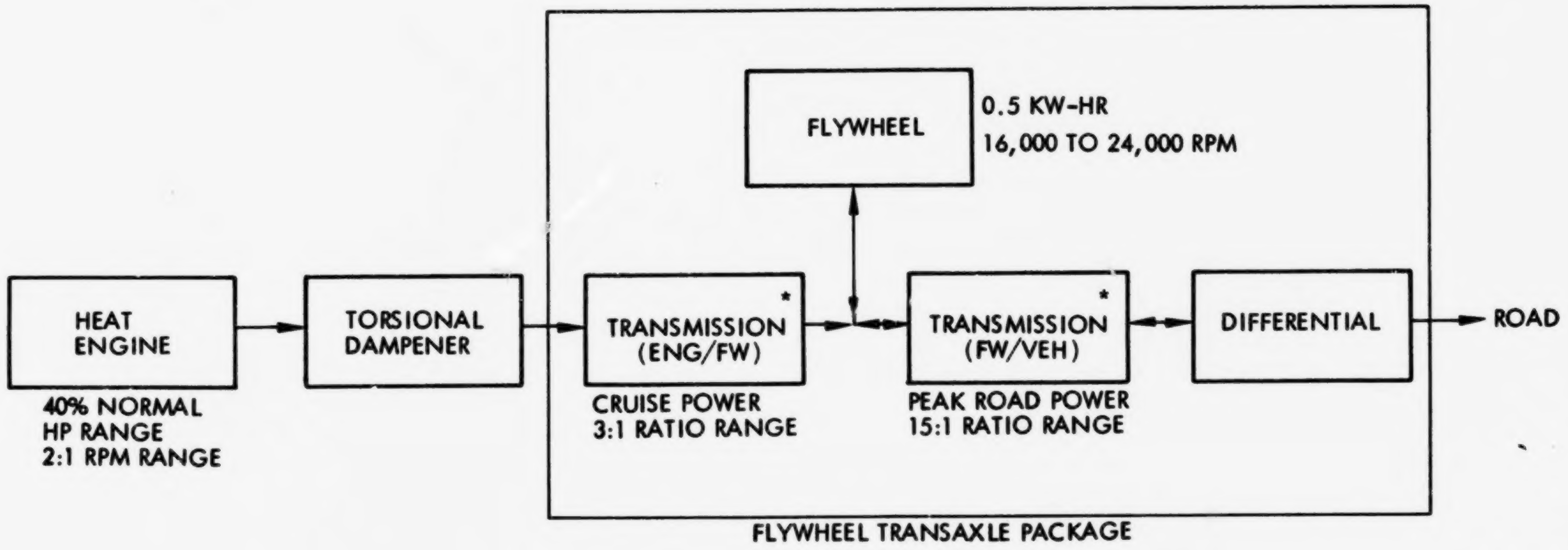
HEAT ENGINE
40% NORMAL HP RANGE
2:1 RPM RANGE
TORSIONAL DAMPENER
TRANSMISSION (ENG/FW) *
CRUISE POWER
3:1 RATIO RANGE
FLYWHEEL
0.5 KW-HR
16,000 TO 24,000 RPM
TRANSMISSION (FW/VEH) *
PEAK ROAD POWER
15:1 RATIO RANGE
DIFFERENTIAL
ROAD
FLYWHEEL TRANSAXLE PACKAGE

*PLANETARY/HYDROSTATIC POWER SPLITTING TRANSMISSION

Fig. 7-6 Transaxle Flywheel/Hybrid Transmission Configuration

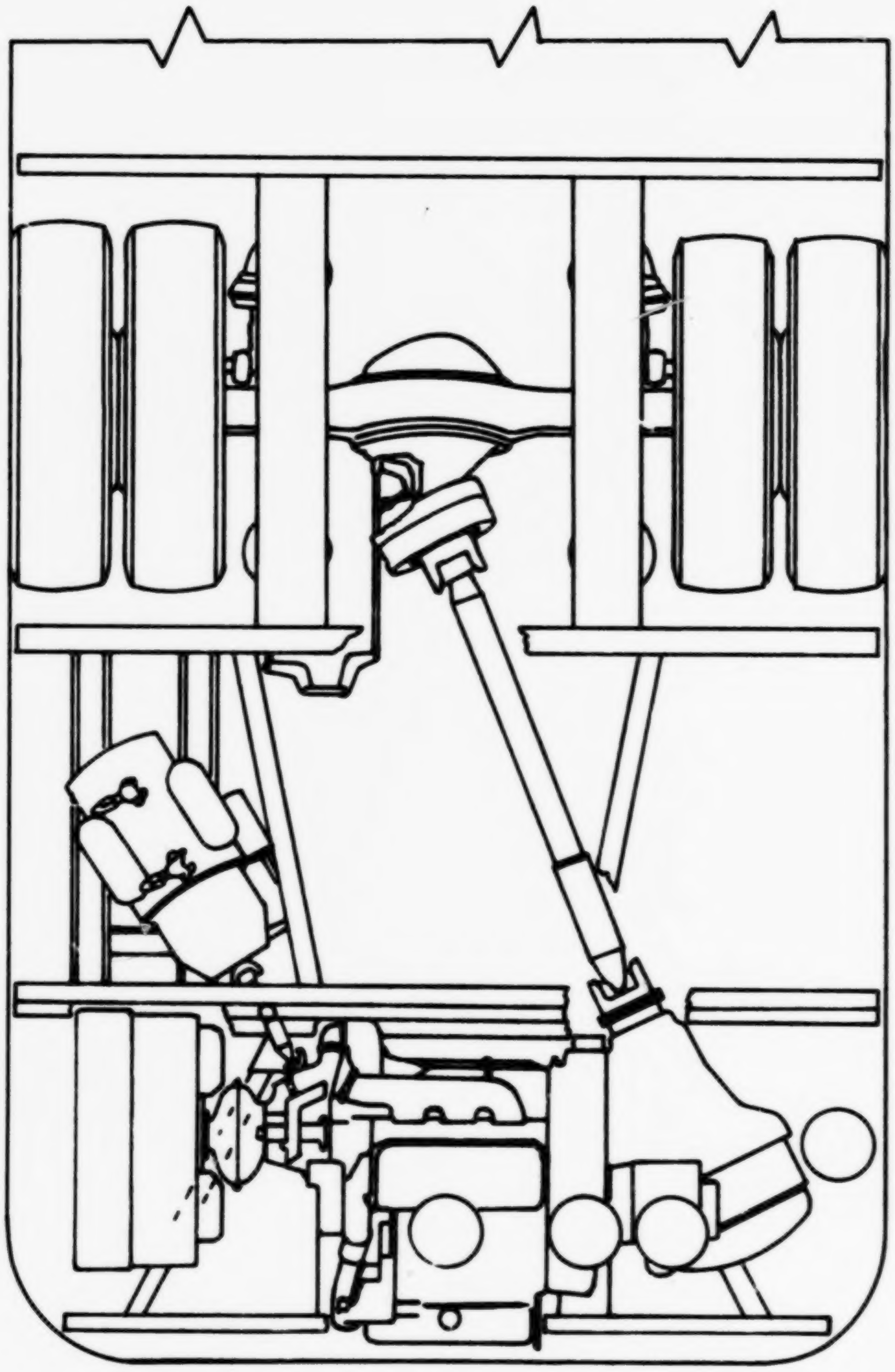

Fig. 7-7 Drivetrain Arrangement for Conventional City Bus

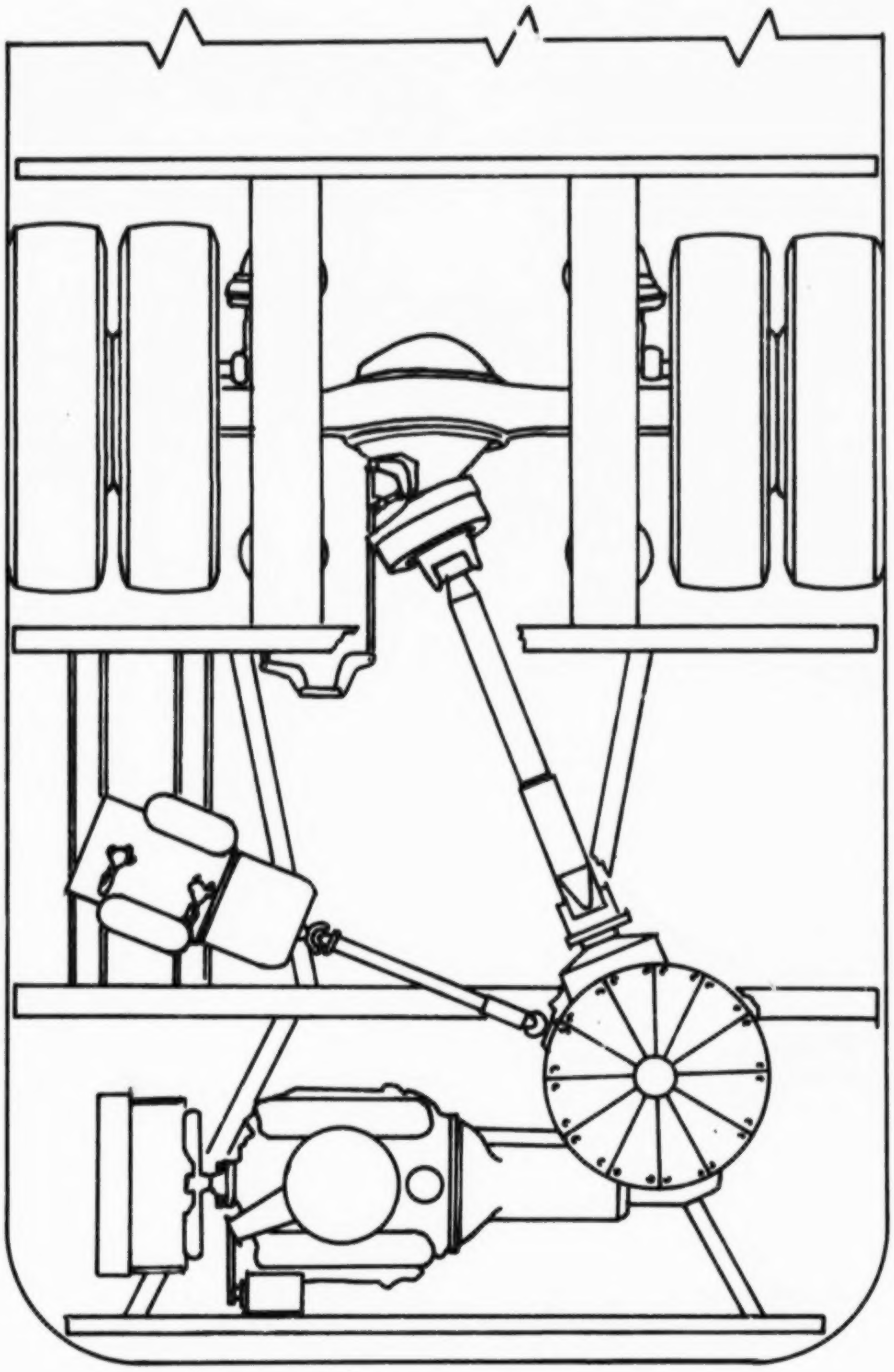

Fig. 7-8 Drivetrain Arrangement for Flywheel/Hybrid City Bus

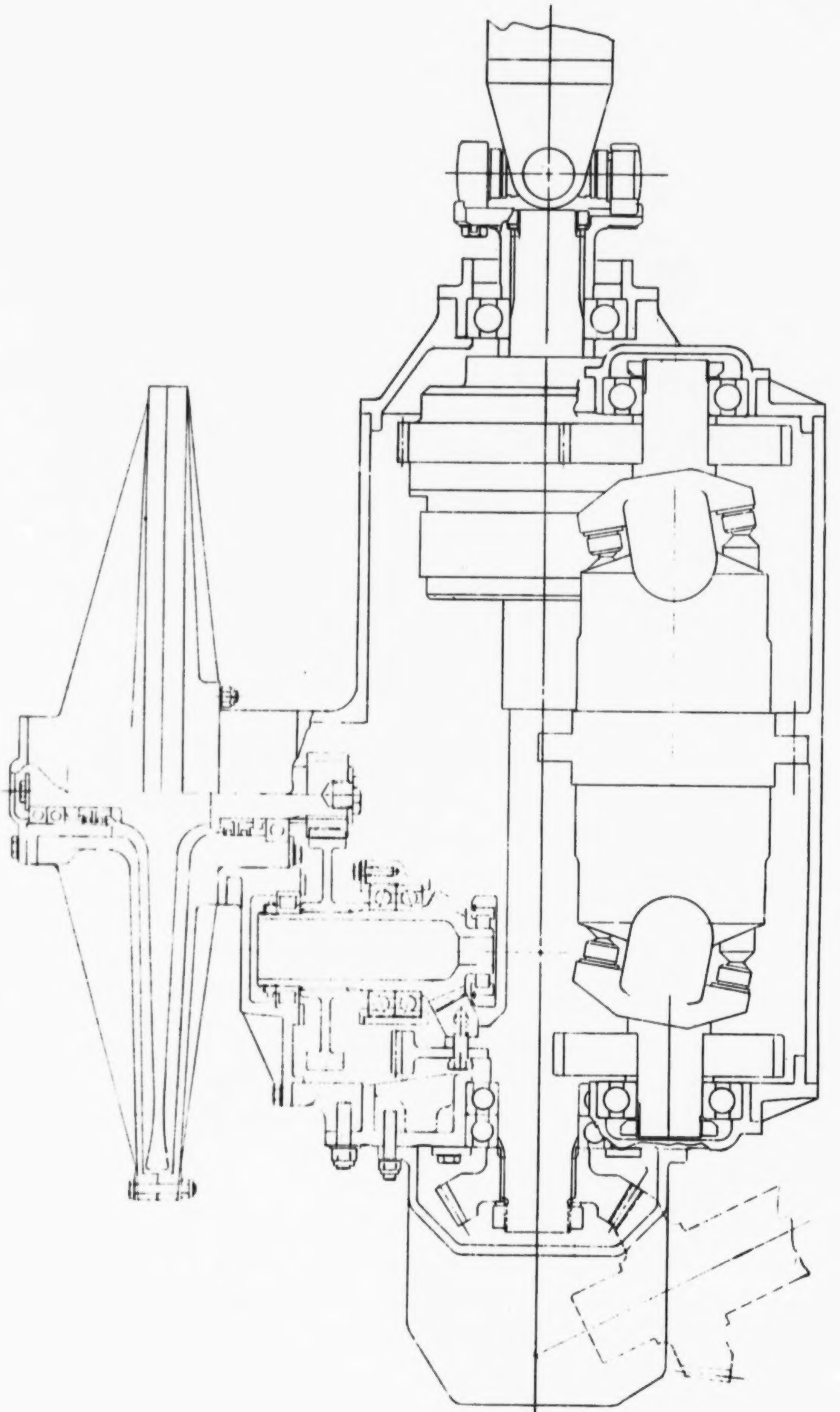

Fig. 7-9 Layout of Flywheel/Hybrid Transmission for City Bus

Section 8
CONCLUSIONS AND RECOMMENDATIONS

The overall conclusion of the Flywheel Feasibility Study and Demonstration program is that flywheel energy storage is a feasible means of emission reduction for full performance vehicles. Although the specific energy of present-day flywheels is not sufficient to make flywheel-only vehicles feasible, flywheel/heat-engine hybrid vehicles are entirely feasible. The flywheel/heat-energy hybrid drive may permit the full size family car to achieve low emission levels while enhancing performance and gas mileage in city driving.

Specific conclusions and recommendations are given in the following paragraphs:

1. Pure flywheel drives are not suitable for any of the four vehicles because the specific energy of the flywheel-only drive system is too low. Using a figure of 25 w-hr/lb as the highest possible flywheel specific energy available today, the family car would require about a 10:1 improvement in specific energy, and the commuter car or delivery/postal van would need roughly a 2:1 improvement. It is not likely that these improvements could be attained within the next 5 years. The city bus is a borderline case; a pure flywheel drive would be suitable if recharging could be accomplished at distances of approximately 10 miles or less. Of course there may be little relative merit in pure energy storage drives if the source of recharge power itself generates more pollution per unit of energy than a flywheel/heat-engine hybrid vehicle (Ref. 8-1).

2. Flywheel/heat engine hybrid drives are suitable for all four vehicles in particular and for most vehicles in general. For hybrid drives, specific energy is not critical; the weight of the steel flywheel is on the order of 1 percent of the gross vehicle weight. Specific power requirements are

easily met by the flywheel per se, but dictate transmission requirements. Although the technical feasibilities of hybrid drives for the three smaller vehicles were indicated, the family car was chosen for further study because of its high population.

3. The proper system control technique is that of total kinetic energy (TKE) control. The TKE approach can give the vehicle a nearly non-history-dependent performance capability and obviates flywheel oversizing for recuperation. For prototype vehicles, an all-electronic control system is recommended so that various control modes can be investigated.

4. The preferred transmission configuration is the double-transmission type because it permits independent speed relationships between flywheel and vehicle as well as between engine and flywheel. The double configuration is essential for prototype vehicles so that various control modes can be evaluated. Evaluation of a single-transmission mode would be made with the proper section of the double-transmission locked up.

5. Of the four types of transmissions studied (mechanical, hydrostatic, hydrokinetic, and electric), the best type is a combination of mechanical and hydrostatic – the power splitting transmission. This transmission is comprised of a planetary differential with a variable hydrostatic bypass. Hydrokinetic transmissions are unsuitable to the flywheel/hybrid by their very nature of operation. Electric transmissions are prohibitively costly.

6. The spark-ignition engine is the best presently available heat engine for hybrid vehicles, both on the basis of minimum cost and on the basis of minimum emissions. The basic flywheel/hybrid approach, however, is applicable to all four engine types investigated (Otto, Brayton, Diesel, and Rankine) and eliminates certain drawbacks with certain types. For instance, in a flywheel/hybrid system, the lag in the gas turbine response would be of no consequence; and for the steam engine, the expander, and more importantly the condenser, would be sized on the basis of cruise plus accessory power rather than peak power.

7. Based on emissions data supplied by EPA/APCO, a flywheel/hybrid family car using a presently available spark-ignition engine can achieve low emission levels.
8. Based on emissions data supplied by EPA/APCO, a flywheel/hybrid family car using one of several engines of projected 1975 availability would have emissions substantially below a flywheel/hybrid with a contemporary engine.
9. Based on emissions data supplied by EPA/APCO, a flywheel/hybrid city bus using a presently available spark-ignition engine would have substantially reduced emissions. In addition, operating cost would be lower than that of a conventional bus.
10. The optimum flywheel geometry is a modified exponential or conical disc with a built-up rim.
11. The optimum flywheel material is common high-strength steel such as AISI 4340.
12. The design of steel disc flywheels is simple and straight forward, and performance is highly predictable. Manufacturing, inspection, and test techniques are well established for similar hardware such as turbine rotors. For these reasons, future development work in steel disc flywheels per se is considered to be unnecessary.
13. The practicality of filamentary composite flywheels remains unproven. The energy density potentials of filamentary composite flywheels is insufficient for pure flywheel vehicles and unnecessary for flywheel/heat-engine hybrid vehicles. For these reasons, little merit is seen in continued development of filamentary composite flywheels.
14. Gyrodynamic effects are not expected to present serious problems, but vehicular testing is recommended. Steering effects should be investigated with various road surface conditions, tire types, vehicle weight distributions, and flywheel attitudes.

15. Flywheel burst containment techniques should be investigated analytically, and empirical tests should be conducted to verify design approaches.

16. Work in the area of aerodynamic shrouding for flywheels at supersonic tip speeds is recommended. Empirical techniques devised for turbine rotor research are directly applicable.

17. Detailed design studies are recommended for flywheel ancillaries such as bearings, seals, and evacuation systems.

18. The development and test of prototype family cars and city buses is recommended. The recommended system components are: spark ignition engine, power splitting transmission (planetary differential plus hydrostatic bypass) of the double configuration, all-electronic controls, and a steel conical disc flywheel. This system would be retrofitted into a full sized six-passenger family sedan of high production. An identical propulsion system would be installed on a dynamometer where emissions could be measured. Various control modes thus could be tested simultaneously for emissions as well as vehicle "feel" and "driveability." The double transmission is required in order to give complete flexibility to the system for testing all types of control modes. For instance, a single transmission would be simulated by "locking-up" the engine-flywheel transmission. The all-electronic controls are also essential for test flexibility.

Program plans for the development and test of prototype vehicles are given in Section 9, Future Program Plans.

Section 9
FUTURE PROGRAM PLANS

The results of the Flywheel Feasibility Study and Demonstration as described in this report show the high potentials for automotive emission reduction offered by kinetic-energy-storage vehicle drives. In particular, the applicability studies conducted for EPA/APCO have shown that the most desirable vehicle drive configurations are flywheel/heat-engine hybrids utilizing spark-ignition engines in a family car and city bus. The results of the computer-aided calculation of emissions from a car meeting the "Vehicle Design Goals — Six-Passenger Automobile" (Revision A, November 30, 1970) when operated over the DHEW Urban Dynamometer Driving Schedule (Federal Register, November 10, 1970) show that low emissions may be possible with a flywheel/spark-ignition engine hybrid drive. Similar reductions in emissions from a city bus result from the flywheel/spark-ignition engine hybrid drive when operated over the stipulated City Bus Cycle. Flywheel/hybrid drives with other engine types may offer the potential of even lower emission levels when and if these engines become available. In addition, anticipated improvements in flywheel materials provide the possibility of even more efficacious flywheels from the standpoint of energy density for future vehicle applications. However, the flywheels that were designed, built, and tested on the present contract have shown that completely acceptable kinetic-energy-storage hybrid propulsion systems can now be demonstrated without further engine or flywheel material improvements. The succeeding paragraphs present plans for a logical sequence of activities that will lead to operational, full-scale, low-pollution cars and busses configured with flywheel/heat-engine hybrid propulsion systems.

A review of various approaches toward the development of practical hybrid vehicle drives has been conducted. As a result, conducting the following three development programs in combination is felt to represent the most expeditious means of achieving the integration of flywheel/spark-ignition engine drives into fully operational prototype passenger cars and buses.

PROGRAM 1 – FLYWHEEL/HYBRID DRIVE SYSTEM DEVELOPMENT

The objective of this program (of approximately 8 months duration) is the full-scale feasibility demonstration and performance verification of a flywheel/spark-ignition engine drive system using presently available components. The system power capability would be in the general range suitable for a bus or car. The "breadboard" drive system would be comprised of the following components:

a. A 0.5 kw-hr or 1.0 kw-hr steel flywheel similar to flywheels built and tested by LMSC on the present contract
b. Flywheel housing consisting of a structure supporting a seal and bearing system based on the findings from the present contract tests
c. Flywheel speed-reducing gearbox
d. Spark-ignition engine of suitable capacity
e. Transmission comprised of hydrostatic components to simulate control interfaces and operation of a power-splitting transmission. (This transmission configuration will be used to simulate the ultimate power-splitting transmission such that tests can be conducted without delay.)
f. Clutch system
g. Ancillary cooling, vacuum, and control systems

The "breadboard" drive would be assembled and extensively tested using a programmable laboratory dynamometer to simulate vehicle rolling, drag, grade, and inertia loads in all four torque-speed quadrants of operation. The specific goals of the planned program are as follows:

a. To verify the operational characteristics of a full-scale flywheel/hybrid drive suitable for ultimate application to a city bus and/or passenger automobile
b. To define the control requirements and control interfaces of a flywheel/hybrid drive
c. To determine the transmission requirements of a flywheel/hybrid drive
d. To select speed ranges for heat-engine and flywheel

PROGRAM 2 – INTEGRATION OF A FLYWHEEL/SPARK-IGNITION HYBRID DRIVE SYSTEM INTO PROTOTYPE PASSENGER CARS

This is a 27-month program culminating in the delivery to EPA/APCO of five flywheel/spark-ignition engine hybrid family cars. The program is divided into logical, serial phases to provide an efficient sequence of work tasks with minimized development risk and several significant program review points. The major objectives and activities of the planned program phases are the following:

Phase 1 – Design, fabricate and test two identical and complete full-sized preprototype drive systems (flywheel, engine, transmission, controls and accessories). Design would be based on dynamometer testing described above of a "breadboard" flywheel/engine/transmission system used to determine general operating characteristics, control interfaces, component requirements, and pollution reduction potentials. The design program would include a computer-aided transmission analysis, flywheel fatigue and failure control studies and tests, and system optimization studies. The air pollution reduction characteristics of one drive would be established by exhaust gas sampling while operating over a simulated DHEW Urban Dynamometer Driving Schedule. The vehicle performance and driver "feel" characteristics would be determined by operating a testbed vehicle with the second drive system in comparison with a conventional control vehicle.

Phase 2 – Fabricate five complete prototype drive systems with spares and assemble into full-sized six-passenger automobiles. Shakedown and performance testing would be conducted prior to delivery of vehicles to EPA/APCO in a ready-to-test condition.

PROGRAM 3 – INTEGRATION OF A FLYWHEEL/SPARK-IGNITION HYBRID DRIVE SYSTEM INTO PROTOTYPE CITY BUSES

The planned 28-month development program, leading to delivery of three full-scale prototype hybrid city buses suitable for operational demonstration in revenue service, is divided into three logical phases. The first phase is directed toward the acquisition and analysis of operational bus data to establish realistic city bus operational cycles and performance requirements.

The second and third phases closely parallel the two phases of the passenger car program described above. The second phase (which could be carried on almost concurrently with the Phase 1 determination of city bus profiles and performance requirements) consists of the design, fabrication, and test of a full-scale preprototype city bus drive suitable for extensive laboratory dynamometer testing. The design would be based on the results of the "breadboard" test program of the flywheel/hybrid drive development described above. Final sizing would be based on the findings of the Phase 1 operational bus data study. The end results of the Phase 2 program would establish the performance and air pollution reduction characteristics of the hybrid bus drive in simulated operations over typical city bus driving cycles. Phase 2 would also include a computer-aided transmission analysis as well as investigation and testing of potential problem areas of flywheel safety, fatigue cycles, and gyrodynamics.

The Phase 3 program plan consists of the fabrication of three full-sized bus drives with spares followed by assembly into three buses. The buses would be extensively tested for performance and safety prior to delivery of vehicles to EPA/APCO in a ready-to-test condition.

Section 10
REFERENCES

1-1 "The Oerlikon Electrogyro, Its Development and Application for Omnibus Service," Automobile Engineer, Dec 1965

2-1 "DHEW Urban Dynanometer Driving Schedule," Federal Register, 10 Nov 1970

4-1 David L. Plett and Harold G. Carlson, "Performance of a Variable Speed Constant Frequency Electrical System," IEEE Transactions on Aerospace, Vol. 2, No. 2, Apr 1964

4-2 Worldwide Diesel and Gas Turbine Catalog, Vol. 35, 1970

4-3 Automotive Industries 52nd Annual Engineering Specifications, 1970

4-4 Listing of U.S. Reciprocating (Gasoline) Engines, U.S. Gas Turbine Engines, and Leading International Gas Turbines; Aviation Week and Space Technology; Mar 1970

4-5 S. William Gouse, Jr., "The Search for Low Emission Vehicle Propulsion," American Society of Mechanical Engineers, No. 69-WA/Enr-4.

4-6 List of Rankine Cycle Engine Companies and Small Gas Turbine Engine Companies transmitted by Dr. Karl Hellman (EPA/APCO) letter dated 16 Jul 1970.

4-7 Report of Hearing Proceedings, Subcommittee on Air and Water Pollution of the Committee on Public Works, Committee on Commerce, U.S. Senate, 90th Congress, 1968

4-8 Brake Specific Emission Curves transmitted by Dr. Karl Hellman (EPA/APCO) for spark ignition, diesel, gas turbine, and Rankine engines as modified by mutual agreement in telephone conversation, 18 Aug 1970

4-9 Arthur F. Underwood, "Requiem for the Piston Engine?", Machine Design, 6 Aug 1970

4-10 R. E. Wolfgang Hempel, "Does Turbocharging Increase Diesel Engine Noise? – Observations on the Generation, Emission, and Reduction of Diesel Engine Noise," SAE Paper No. 680406, May 1968

4-11 Thermo Electron Corporation, Conceptual Design, Rankine-Cycle Power System With Organic Working Fluid and Reciprocating Engines for Passenger Vehicles, Report No. TE4121-133-70, Jun 1970

5-1 D. E. Goldman and H. E. von Gierke, "The Effects of Shock and Vibration on Man," Naval Medical Res. Inst., No. 60-3

5-2 Francis J. Lavoie, "Nondestructive Testing," Machine Design, Sep 4, 1969

5-3 J. W. Daily and R. E. Nece, "Chamber Dimension Effects on Induced Flow and Frictional Resistance of Enclosed Rotating Disks," Journal of Basic Engineering, Mar 1960

5-4 Robert W. Mann and Charles H. Marston, "Friction Drag on Bladed Disks in Housings," Journal of Basic Engineering, Dec 1961

6-1 Lockheed Aircraft Corporation, Stress Memorandum No. 114, S-N Curves, p. 15

8-1 Paul D. Agarwal, "Electricity Not Such a Clean Fuel," Automotive Engineering, Feb 1971

Appendix A

NAPCA VEHICLE DESIGN GOALS – SIX-PASSENGER AUTOMOBILE

(REVISION A, NOVEMBER 30, 1970)

The design goals presented below are intended to provide:

> A common objective for prospective contractors.
>
> Criteria for evaluating proposals and selecting a contractor.
>
> Criteria for evaluating competitive power systems for entering first generation system hardware.

The derived criteria are based on typical characteristics of the class of passenger automobiles with the largest market volume produced in the U.S. during the model years 1969 and 1970. It is noted that most weight and volume characteristics presented are maximum values and the performance characteristics are intended as minimum values. Prospective contractors who take exceptions must justify these exceptions in their proposals and relate these exceptions to the technical goals presented herein.

1. Vehicle weight without propulsion system - W_o.

   W_o is the weight of the vehicle without the propulsion system and includes, but is not limited to: body, frame, glass and trim, suspension, service brakes, seats, upholstery, sound absorbing materials, insulation, wheels (rims and tires), accessory ducting, dashboard instruments and accessory wiring, and all other components not included in the propulsion system. It also includes the air conditioner compressor, the power steering pump, and the power brakes actuating device.

   W_o is 2700 lbs.

2. Propulsion system weight - W_p.

   W_p includes the energy storage unit (including containment), power converter (including both functional components and controls) and power transmission to the driven wheels. It also includes the exhaust system, pumps, motors and fans necessary for operation of the propulsion system, and any propulsion system heating or cooling devices.

   The maximum allowable propulsion system weight, W_{pm}, is 1600 lbs. The propulsion system may be lighter than the maximum allowable.

3. Vehicle curb weight - W_c.

   $W_c = W_o + W_p$.

   The maximum allowable vehicle curb weight, W_{cm}, is 4300 lbs. (2700 + 1600 max. = 4300).

4. Vehicle test weight - W_t.

   $W_t = W_o + W_p + 300$ lbs. W_t is the vehicle weight at which all accelerative maneuvers, fuel economy and emissions are to be calculated. (Items 8 b,c,d).

   The maximum allowable test weight, W_{tm}, is 4600 lbs. (2700 + 1600 max. + 300 = 4600).

5. Gross vehicle weight - W_g.

   $W_g = W_o + W_p + 1000$ lbs. W_g is the gross vehicle weight at which sustained cruise grade velocity capability is to be calculated. (Item 8 e). The 1000 lbs. load simulates a full load of passengers and baggage.

   The maximum allowable gross vehicle weight, W_{gm}, is 5300 lbs. (2700 + 1600 max. + 1000 = 5300).

6. Propulsion system volume - V_p.

   V_p shall be packagable in such a way that the volume encroachment on either the passenger or luggage compartment is not significantly different than today's (1970) standard full size family car. Necessary external appearance (styling) changes will be minor in nature. V_p shall also be packagable in such a way that the handling characteristics of the vehicle do not depart significantly from a 1970 full size family car.

   The maximum allowable volume assignable to the propulsion system, V_{pm}, is 35 ft^3.

7. Emission Goals.

   The vehicle when tested for emissions in accordance with the procedure outlined in the Nov. 10, 1970 Federal Register shall have a weight of W_t. The emission goals for the vehicle are:

Hydrocarbons*	0.14 grams/mile	maximum
Carbon monoxide	6.16 grams/mile	maximum
Oxides of nitrogen**	0.4 grams/mile	maximum
Particulates	0.03 grams/mile	maximum

*Total hydrocarbons (using 1972 measurement procedures) plus total aldehydes. Aldehydes will not be more than 10 percent by weight of the hydrocarbons or 0.014 grams/mile, whichever is greater.

**Measured or computed as NO_2.

The powerplant should not produce objectionable levels of smoke, odors, or other pollutants which are not included above.

8. Start up, Acceleration, and Grade Velocity Performance.

   a. Start up: The time to reach 65 percent full power is 45 sec. Ambient conditions are 14.7 psia pressure, 60°F temperature.

      Cold (-40°F) start-up techniques shall be equivalent to the typical automobile spark-ignition engine.

   b. Acceleration from a standing start: The minimum distance to be covered in 10.0 sec. is 440 ft. The maximum time to reach a velocity of 60 mph is 13.5 sec. Ambient conditions are 14.7 psia, 85°F. Vehicle weight is W_t. Acceleration is on a level grade and initiated with the engine at the normal idle condition.

   c. Acceleration in merging traffic: The maximum time to accelerate from a constant velocity of 25 mph to a velocity of 70 mph is 15.0 sec. Ambient conditions are 14.7 psia, 85°F. Vehicle weight is W_t, and acceleration is on level grade.

   d. Acceleration, DOT High Speed Pass Maneuver: The maximum time and maximum distance to go from an initial velocity of 50 mph with the front of the vehicle 100 feet behind the back of a 55 foot truck traveling at a constant 50 mph to a position where the back of the vehicle is 100 feet in front of the front of the 55 foot truck is, 15 sec. and 1400 ft. The entire maneuver takes place in a traffic lane adjacent to the lane in which the truck is operated. The vehicle speed during the maneuver cannot exceed 80 mph. Ambient conditions are 14.7 psia, 85°F. Vehicle weight is W_t, and acceleration is on level grade.

   e. Grade velocity: The minimum sustained cruise velocity on a 5 percent grade with the air conditioner operating is 65 mph. Ambient conditions are 14.7 psia 85°F. Vehicle weight is W_g.

The vehicle must be capable of providing performance (Paragraphs 8b, 8c, 8d, 8e) within 5% of the stated 85°F values, when operated at ambient temperatures from-20°F to 105°F.

9. Minimum vehicle range without supplementing the energy storage will be 200 miles. The minimum range shall be calculated for, and applied to each of the two following modes: 1) A city-suburban mode, and 2) a cruise mode. Mode 1 is the driving cycle which appears in the Nov. 10, 1970 Federal Register. For vehicles whose performance does not depend on the state of energy storage, the range may be calculated for one cycle and ratioed to 200 miles. For vehicles whose performance does depend on the state of energy storage the Federal driving cycle must be repeated until 200 miles have been completed. Mode 2 is a constant 70 mph cruise on a level road for 200 miles. The vehicle weight for both modes shall be, initially, W_t. The ambient conditions shall be a pressure of 14.7 psia, and temperatures of 60°F, 85°F and 105°F. The vehicle minimum range shall not decrease by more than 5% at an ambient temperature of -20°F.

For hybrid vehicles, the energy level in the power augmenting device at the completion of operation will be equivalent to the energy level at the beginning of operation.

10. System thermal efficiency will be calculated by two methods:

1. A "fuel economy" figure based on the number of Btu per mile required to drive the vehicle over the 1972 Federal driving cycle which appears in the July 15, 1970 Federal Register. Vehicle weight is W_t.

2. A "fuel economy" figure based on the number of Btu per mile required to drive the vehicle at constant speed, in still air, on level road, at speeds of 20, 30, 40, 50, 60, 70, and 80 mph. Vehicle weight is W_t.

In both cases, the system thermal efficiency shall be calculated with sufficient electrical, power steering and power brake loads in service to permit safe operation of the automobile, air conditioning and heater loads being excluded.

Ambient conditions are 14.7 psia and temperatures of 60°F, 85°F and 105°F.

11. Air Drag Calculation: The product of the drag coefficient, C_d, and the frontal area, A_f is to be used in air drag calculations. The product C_dA_f has a fixed value of 13 ft^2. The air density used in computations shall correspond to the applicable ambient air temperature.

12. Rolling Resistance, R, is expressed in the equation $R = W/50 [1 + (1.4 \times 10^{-3}V) + (1.2\ 10^{-5}V^2)]$ lbs. V is the vehicle velocity in ft/sec. W is the vehicle weight in lbs.

13. Accessory power requirements: The accessory power demands are defined to include: the air conditioning compressor, the power steering pump, the alternator, and the power brakes actuating device. The accessories also include a device for heating the passenger compartment if the heating demand is not supplied by waste heat.

    The maximum intermittent accessory load, P_{aim}, is 10 HP (plus the heating load, if applicable). The maximum continuous accessory load, P_{acm}, is 7.5 HP (plus the heating load if applicable).

    If accessories are driven at variable speeds, the above values apply. If the accessories are driven at constant speed, the values will be reduced by 3 HP.

14. Passenger comfort requirements: Heating and air conditioning of the passenger compartment shall be at a rate equivalent to that provided in the present (1970) standard full size family car.

    Present automobile heating rate practice is approximately 30,000 Btu/hr. For an air conditioning system at 110°F ambient, 80°F and 40% relative humidity air to the evaporator, the rate is approximately 13,000 Btu/hr.

15. The propulsion system shall be operable within an expected ambient temperature range of -40° to 125°F.

16. Propulsion system design (normal operation) lifetime will be 3000 hours. Normal maintenance may include replacement of accessable minor parts of the propulsion system via a usual maintenance procedure, but the major parts of the system shall be designed for a 3000 hour minimum life.

17. Noise:
    a. Maximum Noise Test: The maximum noise generated by the vehicle shall not exceed 77 dbA when measured in accordance with SAE J968a. Note that the noise level is 77 dbA whereas in the SAE J968a the level is 86 dbA.

    b. Low Speed Noise Test: The maximum noise generated by the vehicle shall not exceed 63 dbA when measured in accordance with SAE J968a except that a constant vehicle velocity of 30 mph is used on the pass-by, the vehicle being in high gear or the highest gear in which it can be operated at that speed.

c. Idle Noise Test: The maximum noise generated by the vehicle shall not exceed 62 dbA when measured in accordance with SAE J968a except that the engine is idling (clutch disengaged or in neutral gear) and the vehicle passes by at a speed of less than 10 mph. The microphone will be placed at 10 feet from the centerline of the vehicle pass line.

18. The vehicle shall comply with all current Department of Transportation Federal Motor Vehicle Safety Standards.

Revision A (Nov. 30, 1970)

Appendix B
COMPUTER PROGRAM DESCRIPTIONS

Program Name: /F1.O Flywheel/

Size: 13056 characters

Data Inputs:

Variable	Unit
Weight	lb
Frontal area	sq ft
Drag coefficient	
Engine size	hp
Flywheel size	kw-hr
Maximum jerk	mph-sec/sec

File Inputs:

Profile

Contains elapsed time, acceleration, acceleration type (constant horsepower or constant acceleration), and grade for trip profile

Emissions

Contains log plots of HC, CO, and NO_x

Program Functions:

- Develops incremental emissions as a function of heat engine horsepower
- Computes constant road horsepower acceleration limited by jerk rate
- Computes transmission efficiencies

Program Outputs:

For each second:

- Time (sec)
- Acceleration (mph/sec)

- Velocity (mph)
- Drag (lb)
- Rolling resistance (lb)
- Horsepower out
- Cumulative horsepower out
- Average horsepower out
- Horsepower in
- Cumulative horsepower in
- Average horsepower in
- Net horsepower in system
- Flywheel energy
- Distance traveled (ft)
- Cumulative grams of HC
- Cumulative grams of CO
- Cumulative grams of NO_x

Summary Outputs:

- Maximum horsepower required
- Cruise horsepower
- Input horsepower required
- Average horsepower out
- Maximum flywheel energy
- Emissions in:
  - lb
  - lb/hr
  - lb/mi
  - gm
  - gm/hr
  - gm/mi

Comments: Several versions of this program have been developed for specific purposes. For example, some versions initiate with the flywheel energy at zero; others initiate with the flywheel at maximum energy and then automatically continue the run until the flywheel is again at maximum energy. Many subprograms have been developed to simulate different transmission types.

Program Name: /F51.1 VELGRD/

Size: 2304 Characters

Data Inputs:

Variable	Unit
Weight	lb
Frontal area	sq ft
Drag coefficient	
Maximum velocity	mph

Program Functions:

- Calculates road horsepower required to cruise at maximum velocity on 0-percent grade
- Using calculated horsepower (or an optional input horsepower), develops a plot of velocity vs. grade percent for grade from 0 to 30 percent (or higher)

Program Outputs:

- Cruise horsepower on 0-percent grade
- Table of velocity and grade
- File of velocity and grade to be used by X-Y plotter

Program Name: /F10.4 FWGEN/

Size: 1536 Characters

Data Inputs:

Variable	Units
Increment	in.
Radius	in.

Equations

Equations for flywheel
Geometry at varying intervals
From 0 to radius

Program Functions:

- Develops incremental half-thickness of flywheel from 0 to R based on input equations

Program Output:

- A file containing radius increments and half-thickness for use in Program / F10.2 FWSTRESS/

Program Name: /F10.2 FWSTRESS/

Size: 5376 Characters

Data Inputs:

Variable	Unit
Speed	Rad/sec
Material density	lb/cu in.
Poissons Ratio	
Young's Modulus	
Temperature coefficient	
Temperature difference	deg-F
Outside radius	in.

File Inputs: Incremental radius and half-thickness of flywheel from O to R (outside radius)

Program Functions:

- First accepts a trial value of the tangential stress of the outermost increment
- Calculates total force acting on flywheel
- Zeros in by reiteration on the actual outside tangential stress so that the incremental forces will equal the total force
- Generates the following outputs upon finding the correct tangential stress:

Program Outputs

Incremental

- Radius (in.)
- Thickness (in.) from input file
- Temperature (deg-F)
- Tangential stress (psi)
- Radial stress (psi)

Summary:

- Mean tangential stress (psi)
- Moment of inertia (lb-in.-sec^2)
- Kinetic energy (in.-lb)
- Weight (lb)
- Energy density (in.-lb/lb)
- Shape factor

Comments: This program included an option to create a file so that an X-Y plotter can generate a plot of the flywheel cross section and the associated tangential and radial stresses across the cross section

Appendix C

HEAT-ENGINE TREND DATA

MFG	MODEL	TYPE	BHP	WT	COST	VOL	SFC
FARYMANN	R	D	18	240	375	3.9	.460
FARYMANN	P	D	20	335	387	4.3	.460
FARYMANN	S	D	25	370	423	4.3	.460
LYCOMING	W-32	D	18	306	697	8.2	.480
LYCOMING	W-42	D	20	313	702	8.2	.485
LYCOMING	W-34	D	36	433	1177	12.3	.510
LYCOMING	W-44	D	40	433	1185	12.3	.485
VOLKSWAGON	122	S	34	206	375	11.6	.480
VOLKSWAGON	126	S	45	220	412	11.7	.490
PEUGEOT	XDP4/88	D	52	390	590	6.8	.485
PEUGEOT	XDP4/90	D	56	414	608	6.8	.485
PEUGEOT	XDP6/90	D	81	581	1070	11.0	.485
PEUGEOT	XM	S	50	319	401	6.7	.530
PEUGEOT	XN1	S	55	319	431	6.7	.530
DAIMLER	OM636	D	36	425	736	8.4	.450
ONAN	CCKA	S	12	168	239	3.8	.750
ONAN	CCKB	S	14	172	248	3.8	.630
ONAN	NY	S	18	125	265	4.4	.620
ONAN	DJ60	D	12	270	541	5.9	.400
ONAN	DJ120	D	22	438	869	9.6	.400
KOHLER	K321	S	11	119	234	3.2	.620
KOHLER	K482	S	14	180	401	4.7	.690
KOHLER	K662	S	19	250	506	8.6	.600
DEUTZ	FIL410	D	11	264	473	5.6	.488
DEUTZ	F2L410	D	21	359	593	7.4	.461
PERKINS	4.108	D	38	480	744	5.5	.470
PERKINS	3-152	D	35	700	764	12.7	.420
PERKINS	4.154	D	55	555	892	11.3	.430
PERKINS	4.236	D	65	750	852	9.2	.370
PERKINS	NA-120	D	90	1040	1185	18.1	.380
PERKINS	NA-180	D	144	1340	1852	27.2	.415
FORD	091GF	S	44	254	438	5.3	
FORD	104GF	S	60	254	458	5.3	
FORD	B8PE	S	36	535	468	9.9	
FORD	B8PD	S	51	535	489	9.9	
FORD	200GF	S	90	337	520	11.8	
FORD	C5PF	S	113	473	555	15.6	
FORD	C5PG	S	124	473	572	15.6	
FORD	C4PD	S	143	720	583	22.2	
FORD	C4PB	S	158	720	754	22.2	

MFG	MODEL	TYPE	BHP	WT	COST	VOL	SFC
FORD	COPB	D	44	585	869		
FORD	C3PY	D	89	880	1126		
FORD	242DF	D	68	754	913		
FORD	330DF	D	97	965	1320		
FORD	363DF	D	106	956	1356		
G.M.C.	911619	S	41	412	403	10.1	.580
G.M.C.	911620	S	43	450	407	10.0	.530
G.M.C.	991894	S	82	410	413	14.5	.490
G.M.C.	6002802	S	108		336		.490
G.M.C.	6002818	S	120		348		.500
G.M.C.	305C	S	112	950	640	25.8	.446
G.M.C.	351C	S	125	980	710	25.8	.490
G.M.C.	401M	S	150	950	805	25.8	.491
G.M.C.	DH478	D	117	950		25.9	
G.M.C.	DH637	D	159	1271		35.1	
SOLOR	10KW	T	22	45		1.2	1.200
WILLIAMS	WR-26	T	80	225		6.0	.590
KLOCKNER	T216	T	85	176		8.7	1.370
TURBOTRON	?	T	88	85		5.8	.580
MOTOREN	6012L	T	94	96		3.1	1.280
SOLOR	TITAN	T	110	85		3.7	1.070
KLOCKNER	T112	T	120	79		1.5	.960
AIRESEARCH	GTP30	T	130	105		5.2	1.070
WILLIAMS	WR2-6	T	130	56		2.3	1.030
WILLIAMS	WR24-7	T	170	85		2.1	1.080
AIRESEARCH	TSE-36	T	210	178		12.7	.830
MOTOREN	6022 A2	T	210	190		9.0	.740
ALLISON	250C18	T	270	136		9.3	.720
TURBOMECA	TAA230	T	300	290			.880
ALLISON	T63	T	310	155		9.6	.710
MOTOREN &	6022 A3	T	320	320		14.4	.670
TURBOMECA	2C6	T	340	315		12.0	.950
ALLISON	T63	T	340	190		10.7	.650
TURBOMECA	OREDEN4	T	355	250		3.8	.580
AIRESEARCH	TSE231	T	400	174		4.3	.640
TURBOMECA	2A	T	450	285		7.4	.620
TURBOMECA	3B	T	465	400		12.2	.670
TURBOMECA	14A	T	510	352		9.5	.590
UACL (P&W)	ST6	T	510	269		9.8	.680
ROLLS-ROYC	103/503	T	600	655			.860

```
    MFG      MODEL  TYPE  BHP   WT  COST  VOL   SFC
---------- -------   -   ---- ---- ---- ---- -----

CZECH      M601      T    620  299        7.8  .640
AIRESEARCH TPE331    T    680  355       14.6  .650
AIRESEARCH TPT331    T    715  343       13.2  .600
TURBOMECA  24        T    755  341       11.9  .540
LYCOMING   T53       T    935  496       11.5  .700
GEN ELECT  T58       T   1060  315        6.9  .660
GEN ELECT  T58       T   1060  315        7.1  .630
GEN ELECT  T58       T   1130  309       11.5  .620
ROLLS-ROYC H1200     T   1150  314       12.8  .640
```

BLANK PAGE

Appendix D

COMPUTER-AIDED STRESS ANALYSIS OF DISC TYPE FLYWHEELS

by R. Gilbert and J. Spillman

The following stress analysis follows the method of Stodola* (pp. 373f), but the difference form of the equations is used rather than the differential form. An isotropic material is assumed. It also is assumed that there is a negligible stress gradient in the axial direction. Considering an incremental piece of the flywheel,

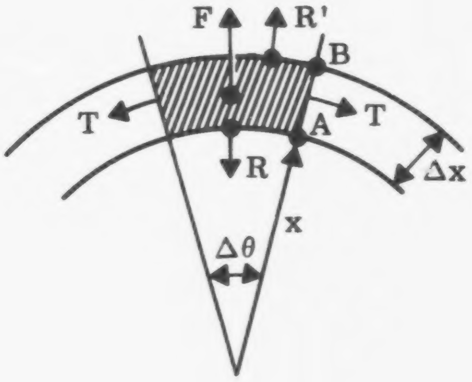

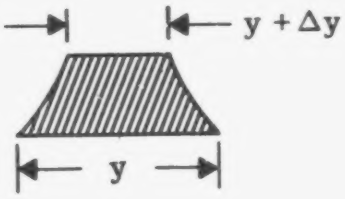

the equation for the summation of forces may be derived.

The volume,

$$\Delta V = (x \Delta \theta)(\Delta x)(y) \tag{D.1}$$

The mass,

$$\Delta m = \frac{\rho}{g} \Delta V = \frac{\rho}{g} x y \Delta x \Delta \theta \tag{D.2}$$

---

*Steam and Gas Turbines, A. Stodola, Vol. I, McGraw-Hill, 1927.

The radial acceleration,

$$a = x\omega^2 \tag{D.3}$$

The centrifugal force on an element due to its own acceleration,

$$F = ma \tag{D.4}$$

$$F = \frac{\rho\omega^2}{g} x^2 y \Delta x \Delta \theta \tag{D.5}$$

The tangential force on each radial face,

$$T = y \Delta x \sigma_t \tag{D.6}$$

The radial force on inner circumferential face,

$$R = y x \Delta \theta \sigma_r \tag{D.7}$$

The radial force on outer circumferential face,

$$R' = (y + \Delta y)(x + \Delta x) \Delta\theta (\sigma_r + \Delta\sigma_r) \tag{D.8}$$

The sum of the forces in the radial direction = 0 .

$$R' - R - T\Delta\theta + F = 0 \tag{D.9}$$

Expanding Eq. (D.8)

$$R' = (yx + y\Delta x + x\Delta y + \Delta y \Delta x)(\sigma_r + \Delta\sigma_r)\Delta\theta \tag{D.10}$$

$$R' = (xy\sigma_r + y\sigma_r \Delta x + x\sigma_r \Delta y + xy\Delta\sigma_r)\,\Delta\theta \qquad \text{(D.11)}$$

$$R' = \left(xy\sigma_r + \Delta\,(xy\sigma_r)\right)\Delta\theta \qquad \text{(D.12)}$$

$$R' = \Delta\,(xy\sigma_r)\,\Delta\theta + xy\sigma_r\Delta\theta \qquad \text{(D.13)}$$

$$R' - R = \Delta(xy\sigma_r)\,\Delta\theta \qquad \text{(D.14)}$$

Combining Eqs. (D.5), (D.6), and (D.14) into (D.9):

$$\Delta(xy\sigma_r)\,\Delta\theta - y\Delta x\sigma_t\,\Delta\theta + \frac{\rho\omega^2}{g}x^2 y\Delta x\Delta\theta = 0 \qquad \text{(D.15)}$$

Dividing through by $\Delta x\Delta\theta$,

$$\frac{\Delta(xy\sigma_r)}{\Delta x} - y\sigma_t + \frac{\rho\omega^2}{g}x^2 y = 0 \qquad \text{(D.16)}$$

which is the equation for the summation of forces.

Now, still following the method of Stodola, Eq. (D.16) is to be combined with the stress compatibility equation.

DERIVATION OF STRESS COMPATIBILITY EQUATION

$$\epsilon_r = \frac{1}{E}(\sigma_r - \nu\sigma_t) \qquad \text{(D.17)}$$

$$\epsilon_t = \frac{1}{E}(\sigma_t - \nu\sigma_r) \qquad \text{(D.18)}$$

from Eq. (D.17),

$$\sigma_r = E\epsilon_r + \nu\sigma_t \tag{D.19}$$

from Eq. (D.18),

$$\sigma_r = \frac{\sigma_t - E\epsilon_t}{\nu} \tag{D.20}$$

from Eqs. (D.19) and (D.20)

$$E\epsilon_r + \nu\sigma_t = \frac{\sigma_t - E\epsilon_t}{\nu} \tag{D.21}$$

$$E\nu\epsilon_r + \nu^2\sigma_t = \sigma_t - E\epsilon_t \tag{D.22}$$

$$\sigma_t - \nu^2\sigma_t = E\nu\epsilon_r + E\epsilon_t \tag{D.23}$$

$$\sigma_t = \frac{E}{1 - \nu^2}(\epsilon_t + \nu\epsilon_r) \tag{D.24}$$

Similarly, by symmetry,

$$\sigma_r = \frac{E}{1 - \nu^2}(\epsilon_r + \nu\epsilon_t) \tag{D.25}$$

The circumferential strain at A,

$$\epsilon_t = \frac{2\pi(x + \xi) - 2\pi x}{2\pi x} \tag{D.26}$$

$$\epsilon_t = \frac{\xi}{x} \tag{D.27}$$

$$\xi_B = \xi + \frac{\Delta\xi}{\Delta x}\Delta x \tag{D.28}$$

The length of A - B after elongation,

$$\Delta x + \Delta(\Delta x) = (x + \Delta x + \xi_B) - (x + \xi) \tag{D.29}$$

$$= \xi_B - \xi + \Delta x \tag{D.30}$$

$$= \xi + \frac{\Delta\xi}{\Delta x}\Delta x - \xi + \Delta x \tag{D.31}$$

$$= \frac{\Delta\xi}{\Delta x}\Delta x + \Delta x \tag{D.32}$$

$$\Delta(\Delta x) = \frac{\Delta\xi}{\Delta x}\Delta x \tag{D.33}$$

$$\frac{\Delta(\Delta x)}{\Delta x} = \frac{\Delta\xi}{\Delta x} \tag{D.34}$$

But by definition,

$$\frac{\Delta(\Delta x)}{\Delta x} = \epsilon_r \tag{D.35}$$

$$\epsilon_r = \frac{\Delta\xi}{\Delta x} \tag{D.36}$$

From Eq. (D.27)

$$\xi = x\epsilon_t \tag{D.37}$$

Combining above with Eq. (D.18)

$$\xi = \frac{x}{E}(\sigma_t - \nu\sigma_r) \tag{D.38}$$

Combining Eqs. (D.36) and (D.17),

$$\frac{\Delta\xi}{\Delta x} = \frac{1}{E}(\sigma_r - \nu\sigma_t) \tag{D.39}$$

From Eq. (D.38),

$$\xi = \frac{1}{E}(x\sigma_t - x\nu\sigma_r) \tag{D.40}$$

$$\Delta\xi = \frac{1}{E}(x\Delta\sigma_t + \sigma_t\Delta x - x\nu\Delta\sigma_r - \nu\sigma_r\Delta x) \tag{D.41}$$

$$\frac{\Delta\xi}{\Delta x} = \frac{1}{E}\left(x\frac{\Delta\sigma_t}{\Delta x} + \sigma_t - x\nu\frac{\Delta\sigma_r}{\Delta x} - \nu\sigma_r\right) \tag{D.42}$$

Combing Eqs. (D.39) and (D.44)

$$\frac{1}{E}(\sigma_r - \nu\sigma_t) = \frac{1}{E}\left(x\frac{\Delta\sigma_t}{\Delta x} + \sigma_t - x\nu\frac{\Delta\sigma_r}{\Delta x} - \nu\sigma_r\right) \tag{D.43}$$

$$\sigma_r + \nu\sigma_r - \sigma_t - \nu\sigma_t = x\left(\frac{\Delta\sigma_t}{\Delta x} - \nu\frac{\Delta\sigma_r}{\Delta x}\right) \tag{D.44}$$

$$\frac{\Delta \sigma_t}{\Delta x} - \nu \frac{\Delta \sigma_r}{\Delta x} = (1 + \nu) \frac{\sigma_r - \sigma_t}{x} \qquad \text{(D.45)}$$

which is the stress compatibility equation.

The summation of forces Eq. (D.16) and the stress compatibility Eq. (D.45) can now be combined to determine the tangential and radial stresses in a flywheel of given shape, material, and peripheral velocity.

COMPUTER METHOD

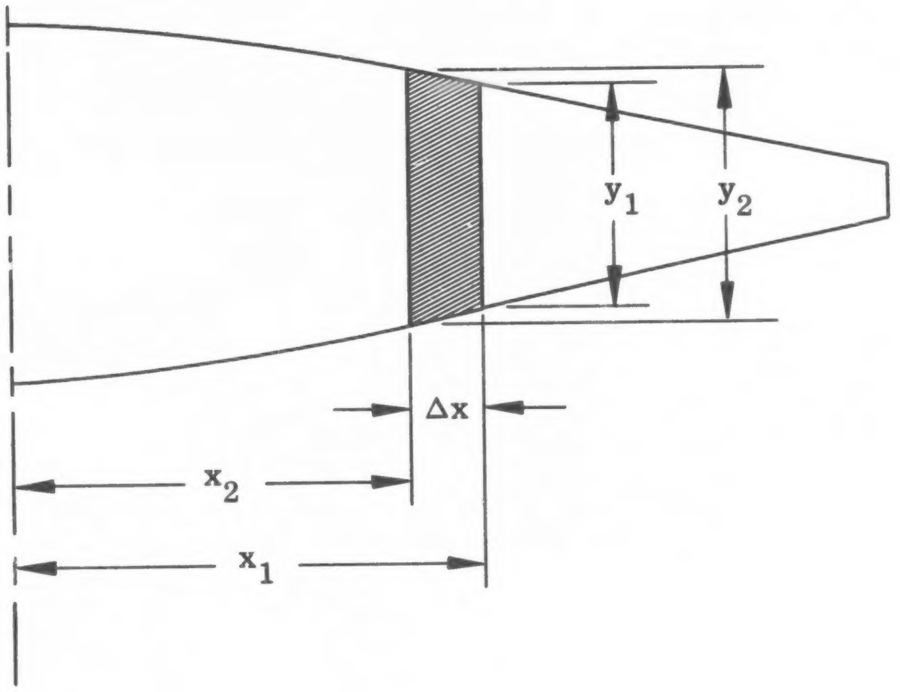

The wheel is divided into a number of circumferential elements (onion rings) and the stresses are calculated starting from the outside of the outermost element and working inward.

From (D.16),

$$\Delta xy\,\sigma_r = y\,\sigma_t\,\Delta x - \frac{\rho\omega^2}{g}\,x^2\,y\,\Delta x \qquad \text{(D.46)}$$

$$\Delta xy\,\sigma_r = (xy\,\sigma_r)_1 - (xy\,\sigma_r)_2 \qquad \text{(D.47)}$$

$$(xy\,\sigma_r)_2 = (xy\,\sigma_r)_1 - y\,\sigma_t\,\Delta x + \frac{\rho\omega^2}{g}\,x^2\,y\,\Delta x \qquad \text{(D.18)}$$

$$\sigma_{r_2} = \left[(xy\,\sigma_r)_1 - y\,\sigma_t\,\Delta x + \frac{\rho\omega^2}{g}\,x^2\,y\,\Delta x\right] \Big/ (xy)_2 \qquad \text{(D.49)}$$

where variables $(x, y, \sigma_r, \sigma_t)$ without subscripts (1 or 2) are mean values. For thin slices, sufficient accuracy can be obtained by using arithmetic averages.

For the outermost slice, $\sigma_{r_1} = 0$, but σ_{t_1} is not known. A value for σ_{t_1} must be assumed and total stress plots obtained. The tangential stress profile when integrated over the half wheel will deviate from the known mean targential stress as calculated from the following equation:

$$(\sigma_t)\,\text{mean} = \frac{\rho\omega^2}{g}\,\frac{\sum\limits_{x=o}^{x_o} x^2\,y\,\Delta x}{\sum\limits_{x=o}^{x_o} y\,\Delta x} \qquad \text{(D.50)}$$

A second assumption for σ_{t_1} at the outside is then made and successive iteration eventually brings the integrated stress profile and the mean tangential stress into agreement. The resulting stress profiles are then correct. The computer program employs a binary closure technique such that the initial assumption for σ_{t_1} need not be at all close to the actual value. For near-optimum energy storage flywheels of the kind considered here, a reasonable initial assumption for σ_{t_1} at the outside element is one half the mean tangential stress per Eq. (D.50).

Since Eq. (D.49) requires the mean value of σ_t, an initial calculation is made using σ_{t_1} for σ_t, and after σ_{t_2} is calculated (see Eq. (D.53) below) σ_t is set to $\frac{1}{2}(\sigma_{t_1} + \sigma_{t_2})$ and σ_{r_2} and σ_{t_2} are recalculated. An interation process is used until the values of σ_t for successive trials close.

With the radial stress known, the tangential stress is then derived from the stress compatibility Eq. (0.45):

$$\Delta\sigma_t = \nu\Delta\sigma_r + (1 + \nu)\frac{\sigma_r - \sigma_t}{x}\Delta x \tag{D.51}$$

$$\Delta\sigma_t = (\sigma_t)_1 - (\sigma_t)_2 \tag{D.52}$$

$$(\sigma_t)_2 = (\sigma_t)_1 - \nu\left(\sigma_{r_1} - \sigma_{r_2}\right) - (1 + \nu)\frac{\sigma_r - \sigma_t}{x}\Delta x \tag{D.53}$$

Thermal stresses due to a radial temperature gradient may be superimposed by adding the term $E\epsilon\,(t_2 - t_1)$ to the right hand side of Eq. (D. 53),

where

E = Young's Modulus, lb/in.^{2} (30×10^6 for steel)

ϵ = thermal coefficient of expansion, °F^{-1} (7.3×10^{-6} for steel)

t_2 = temperature, °F, at the end (inside) of the increment

t_1 = temperature, °F, at the beginning (outside) of the increment

Calculations of total weight, inertia, kinetic energy, etc., are calculated in the normal fashion by summing the values for each increment. The flywheel shape is provided by a data file which may be loaded from tabular data or from an equation or sets of equations.

The computer program and a typical run are attached.

PROGRAM /F10.2 FW STRESS/

```
100     A$="PROGRAM /10.2 FWSTRESS/"  !UPDATED OCT 7,1970

110     REAL A,A1,B,C,D,D1,E,F1,G,I,M,N,P,Q,R,S,T,T1,T2,V
        ,W,W1,X,X1,X2,Y,Y1
120     DIM R(3),T(3),X(300),Y(300)
130     PRINT FOR I=1 TO 10
140     PRINT "DATE OF RUN: ":DATE
150     PRINT FOR I=1 TO 3
160     A=1,M=2,E=3,Q=0,D1=2↑6,S2=1,S3=0
170     READ W,P,V,E2,E3,T5
180     G=386.089
190     GOSUB 2000
200     S,T2=1.2*P*W↑2/G*F1/A1/2
210     J=.1*S
220     FOR I=-10 TO 25 STEP+1
230     IF 2↑(I+1)<J THEN D1=2↑I
240     NEXT I
250     IF Q=0 THEN 580
260     PRINT FOR I=1 TO 10
270     PRINT SPACE(30):"DATE OF RUN: ":DATE
280     PRINT FOR I=1 TO 2
290     PRINT A$
300     PRINT FOR I=1 TO 2
310     F="3Z.4D 4B 2Z.4D 6B 3Z.D 6B -6ZD 2B -6ZD/"
320     PRINT "FLYWHEEL PARAMETERS"
330     PRINT
340     PRINT IN FORM "'     SPEED ----------------------
        - ' 4Q' RAD/SEC'/":W
350     PRINT IN FORM "'     MATERIAL DENSITY -----------
        - ' Q.3D' LBS/CU-IN'/":P
360     PRINT IN FORM "'     POISSONS RATIO -------------
        - ' Q.DD/":V
370     PRINT IN FORM "'     YOUNGS MODULUS -------------
        - ' QQ.DESDD/":E2
380     PRINT IN FORM "'     TEMP. EXP. COEFFICIENT -----
        - ' Q.DESDD/":E3
390     PRINT IN FORM "'     TOTAL TEMP. DIFFERENCE -----
        - ' QQQ.Q ' DEG-F'/":T5
400     PRINT IN FORM "'     OUTSIDE RADIUS -------------
        - '3Q.4D' INCHES'/":X(1)
410     PRINT
420     PRINT "FLYWHEEL DESIGN FACTORS"
430     PRINT
440     PRINT IN FORM "'     MEAN TANGENTIAL STRESS -----
        - ' 7Q ' PSI'/":P*W↑2/G*F1/A1
450     PRINT IN FORM "'     MOMENT OF INERTIA ----------
        - ' 3Q.3D ' LB-IN-SEC↑2'/":M2
460     PRINT IN FORM "'     KINETIC ENERGY -------------
        - '10Q' IN-LBS'/":K
```

BLANK PAGE

PROGRAM /F10.2 FW STRESS/

```
3050     IF S3>1 THEN 3080
3060     IF T1<P*W↑2/G*F1 THEN S4=1 ELSE S4=-1
3070     GO TO 3130
3080     IF S2=-1 THEN 3130
3090     IF T1<P*W↑2/G*F1 THEN 3100 ELSE 3120
3100     IF S4=-1 THEN S2=-1
3110     GO TO 3130
3120     IF S4=1 THEN S2=-1
3130     IF Z=0 THEN PRINT T1,T2
3140     IF Z=-1 THEN PRINT "TOO LOW        ":T2
3150     IF Z=1 THEN PRINT "TOO HIGH       ":T2
3160     IF S2=1 THEN D1=D1*2 ELSE D1=D1/2
3170     IF T1<P*W↑2/G*F1 THEN 3180 ELSE 3200
3180     T2=T2+D1
3190     GO TO 3210
3200     T2=T2-D1
3210     S=T2
3220     GO TO 3260
3230     S2=1000
3240     PRINT T1,T2
3250     S=T2
3260     RETURN
4000     IF Q=0 THEN RETURN
4010     PRINT IN FORM F:X,Y,T6,T,R
4020     RETURN
10000    !ENTER SPEEDDENSITYPOISSONS RATIOYOUNGS MODULUSTE
         MP. EXP COEF.TOTAL TEMP. DIFF.
10050    DATA 2512,.285,.3,30E6,7.3E-6,0
```

```
PROGRAM /F10.2 FW STRESS/

860     GOSUB 4000
870     GO TO 920
880     I=N-1
890     GO TO 920
900     I=N-1
910     IF T1<0 THEN Z=-1 ELSE Z=1
920     NEXT I
930     IF X(N-1)<>0 THEN 970
940     T1=T1+T(A)*Y(N-1)*D
950     W2=W2+Y*D*PI*P*X(N-2)
960     M2=M2+(Y*D*PI*P*X(N-2))/G*X↑2
970     R1=SQRT(M2*G/W2)
980     K=(W2/(2*G))*R1↑2*W↑2
990     K1=K/W2
1000    IF Q=1 THEN 1030
1010    GOSUB 3000
1020    GO TO 250
1030    IF X(N-1)<>0 THEN 1050
1040    PRINT IN FORM "3Z.4D 4B 2Z.4D 6B 3Z.D/":0,Y(N-1),
        T6
1050    PRINT FOR I=1 TO 10
1060    STOP
2000    OPEN /D10.2 DATA/,INPUT,1
2010    ON ENDFILE(1) GO TO 2150
2020    N=1
2030    DIM X(300),Y(300)
2040    INPUT FROM 1:X(N),Y(N)
2050    F1,A1=0
2060    N=N+1
2070    INPUT FROM 1:X(N),Y(N)
2080    D=X(N-1)-X(N)
2090    X=X(N-1)-D/2
2100    Y=(Y(N)+Y(N-1))/2
2110    F1=F1+X↑2*Y*D
2120    A1=A1+Y*D
2130    N=N+1
2140    GO TO 2070
2150    CLOSE 1
2160    PRINT
2170    PRINT "TOTAL FORCE=":F1*P*W↑2/G
2180    PRINT
2190    PRINT "CALC FORCE     O.S.STRESS"
2200    PRINT "----------     ----------"
2210    RETURN
3000    IF S2<100 THEN 3030
3010    Q=1
3020    RETURN
3030    S3=S3+1
3040    IF ABS(P*W↑2/G*F1-T1)<10 THEN 3230
```

```
                                       DATE OF RUN: 10/08  16:34

PROGRAM /10.1.2 FWSTRESS/

FLYWHEEL PARAMETERS-

     SPEED ------------------------ 2512 RAD/SEC
     MATERIAL DENSITY ------------- .285 LBS/CU-IN
     POISSONS RATIO --------------- .3
     YOUNGS MODULUS --------------- 30.0E+06
     TEMP. EXP. COEFFICIENT ------- 7.3E-06
     TOTAL TEMP. DIFFERENCE ------- .0 DEG-F
     OUTSIDE RADIUS --------------- 10.2230 INCHES

FLYWHEEL DESIGN FACTORS

     MEAN TANGENTIAL STRESS ------ 116867 PSI
     MOMENT OF INERTIA ----------- 5.049 LB-IN↑2-SEC
     KINETIC ENERGY -------------- 15931389 IN-LBS
                                   .5000 KWH
     WEIGHT ---------------------- 46.40 LB
     ENERGY DENSITY -------------- 343325.93 IN-LBS/LB
                                   10.8 WH/LB
     SHAPE FACTOR ---------------- .7547

 RADIUS    THICKNESS  TEMPERATURE  TANGENTIAL  RADIAL
  (IN)       (IN)       (DEG-F)      STRESS    STRESS
                                     (PSI)     (PSI)
-------    -------      -----       -------   -------

10.2230     .2560        .0          62032          0
 9.7119     .2878        .0          71740      19683
 9.2007     .3217        .0          80151      36515
 8.6896     .3574        .0          87458      50947
 8.1784     .3947        .0          93818      63352
 7.6673     .4332        .0          99362      74035
 7.1561     .4727        .0         104201      83249
 6.6450     .5126        .0         108425      91200
 6.1338     .5526        .0         112110      98064
 5.6227     .5922        .0         115320     103983
 5.1115     .6308        .0         118109     109076
 4.6004     .6679        .0         120522     113444
 4.0892     .7029        .0         122595     117167
 3.5781     .7353        .0         124360     120314
 3.0669     .7646        .0         125843     122942
 2.5558     .7903        .0         127065     125095
 2.0446     .8120        .0         128042     126811
 1.5335     .8293        .0         128787     128119
 1.0223     .8418        .0         129306     129045
  .5112     .8494        .0         129566     129643
  .0000     .8520        .0
```

Appendix E

ANALYSIS OF FLYWHEEL/HYBRID FAMILY CAR PERFORMANCE IN DOT HIGH-SPEED PASS MANEUVER

An analysis of the family car with a flywheel/heat-engine hybrid drive in repetitive cycles of the DOT High-Speed Pass Maneuver was conducted.

The DOT High-Speed Pass Maneuver is described in the "NAPCA Vehicle Design Goals – Six-Passenger Automobile (Revision A, November 30, 1970)" as follows:

> "The maximum time and maximum distance to go from an initial velocity of 50 mph with the front of the vehicle 100 feet behind the back of a 55 foot truck traveling at a constant 50 mph to a position where the back of the vehicle is 100 feet in front of the front of the 55 foot truck is, 15 sec. and 1400 ft. The entire maneuver takes place in a traffic lane adjacent to the lane in which the truck is operated. The vehicle speed during the maneuver cannot exceed 80 mph. Ambient conditions are 14.7 psia, 85° F. Vehicle weight is W_t , and acceleration is on level grade."

E.1 INITIAL ASSUMPTIONS

The family car hybrid drive was assumed to have the following characteristics in accordance with the aforementioned "Vehicle Design Goals":

Family car length = 20 ft
Continuous hp available to road = 65.9 hp
Maximum hp to road during constant hp acceleration = 184 hp
Flywheel energy storage capacity = 391 w-hr
Maximum flywheel energy required for acceleration = 355 w-hr
Vehicle weight = 4000 lb
Maximum transmission hp output = 184 hp
Average transmission efficiency during maneuver = 90%
Minimum deceleration (braking) time = 1/3 acceleration time

E.2 ANALYSIS

Two boundary cases were analyzed to verify the suitability of the flywheel/heat-engine drive for repetitive maneuvers. The first case represents the poorest vehicle performance that will meet the maneuver criteria. Here, the family car is accelerated at constant horsepower such that it travels exactly 375 ft further than the truck in 15 sec. The car is then decelerated to 50 mph in 5 sec, at which time the maneuver is repeated.

E.3 CASE 1 CALCULATIONS

Based on the Total Kinetic Energy (TKE) concept, the available flywheel kinetic energy (KE) at the start of the maneuver is:

$$\text{Initial Flywheel KE} = \left[1 - \frac{(\text{initial velocity})^2}{(\text{final velocity})^2}\right] (\text{Max KE Reqd}) + \text{Reserve KE}$$

or

$$\text{Initial Flywheel KE} = \left[1 - \frac{(50)^2}{(80)^2}\right](355) + 36 = 252 \text{ w-hr}$$

During acceleration, the rolling, drag, and transmission losses are supplied by the heat engine. At end of acceleration, velocity is 78.5 mph and remaining flywheel energy is

$$KE_f = 355\left[1 - \frac{(78.5)^2}{(80)^2}\right] + 36 = 49 \text{ w-hr}$$

The recuperated vehicle kinetic energy during deceleration (without increasing transmission hp) then is

$$KE_d = \frac{184\ (0.9)\ (746)\ (5)}{3600} = 172 \text{ w-hr}$$

In addition, the heat engine can simultaneously supply energy to the flywheel as follows

$$KE_{eng\text{-}fw} = \frac{65.9\ (746)\ (5)}{(0.9)\ 3600} = 76 \text{ w-hr}$$

Thus, the total energy available to the flywheel at the end of the maneuver is 297 w-hr. However, the TKE control would hold the flywheel at approximately 252 w-hr. Thus, the maneuver could be repeated continuously.

E.4 CASE 2 CALCULATIONS

The second case analyzed was for the highest performance available, by using the flywheel and heat engine to supply a constant 184 hp to the road until the car is 375 ft ahead of the truck. The time of 1/3 the acceleration period is then used for recuperative braking. This scenario would be the most probable in actual two-lane road driving operations since the exposure is minimized.

Again, as in Case 1, the initial flywheel KE is 252 w-hr at the start of the maneuver. The acceleration time (at constant hp) to reach a point 375 ft ahead of the truck is 11.5 sec and the final velocity reached is 80 mph.

The flywheel KE at the end of acceleration is

$$KE_f = 0 + 36 = 36 \text{ w-hr}$$

The energy recuperated during braking is

$$KE_d = \frac{184\ (0.9)\ (746)\ (3.83)}{3600} = 132 \text{ w-hr}$$

The make-up energy simultaneously available during deceleration from the engine is

$$KE_{eng-fw} = \frac{65.9\,(746)\,(3.83)}{(0.9)\,(3600)} = 58 \text{ w-hr}$$

Thus, the available energy to the flywheel is 226 w-hr. Since only 216 w-hr of flywheel energy is required to repeat the maneuver immediately, the flywheel status is sufficient for an identical maneuver on the second pass. On the third and successive repetitive pass maneuvers without dwell, the time to pass is increased from 11.5 sec to 13 sec (still well within the 15-sec limit). In order to provide for repetitive high-performance pass maneuvers up to the 200-mile family car range, the imposition of a dwell time of 0.5 sec after the second and subsequent repetitive pass maneuvers is required.